Detectors in astronomy

G. Finger
European Southern Observatory

Outline

- Optical detectors
  - deep depletion CCD, L3 CCD, Orthogonal transfer CCD
  - Si-PIN CMOS arrays
- Infrared detectors
  - Hybrid structure, readout architectures, size limitation
  - Mid infrared blocked impurity band arrays
  - AO sensors
  - Results with HgCdTe arrays
    - LPE HgCdTe/CdZnTe and MBE HgCdTe/CdZnTe
    - Dark current for different materials
    - Interpixel crosstalk and conversion gain
    - Noise, persistence, glow, reference pixels
    - Guide mode of Hawaii-2RG, ASIC
- Readout controller and ASIC

ESO VLT

Paranal Observing Platform with AT1 and AT2

ESO PR Photo 07a/05 (14 March 2005)

- In Chile on Cerro Paranal at 2400m
- 4 x 8 m telescopes + 2 x 1.8 m telescopes
- Interferometry
- Active optics adaptive optics fringe tracking

ESO VLT

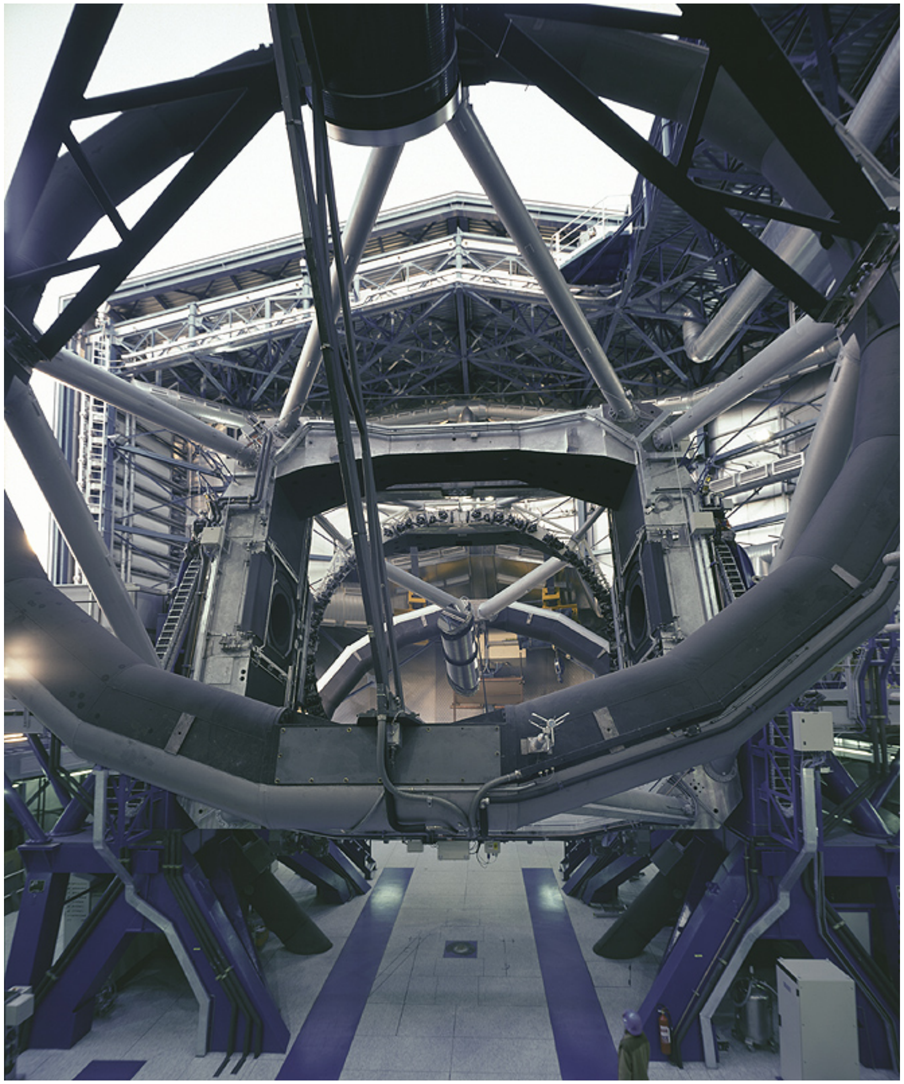

- In Chile on Cerro Paranal at 2400m
- 4 x 8 m telescopes + 2 x 1.8 m telescopes
- Interferometry
- Active optics adaptive optics fringe tracking

VLT Interferometer: VLTI

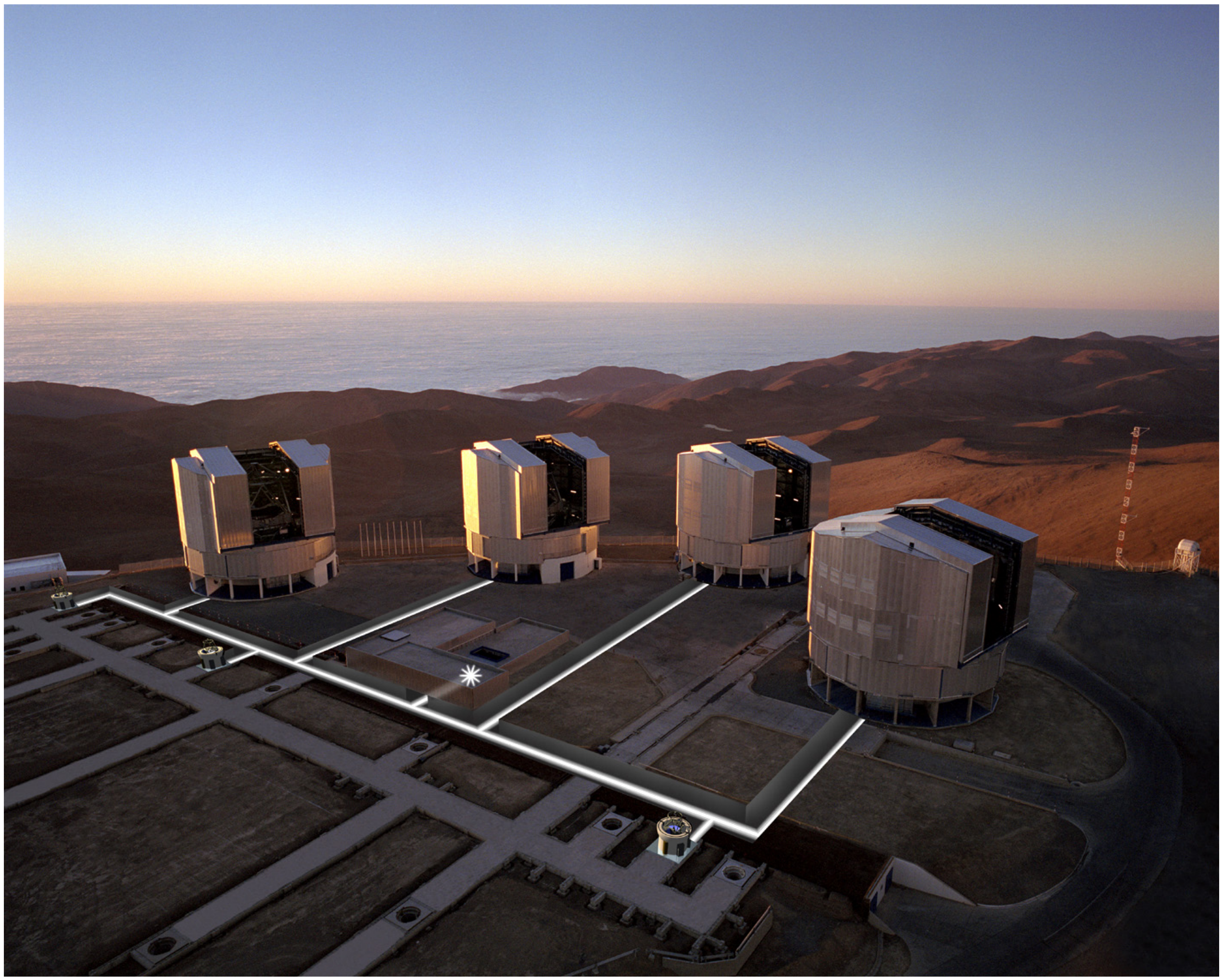

- From the beginning the VLT was built to be an interferometer
- Four 8-m Unit Telescopes Max. Baseline 130m
- Three 1.8-m Auxiliary Telescopes Baselines 8 – 200m
- Near IR to MIR angular resolution 1-20 milliarcsec
- Excellent uv plane coverage

Instruments of the ESO VLT / VLTI need detectors covering the UV, visible and IR (300 nm to 28 μm)

and many more to come……

Intrinsic photon detectors

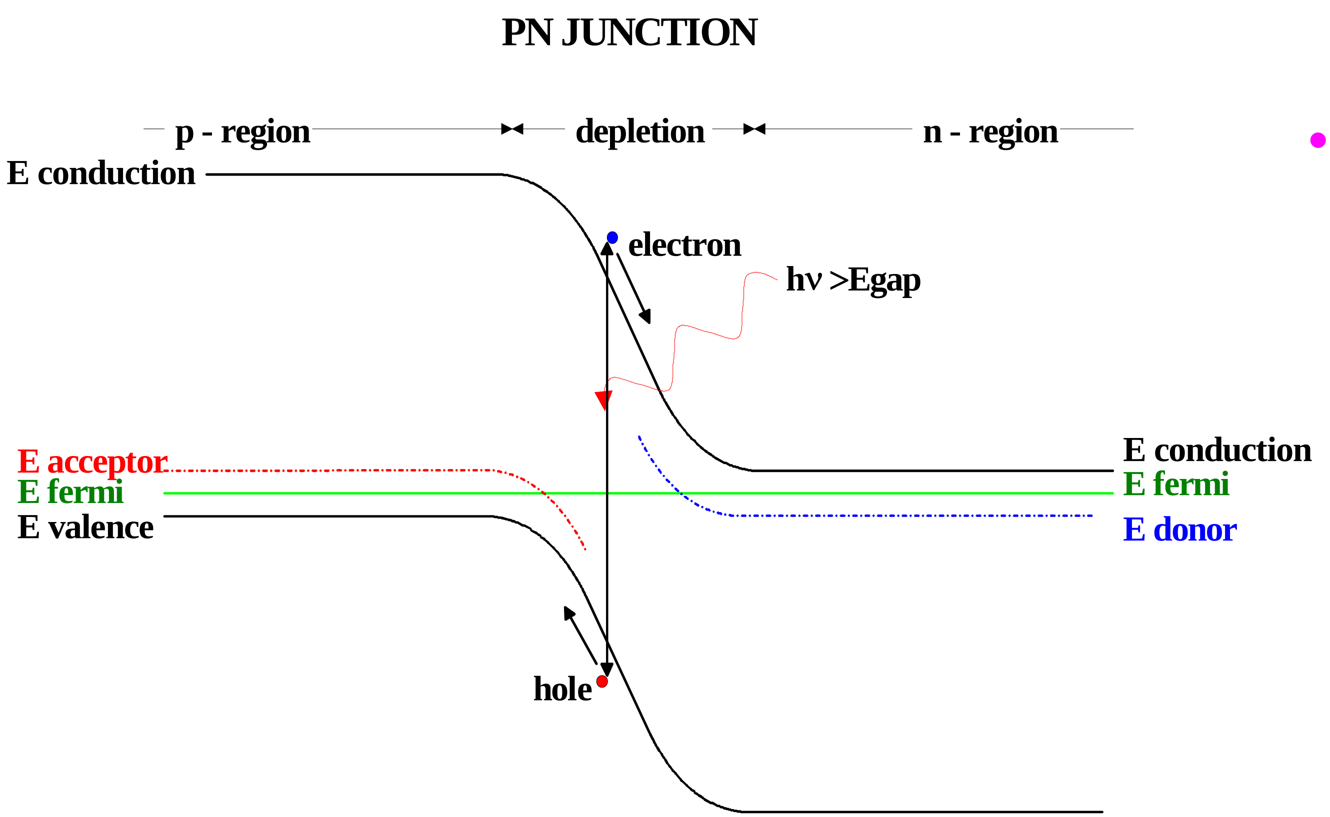

- Absorbed photon generates transition from valence to conduction band
- Si bandgap 1.12 eV
  $\Rightarrow \lambda_c \sim 1\ \mu m$

CCD operating principle

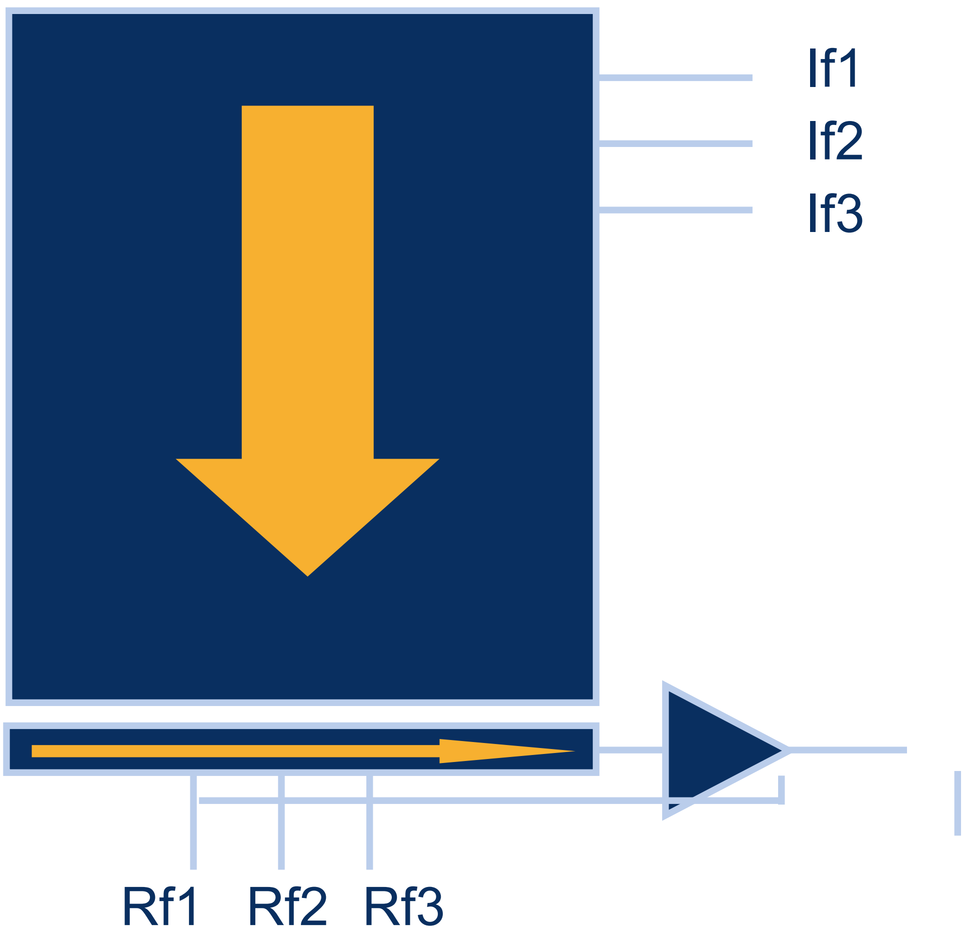

Basic CCD Structure

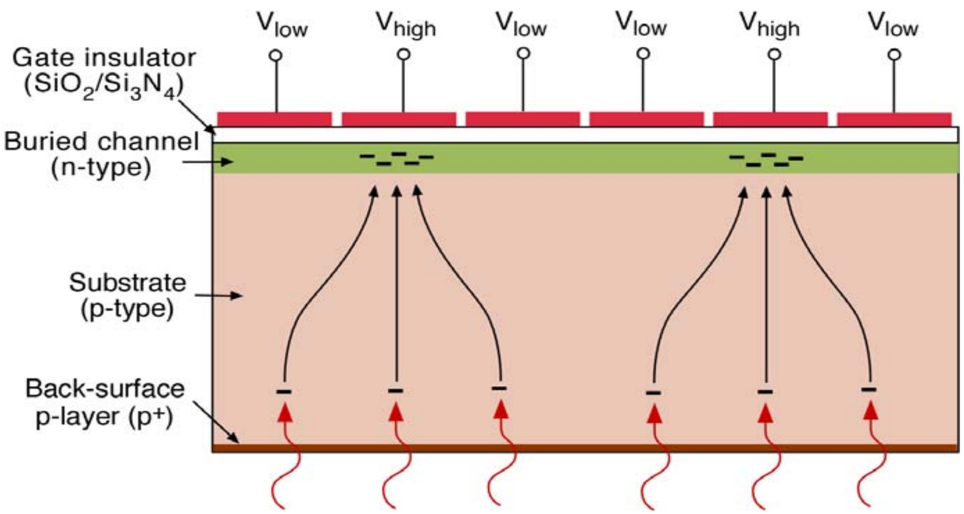

View along charge-transfer direction

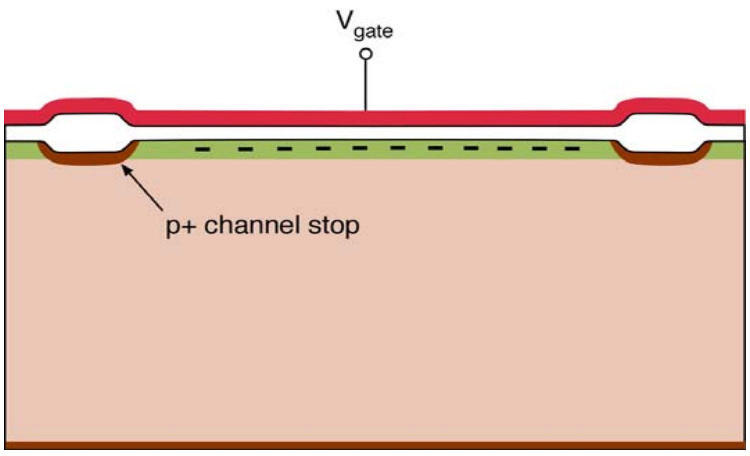

View across CCD channel

Effects of Partial Depletion

- Full depletion essential for minimal charge spreading (high MTF)
- Methods to ensure full depletion
  - » Thin device
  - » High-resistivity substrate
  - » High clock voltages
  - » Bias back-surface p^+ negative

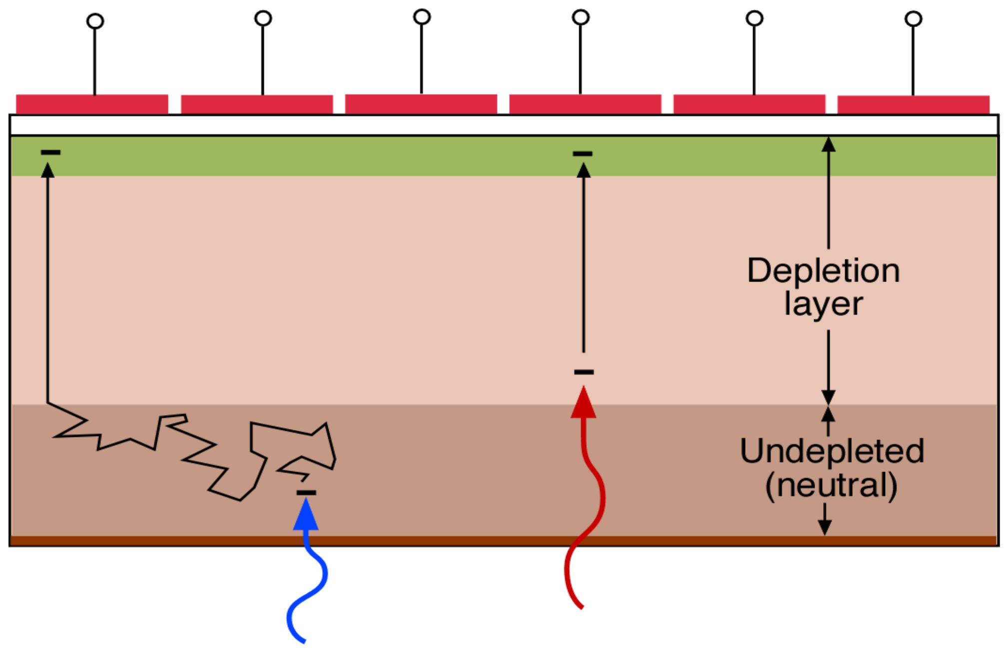

QE- fully depleted, very thick devices

20-100 ohm-cm Si is usually thinned to 10-16 um

Use 1500 or 10,000 ohm-cm for deeper depletion, and thicker devices

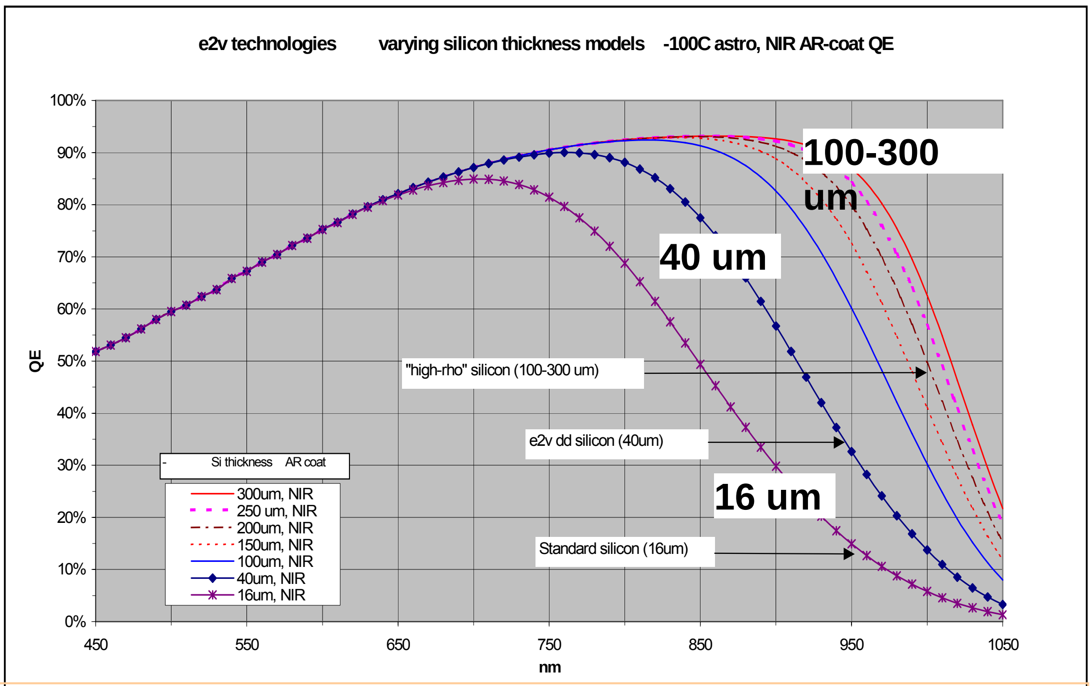

Spectral response for differing silicon thickness

LBNL QE measurements (Lick), from Bebek et al SPIE 5167. 280 um thick CCD at –130C

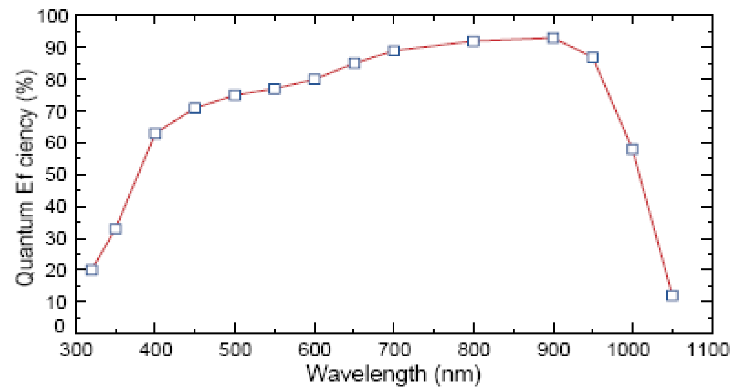

Considerations

Red wavelength fringes reduce for thicker devices.

Cosmic ray collection increases for thick devices

Large undepleted depth increases PSF

Examples of CCD detectors systems

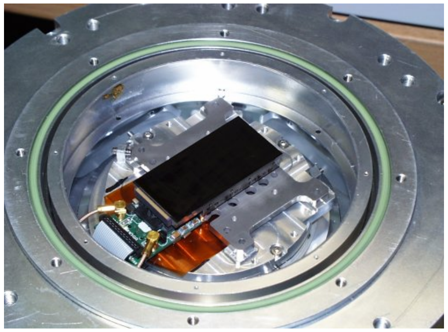

Single E2V
2kx4k CCD

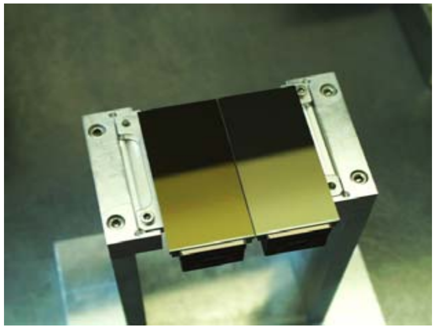

Mosaic of two
E2V 2kx4k CCD

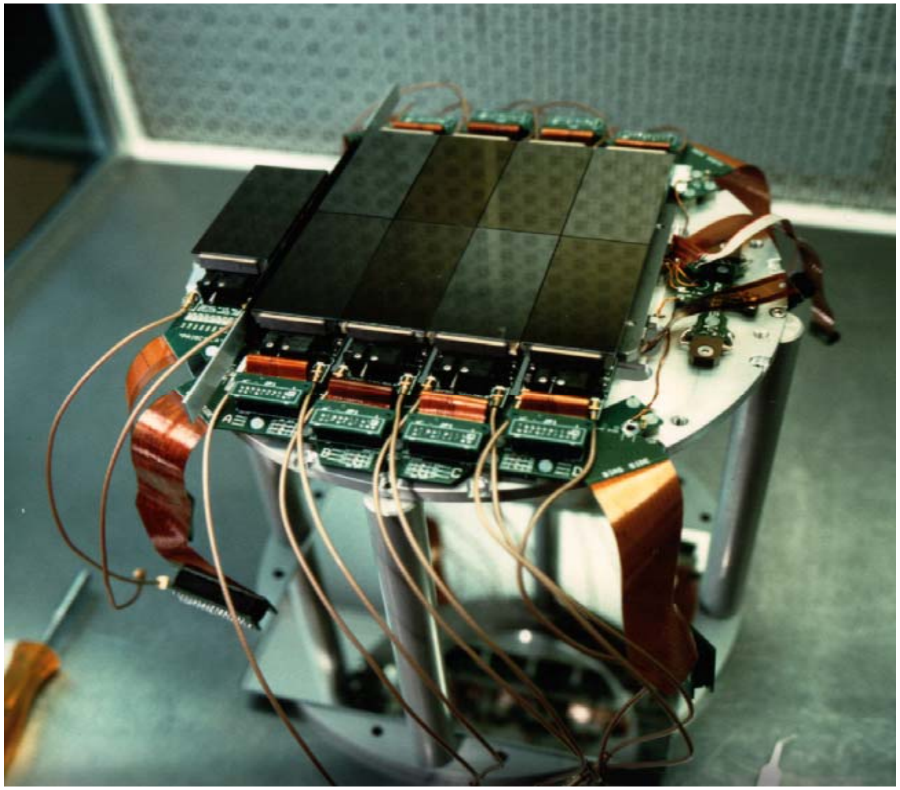

Wide Field Imager
8k x 8k mosaic, 72 million pixels

OmegaCAM detector mosaic

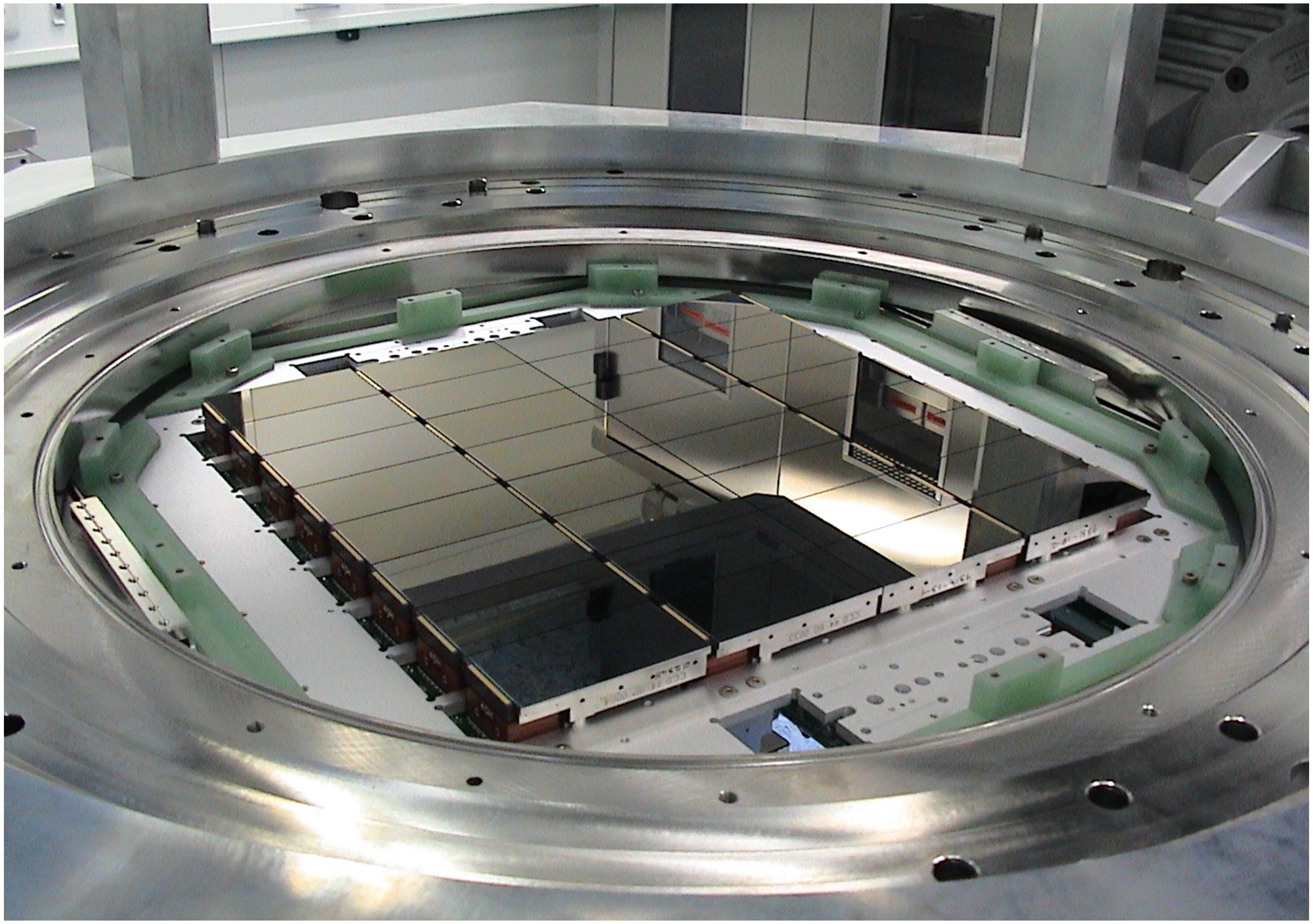

32 CCDs - 16 x 16 k - 1x1° FOV + 4 tracker - **288** million pixels !

Readout noise

Readout noise (with QE) is a key factor in determining signal/noise

Low noise floor is essential- needs small node. Two stage outputs are usual to provide adequate drive capability

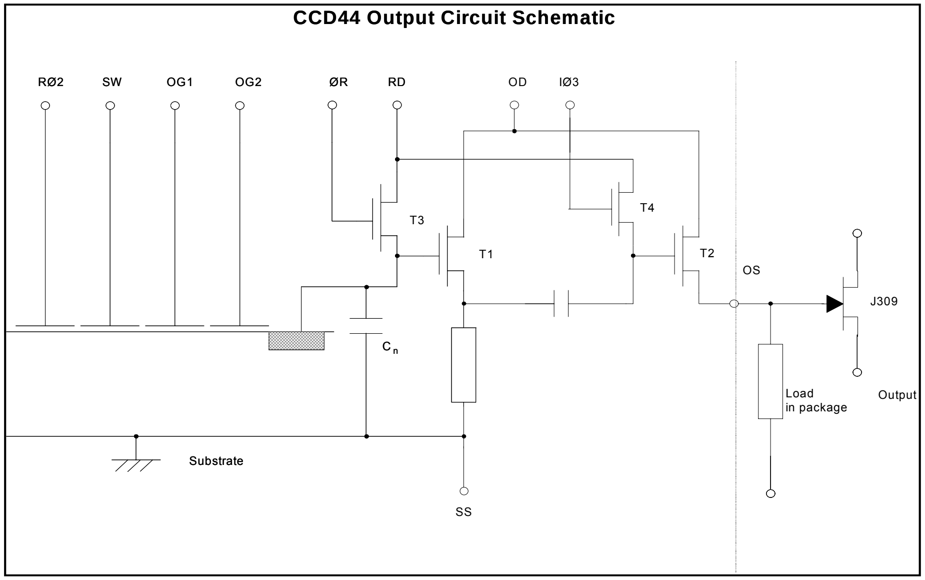

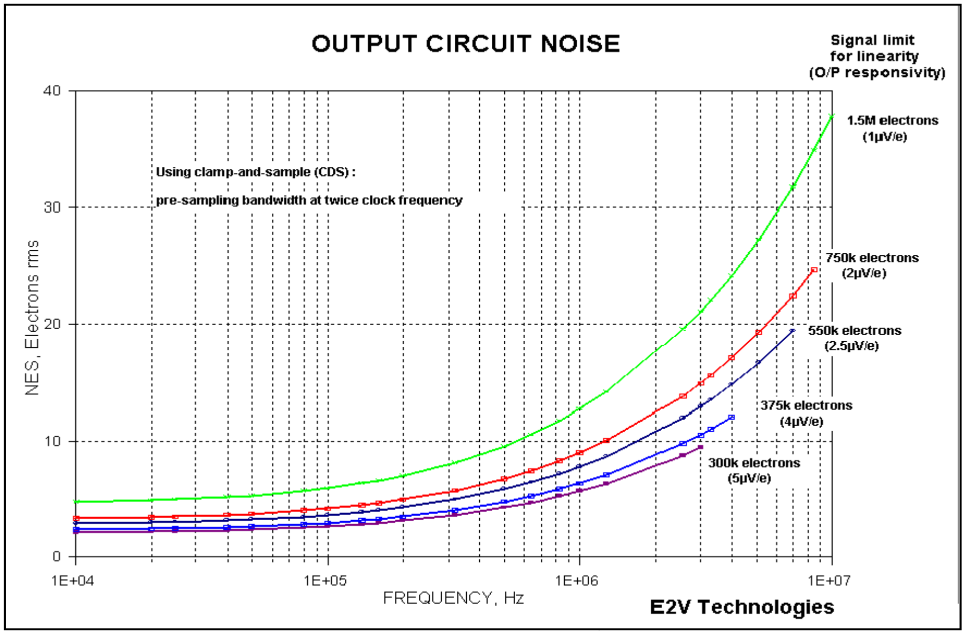

L3Vision CCD

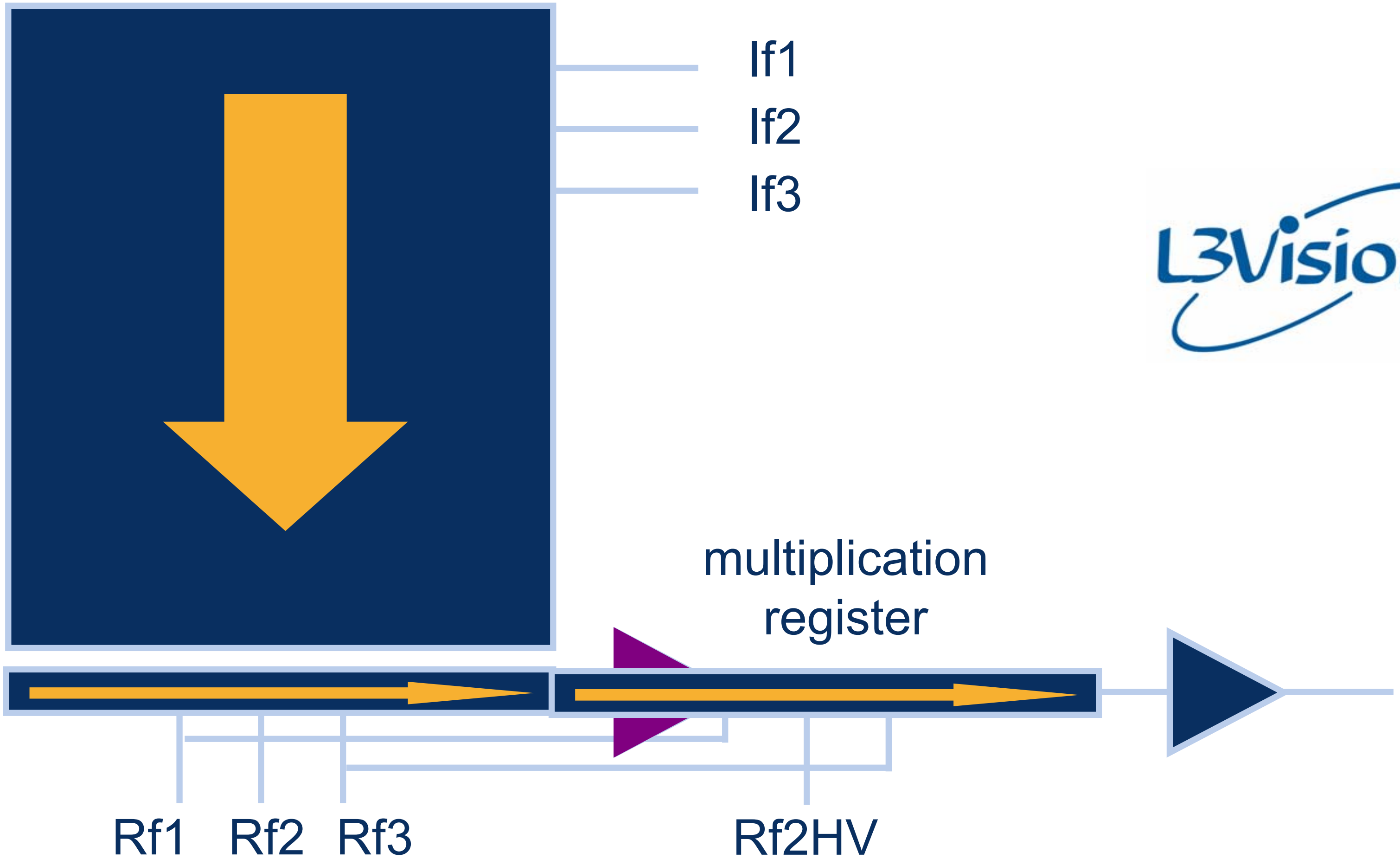

L3Vision technology

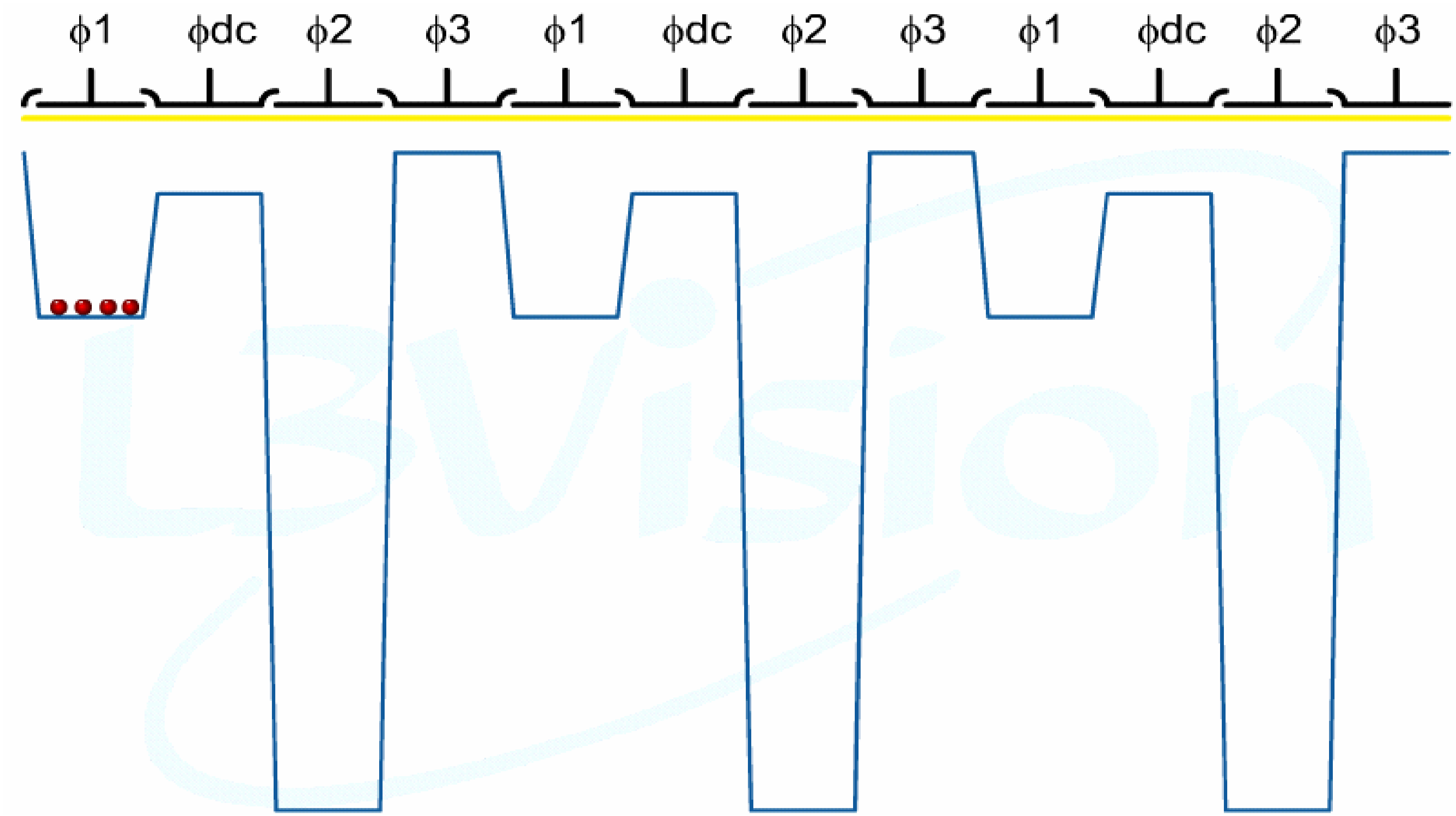

Sub-electron readout noise CCD (electron multiplication)

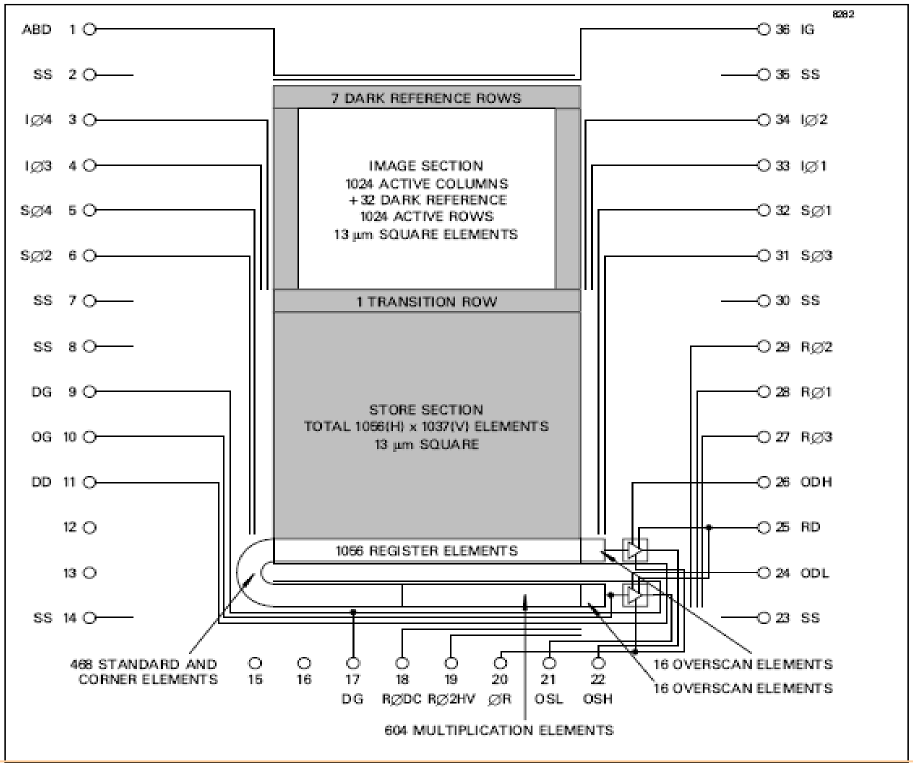

Example of avalanche-gain architecture (e2v CCD65)

•Scientific CCDs normally have readout noise floors of 2-5 e- rms.

•Avalanche gain technology (electron multiplication) allows sub-electron read-noise.

•**Several important considerations:**

•Cooling to suppress dark current becomes very important

•Good control of operating temperature and HV-clock level are important for gain stability

•Noise statistics are non-Gaussian resulting from the stochastic gain process

L3Vision

8 output WFS CCD. See Downing et al, SDW2005

Conventional vs. Orthogonal-Transfer CCDs

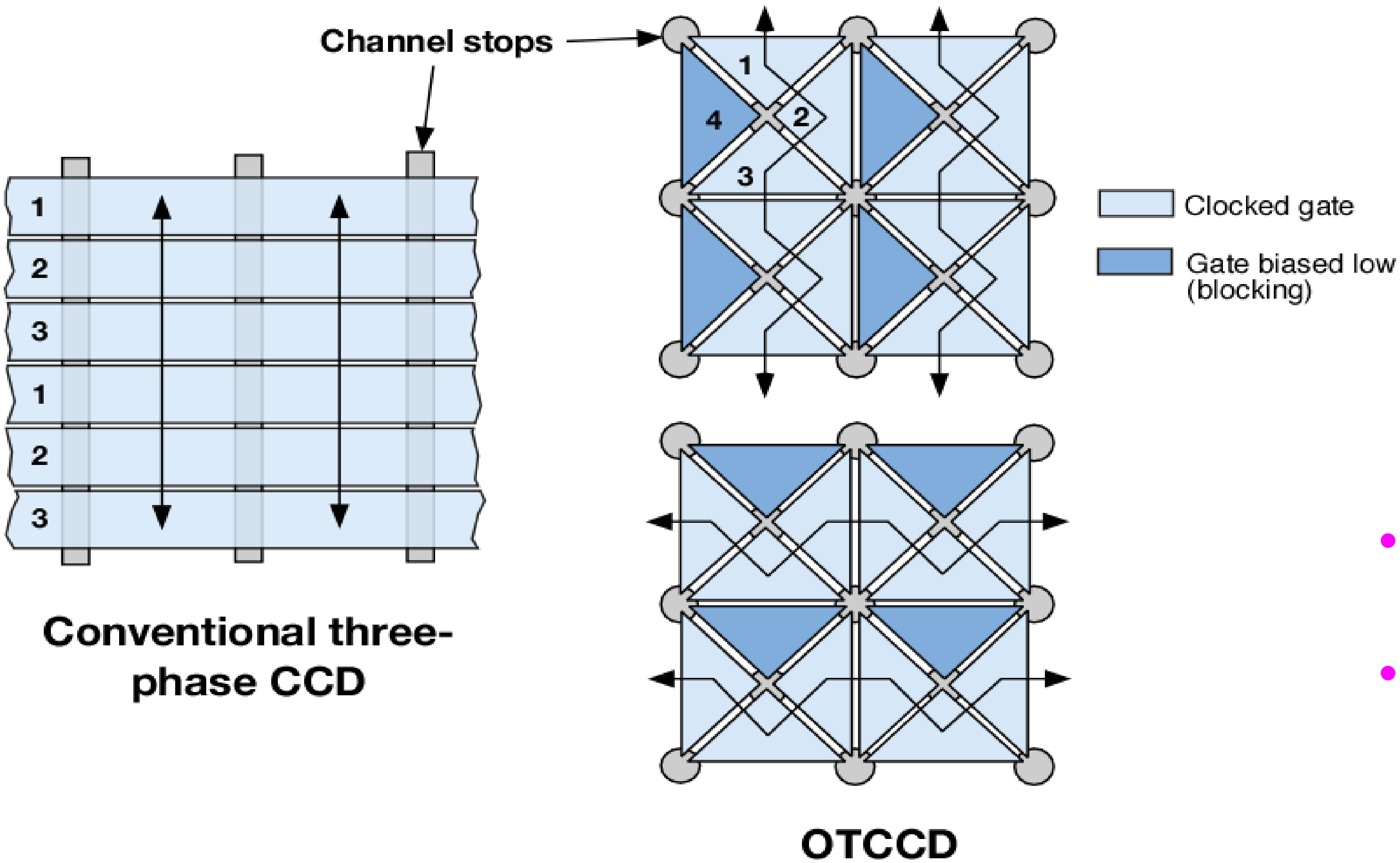

- Move charge in both x and y
- Follow tip-tilt motion of object

SI-PIN/Visible hybrid device architecture

Main difference:
SI-PIN array is a fully depleted bulk detector

IR array is a per pixel depleted detector.

Properties of SI-PIN arrays:
- 100 % fill factor
- High electric field strength (Vsub ~10 Volts)
- Lower integrating node capacity than IR detectors => lower noise
- Fully depleted bulk => good QE
- All features of the Hawaii2RG multiplexer can be used

Silicon Hybrid Architecture (backside illumination)

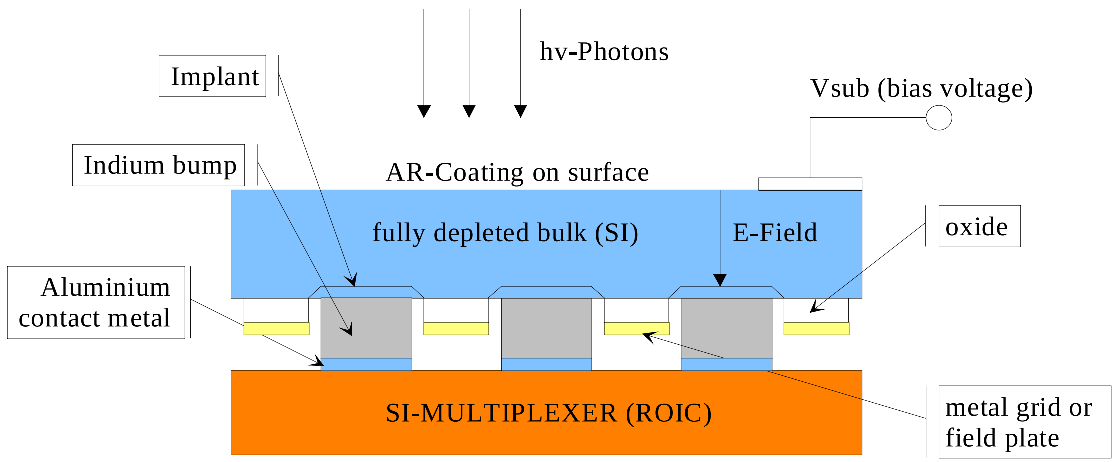

Note that Hybrids differ substantially from monolithic CMOS where photon detection and readout take place in the same piece of silicon.

HyViSI quantum efficiency

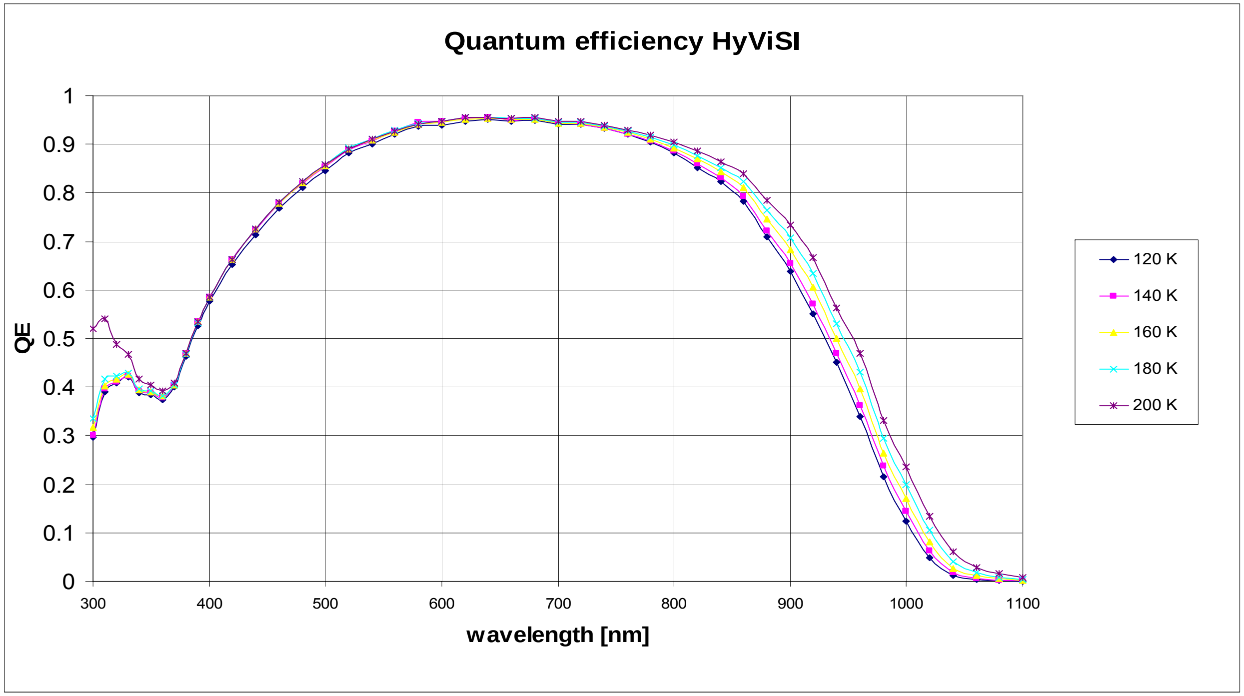

In the past the Quantum efficiency measurements have been interpreted wrong due to the overestimation of the nodal capacity (conversion factor).

Now measured data fits well to modeled values from Rockwell.

In the near IR the QE depends on operating temperature. As the temperature get lower, the photon absorption length increases (bigger Si bandgap).

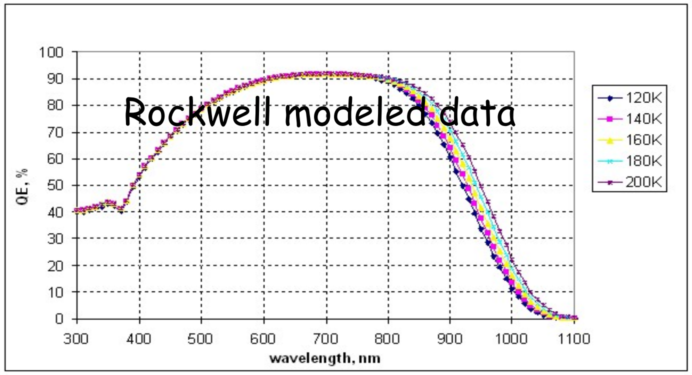

Principle of CMOS Sensors operating in capacitive discharge mode

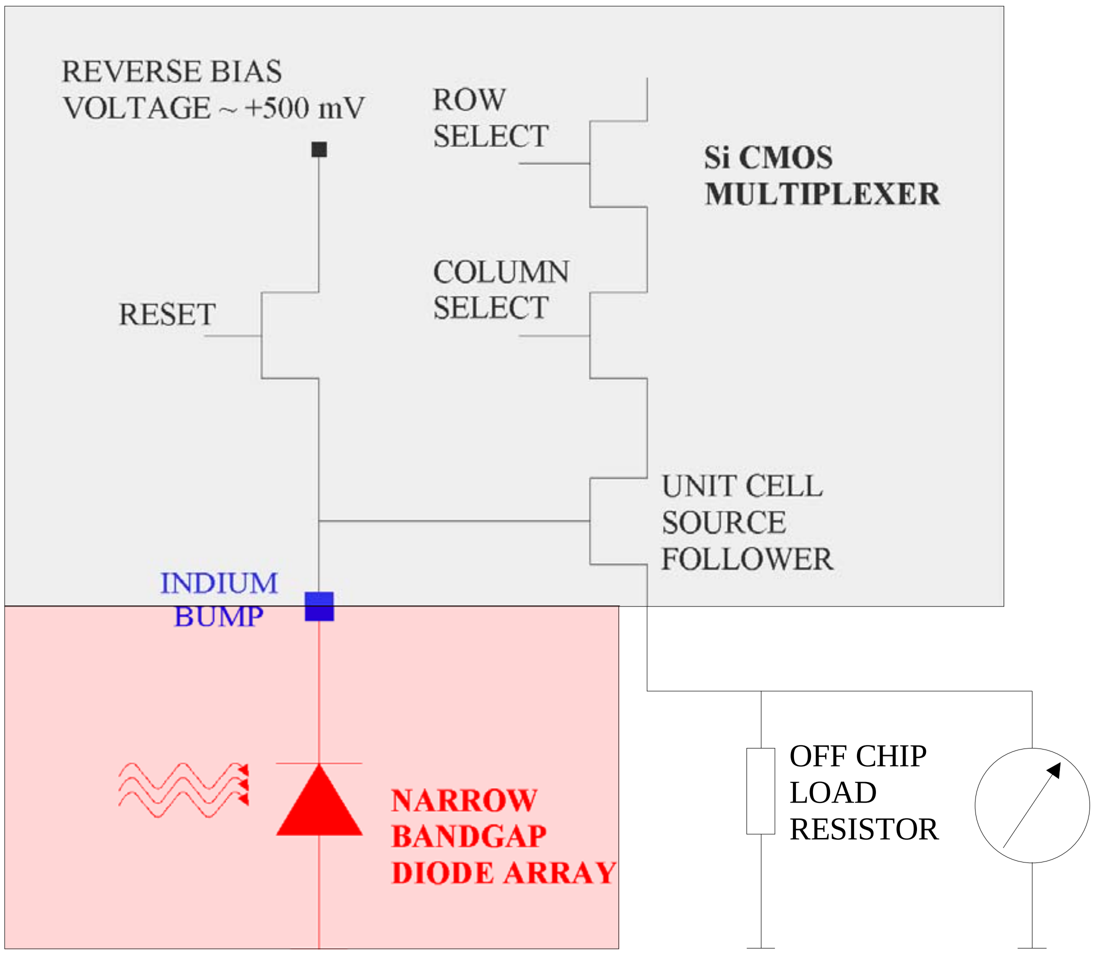

Structure:

- Silicon readout multiplexer
- Narrow band-gap infrared diode array
- Hybridization with In bumps

Operation:

- charge diode capacity by reverse bias voltage
- floating capacity is discharged by absorbed photons
- Read voltage across diode capacity several times during integration by addressing unit cell source follower

comparison Si-PIN COMOS / CCD

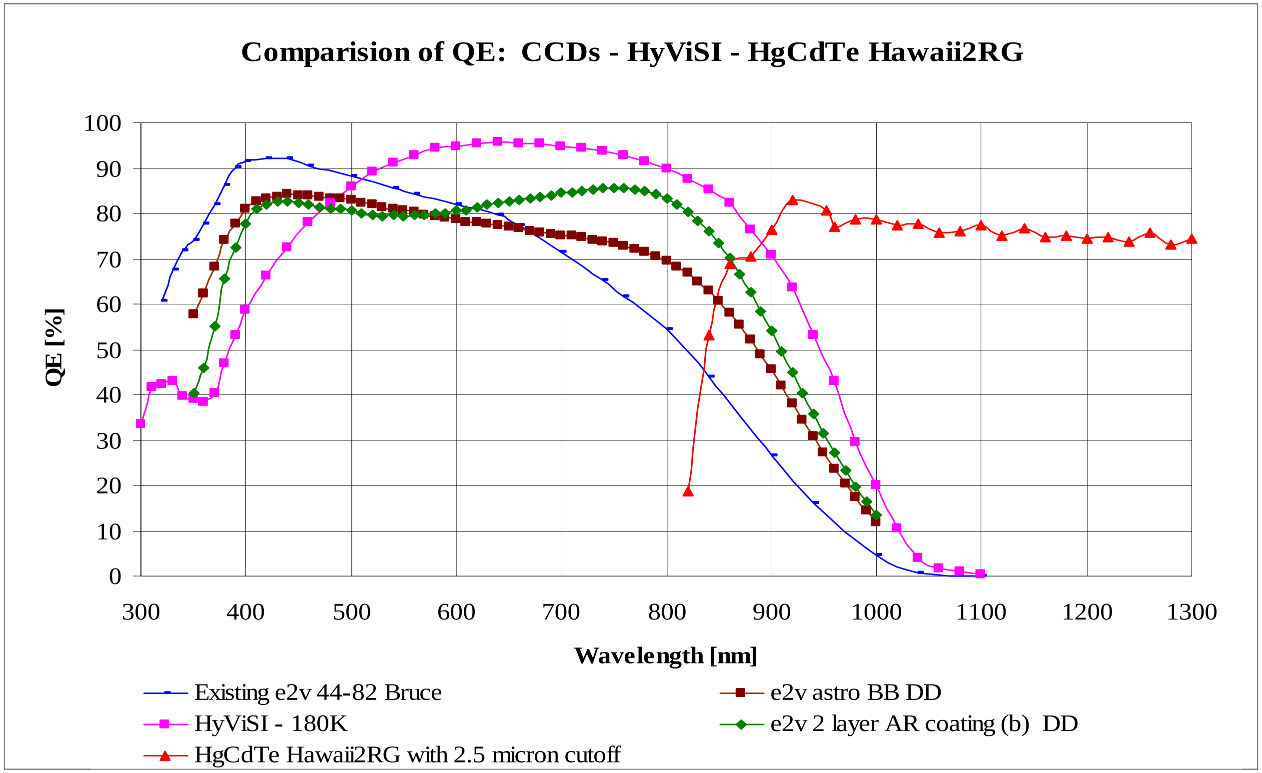

The HyViSI detector outperforms all CCDs above 500 nm and shows a higher overall QE compared to the CCDs.

The e2v astro is a curve provided by e2v for a broad band deep depletion device.

The green curve the QE for a 2 layer AR coating of the deep depletion CCD.

The blue curve is the QE of the CCD currently installed in Giraffe at the VLT.

Red curve is a IR Hawaii2RG HgCdTe detector

Noise reduction by multiple nondestructive readouts

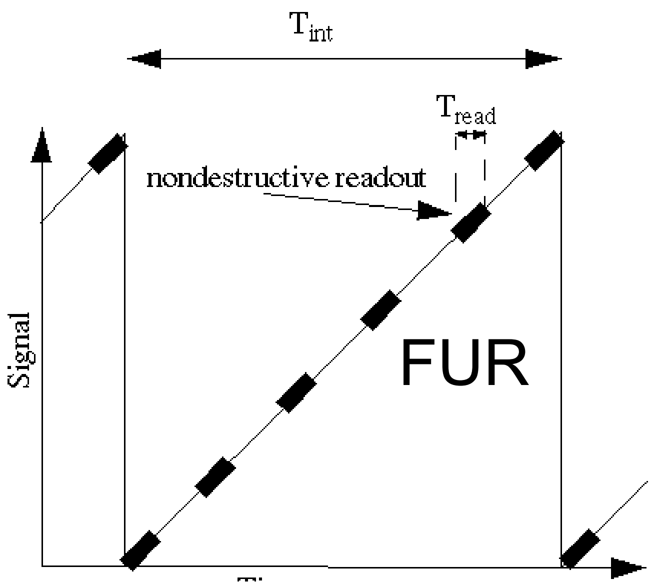

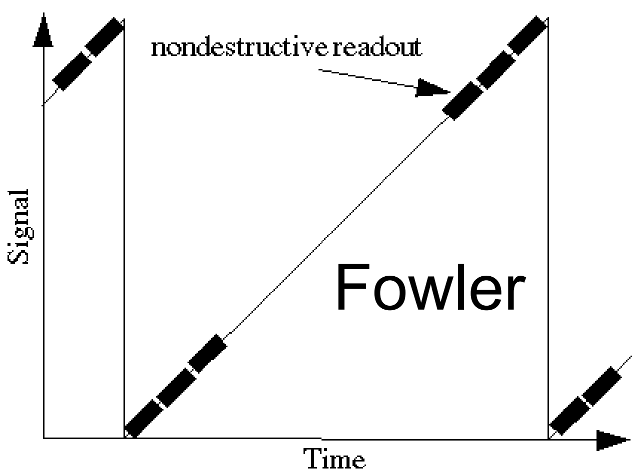

- Multiple readouts of array possible without disturbing ongoing integration : nondestructive readout
- Follow-up-the-ramp sampling (FUR):
  at equidistant time intervals nondestructive readouts
  least squares fit: slope of integration ramp

$$SNR_{FUR} = SNR_{DC}\sqrt{\frac{n(n+1)}{6(n-1)}}$$

- Fowler sampling:
  nondestructive readouts at start and at end of ramp
  least squares fit: slope of integration ramp
  for n>>1:

$$SNR_{Fowler} = SNR_{DC}\sqrt{\frac{n}{2}} \cong SNR_{FUR}\sqrt{3} \Leftrightarrow T_{int} >> nT_{Read}$$

Si-PIN COMOS detectors

- Noise <2erms at T<115K with multiple sampling
  but >6erms at T>140K
- CMOS devices are dc-coupled: require low 1/f noise
- Dark current 10 e/hour at T<140K (CCD < 1 e/hour)
- Interpixel crosstalk 10 % due to capacitive coupling between pixels

ADVANTAGES OF CMOS detectors

- No CTE degradation and reduced “blooming” for bright objects
- No shutter required and less power consumption
- Advanced features of Hawaii2RG multiplexer with Si-PIN (i.e. fast reads, guide mode feature, non destructive readout modes , common readout electronics with IR arrays etc., ASIC)
- Performance of Si-PIN CMOS arrays will improve

Low Frequency Noise Infrared / CCD

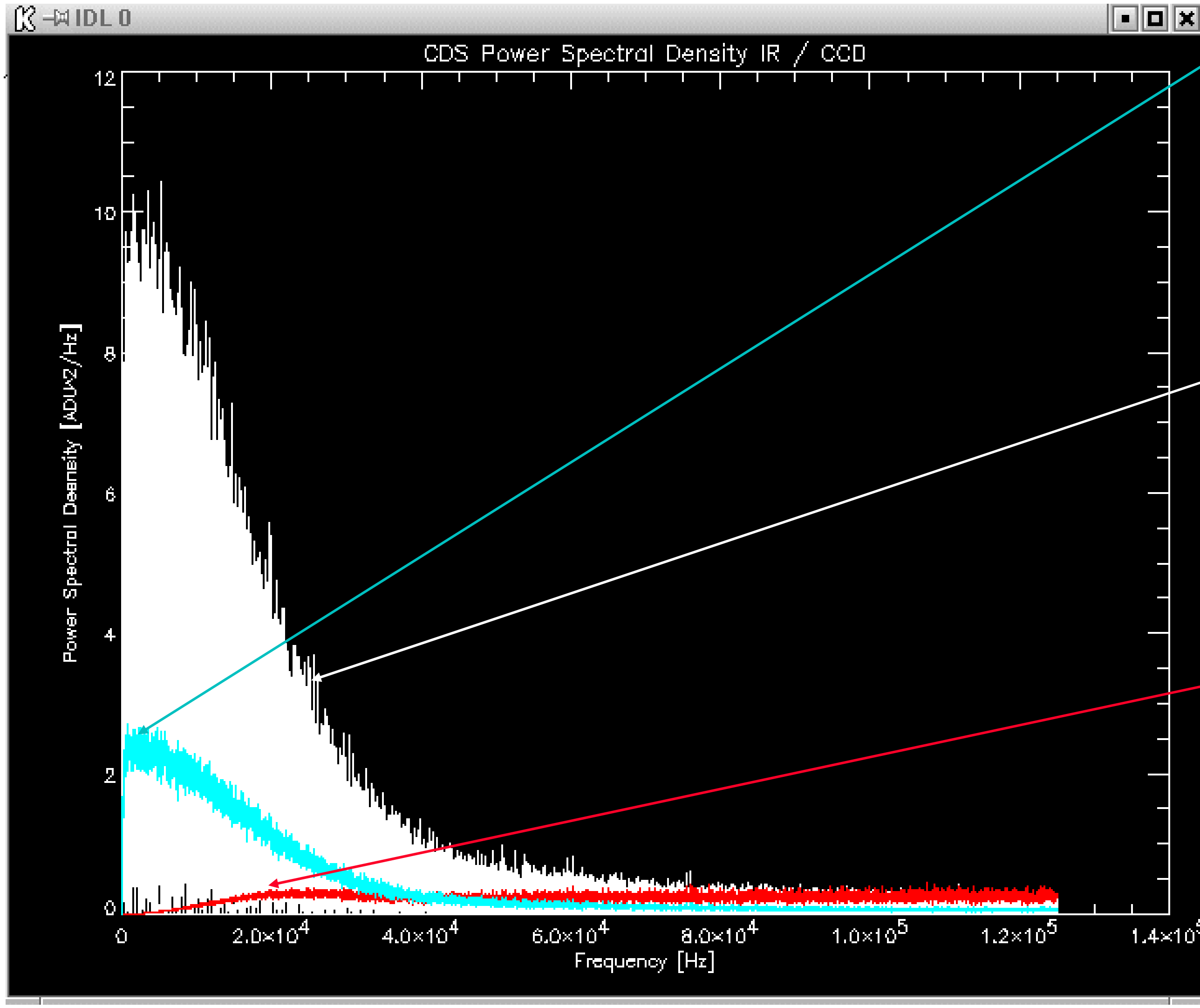

- Blue curve:
  power spectral density of
  Picnic 256x256 MBE
- $|N_{CDS}|^2=|N_{DET}|^{2*} \ |H_{CDS}|^2$
  $|H_{CDS}|^2=[2-2\cos(2\pi f t_s)]$
- White Curve Infrared:
  dc coupled
  t_s = 1 sec (can be >1000s)
  fully sensitive to
  1/f noise and 50 Hz
- Red curve CCD
  $t_s = 4 \ \mu sec$
  no 1/f noise and 50Hz
- subtract low frequency
  noise by reference cell

comparison Si-PIN COMOS / CCD

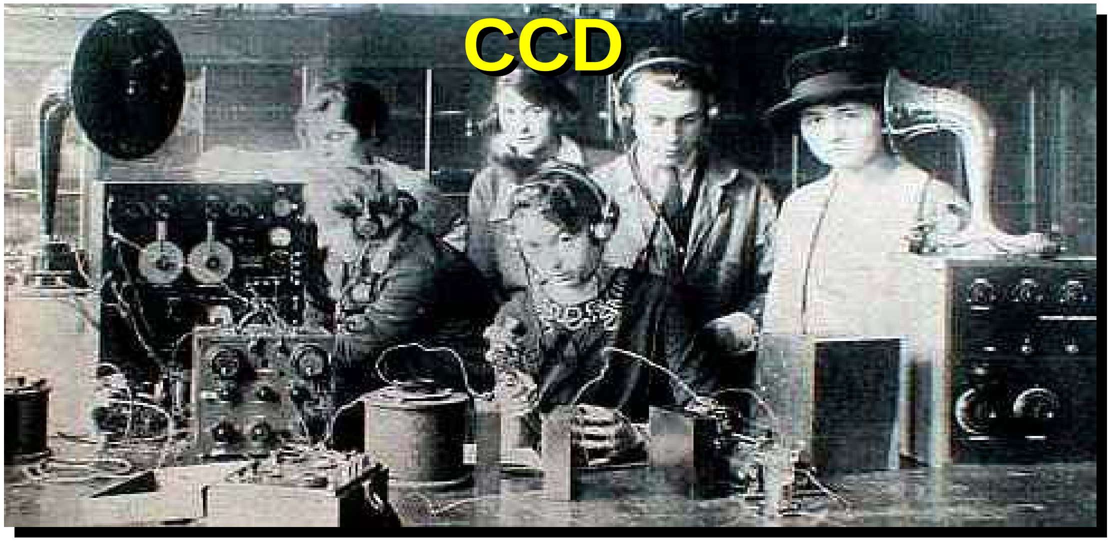

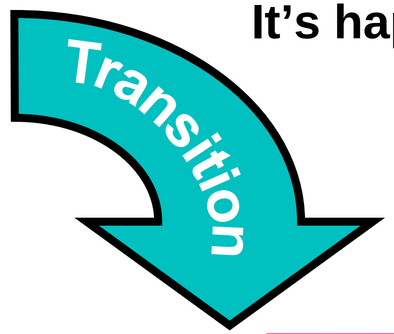

It's happening!

Intrinsic infrared photon detectors

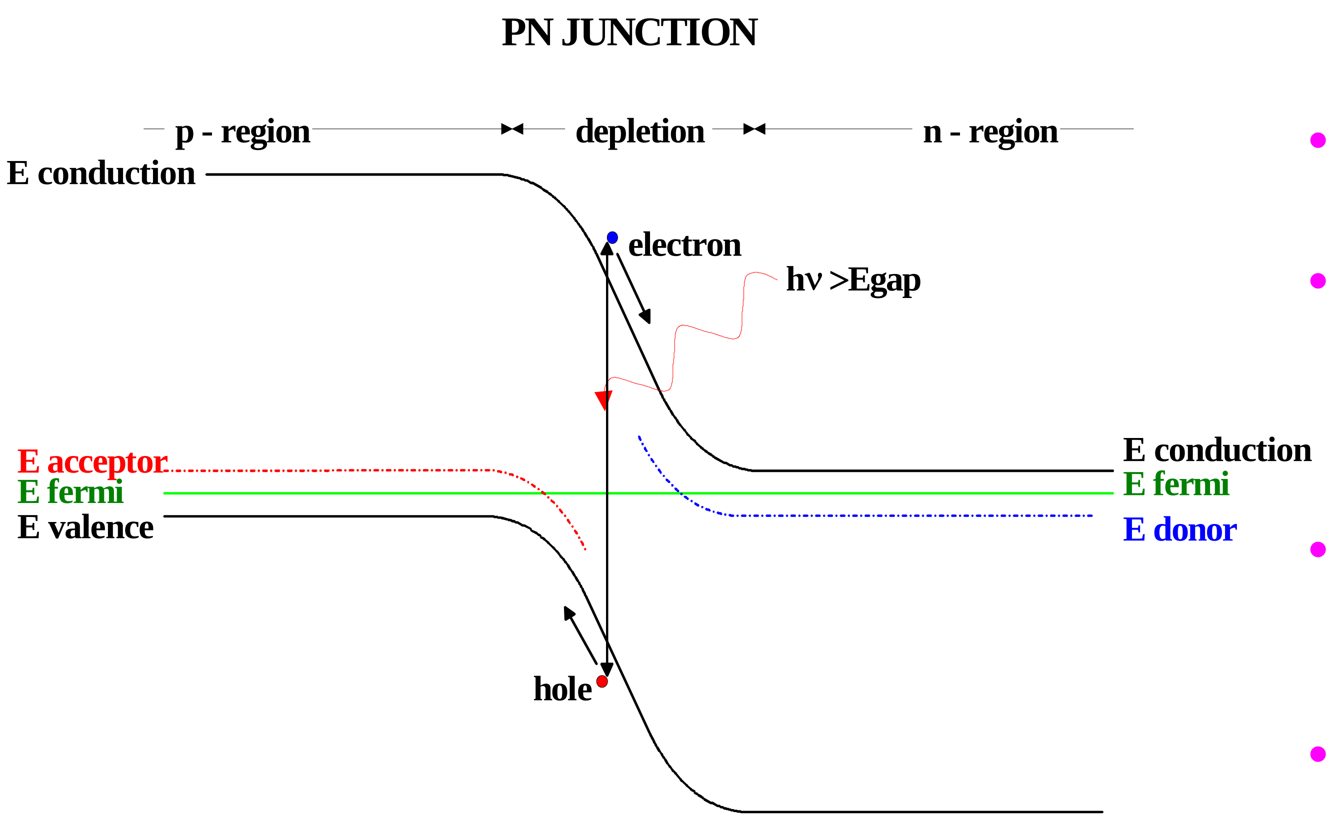

- Absorbed photon generates transition from valence to conduction band
- Si bandgap 1.12 eV
  $\Rightarrow \lambda_c \sim 1\ \mu m$
- for intrinsic infrared photon detectors at $\lambda > 1\ \mu m$ narrow bandgap semiconductor required
- $Hg_{(1-x)}Cd_xTe$
  tuneable with x
  $\lambda_c = 1.7 - 14\ \mu m$
- InSb
  $\lambda_c = 5.2\ \mu m$

Infrared hybrid arrays

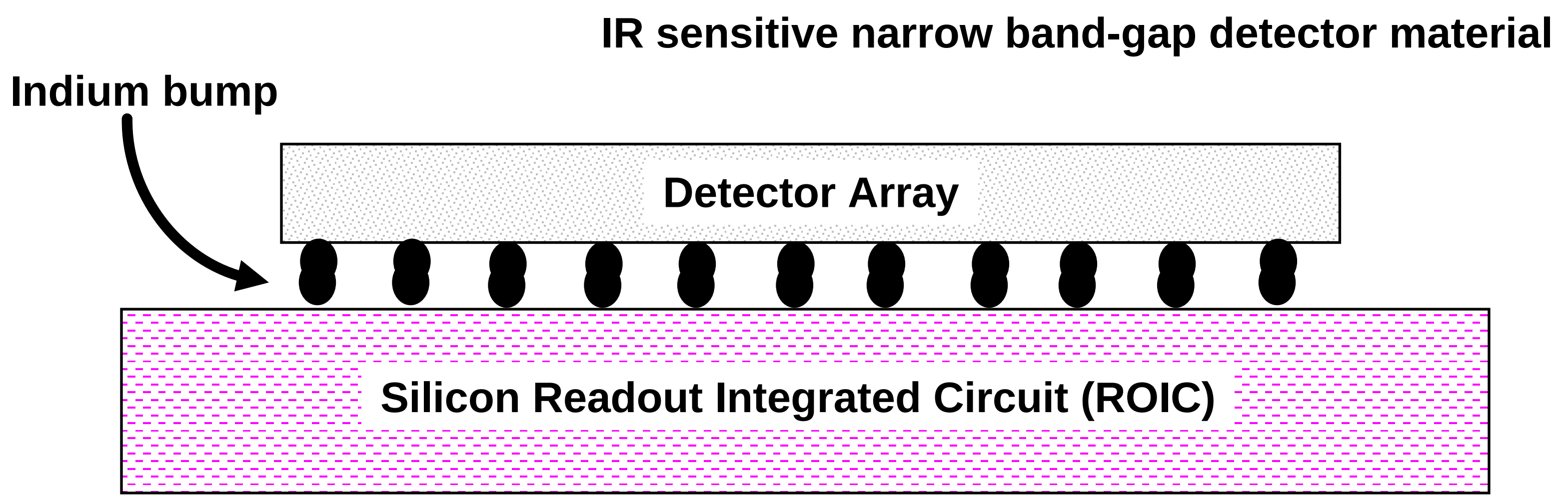

Hybrid focal plane array structure of LPE HgCdTe (PACE)

ROCKWELL SCIENTIFIC

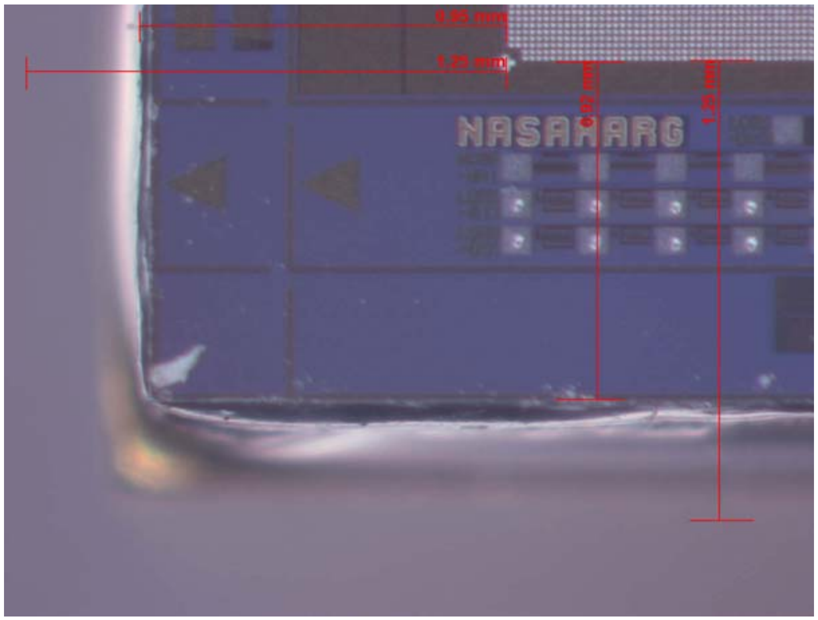

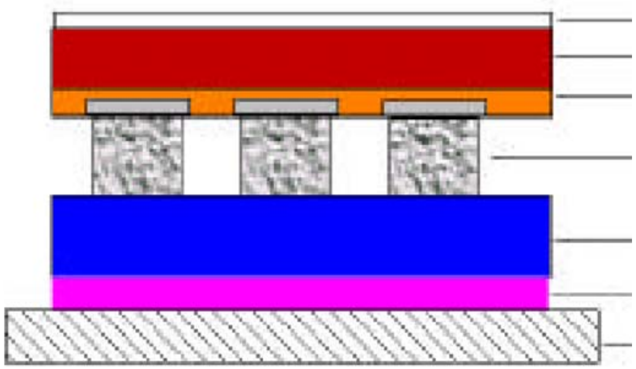

- Sapphire substrate
- CdTe buffer layer
- Liquid phase epitaxy grown HgCdTe
- Implant boron ions to form n-on-p junctions
- Passivate surface with ZnS
- In bumps
- Si mux
- Balanced composite structure to minimize thermal stress

Input circuit schematics

SFD

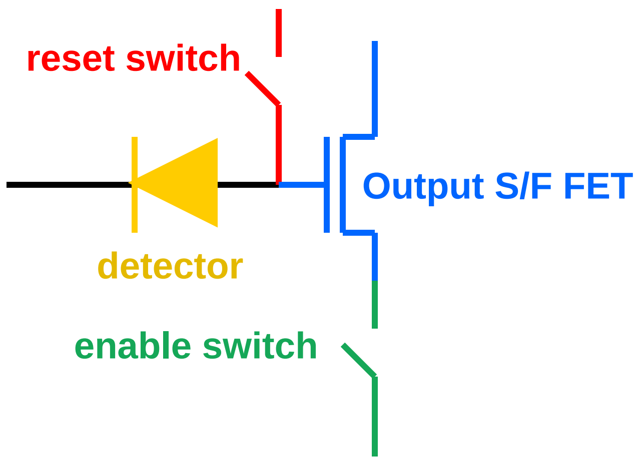

Low flux

Low noise

CTIA

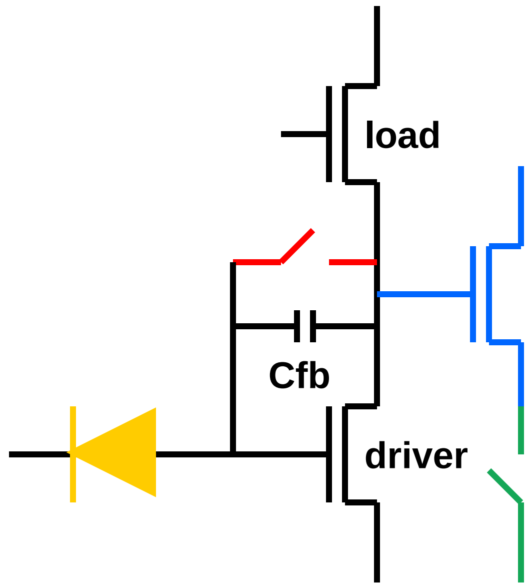

High speed

Low noise

DI

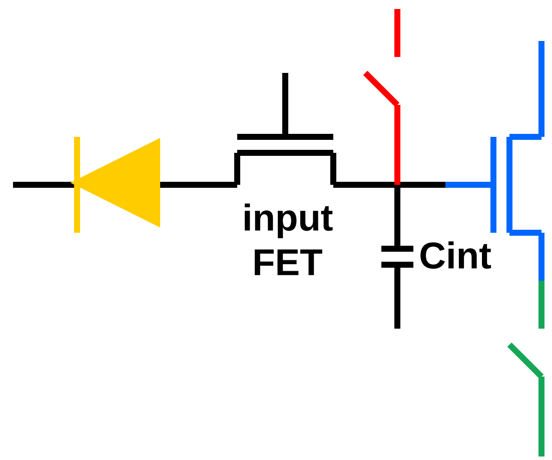

High flux

Thermal infrared

Temperature and Wavelengths of Detector Materials

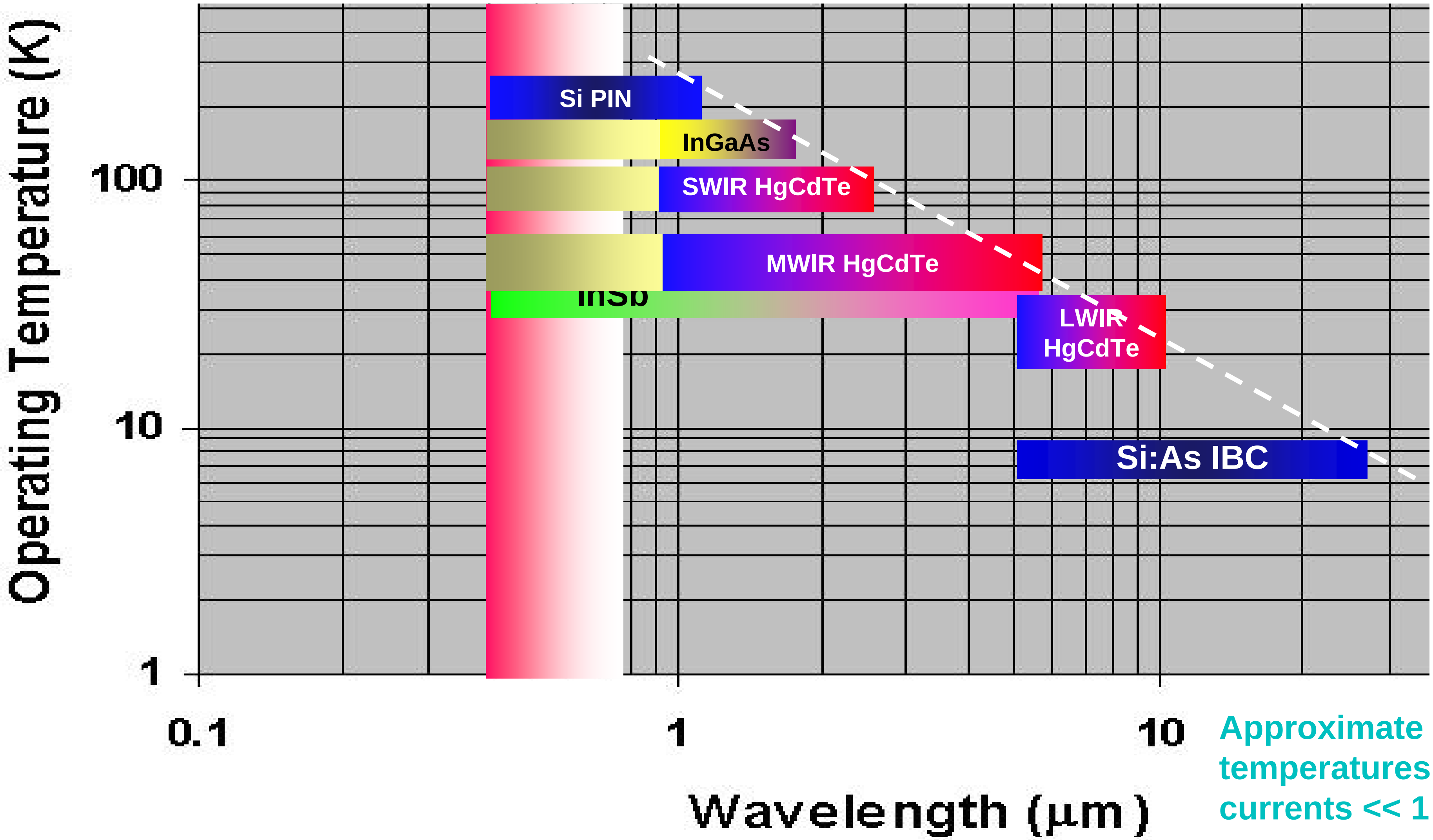

Approximate detector temperatures for dark currents << 1 e-/sec

Extrinsic infrared photon detectors

BIB Detector Energy Band Diagram

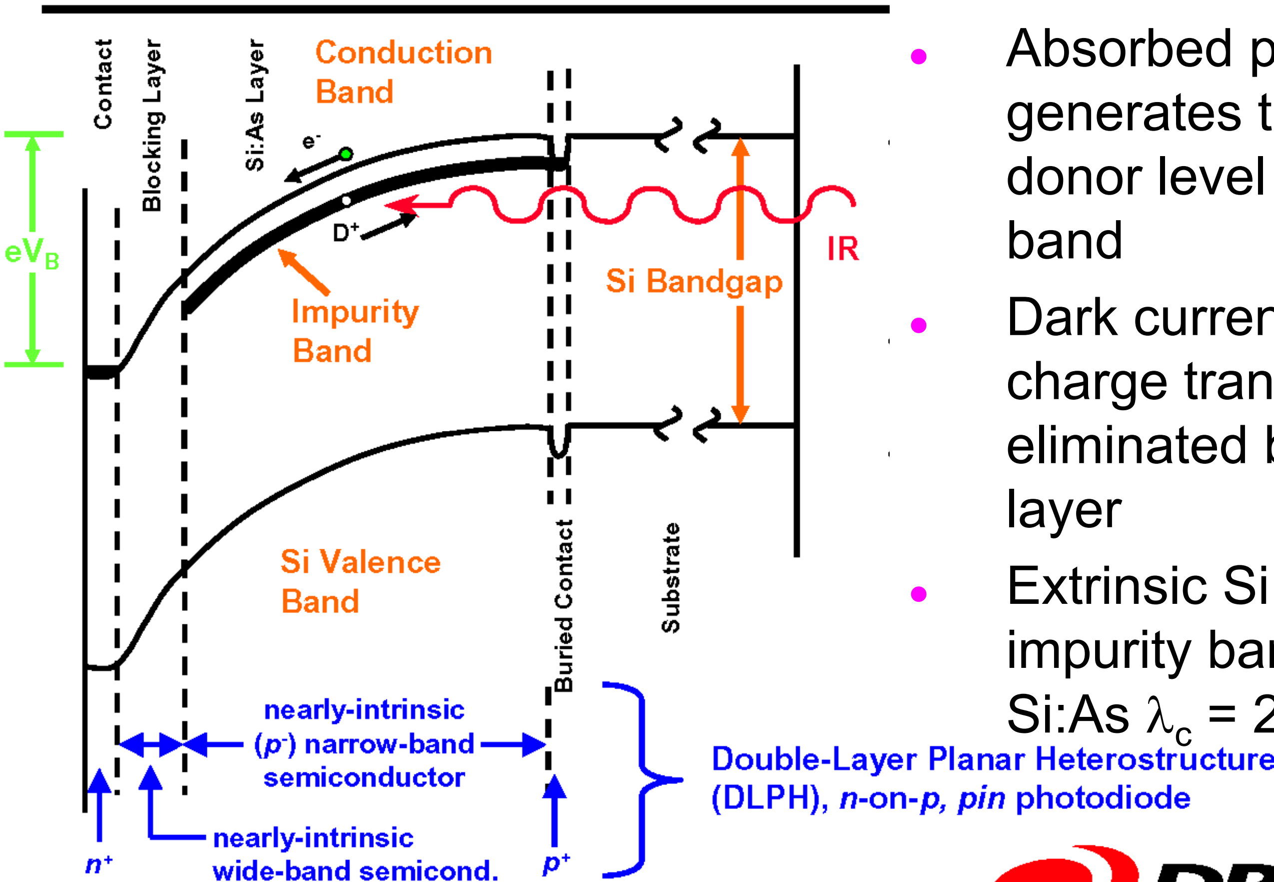

- Absorbed photon generates transition form donor level to conduction band
- Dark current from D+ charge transport eliminated by blocking layer
- Extrinsic Si blocked impurity band for LWIR Si:As λ_c = 28 μm

DRS TECHNOLOGIES

Atmospheric radiance

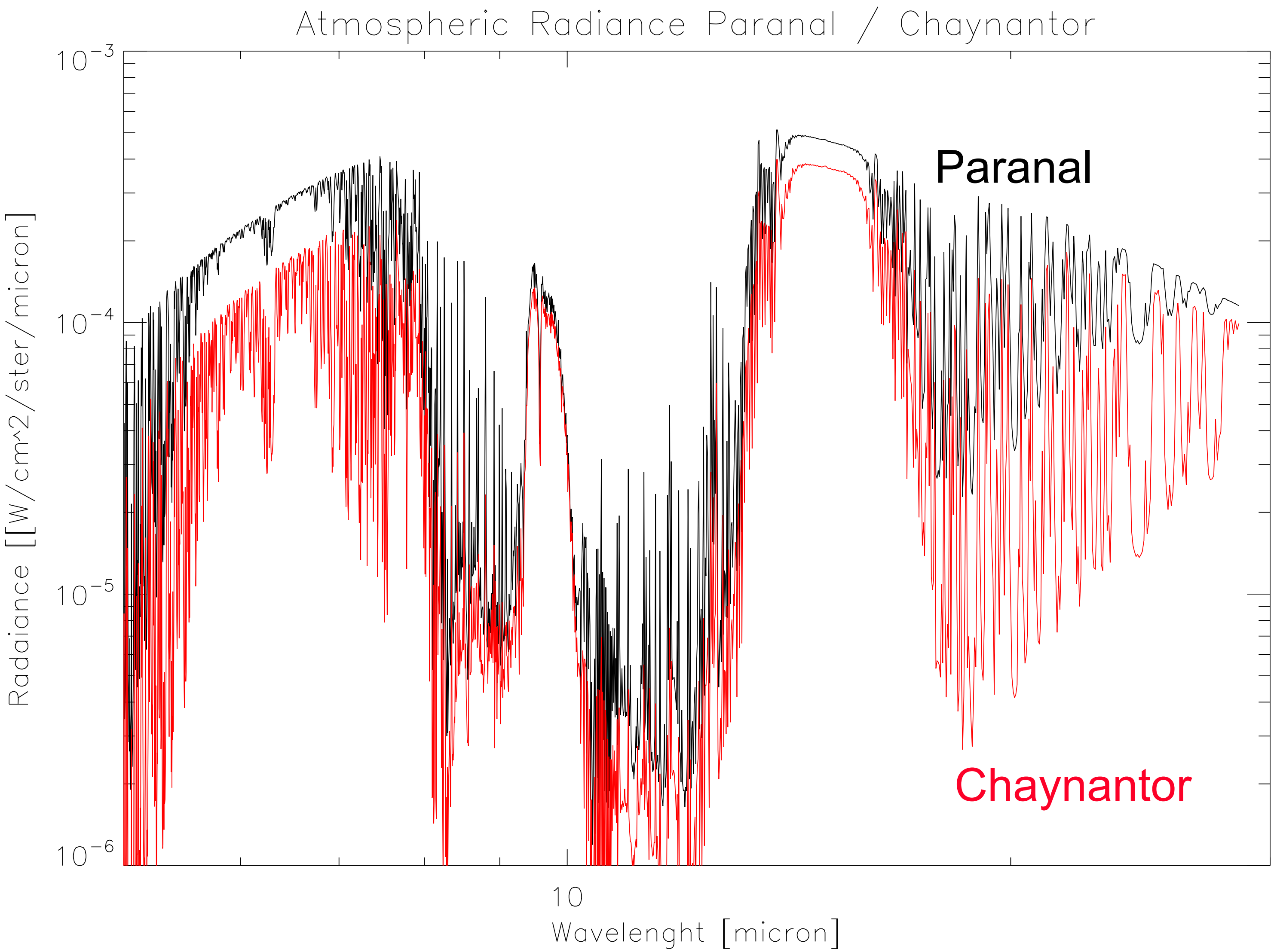

- Modtran
- US standard atmosphere
- Water vapor profile subarctic winter
- Zenith angle 0 degree
- Paranal 2600m
- Chaynantor 5000m

Floorplan for Aquarius 1024 x 1024 Readout

- Bond pads on top and bottom of chip
  - » Multiple chips can be close-butted side by side
- Row shift register structure:
  - » Top half of array reads out top-to-bottom
  - » Bottom half of array reads out bottom-to-top
  - » Windowing reduces number of rows read for increased frame rate
- Column shift register structure:
  - » 16 or 64 outputs (selectable)
    - – 8 or 32 outputs on each half of array
  - » Each output reads out a block of pixels
    - – 16 output mode:
      Each block is 128 columns wide x 512 rows tall
    - – 64 output mode:
      Each block is 32 columns wide x 512 rows tall

8 or 32 outputs (selectable)

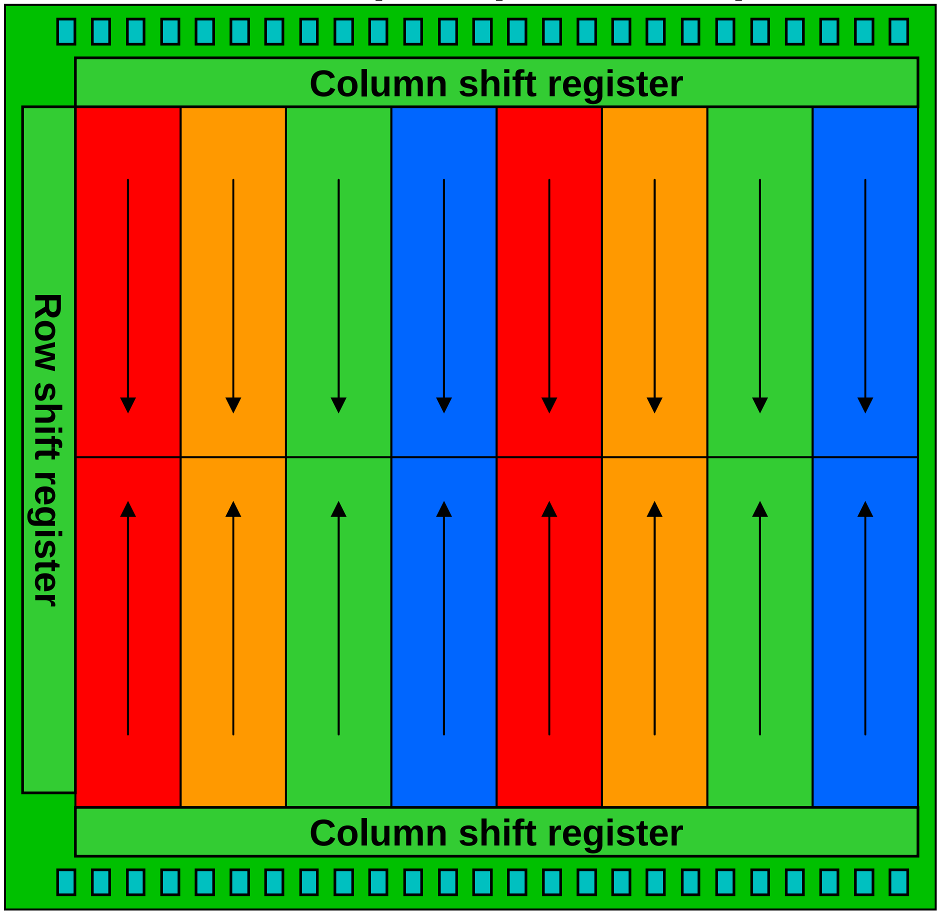

8 or 32 outputs (selectable)

Aquarius basic specs

- Format 1Kx1K
- Pixel pitch 30 μm
- Number of outputs 64
- Maximum frame rate:150 Hz
- Storage capacity switchable 1.5E7 e-
  (imaging)
  and 1E6 (spectroscopy)
- Frame rate 150 Hz
- Readout noise < 200 erms with multiple
  sampling

Limitations of Array Format

- With reticle-stiching of submicron masks readout multiplexer size is scalable to any large format

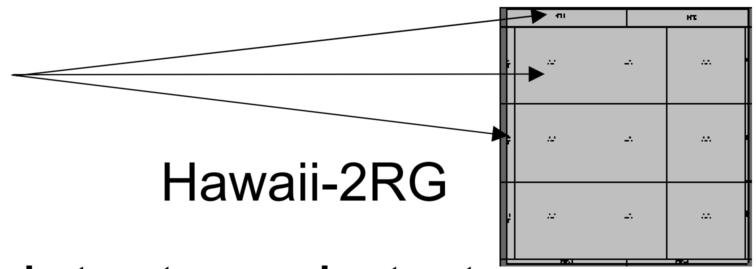

Hawaii-2RG

- Detector array size limited by the size of detector substrates
  - » InSb 2Kx2K , 4Kx4K under development
  - » HgCdTe
    - – CdZnTe (6 cm x 6 cm substrate) 2Kx2K
    - – Si and Al_2O_3 substrate no limit >4Kx4K performance limited
  - » Si:As : 320 x 240, 1Kx1K under development
- lager formats with mosaics of buttable arrays

InSb mosaic for
Cryogenic Echelle Spectrograph CRIRES

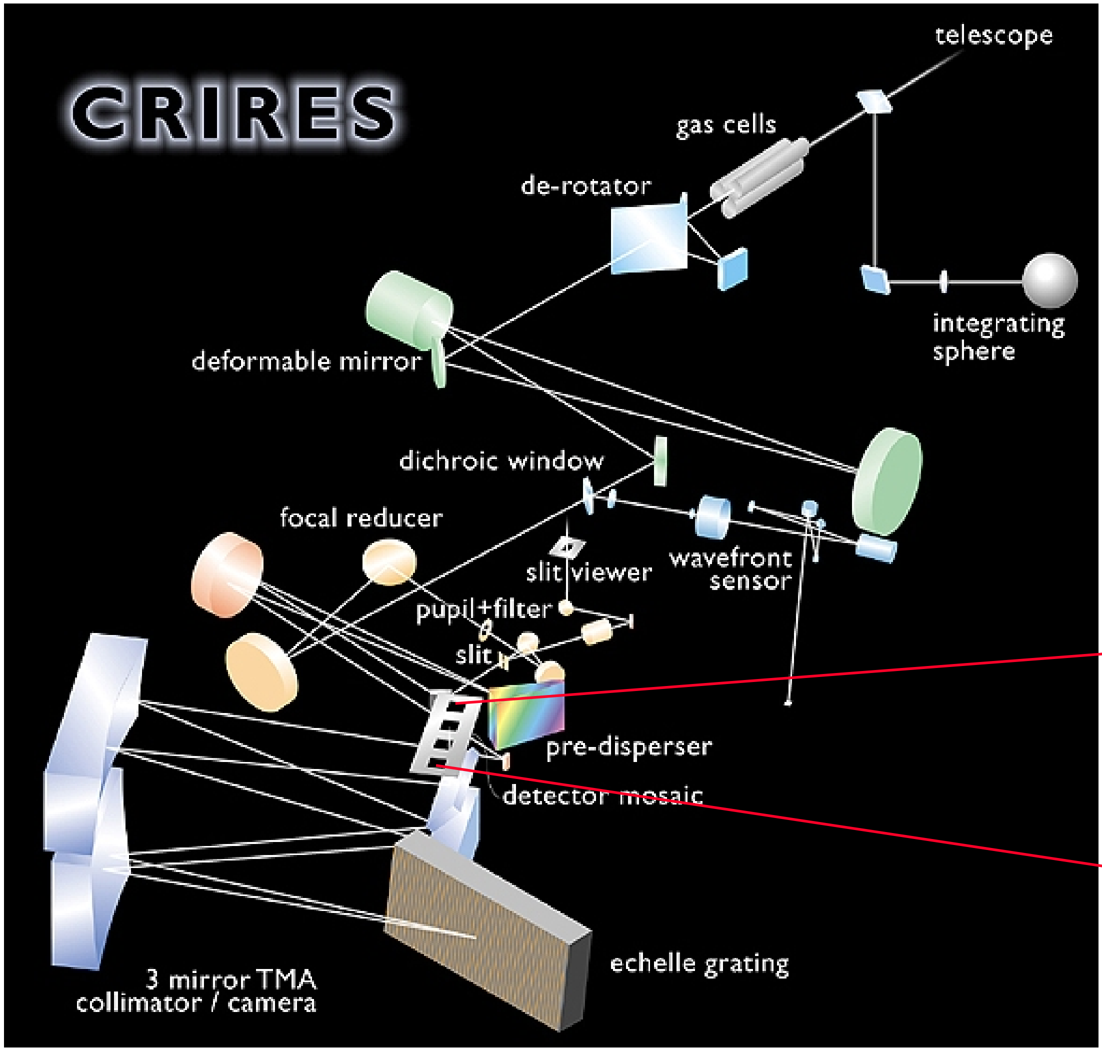

- curvature AO: 0.1 arcsec / pixel
  512 pixels in spatial direction
- High resolution R=100000 echelle
- prism predisperser for order sorting and photon background suppression

Four **Aladdin**1Kx1KInSb arrays

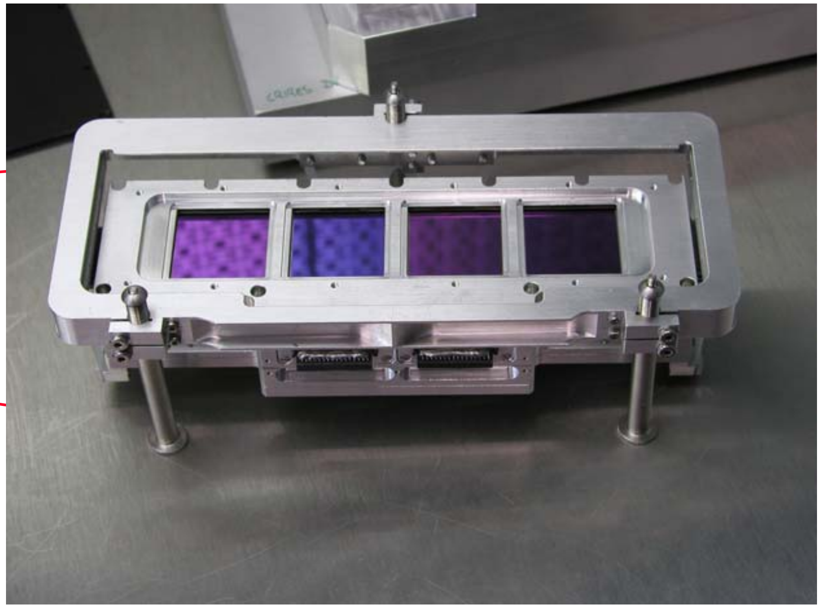

CRIRES Detector setup overview

- AlN multilayer ceramic mother board with Aladdin detector
- 2 layer flexible manganin board to maintain temperature difference between detector (30K) and radiation shield (60K)
- light tight connector at radiation shield to block thermal radiation of cryogenic amplifiers
- flex rigid daughter board with cryogenic amplifiers, bias and clock filters & antistatic protection

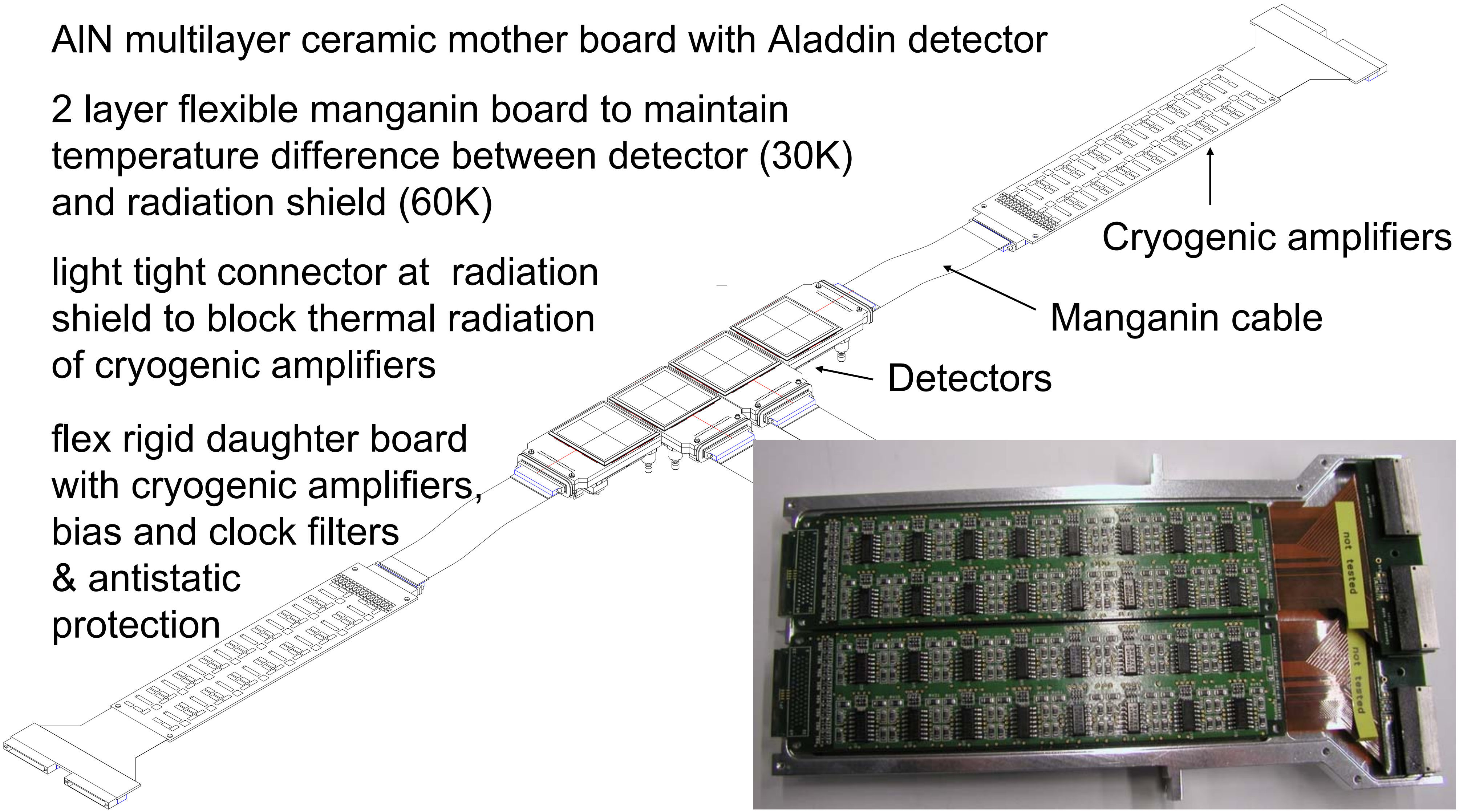

VIRGO 16x2Kx2K HgCdTe mosaic for VISTA

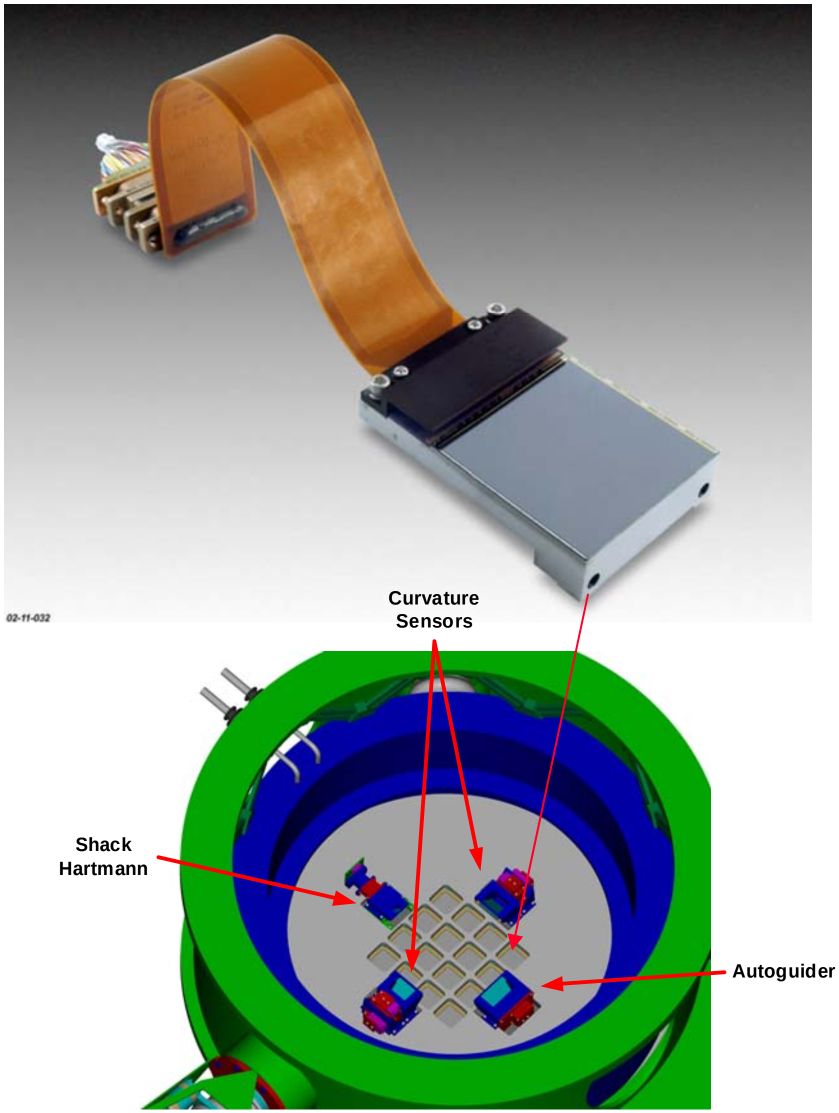

- Built by RAL & UKATC
- HgCdTe grown by LPE on CdZnTe substrate
- Pixel size 20 μm
- 16 parallel outputs
- Pixel rate 400KHz
- Frame rate 1.45 Hz
- 3-side buttable
- Multilayer ceramic mother board on metal pedestal
- Reference cells included in video data stream
- ESO is building 256 channel data acquisition system (IRACE)

VISTA infrared survey camera for VLT

- 4 meter survey telescope for ESO VLT
- Field of view 1.65 degrees
- Pixel scale 0.3 arcsec/pixel
- Wavelength range 1-2.5 μm
- 16x2Kx2K InSb VIRGO arrays

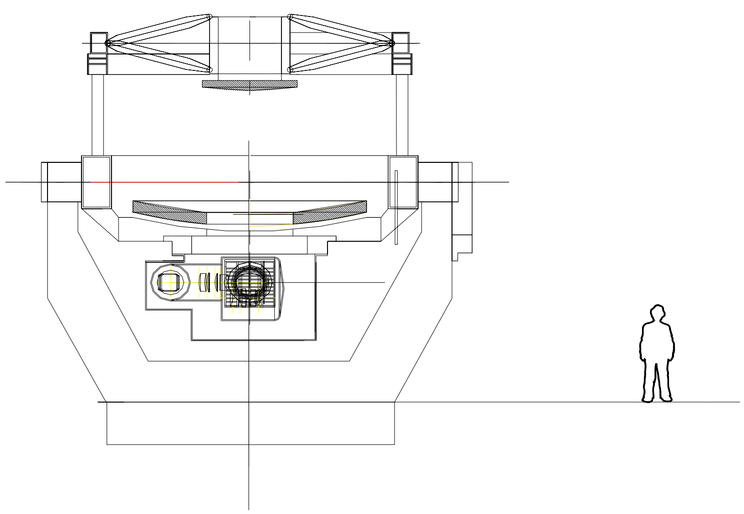

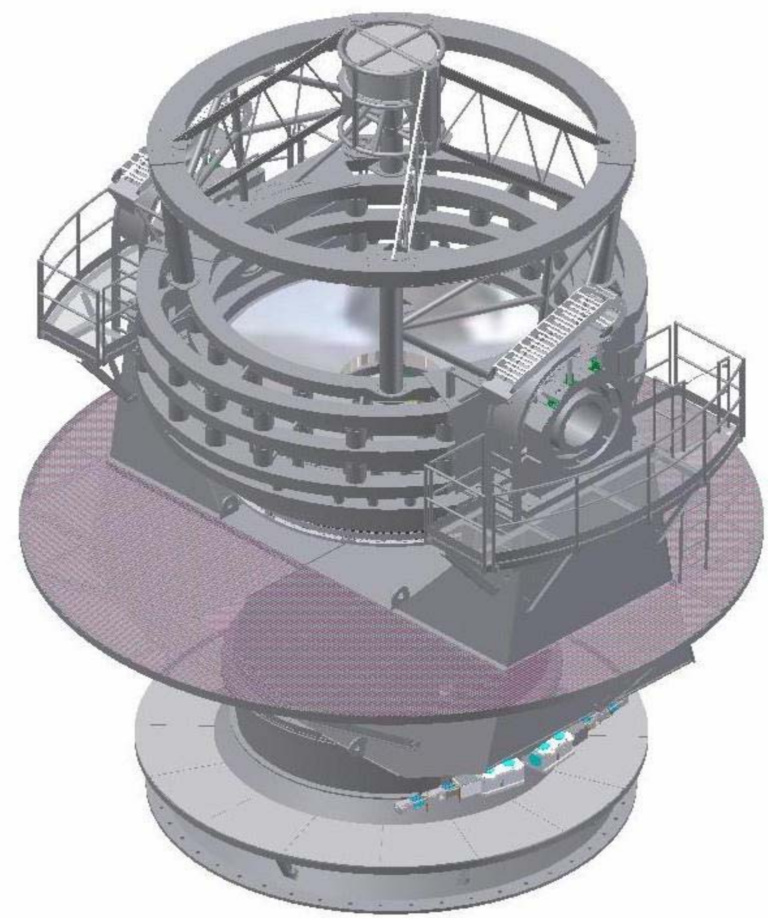

VISTA infrared camera

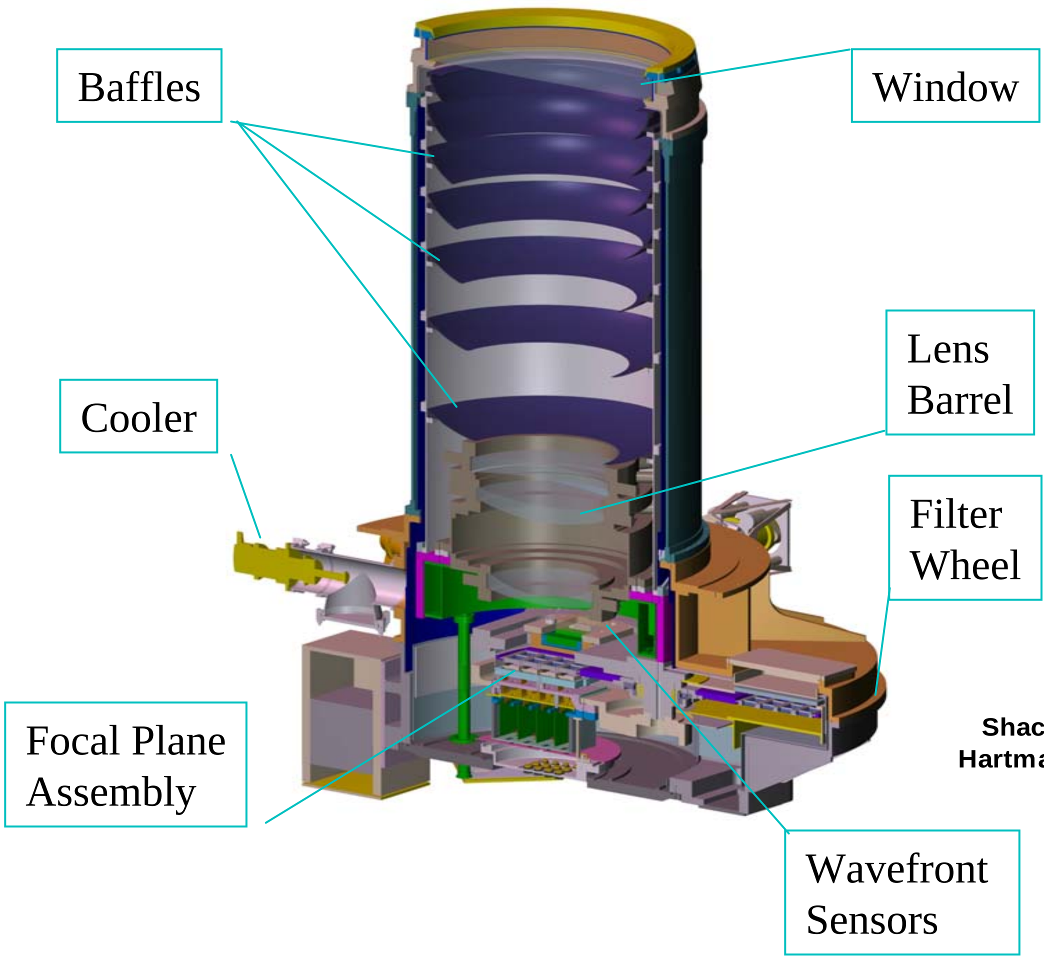

- Cold baffle long-cryostat design without imaging pupil minimizes thermal radiation
- Internal annular baffles to reduce scattering
- Detectors at 90% / 45% spacing

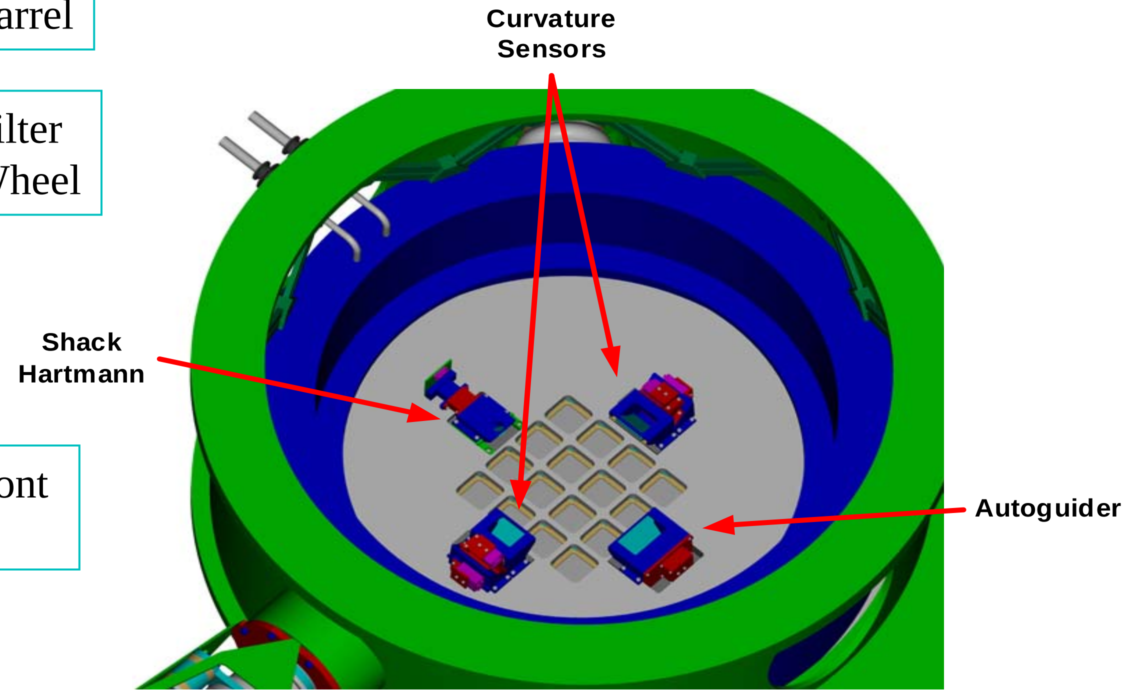

VIRGO 16x2Kx2K HgCdTe mosaic for VISTA

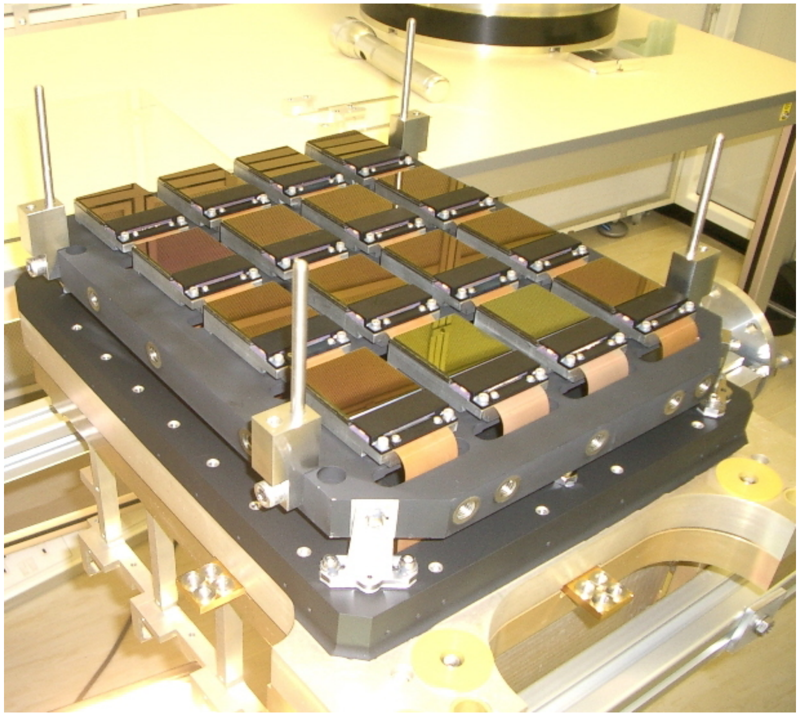

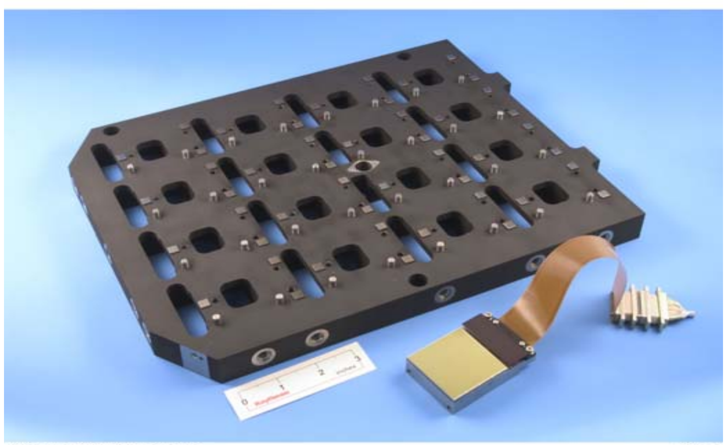

VISTA Mounting Plate, with Module - 3/17/05 05-03-148

Virgo arrays

Flatness $< 25\ \mu m$

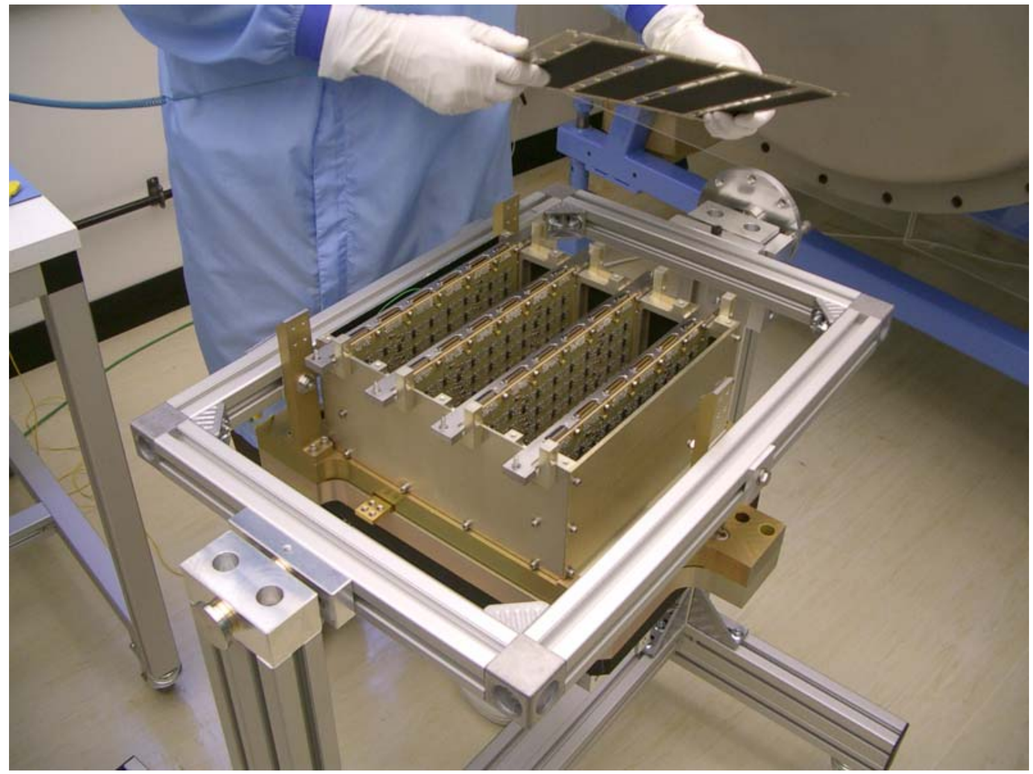

Symmetric cryo-opamps

VISTA - Telescope and IR Camera

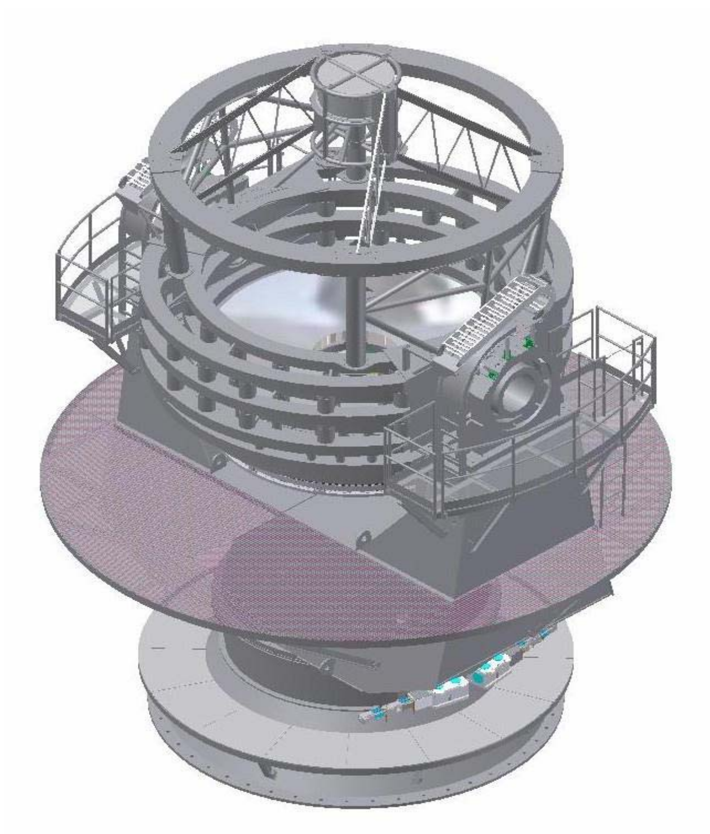

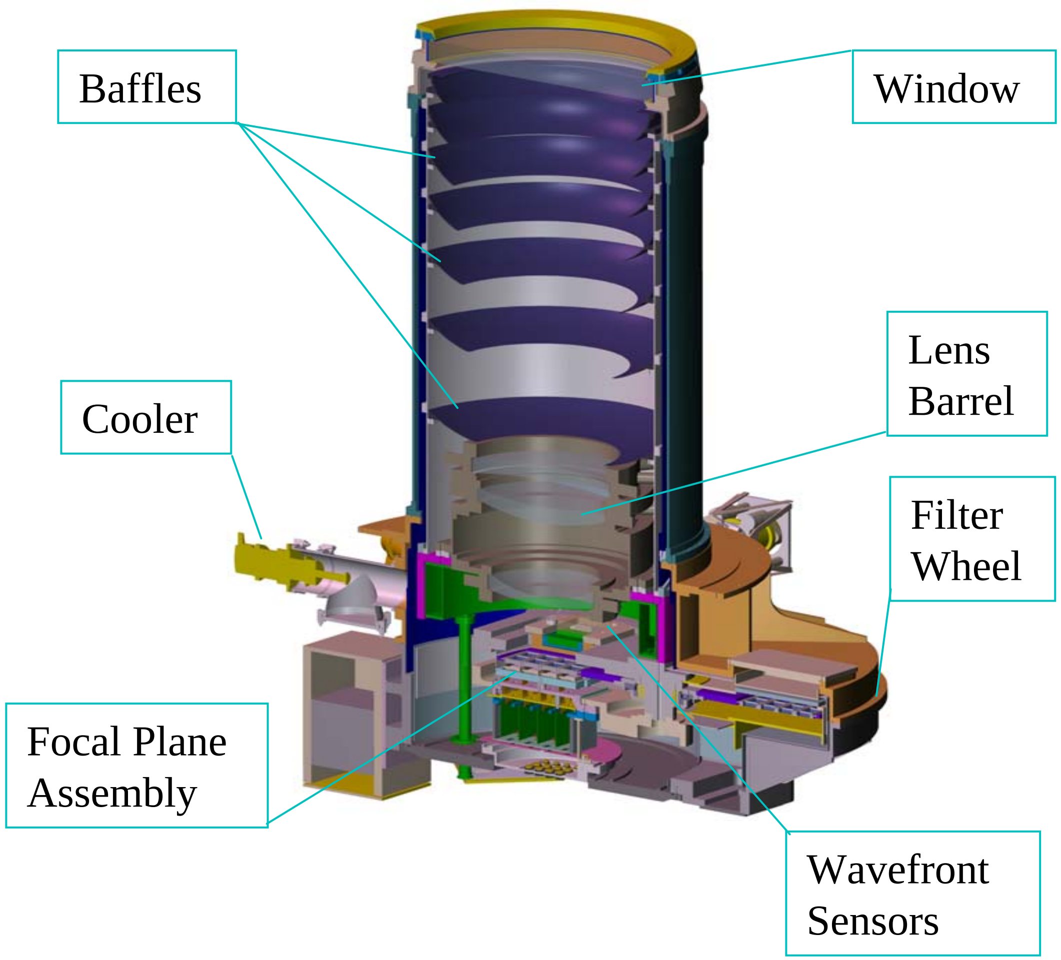

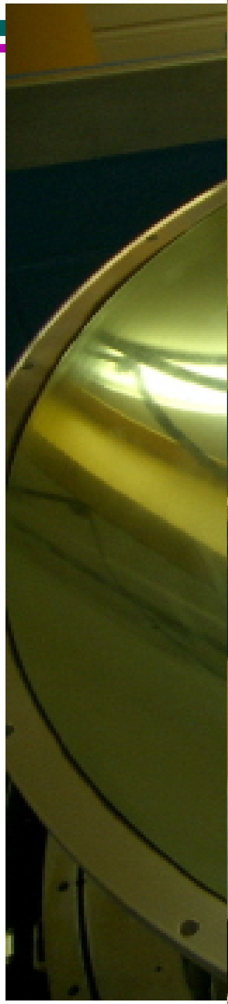
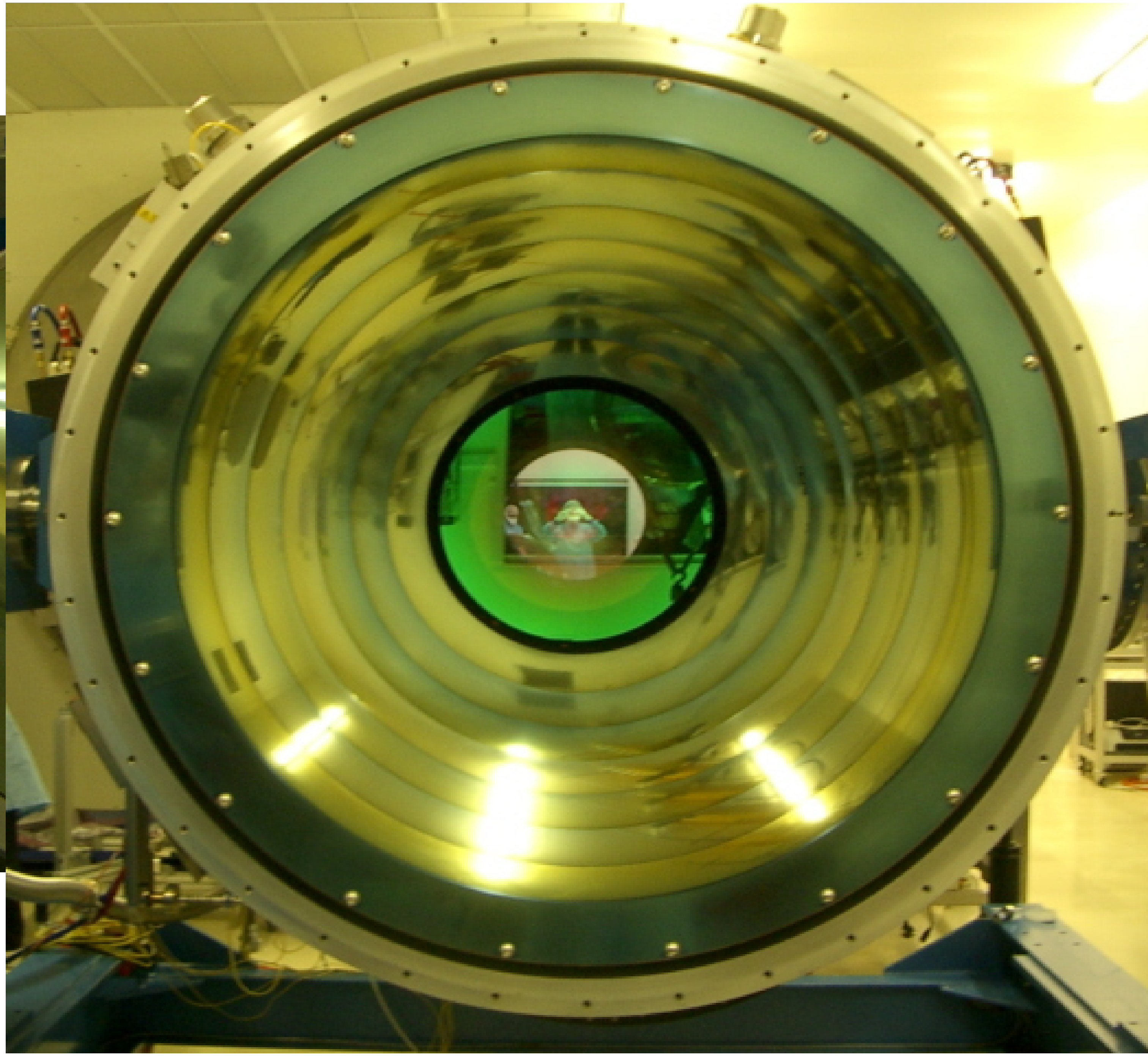
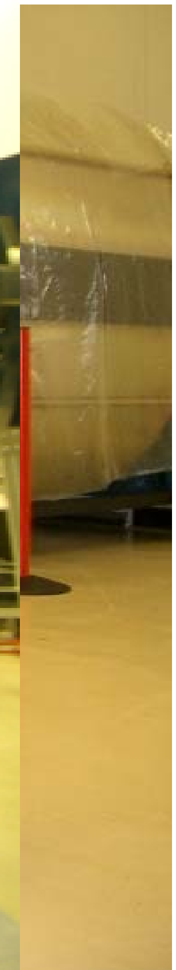

Focal Plane Assembly Details

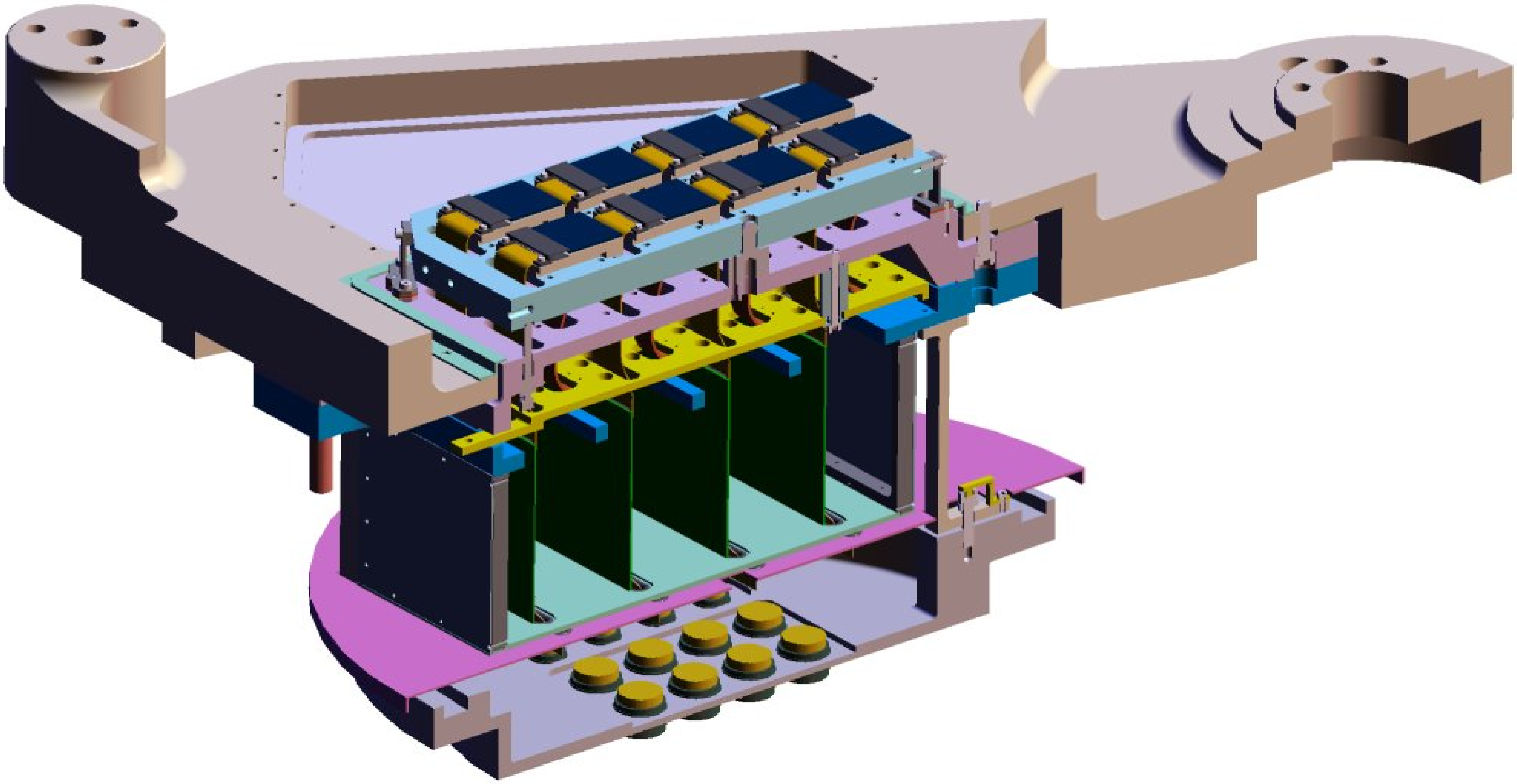

VIRGO 16x2Kx2K HgCdTe mosaic for VISTA

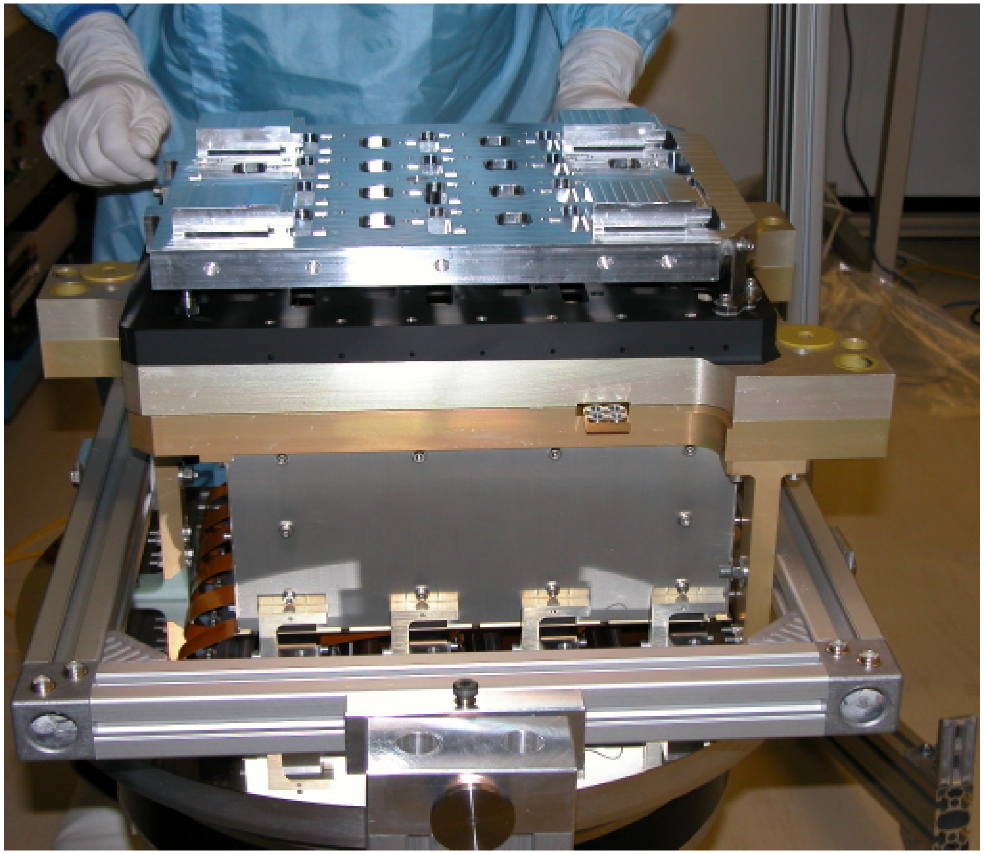

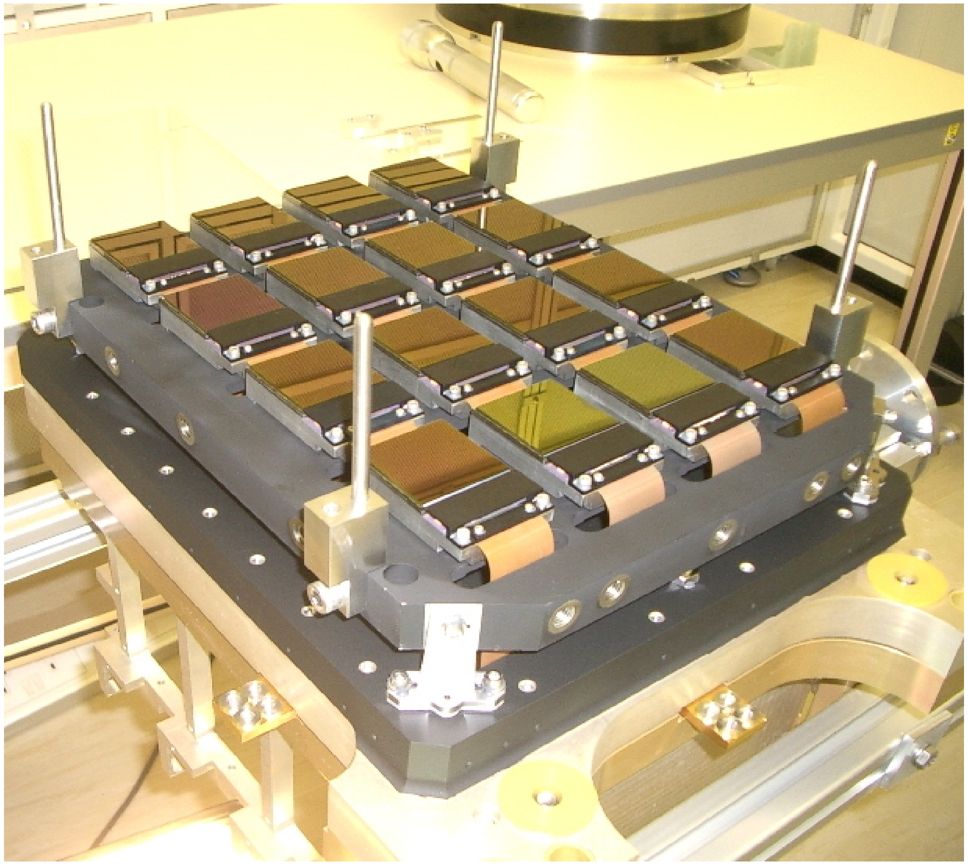

Detector co-planarity: all pixels within ±25µm (Thanks Raytheon!)

VIRGO 2Kx2K for VISTA

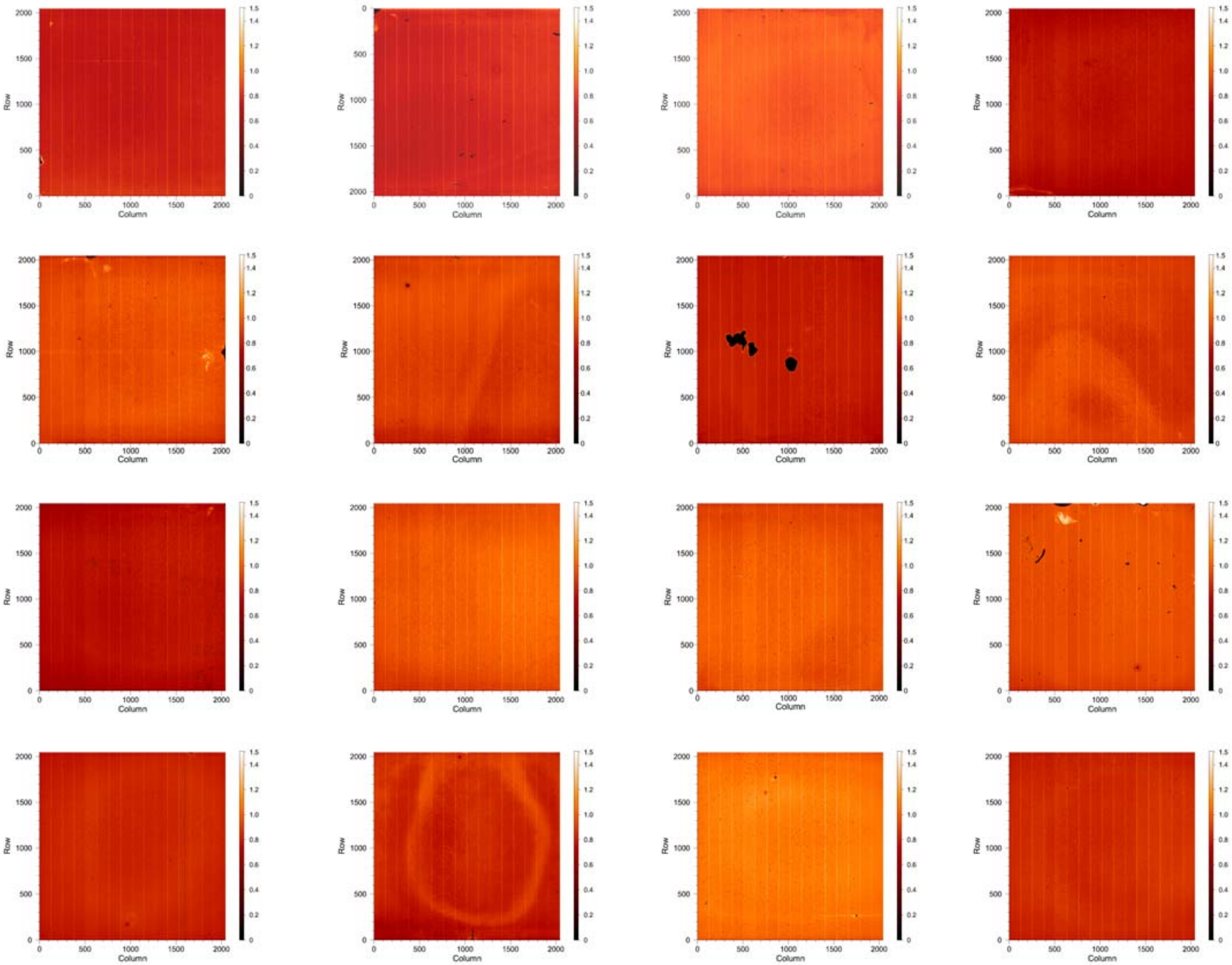

- 16 science grade arrays delivered
- Read noise 15 erms for DC readout
- IRACE 256-channel system

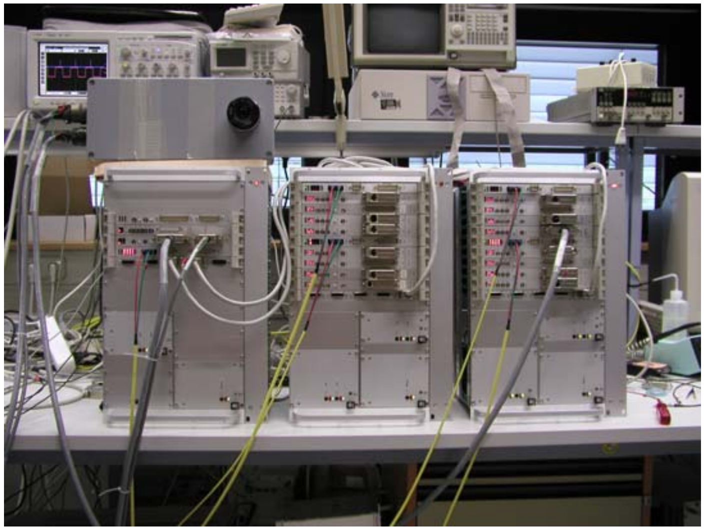

Q.E. Performance* Summary for 16 Science Grade Modules

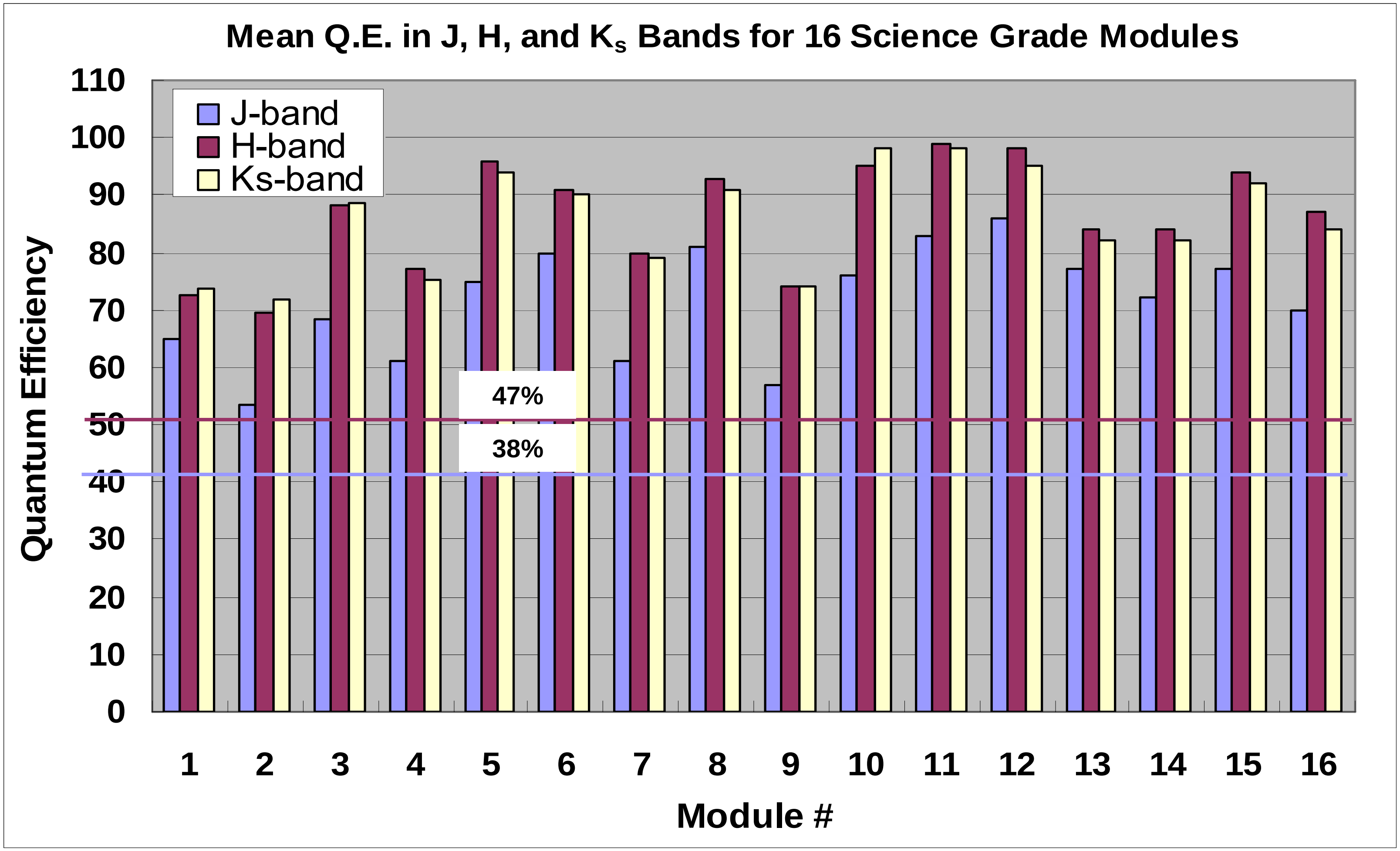

VISTA requirement:

J-band: > 38%

H-band: > 47%

K_s-band: > 47%

* With single-layer AR coating with minimum reflectance at 1.4 μm

Hawk-I Mosaic Package

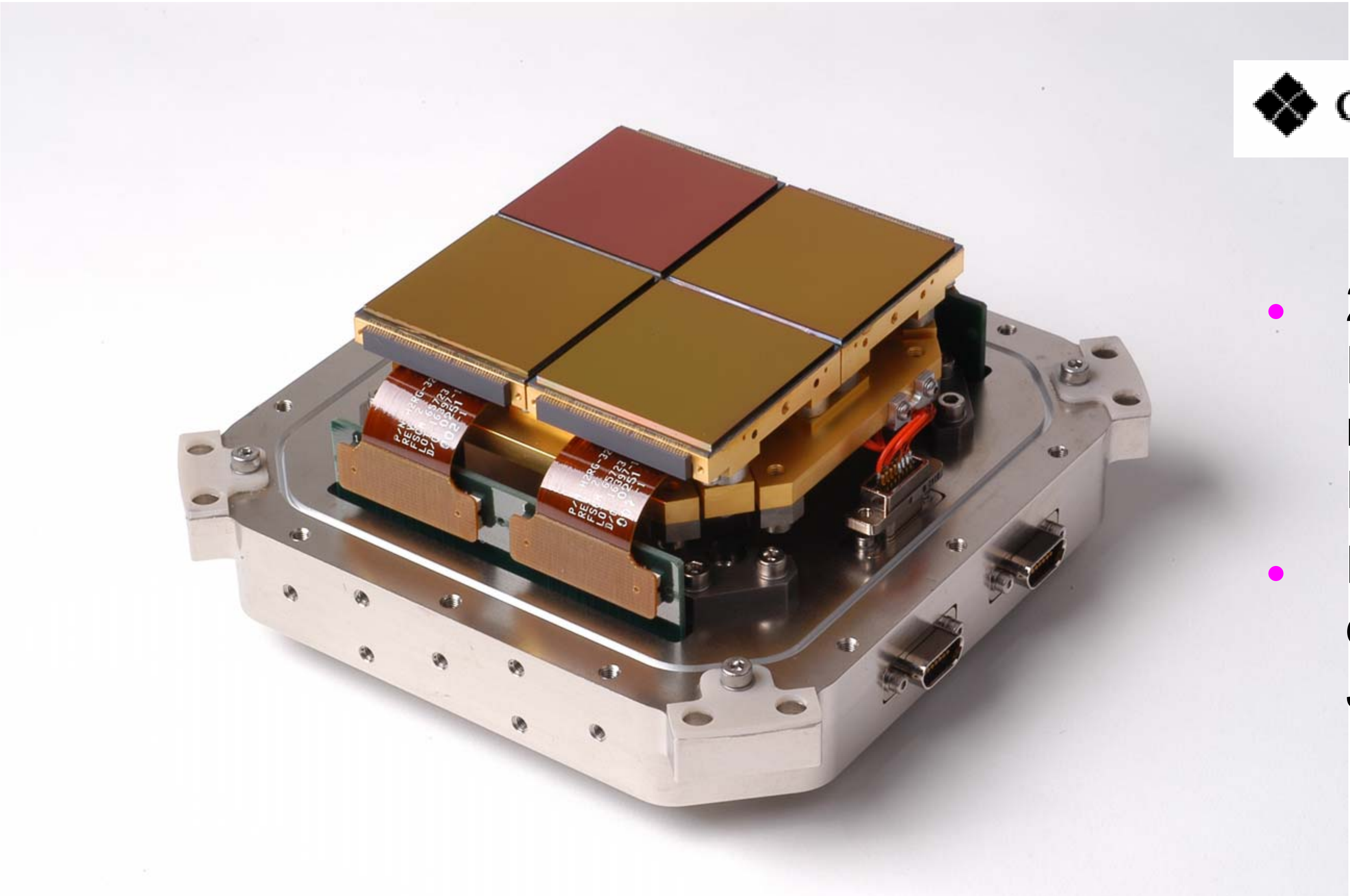

GL SCIENTIFIC

- 2x2 2Kx2K Hawaii-2RG mosaic for Hawk-I
- Package developed for JWST

Hawk-I Mosaic Package

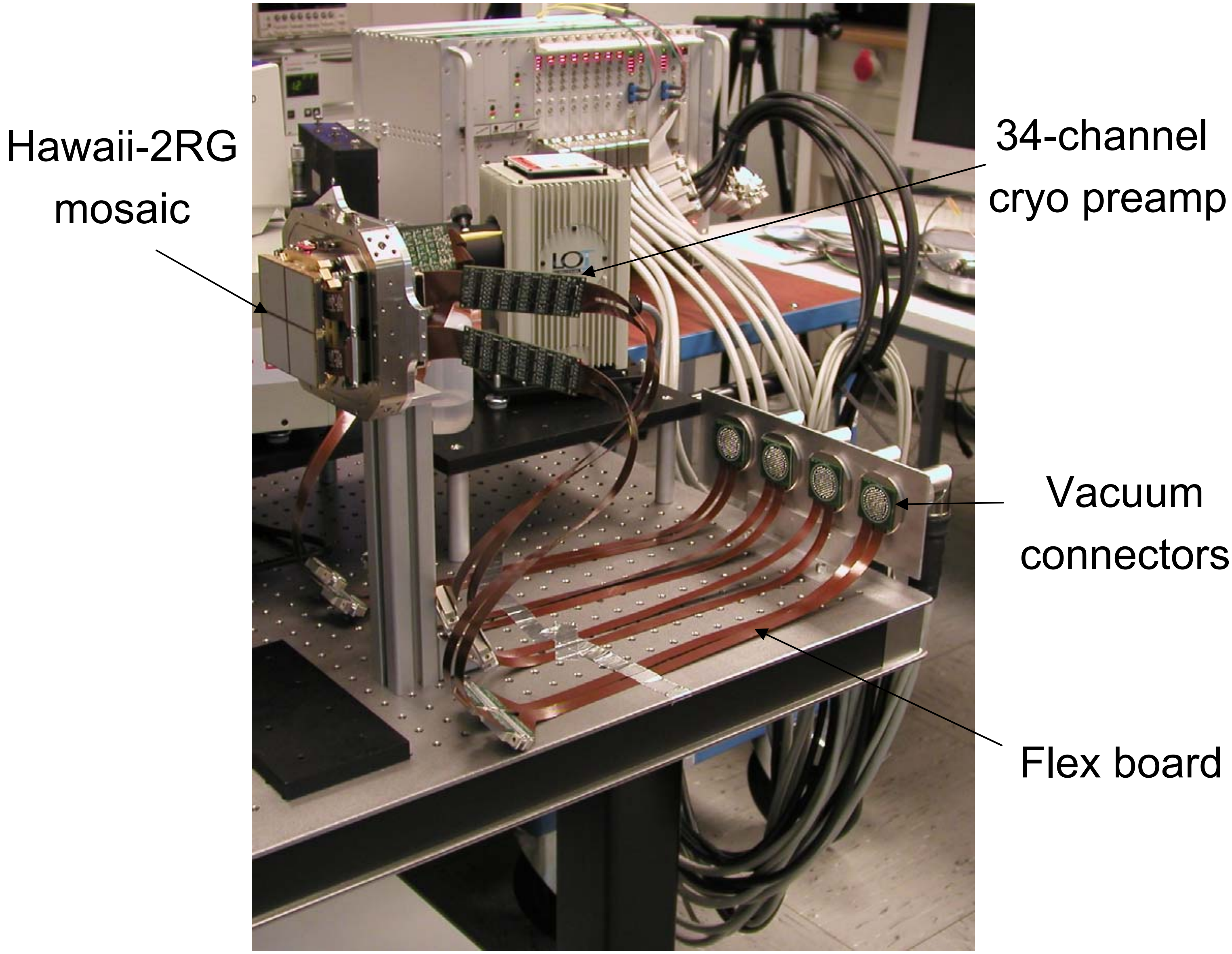

SNAP focal plane

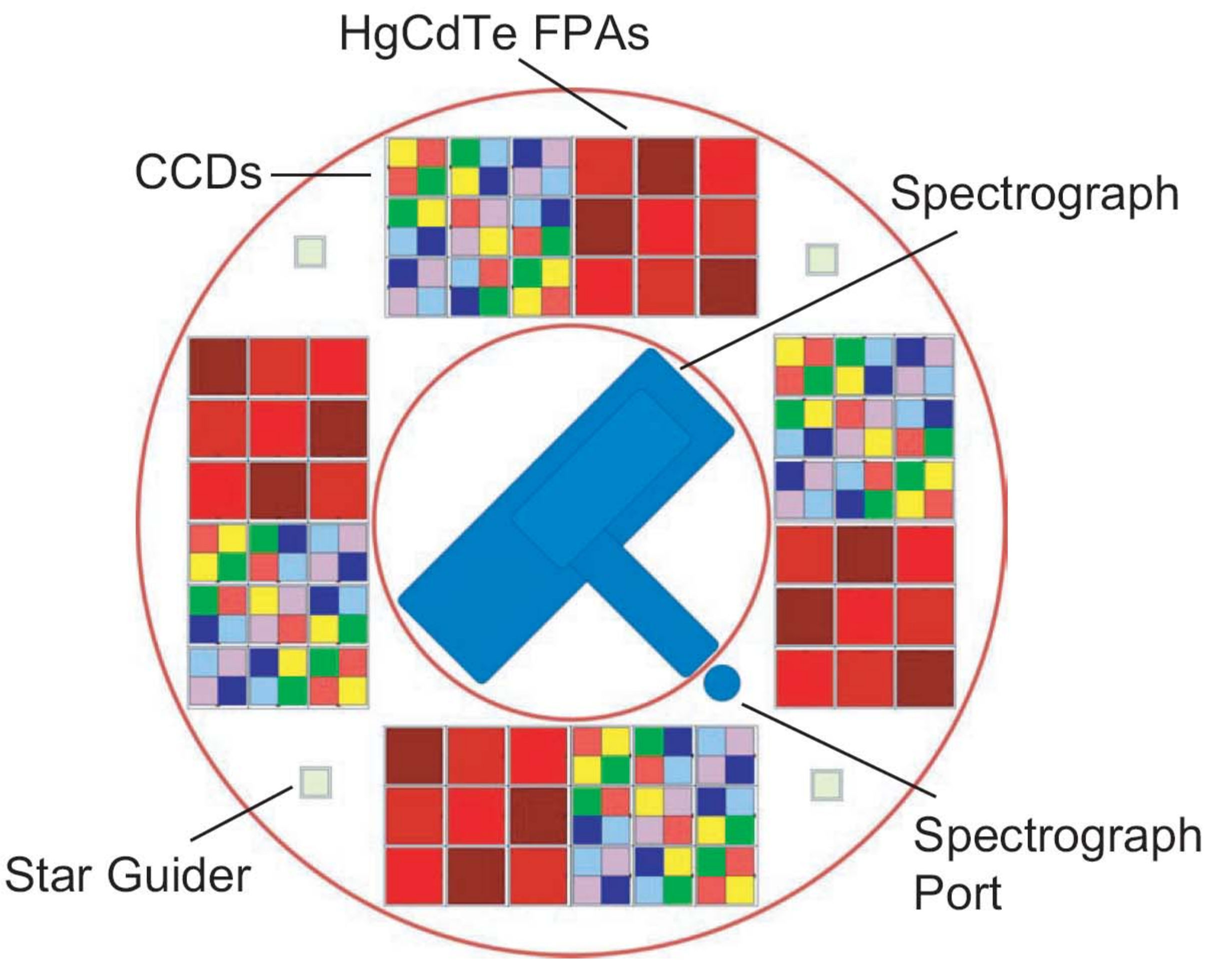

- SuperNova/Acceleration Probe (SNAP) will
- obtain precision calibrated light curves and spectra for over 2500 Type Ia supernovæ at redshifts 0.1 to 1.7
- determine the nature of the dark energy.
- 36 HgCdTe arrays λ_c=1.7 μm with 3 filers
- 36 CCD's with 6 filters
- Change filters by scanning telescope

IR sensor for adaptive optics

NAOS

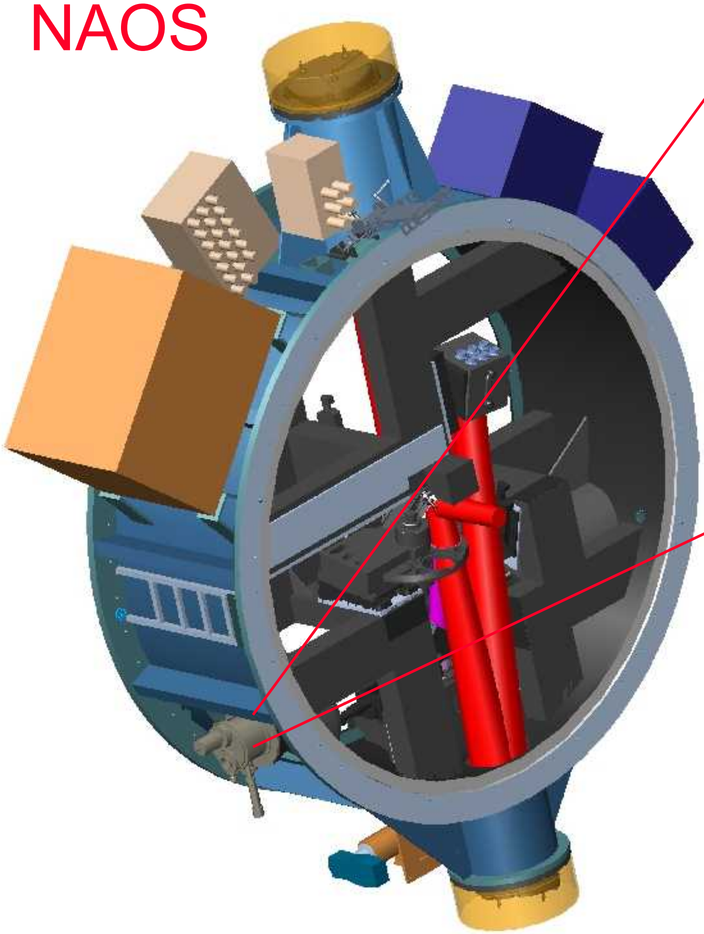

Hawaii1 1Kx1K HgCdTe

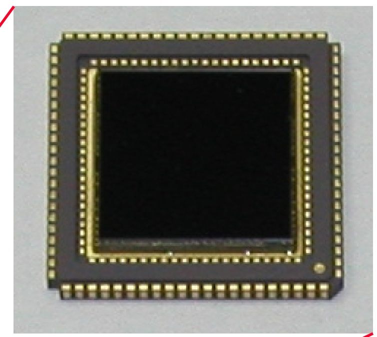

- Measure wavefront distortion by atmosphere to correct it with AO mirror
- NAOS CONOCA at the VLT
- Shack-Hartmann AO system
- optical and infrared wavefront sensor
- one quadrant of Hawaii 1Kx1K HgCdTe
- 7x7 and 14x14 subapertures

Adaptive optics

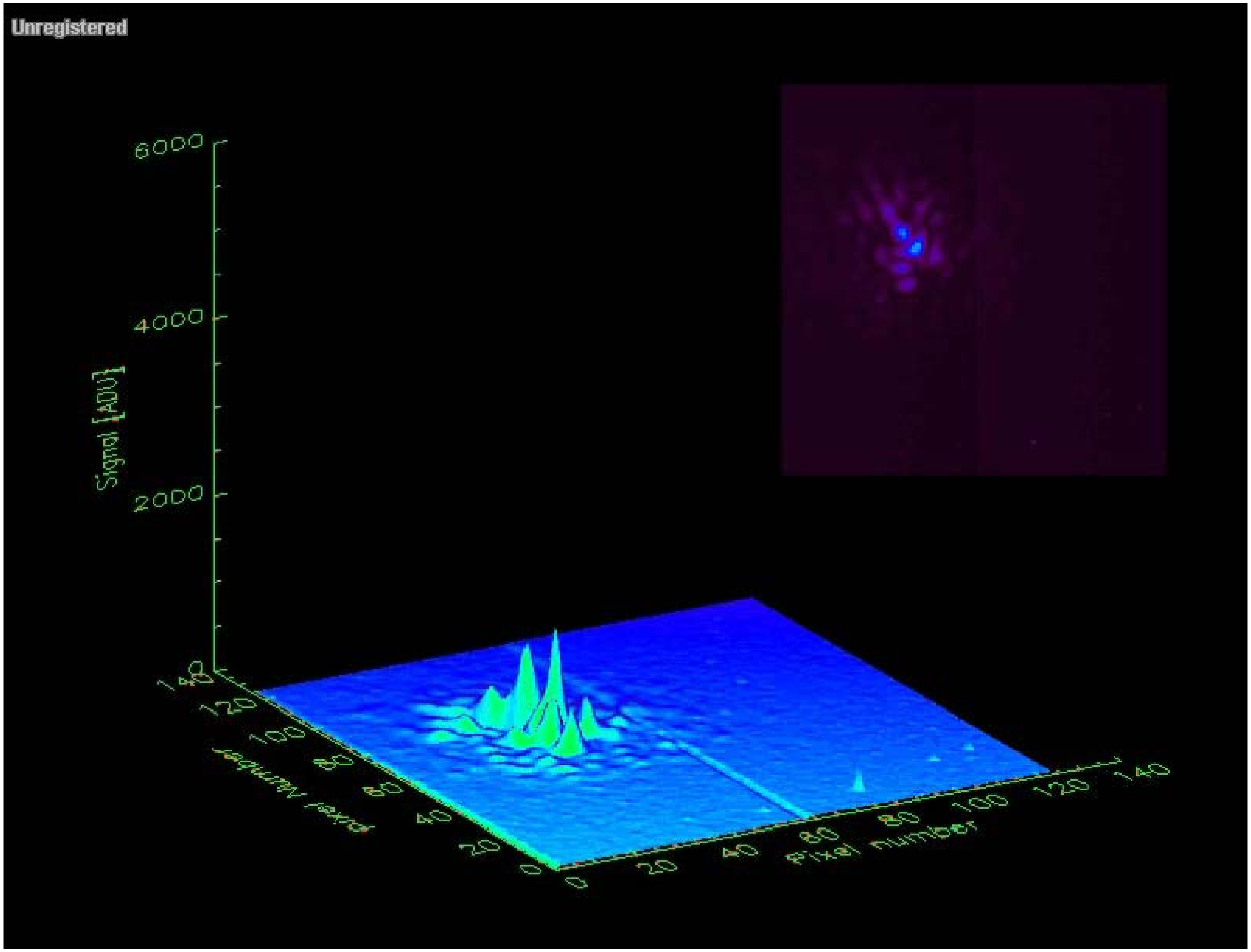

- Closed loop with a 60 element MACAO curvature system and the AO-IR 1k x 1k test camera at 2.2 μm
- Best image quality with AO at λ=2 μm
- Strehl ratio for 8 m telescope 60 %

Saturnian moon Titan

- Aladdin array in NACO
- High contrast with adaptive optics and spectral differential imaging (SSDI): in methane absorption band and in methane window
- Attenuate speckle noise
- Diameter 0.7 arces
- Resolution 0.06 arcsec

Geiger APD's for AO

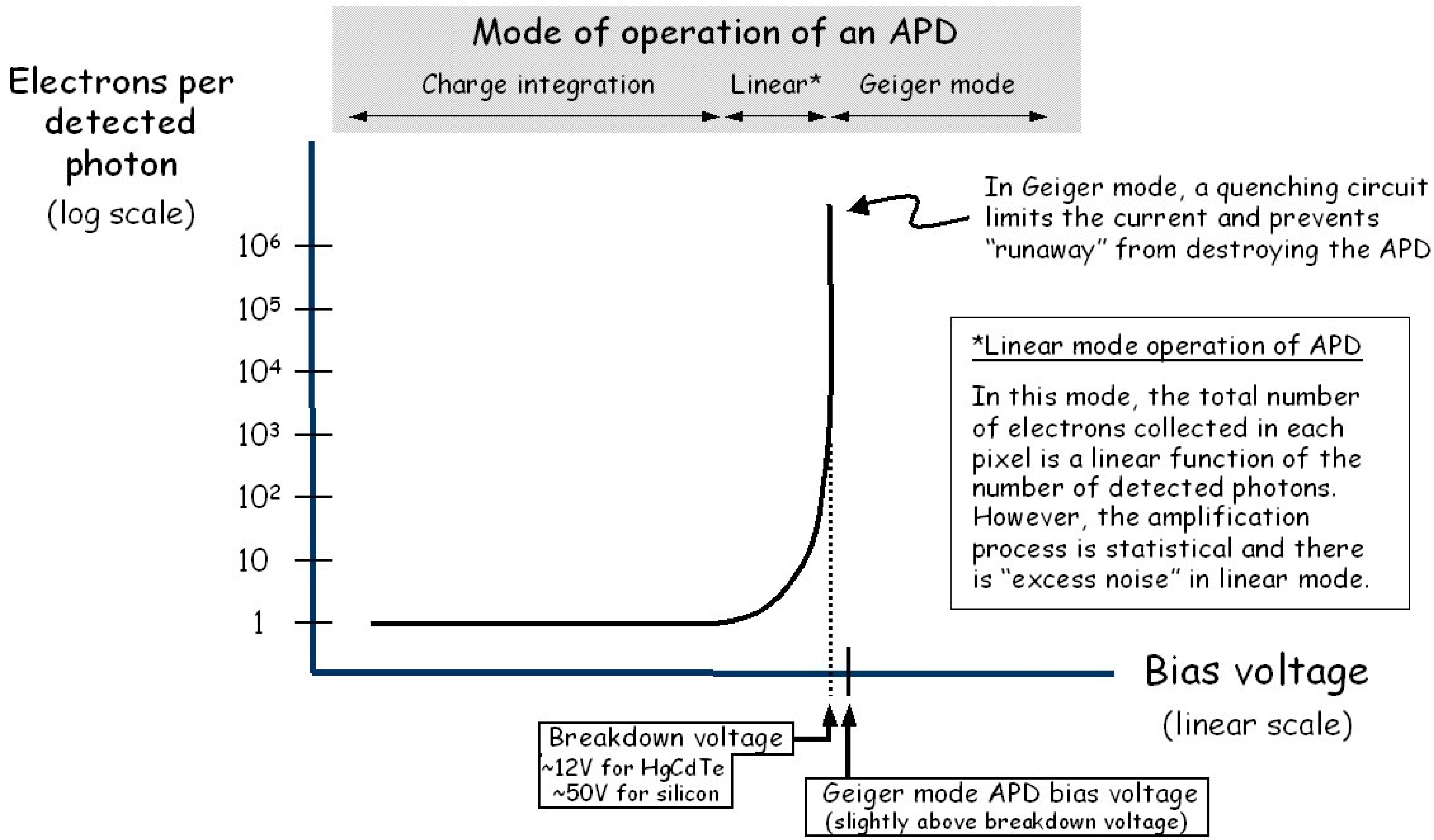

Geiger APD's for AO

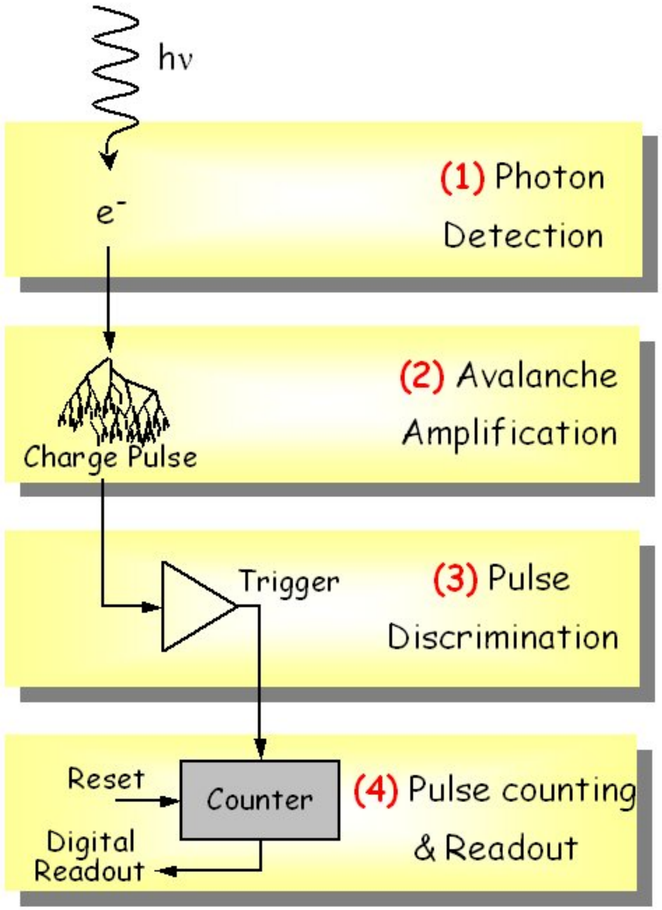

- Geiger mode zero readout noise
- Each pixel has its counter
- Format 128x128, pitch 30 μm
- Frame rate > 1KHz
- Both Si-PIN and HgCdTe possible

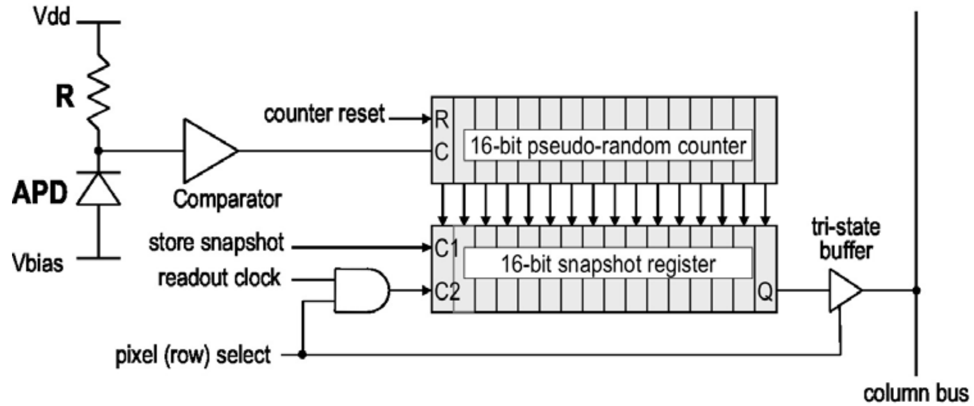

Test results with λ_c=2.5 μm
2Kx2K HgCdTe arrays on CdZnTe substrates

Dark current density of different detector materials

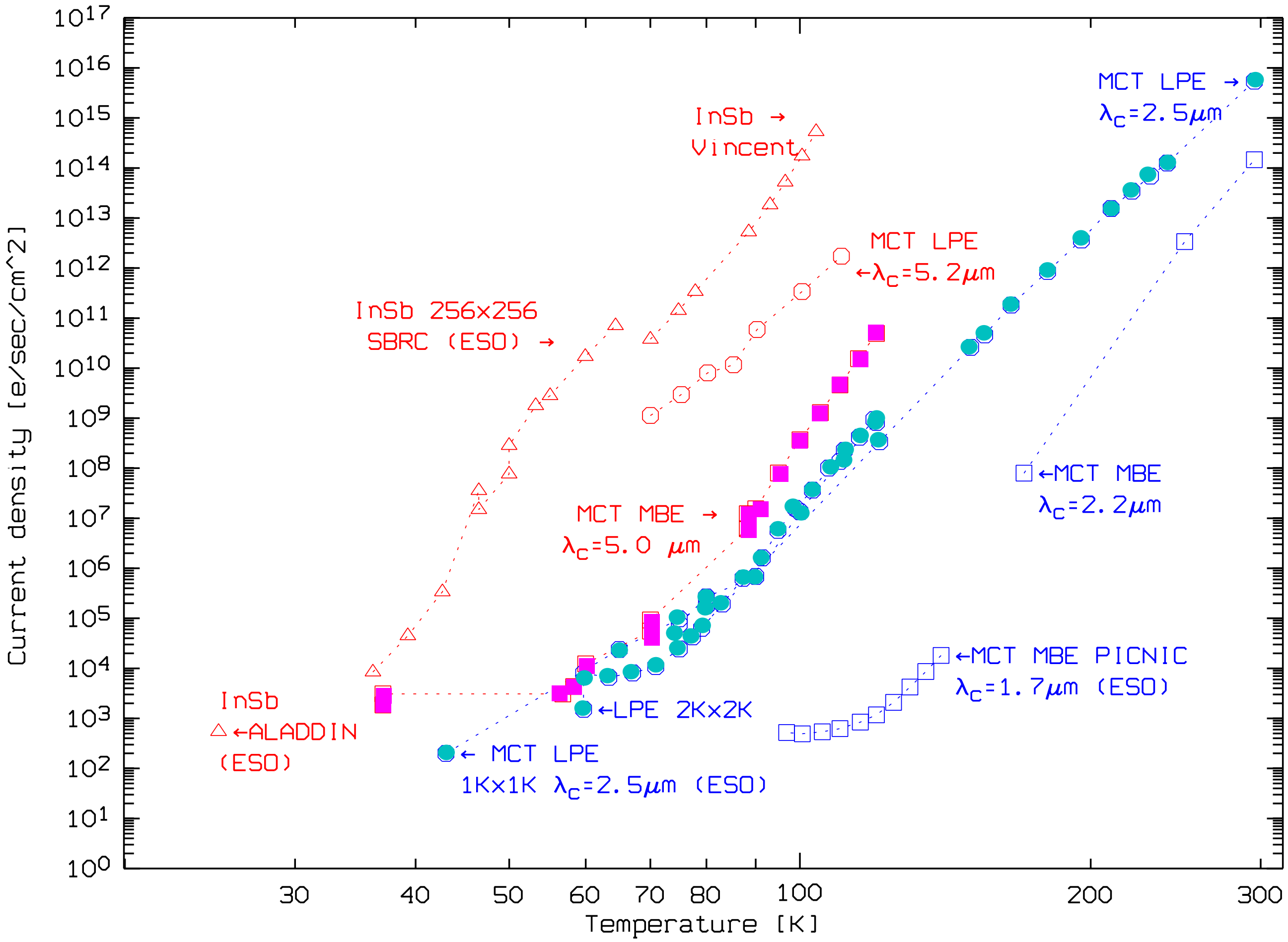

- Red : long wavelength detectors (λ_c=5.0µm-5.2µm)
- Blue: short wavelength detectors (λ_c=1.7µm-2.5µm)
- Triangles:InSb
- Circles: LPE HgCdTe
- Squares:MBE HgCdTe

  best Material at 60 K (MBE HgCdTe / InSb 10^{-6})
- InSb as good as MBE HgCdTe at 30 K
- HgCdTe MBE λ_c=5.0µm as good as LPE λ_c=2.5µm

MBE grown HgCdTe double layer planar heterostructure

Rockwell Scientific

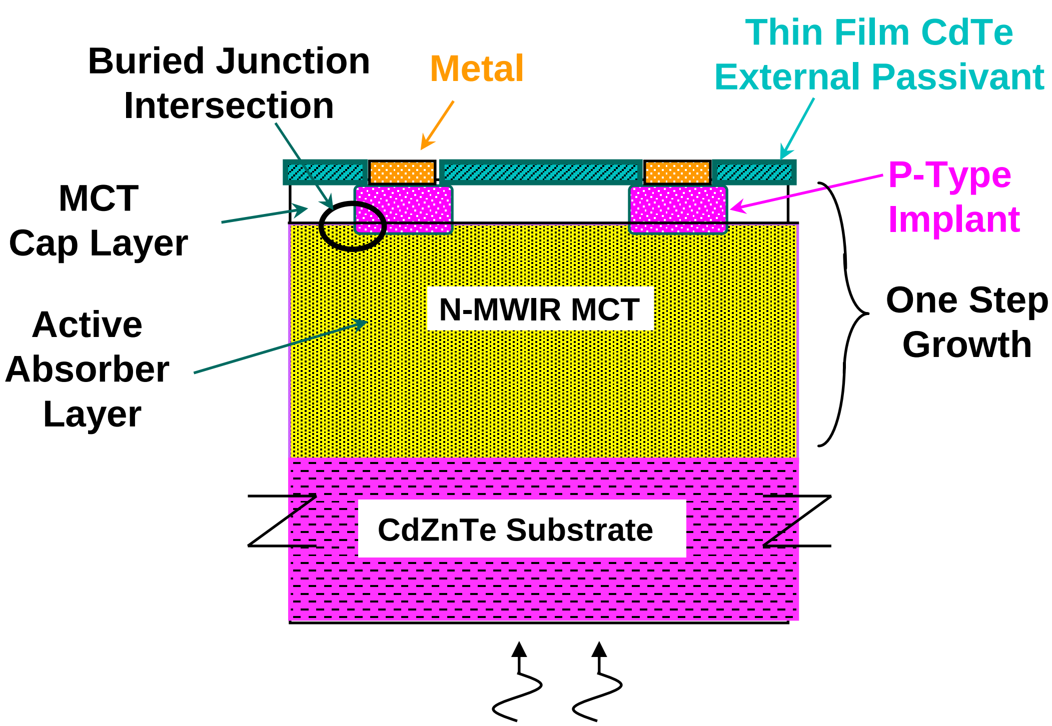

- CdZnTe substrate
- Molecular beam epitaxy grown HgCdTe n-type absorbing layer
- Wide band-gap HgCdTe cap layer: junction in bulk
- P-type arsenic implant forms p-on-n junction
- Cap layer and lattice match of CdZnTe substrate and HgCdTe results in almost ideal pixel performance

Dark current versus temperature
HgCdTe LPE / MBE

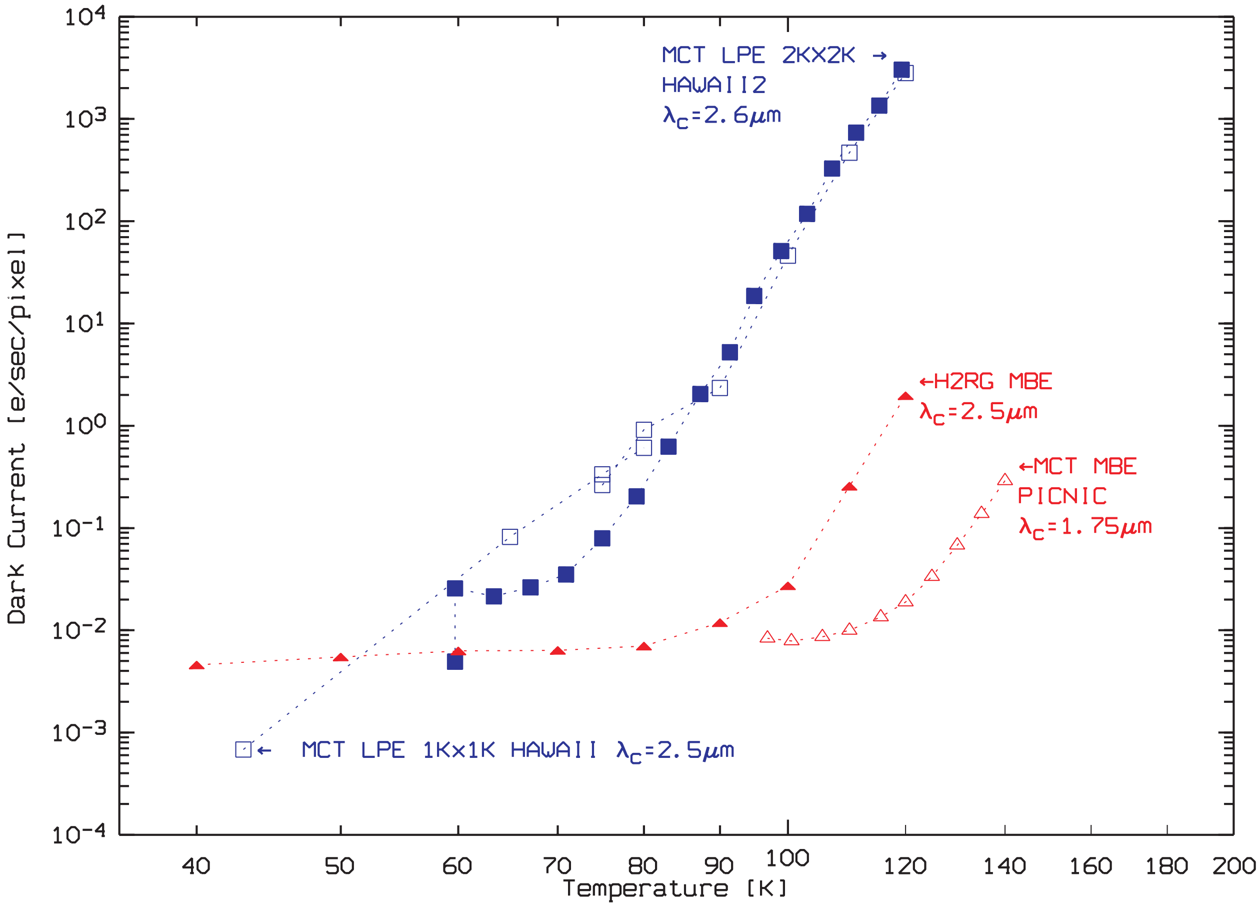

- LPE λ_c=2.5μm
  - ■ Hawaii2 2Kx2K
  - □ Hawaii1 1Kx1K
- MBE λ_c=2.5 / 1.7 μm
  - ▲ Hawaii-2RG 2Kx2K λ_c=2.5μm
  - Δ PICNIC 256x256 λ_c=1.7μm
- MBE at T<80K I_{dark} < 0.01 e/s/pixel
- at T=100K $I_{MBE}=I_{LPE}$ /1660
- Good λ_c=2.5μm MBE material can be used in liquid bath cryostats

Dark current versus temperature
HgCdTe LPE / MBE

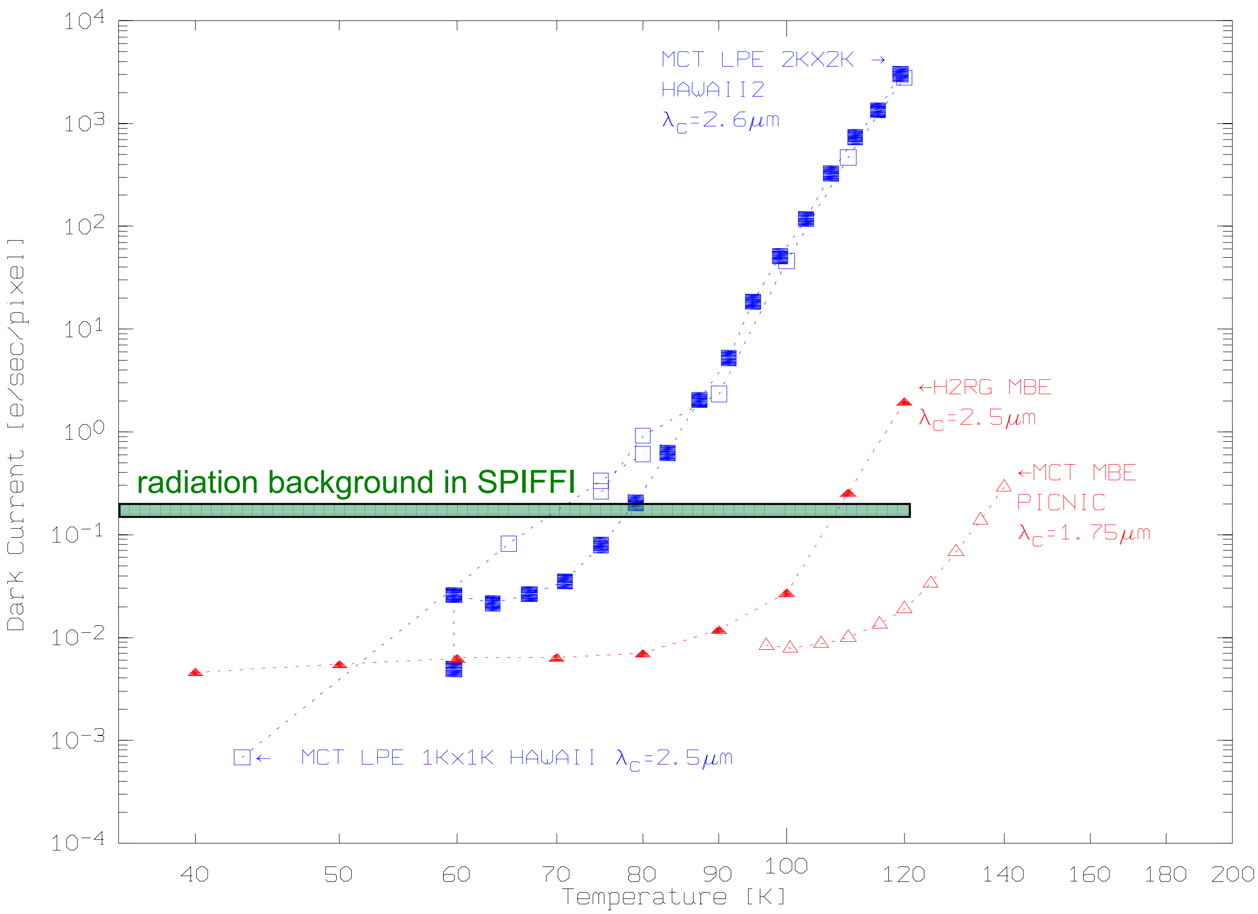

- LPE λ_c=2.5µm

  ■ Hawaii2 2Kx2K
  □ Hawaii1 1Kx1K

- MBE λ_c=2.5 / 1.7 µm

  ▲ Hawaii-2RG 2Kx2K λ_c=2.5µm
  Δ PICNIC 256x256 λ_c=1.7µm

- MBE at T<80K I_{dark} < 0.01 e/s/pixel

- at T=100K $I_{MBE}=I_{LPE}$ /1660

- Good λ_c=2.5µm MBE material can be used in liquid bath cryostats

Dark Current vs. Inverse Temperature VIRGO LPE array on CdZnTe substrate

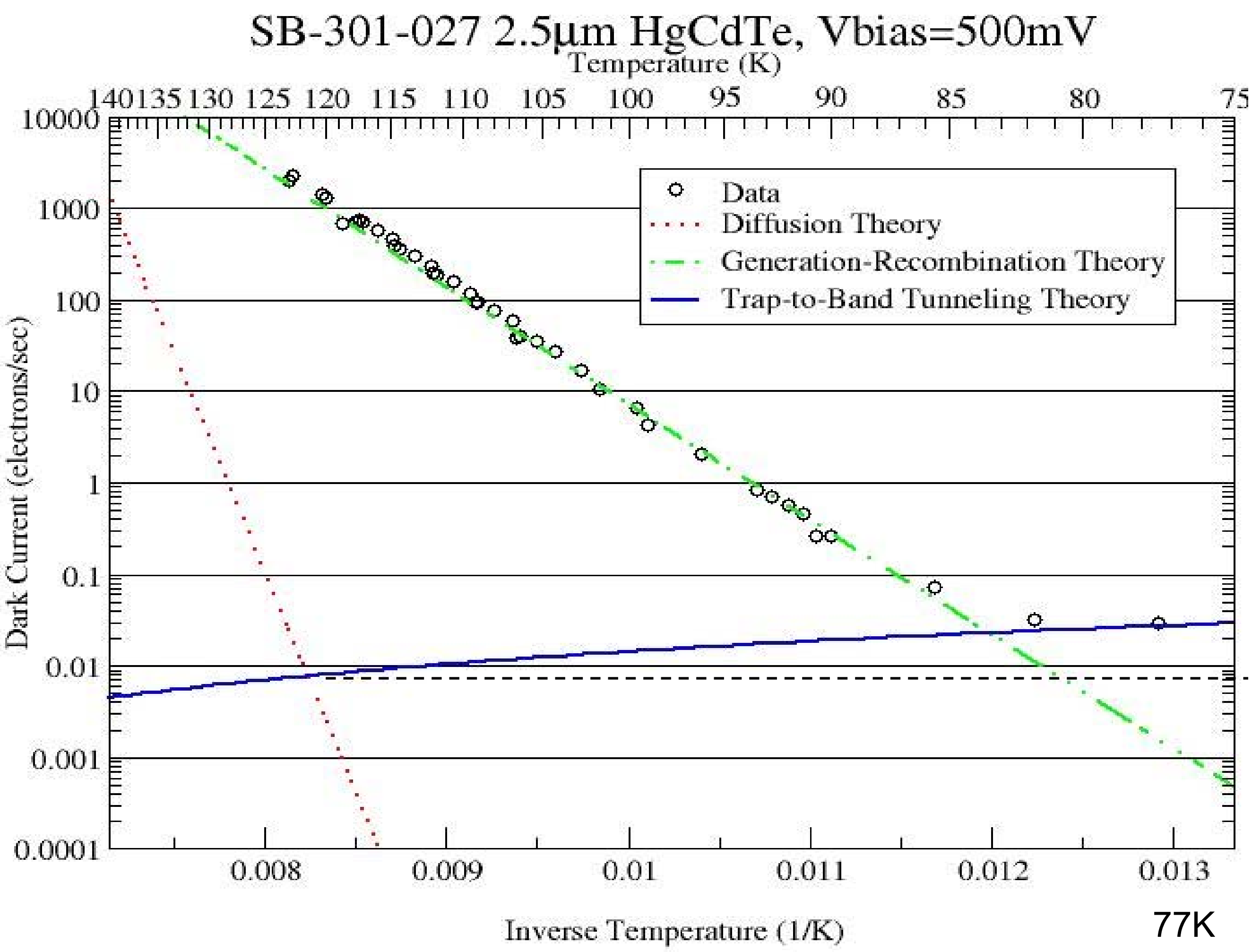

- Three dark current mechanisms:
- Diffusion: $I_D \sim \exp(-E_g/KT)$
- Generation-Recombination: $I_D \sim \exp(-E_g/2KT)$
- Tunneling weak temperature dependence
- Diffusion limited performance down to T=60K only by MBE grown λ_c=5 μm HgCdTe perfect lattice match between CdZnTe and HgCdTe

T=60K

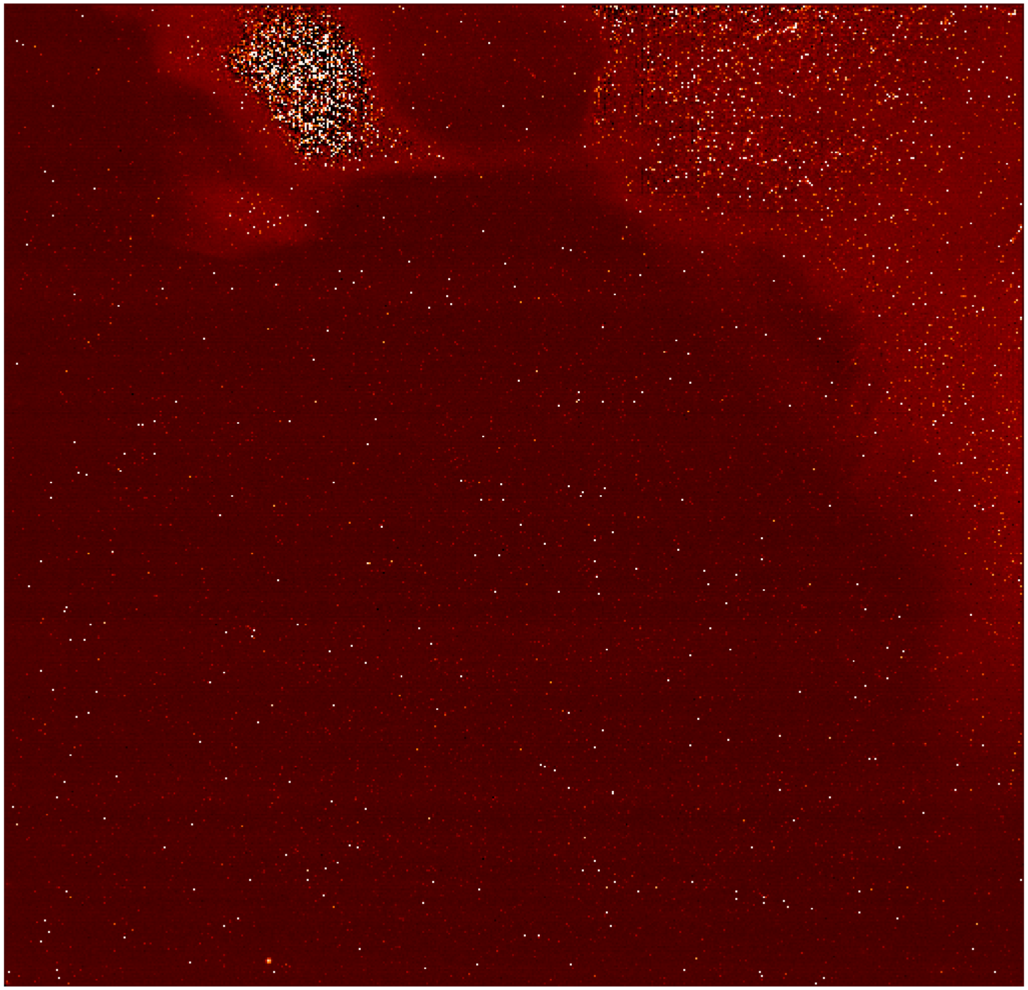

- Cut level -0.5/2 e/s/pix
- Integration time 11 min

T=80K

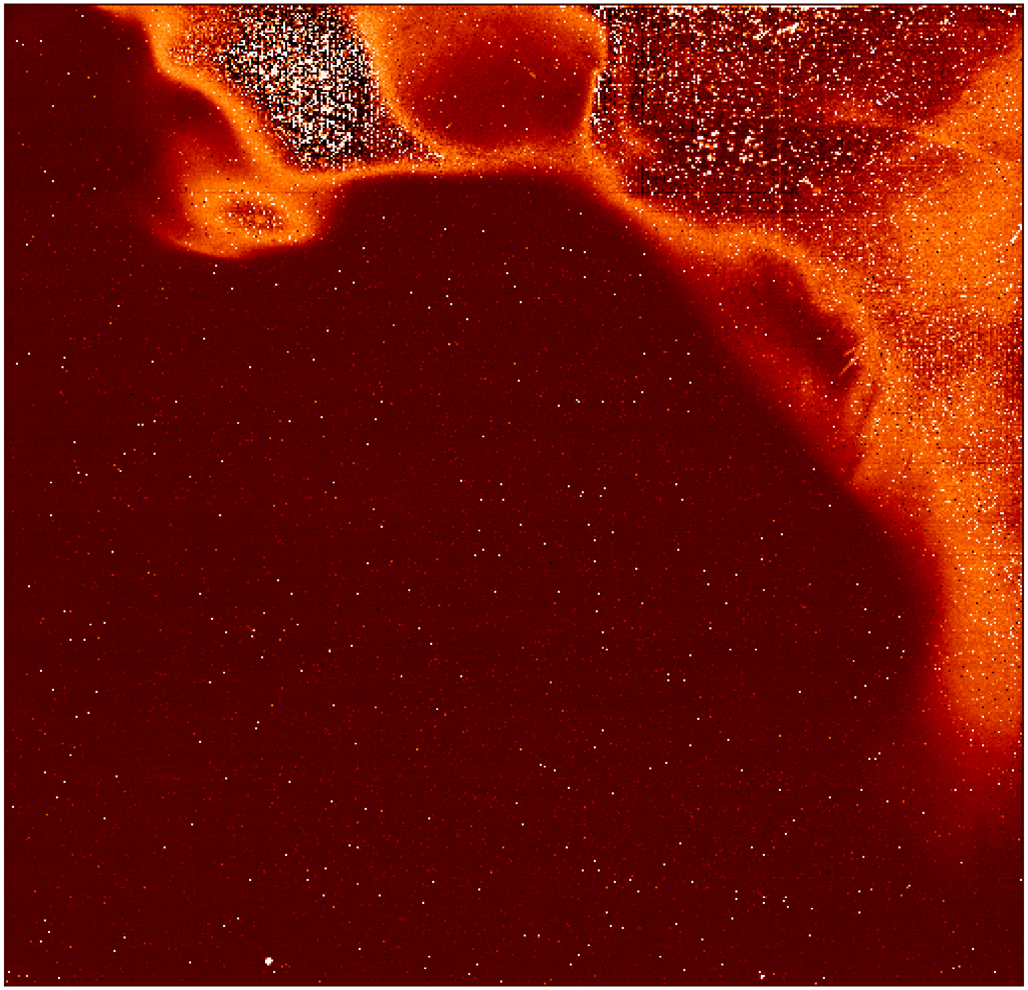

- Cut level -0.5/2 e/s/pix
- Integration time 11 min

Detector operating temperature

- for a perfect science grade array
  $I_{dark} < 0.01$ e/s at $T < 80$ K
- for a real array cosmetic quality improves
  if array cooled to $T < 60$ K
- Required operating temperature depends on quality
  of science grade array

32 channel package for Hawaii-2RG

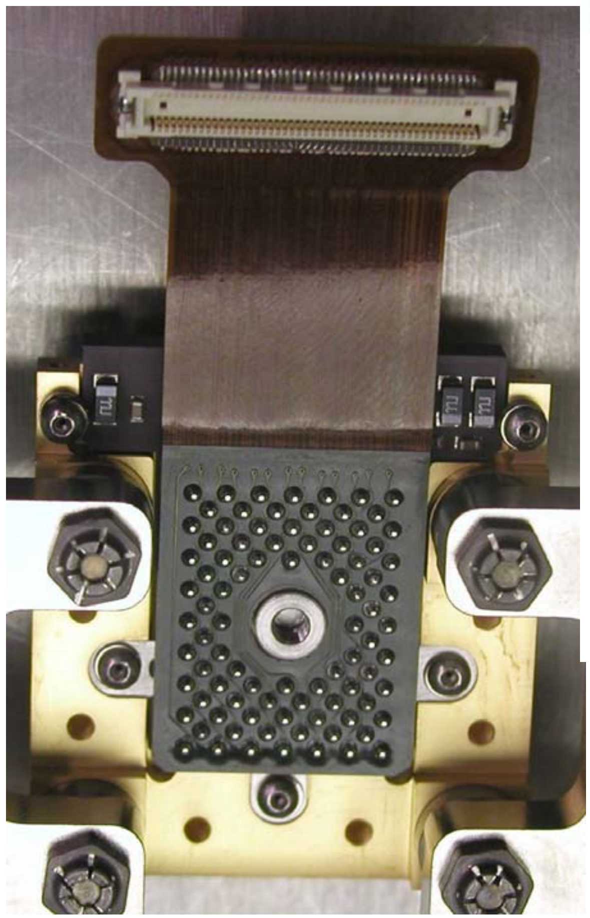

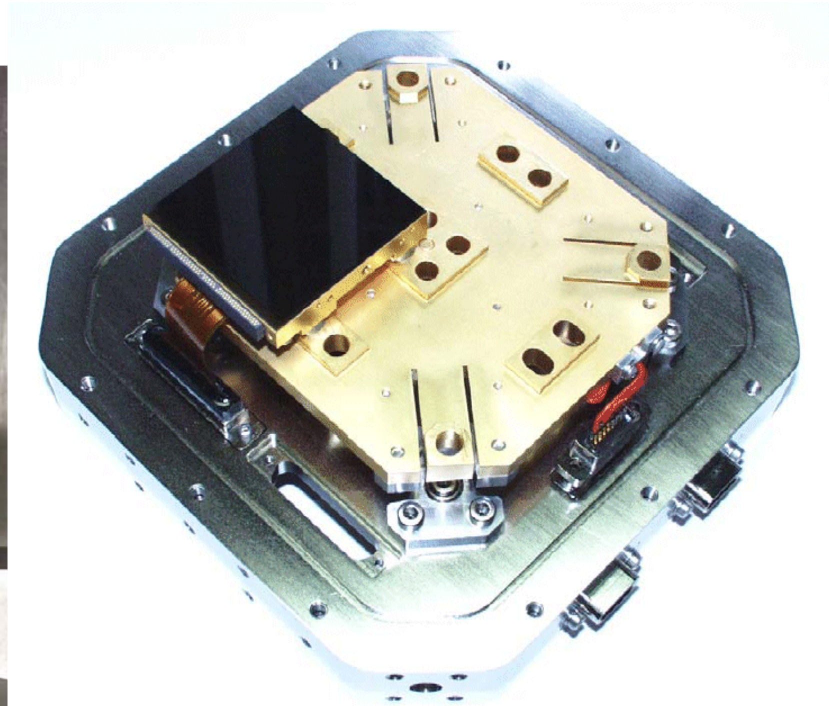

- 32 channel package without ASIC developed for ESO
- Mosaic for Hawk-I and KMOS ? In collaboration with GL Scientific

32 channel package for Hawaii-2RG

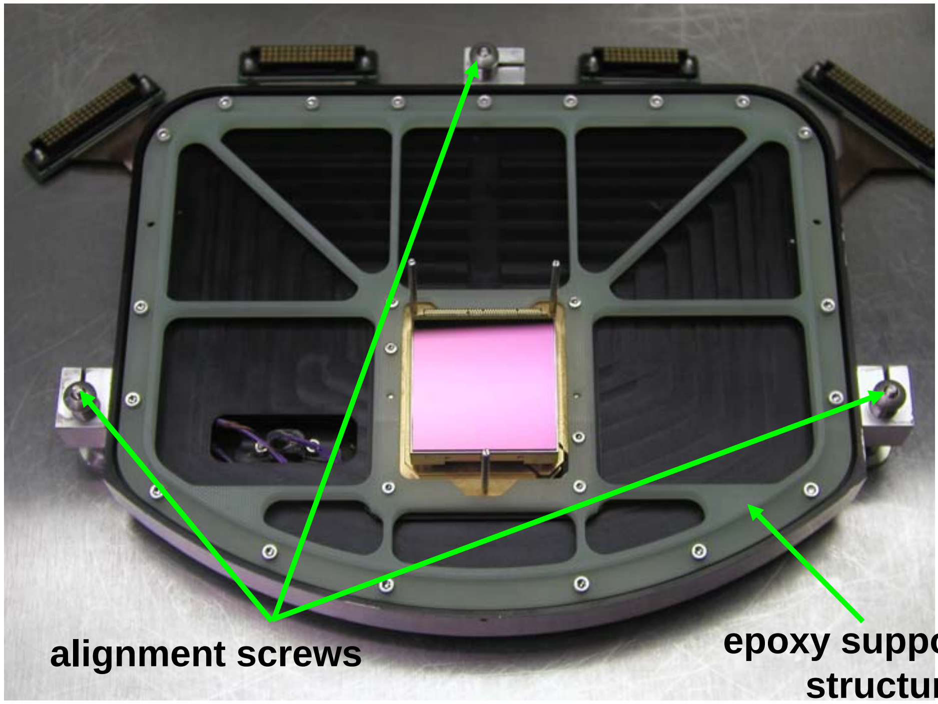

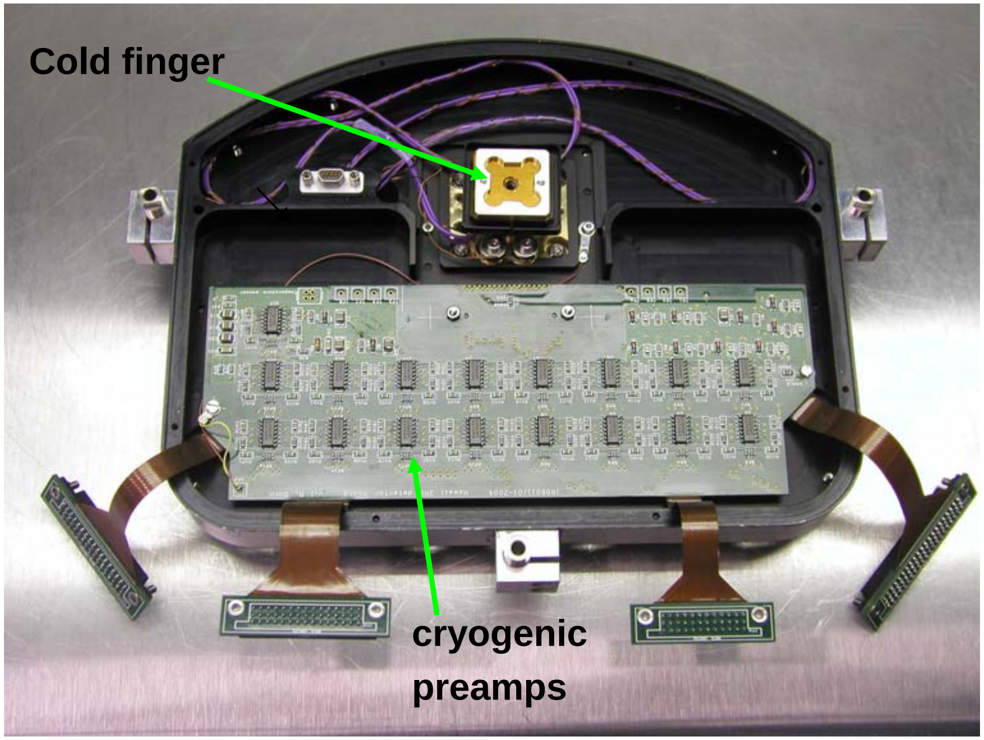

- Tip tilt and focus adjustment by 3 alignment screws
- Detector cooled by cold finger on the backside of the array
- Use of cryogenic CMOS preamplifiers

32 channel package for Hawaii-2RG

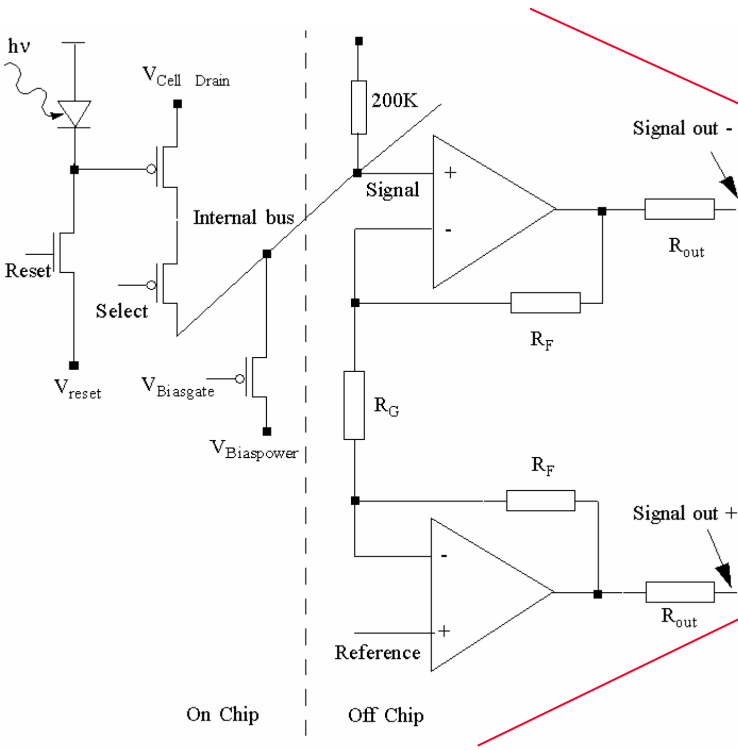

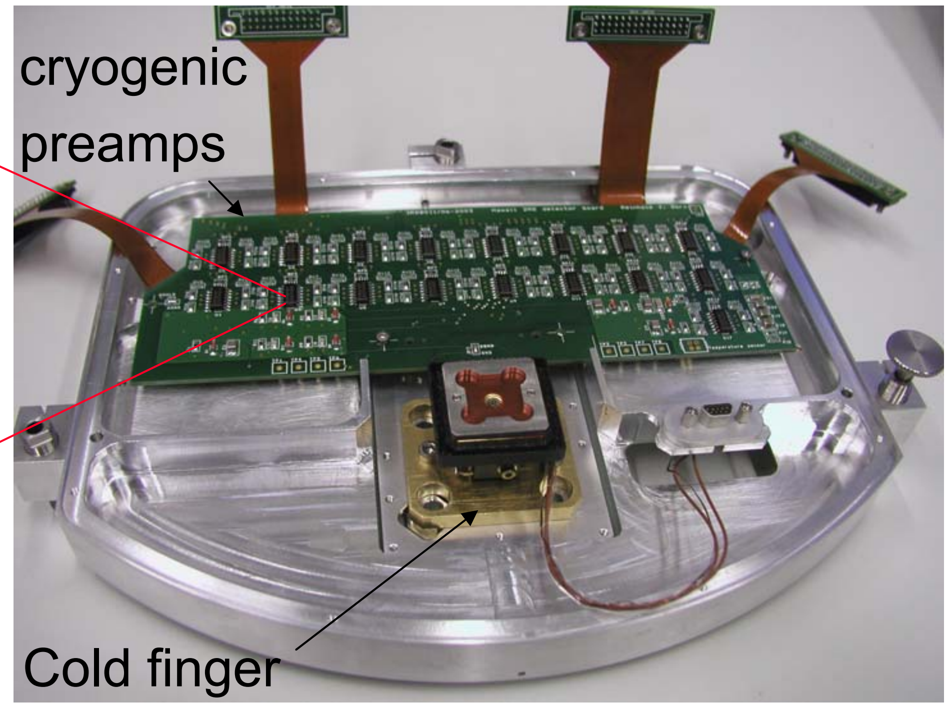

- Internal bus of array accessed directly by cryogenic CMOS amplifiers
- Symmetric amplifier design for differential signal chain
  32 video + 1 reference + 1 guide channel used in slow mode (100 KHz)
- Bias and clock filtering at detector

Quantum efficiency versus wavelength

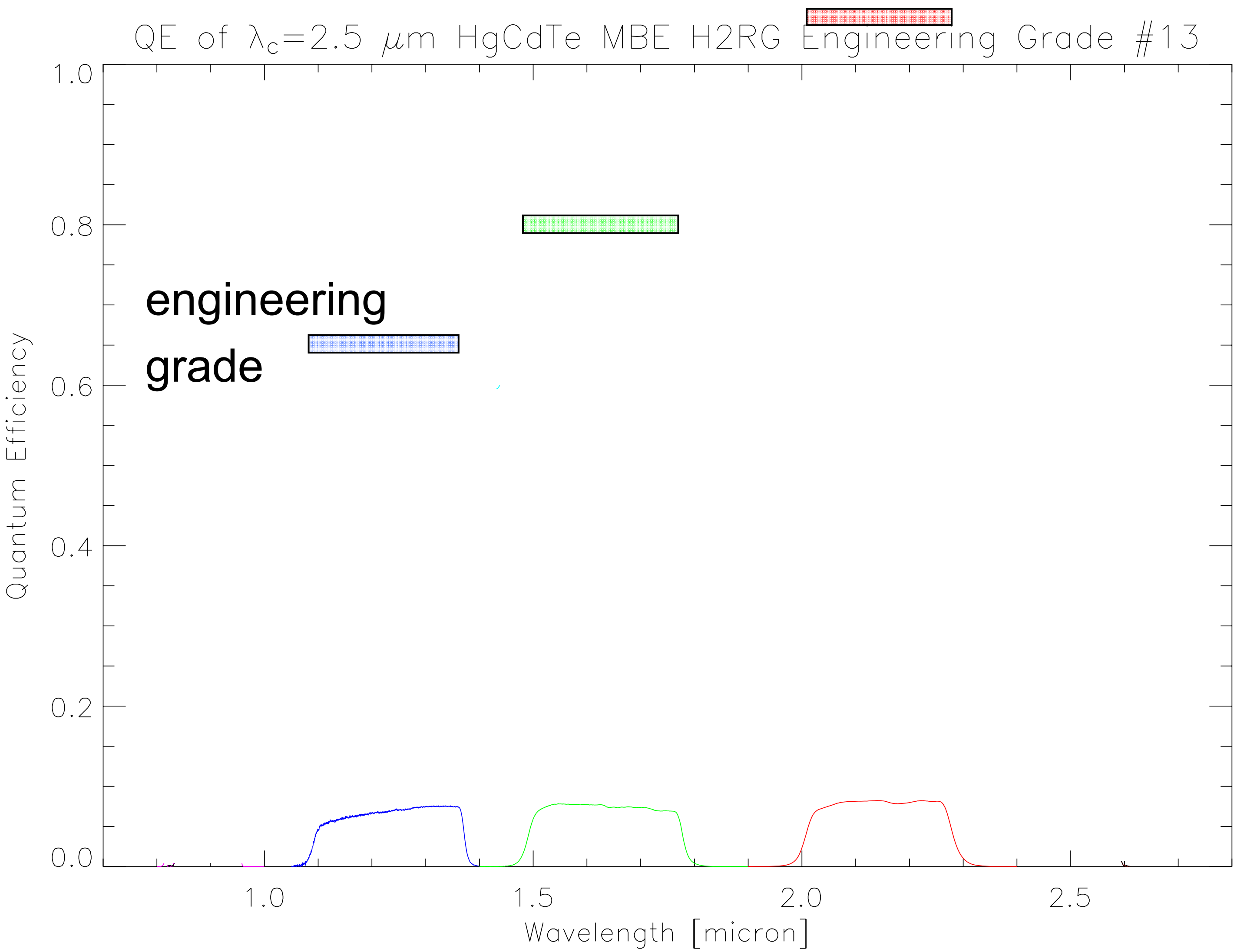

- Smooth curve to obtain final result
- Engineering grade using shot noise:

K: 1.05
H: 0.81
J: 0.65

something must be wrong with QE measurement!

- After re-checking blackbody, filter transmission, filter leaks, geometry…
- QE K:105%
- only parameter left was conversion gain

Conversion Gain

- Conversion gain = electron charge / capacitance,

$$V = Q / C$$

expressed as microvolts per electron, or electrons per millivolt.

- Estimate conversion gain from design, but must measure to take into account all effects.
- Three ways to measure conversion gain:
  1. Poisson statistics of light detection
  2. Radioactive source
  3. Measurement of reset current as function of output signal.

Statistics of Photon Noise

Photon detection described by Bose-Einstein statistics

(1) $$\langle N^2 \rangle = \langle N \rangle \frac{\exp(hc/\lambda KT)}{\exp(hc/\lambda KT) - 1}$$

(2) $$hc/\lambda >> KT \Rightarrow \langle N^2 \rangle = \langle N \rangle$$

$hc/\lambda = 4.8$ at $\lambda = 10\ \mu m$!

(3) $$\langle N \rangle e = C \langle V \rangle$$

substitute (3) *in* (2) $$\frac{C^2 \langle V^2 \rangle}{e^2} = \frac{C \langle V \rangle}{e}$$

(4) $$\frac{\langle V \rangle}{\langle V^2 \rangle} = \frac{C}{e} \quad in \quad electrons/Volt$$

Photon Shot Noise follow
<u>Poisson Statistics</u>

Variance = Mean

Conversion gain with shot noise STDEV : time series

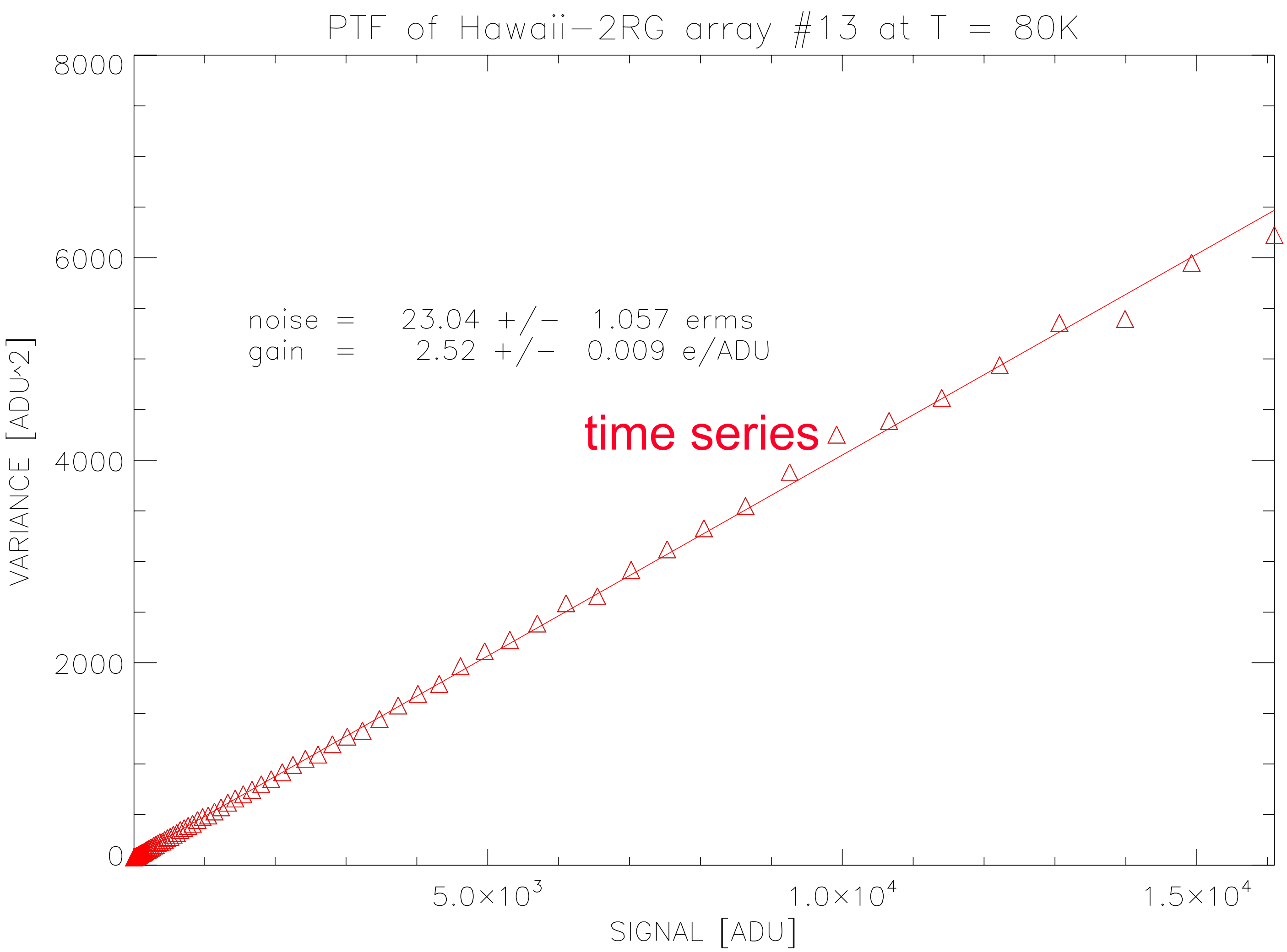

- Plot variance versus signal
- Inverse slope is conversion gain C_o/e in e/V or e/ADU
- Take a series of exposures and from the time series of pixel intensity determine standard deviation for each pixel

Conversion gain with shot noise STDEV : pixel to pixel variation

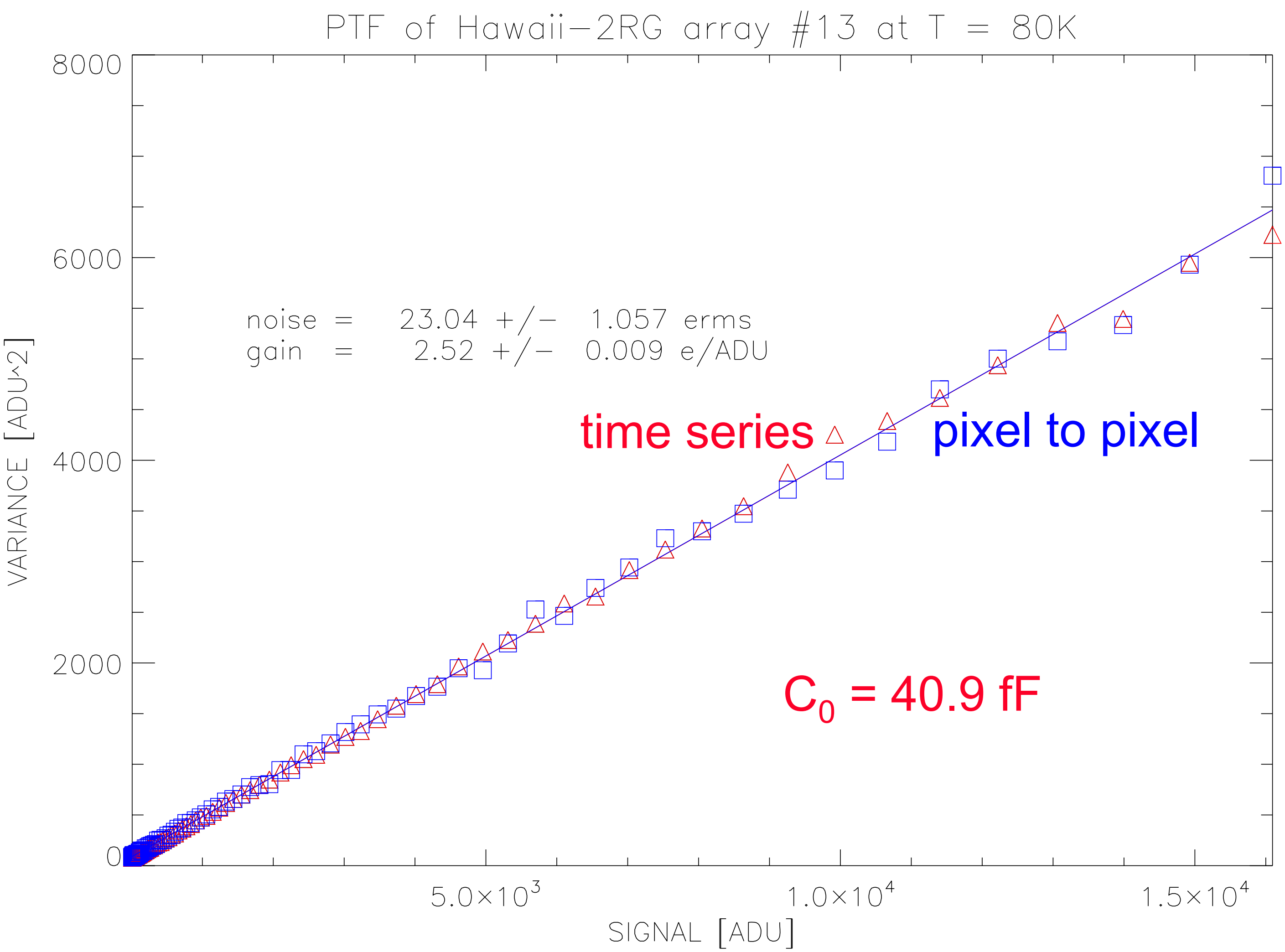

- Plot variance versus signal
- Inverse slope is conversion gain C_o/e in e/V or e/ADU
- Take a difference of two exposures and from pixel to pixel variation determine standard deviation
- Divide by $\sqrt{2}$
- Ergodic system: same result

Conversion gain

- assumtion: noise is dominated by photon shot noise

$$\textit{Photon Statistics}: \langle N^2 \rangle = \langle N \rangle \quad \textit{and} \quad \langle N \rangle e = C_0 \langle V \rangle$$

$$\frac{\langle V \rangle}{\langle V^2 \rangle} = \frac{C_0}{e} \quad \textit{in} \quad \textit{electrons / Volt}$$

- We need a smaller capacitance to bring QE down to below 100 %
- We need larger noise
- Does the shot noise method see a larger capacitance ?
  Is there capacitive coupling between pixels?
- Answer: measure nodal capacitance C_0 directly by capacitance comparison (cap method)

Conversion gain by capacity comparison

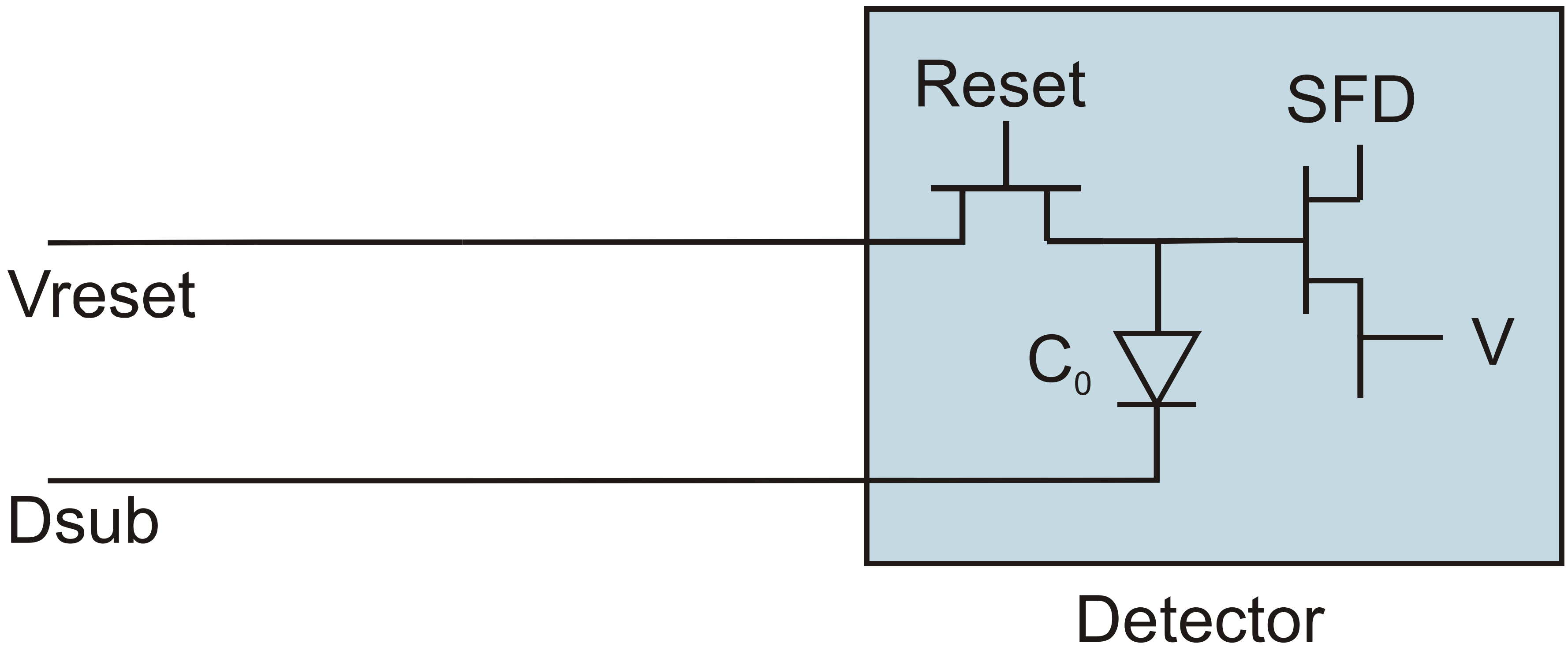

- Charge for resetting node capacity is provided by bias voltage Vreset

Conversion gain by capacity comparison

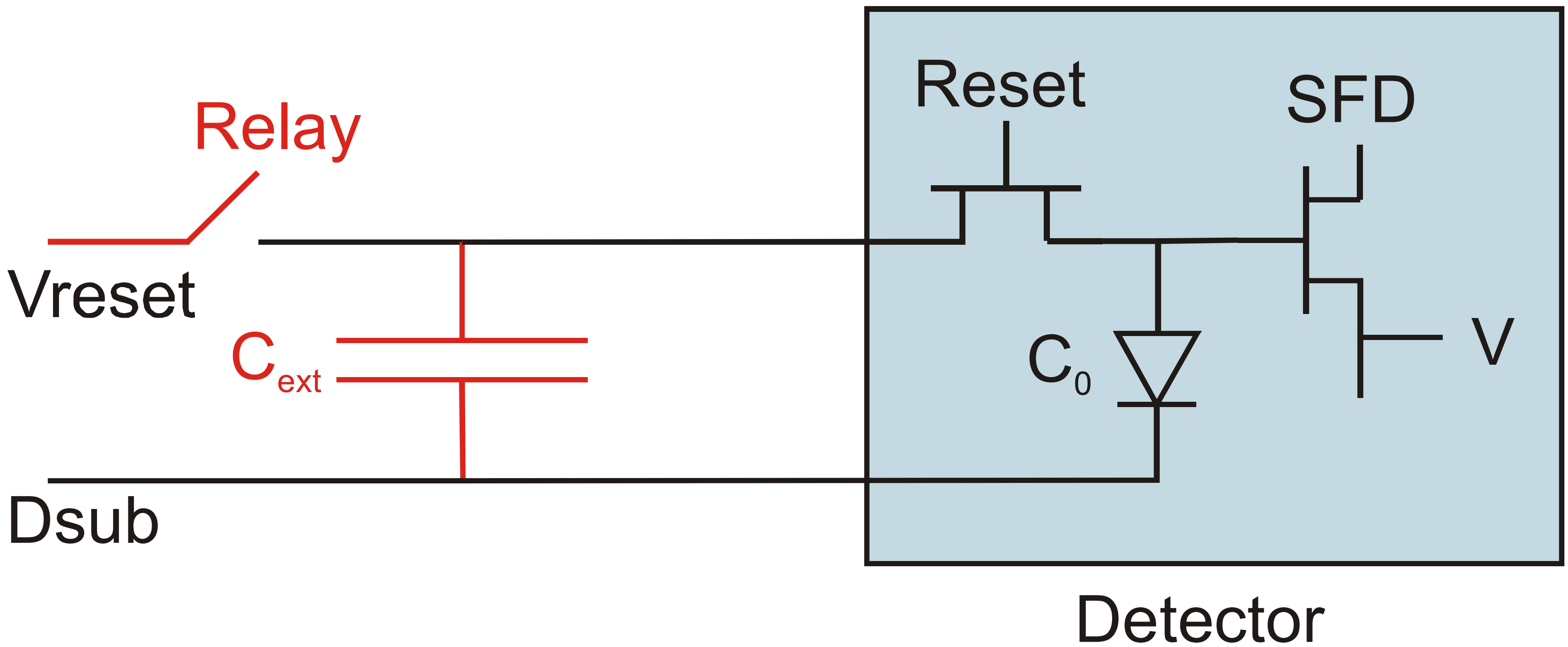

$$(V_{ext,1} - V_{ext,2})C_{ext} = \sum_{n=1}^{nframes} \sum_{i=1}^{npixel} V_{n,i} C_0$$

Conversion gain by capacitance comparison method

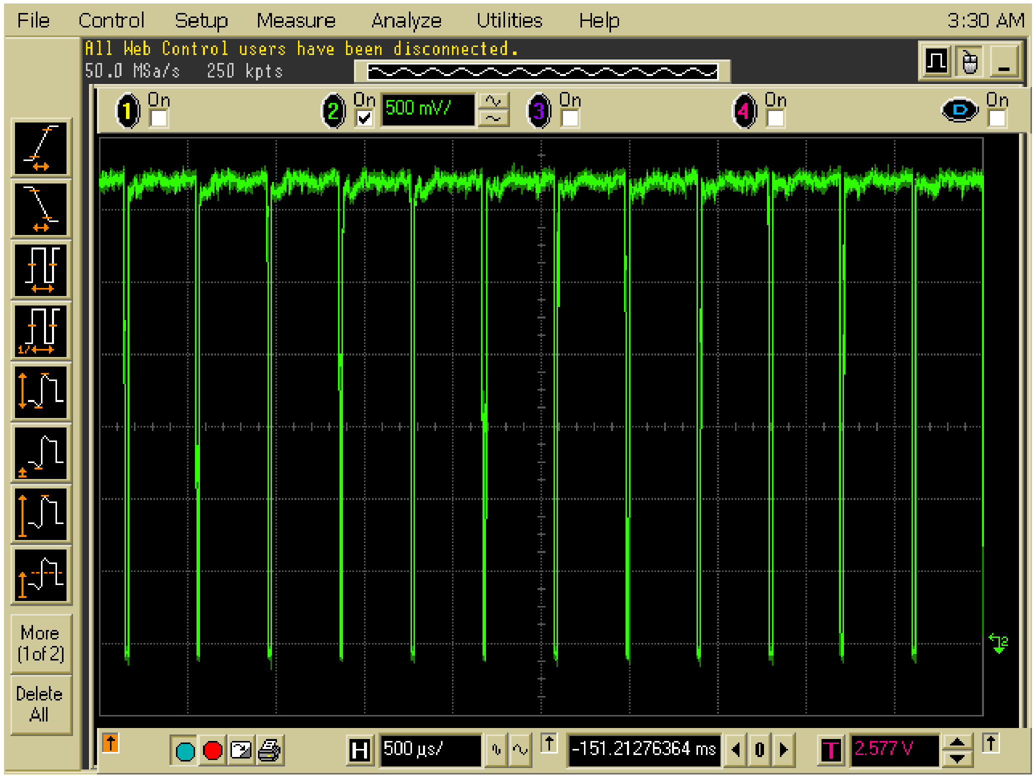

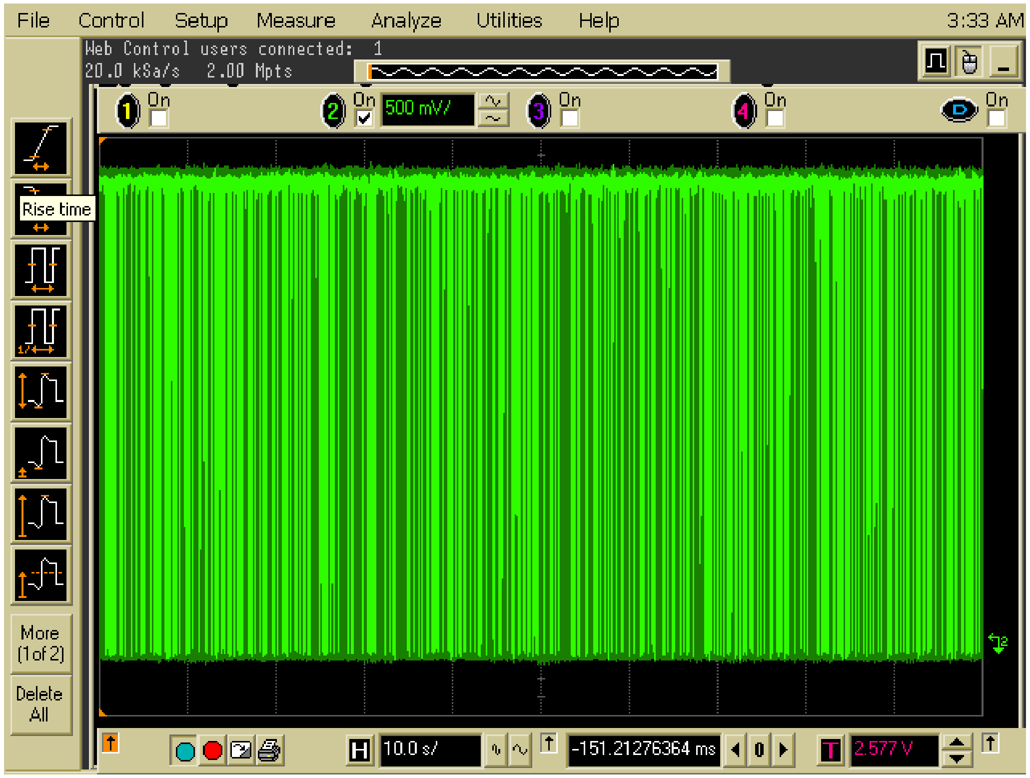

No photon flux

Conversion gain by capacitance comparison method

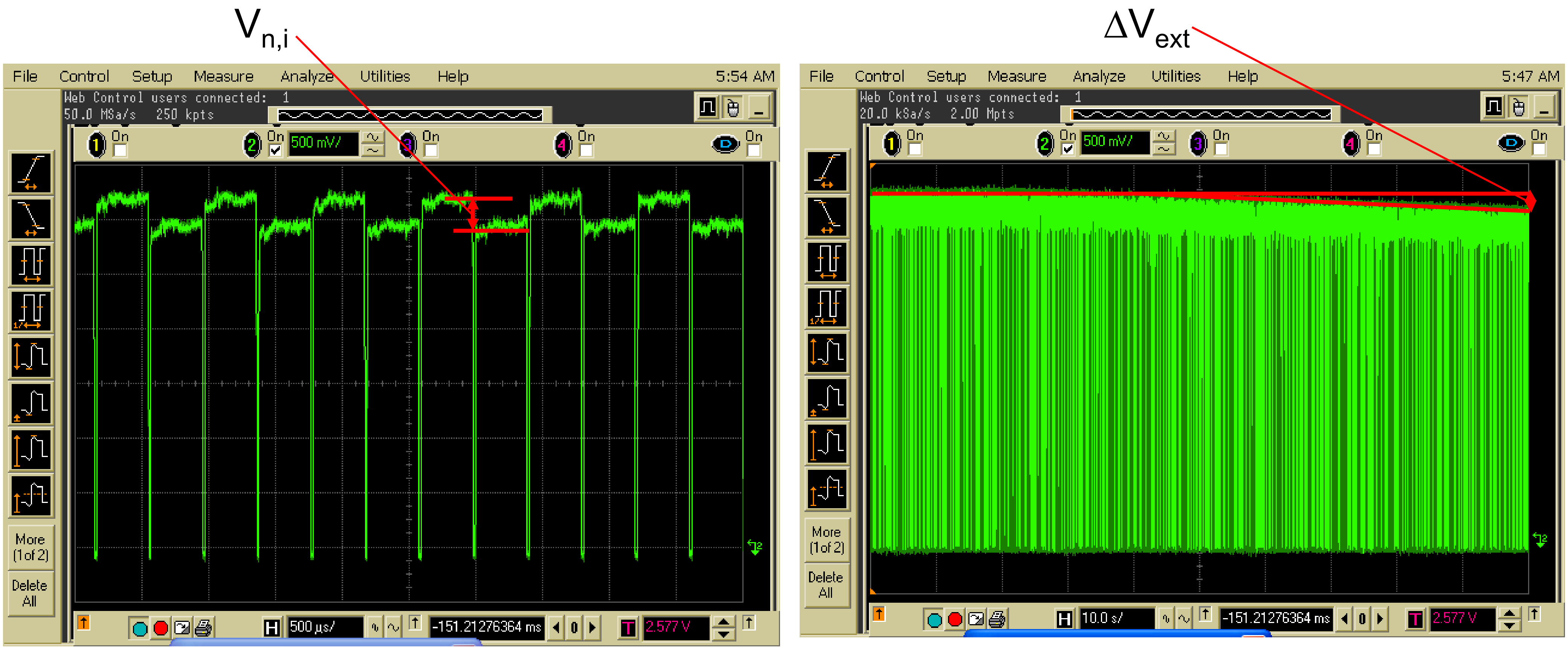

small photon flux

Conversion gain by capacitance comparison method

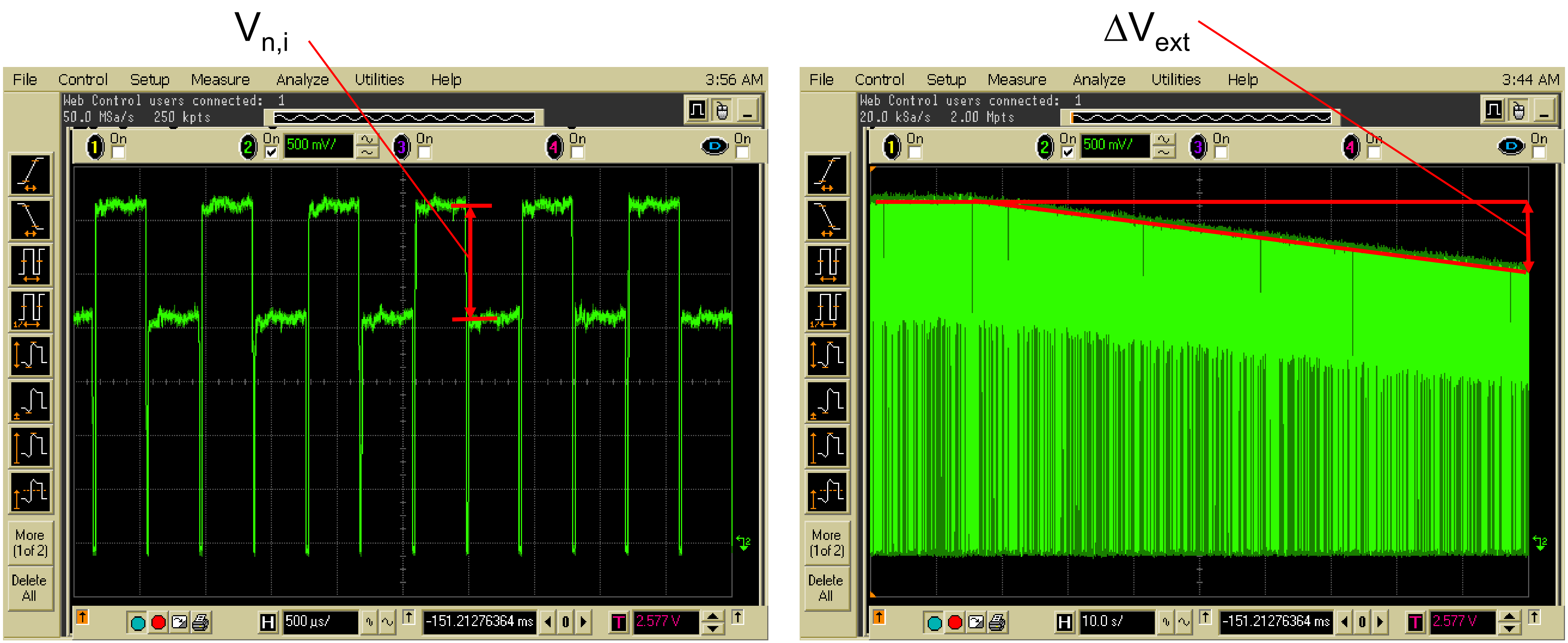

large photon flux

Conversion gain by capacitance comparison method

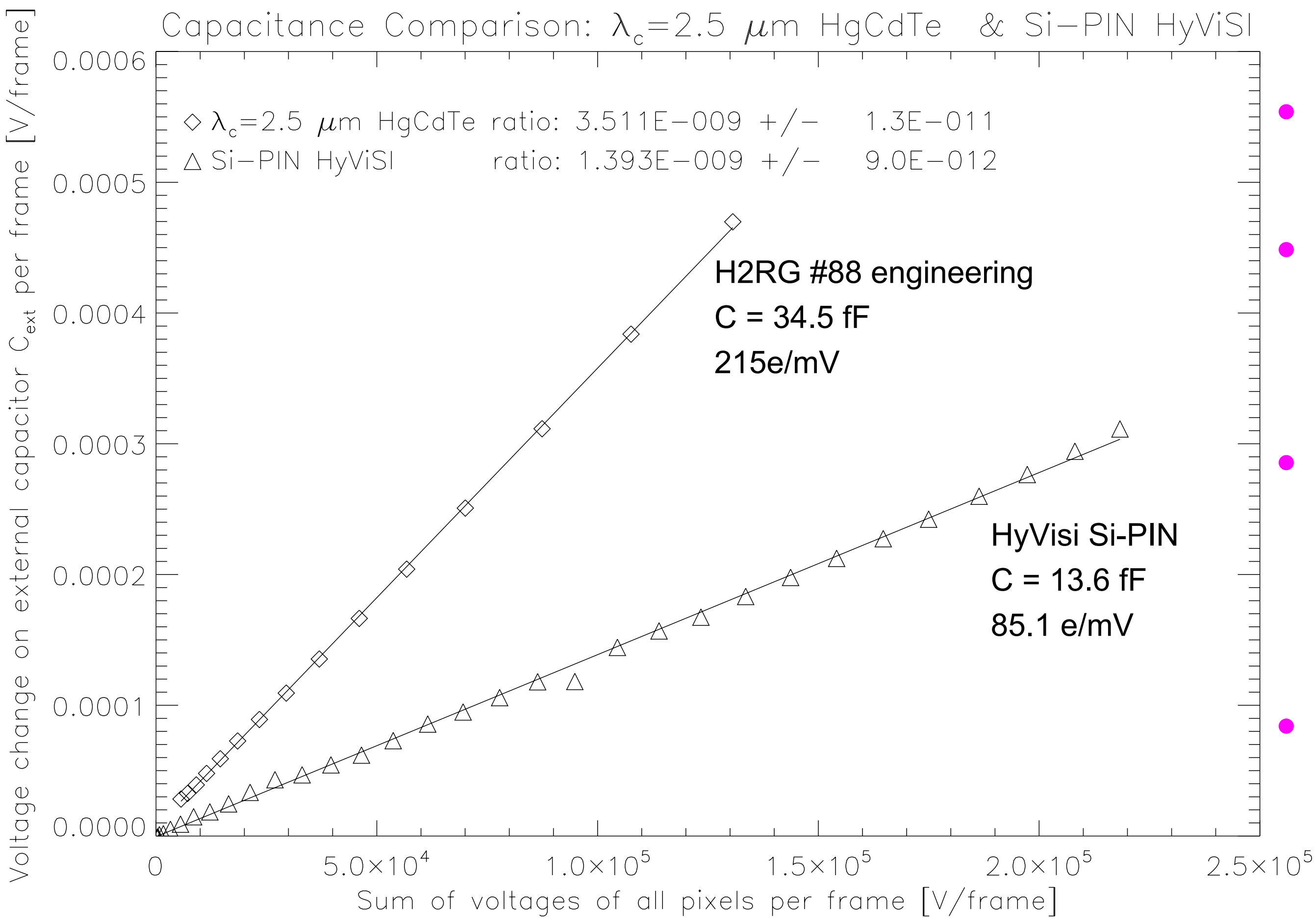

- nodal capacitance
  $C_0 = C_{ext}$ * slope
- Slope:
  voltage change on C_{ext} /
  sum of voltages of all pixels
- H2RG #88
  215 e/mV
  C_0 = 34.5 fF
  (C_0= 40.3 fF shot noise)
- HyVisi Si-PIN
  85.1 e/mV
  C_0 = 13.6 fF
  (C_0= 27 fF shot noise)

Test of shot noise versus capacitance comparison with Fe55

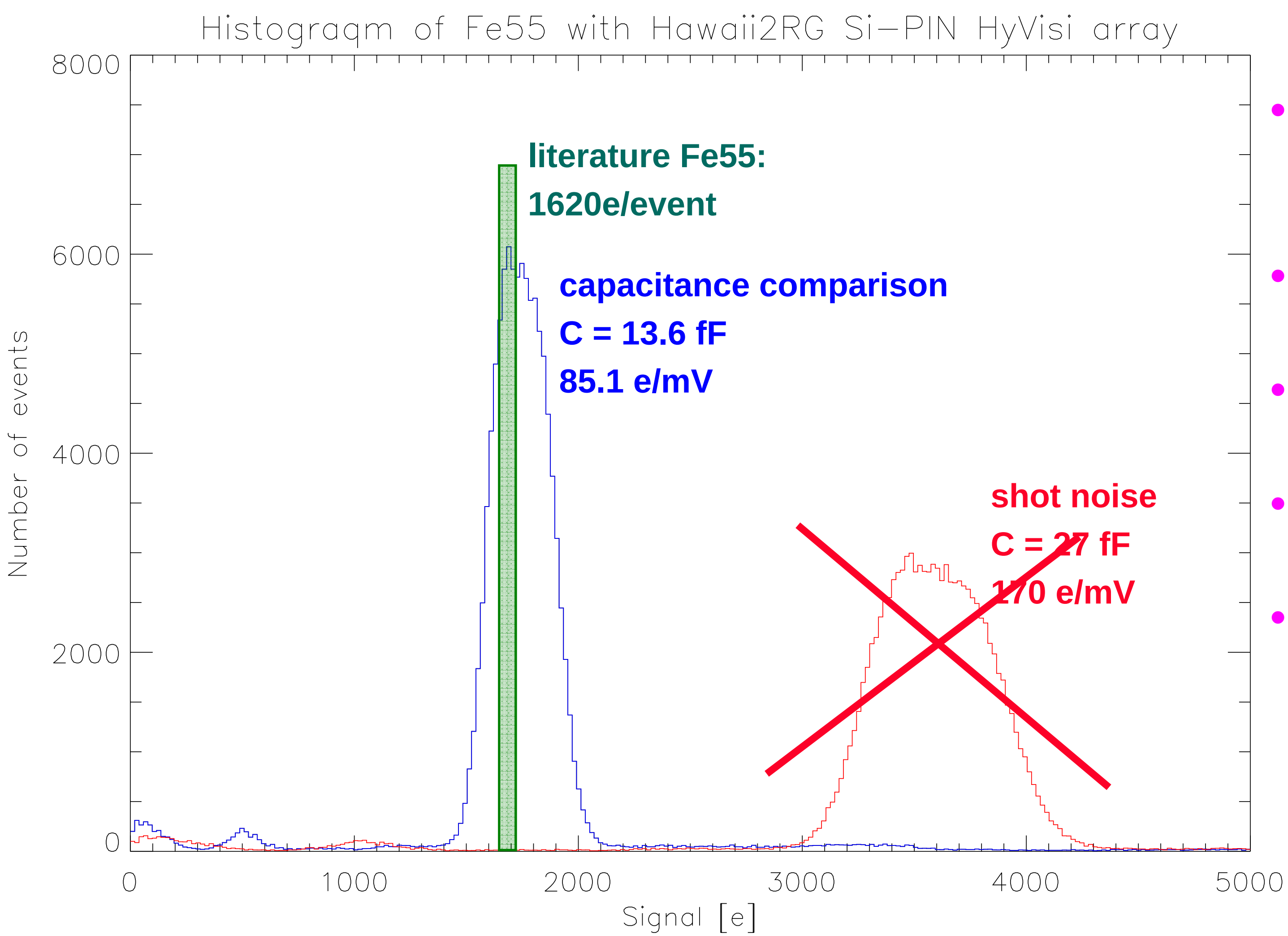

- HyViSi Si-PIN array hybridized to Hawaii2RG mux
- Fe55 ideal for verifying PTF methods
- Shot noise: C_{node} = 27 fF
- Capacitance comparison: C_{node} = 13.6 fF
- Shot noise method wrong

Need good radioactive sources for IR detectors

- For Infrared Hybrids
  - No known good radioactive source
  - Amount of charge deposited into HgCdTe depends on bandgap / cutoff wavelength
  - Possibly Fe55 can be used for InSb?
    - ~2500 electrons deposited
- This area needs investigation

Photon counting in InSb with spectral resolution

- Aladdin 1Kx1K InSb array
- Fe55
- K_α line 6KeV
- 1620 e- / photon in Si

Photon counting in InSb with spectral resolution

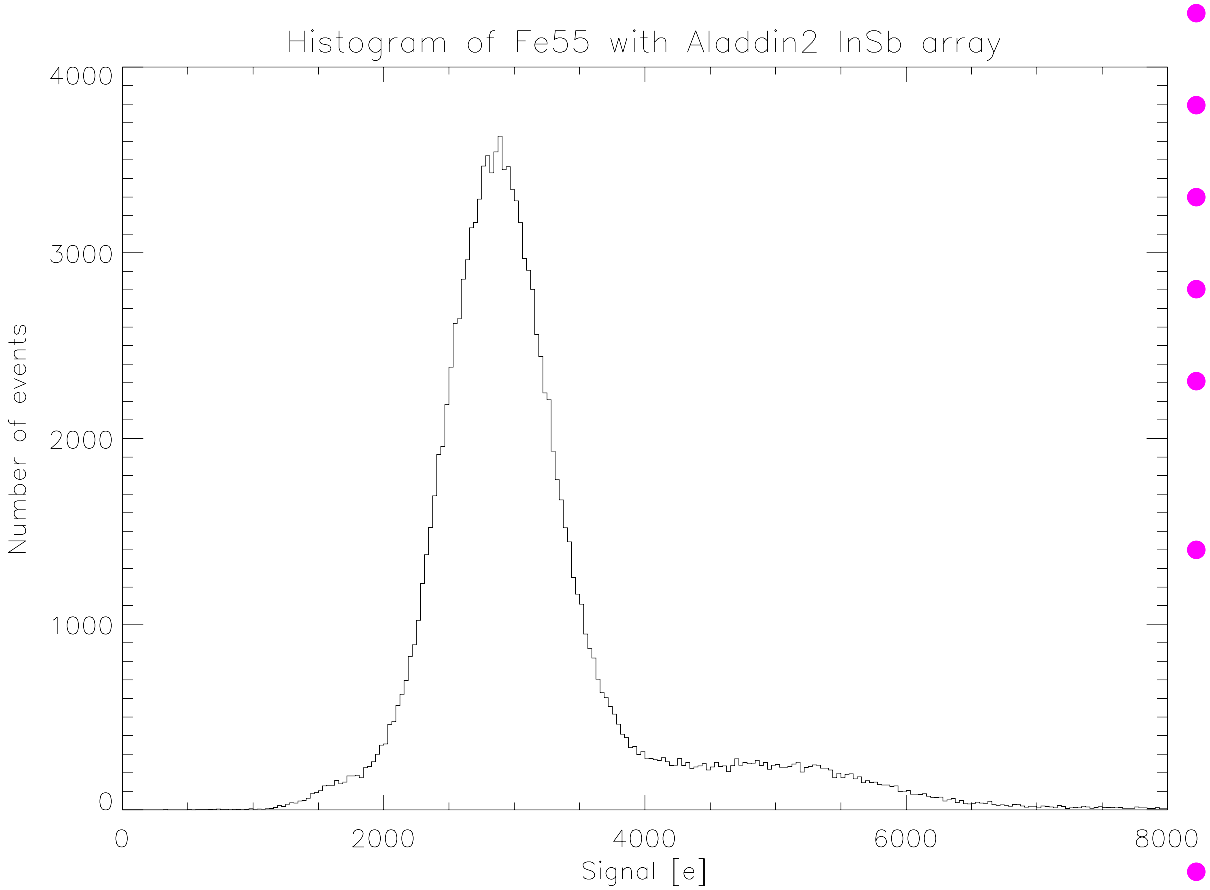

- Aladdin 1Kx1K InSb array
- Fe55
- K_α line 6KeV
- 1620 e / photon in Si
- Measured:
  2500 e / photon in InSb
- Because of smaller bandgap InSb is expected to have better energy resolution than Si
- Who knows ???? e/photon for K_α in InSb

Interpixel capacitive coupling

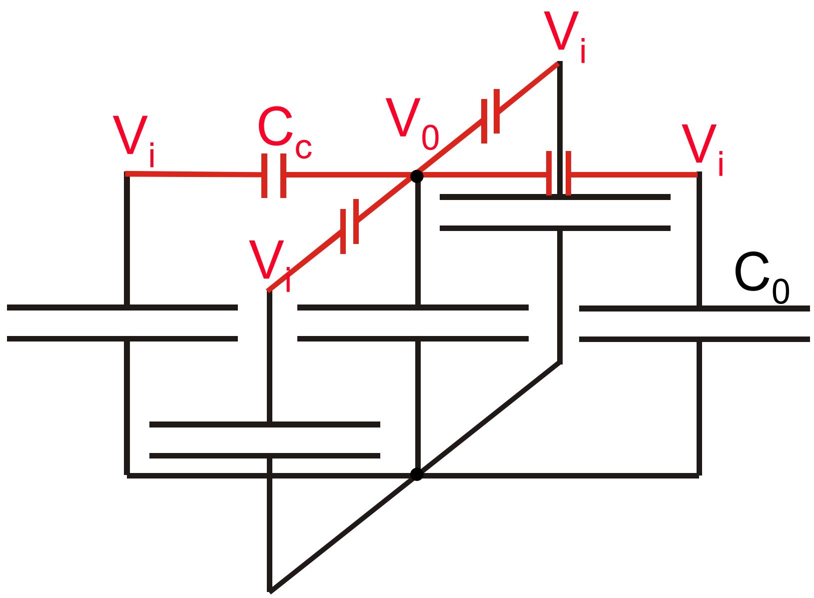

- C_0 node capacity of pixel
- Introduce coupling capacity C_c
  $x = C_c/C_0$
- Apparent capacity for shot noise:
  $C=C_0\,(5x+1)/(x+1)$
- V_0+4V_i

Interpixel capacitive coupling

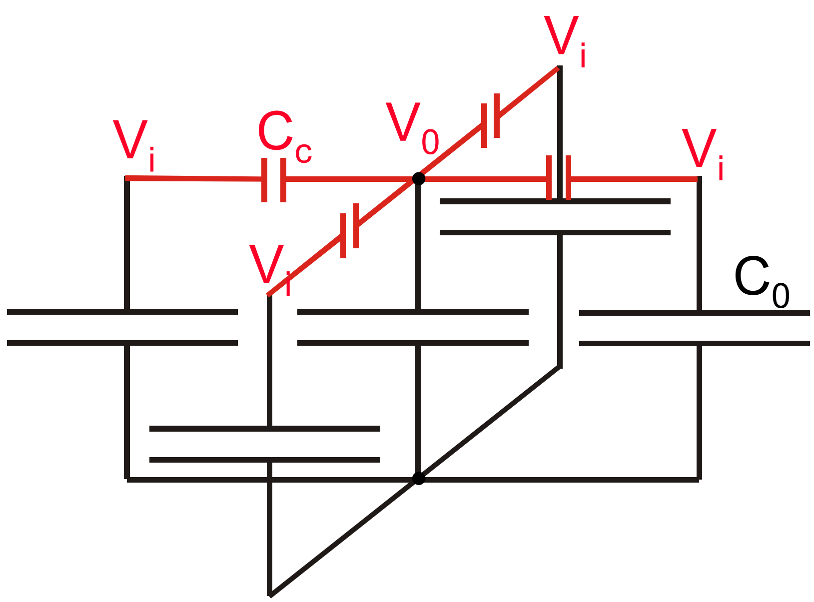

See Andrew Moore et al.
Interpixel capacitance in
Non-destructive FPA's
SPIE 5167,204 (2004)

- C_0 node capacity of pixel
- Introduce coupling capacity C_c
  $x = C_c/C_0$
- Apparent capacity for shot noise:
  $C=C_0\,(5x+1)/(x+1)$
- $V_0+4V_i = V$
- photometry conserved
- for uniform illumination no signal charge stored on C_c
- C_c reduces noise , but also sharpness and contrast

Interpixel capacitive coupling

snapshot:
single
photons

integrated
Image:

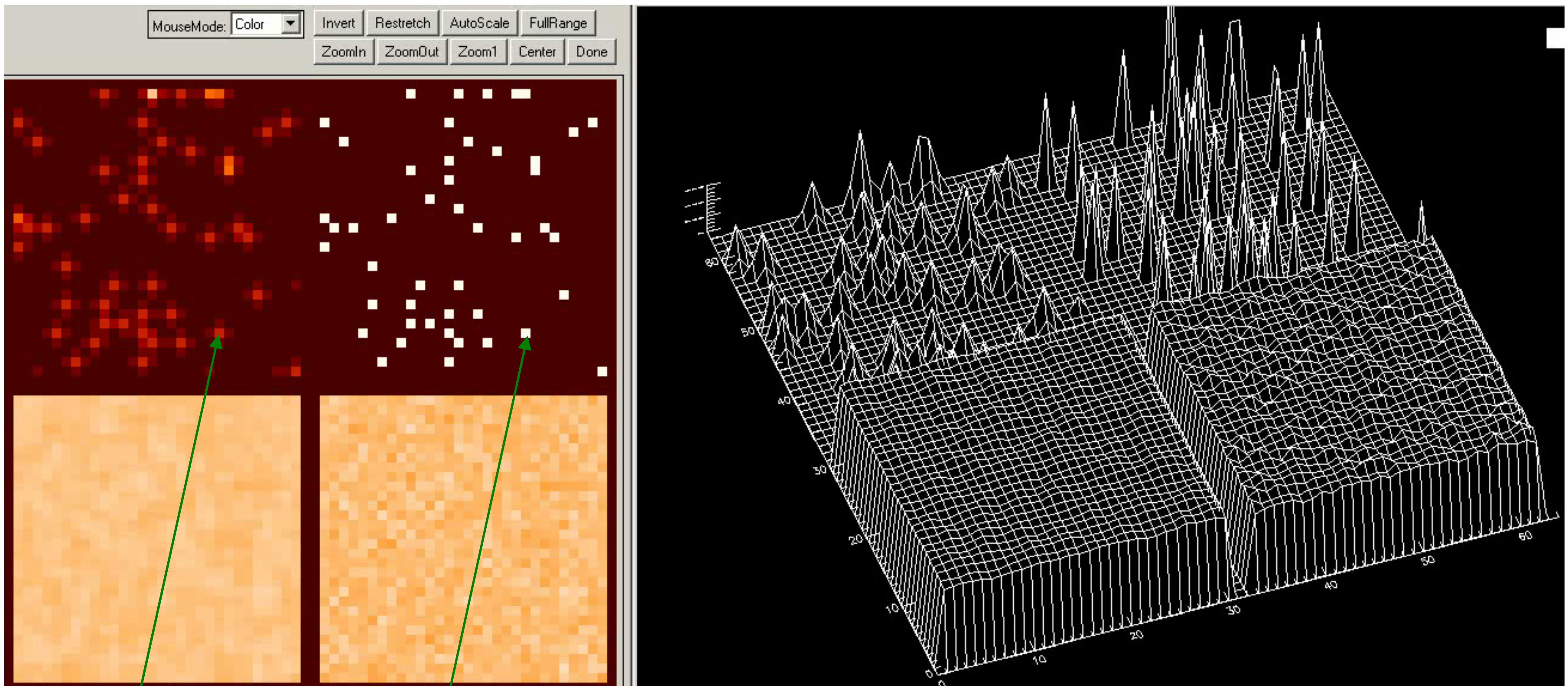

coupling | no coupling

response on
neighbor pixels

same signal

low noise | high noise

coupling | no coupling

same signal

low noise | high noise

Interpixel capacitive coupling

snapshot: single photons

integrated Image:

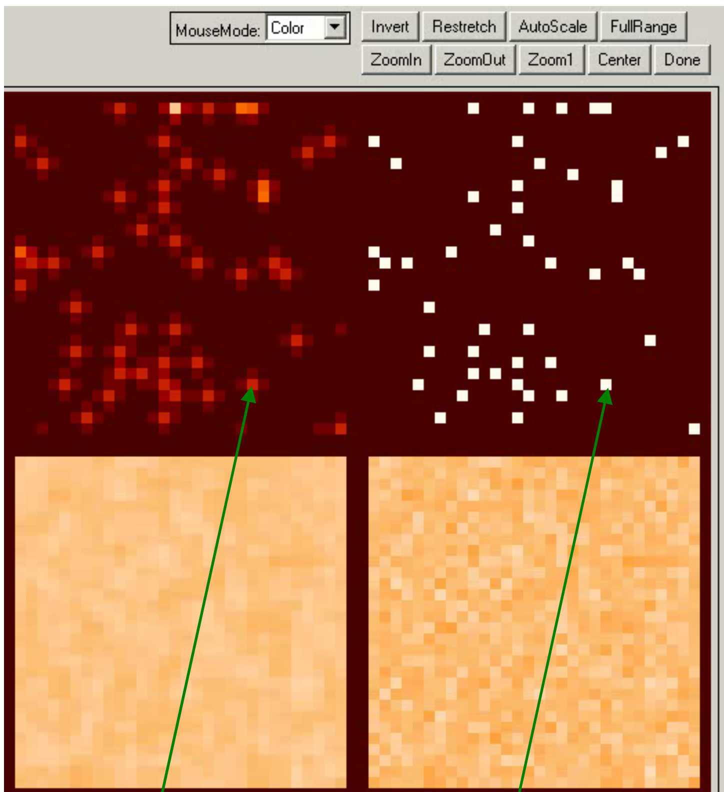

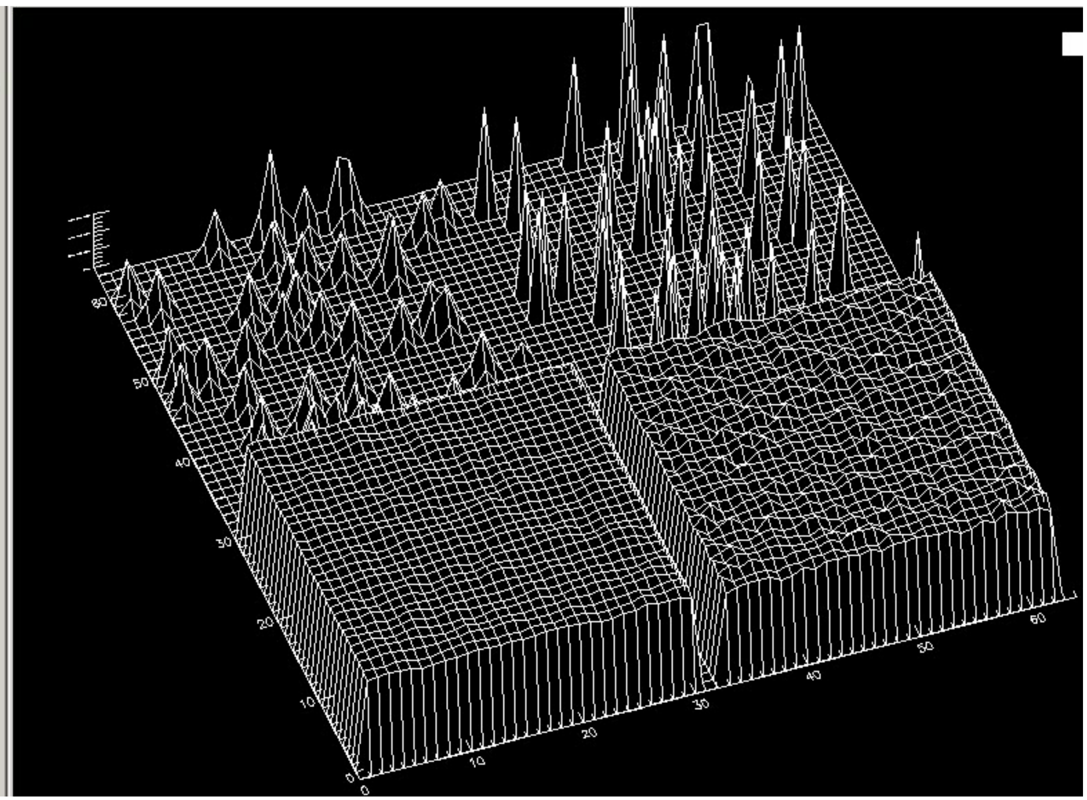

coupling

no coupling

response on neighbor pixels

same signal

low noise

high noise

coupling

no coupling

same signal

low noise

high noise

Shot noise reduction versus coupling capacity

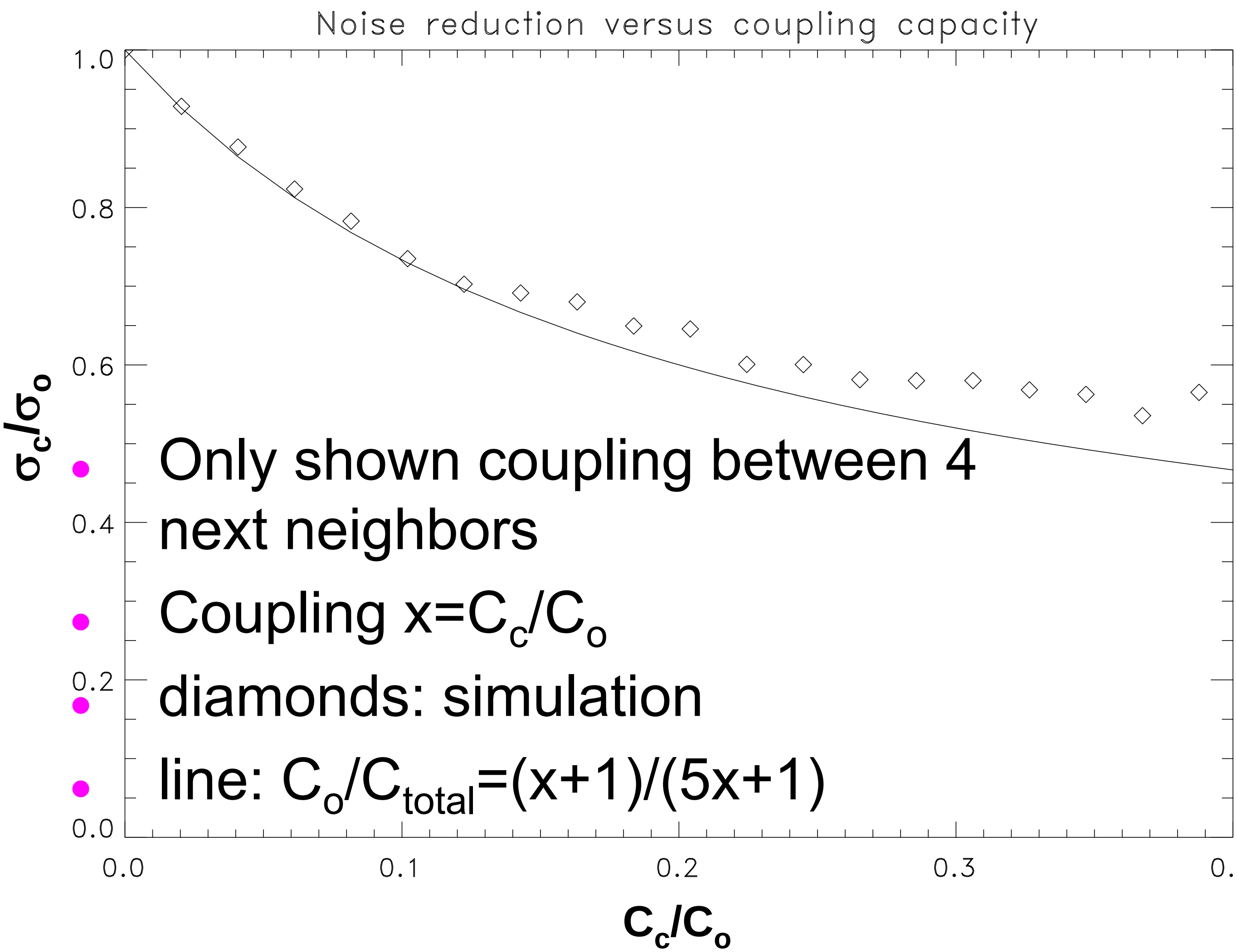

- Only shown coupling between 4 next neighbors
- Coupling $x=C_c/C_o$
- diamonds: simulation
- line: $C_o/C_{total}=(x+1)/(5x+1)$

Quantum efficiency versus wavelength

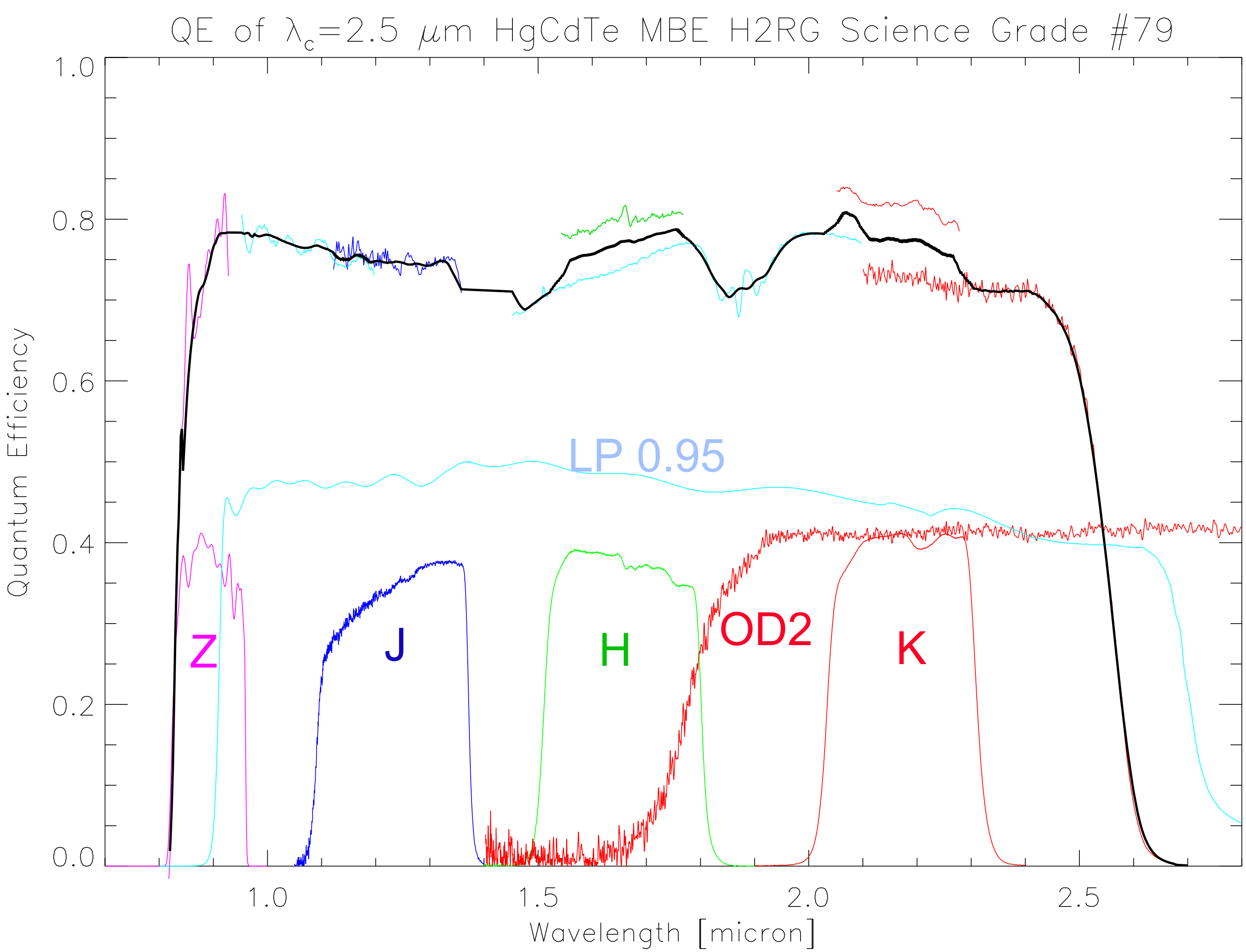

- Science grade #79
- K: 0.82
  H: 0.80
  J: 0.75
  Z: 0.78

  (transmission of used filters indicated)
- QE with Si-PIN < 100%
  (see R. Dorn)

HgCdTe
p^+-n junction under bias

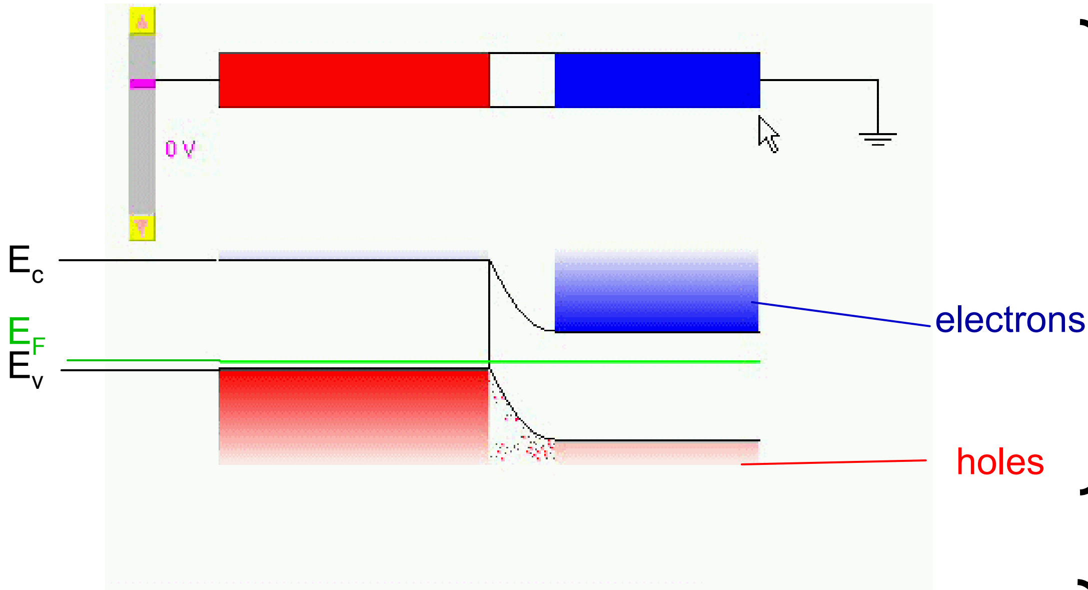

p^+ : $N_A >> N_D$

Band diagram and current components

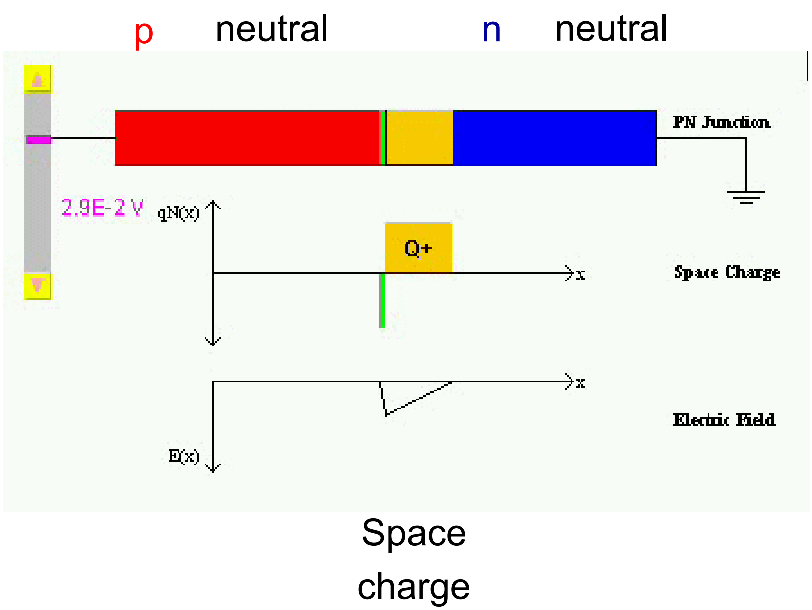

Space charge and electric field

p$^+$-n junction under bias

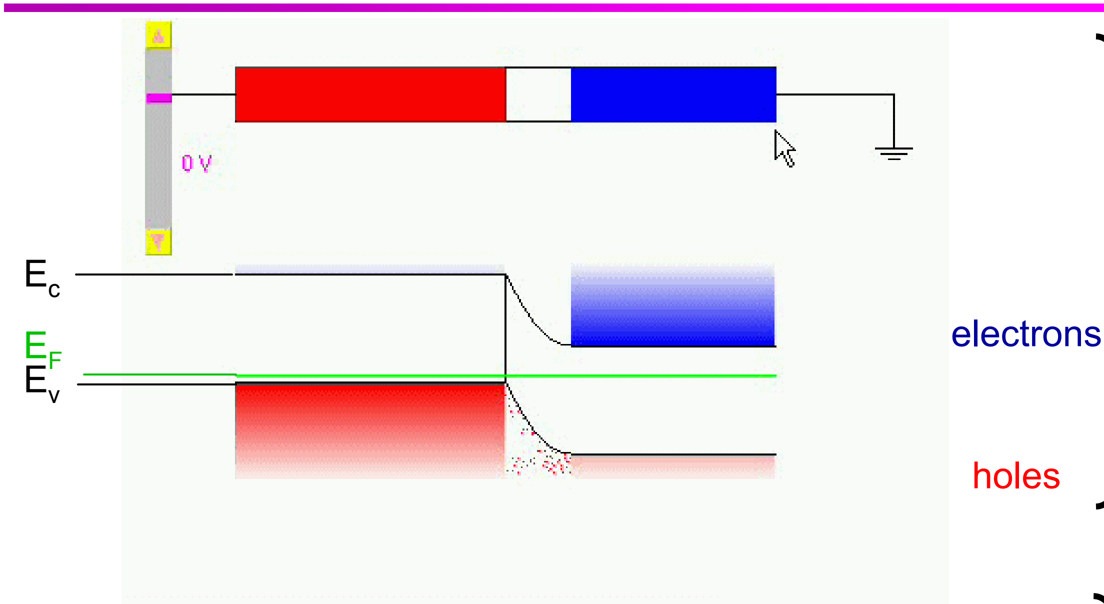

p neutral n neutral

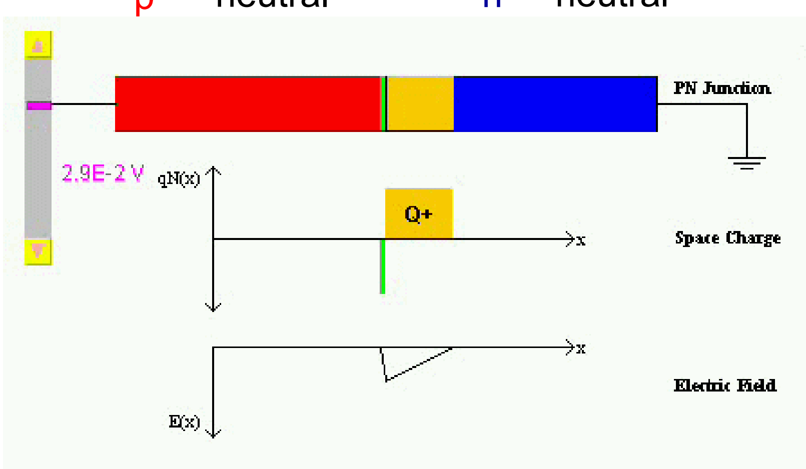

Space charge

Increase bias voltage

Band diagram and current components

$$C(V) = \sqrt{\frac{e\varepsilon}{2(V_{bi} + V_{DSUB} - V_{RESET})} \frac{N_a N_d}{N_a + N_d}}$$

Space charge and electric field

Capacitance versus bias voltage

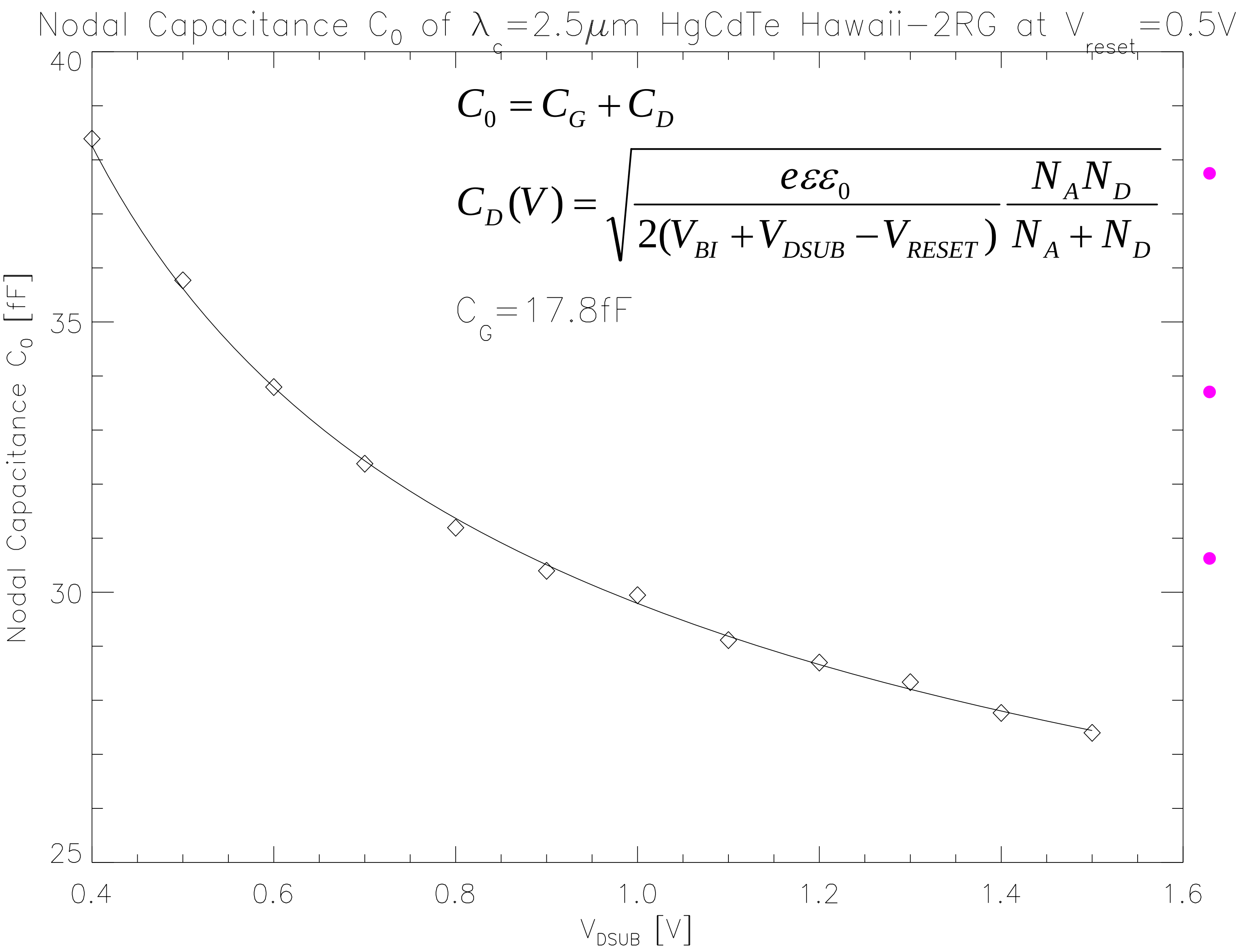

- Diode capacitance is dependent on voltage across diode
- Can be measured with capacitance comparison method
- Capacitance is changing during detector integration

$1/C^2$ plot

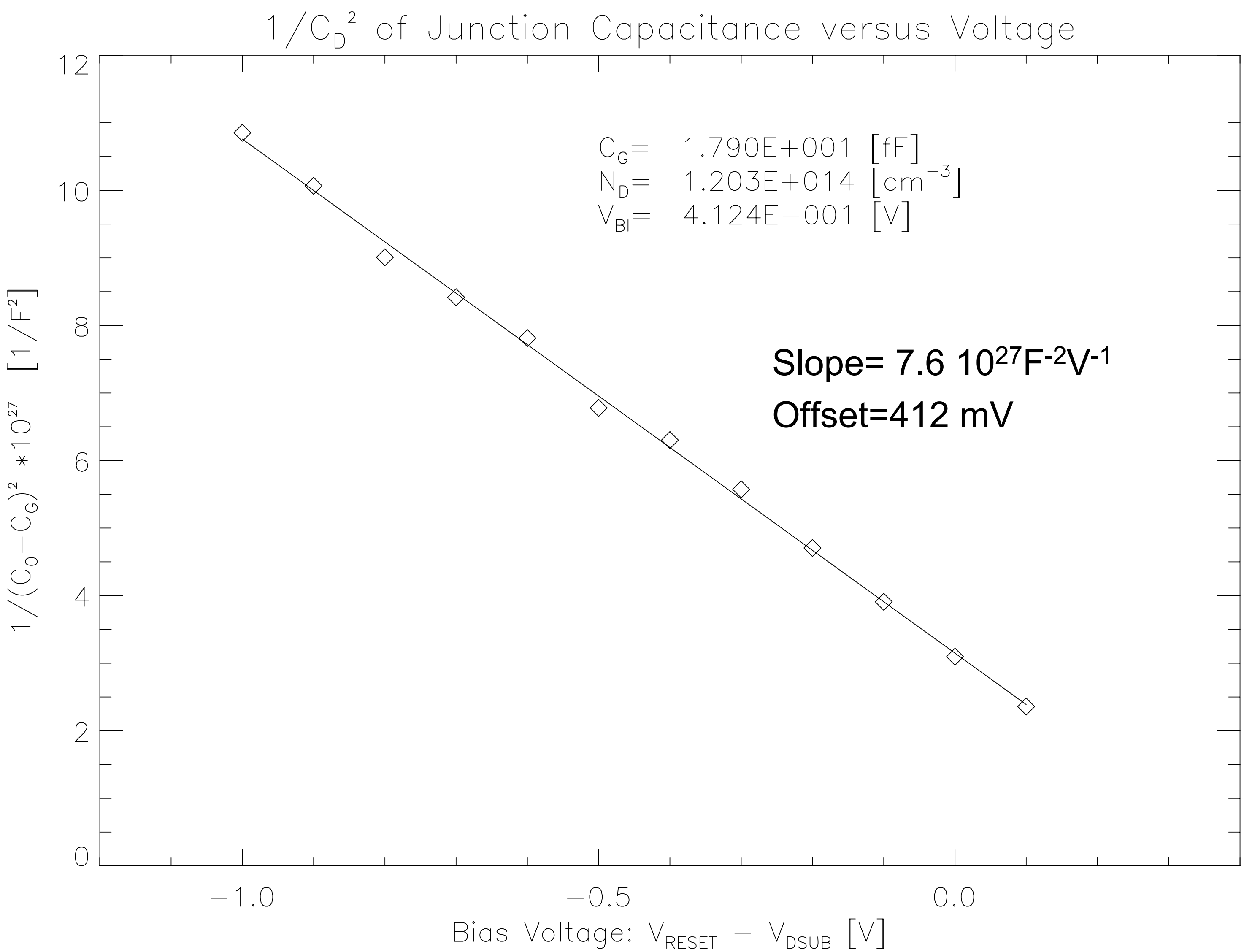

- For p^+-n diode
  $N_A >> N_D$

  $$N_D = -\frac{2}{e\varepsilon\varepsilon_0}\frac{1}{d(1/C_D{}^2)/dV}$$

  with ε=14.67 and
  slope of $7.6\ 10^{27} F^{-2} V^{-1}$
  doping concentration
  $N_D = 1.2\ 10^{14}\ cm^{-3}$
- V_{BI}=412 mV
- Maximum of linear correlation coefficient
  C_G=17.9 fF

Capacitance versus bias voltage

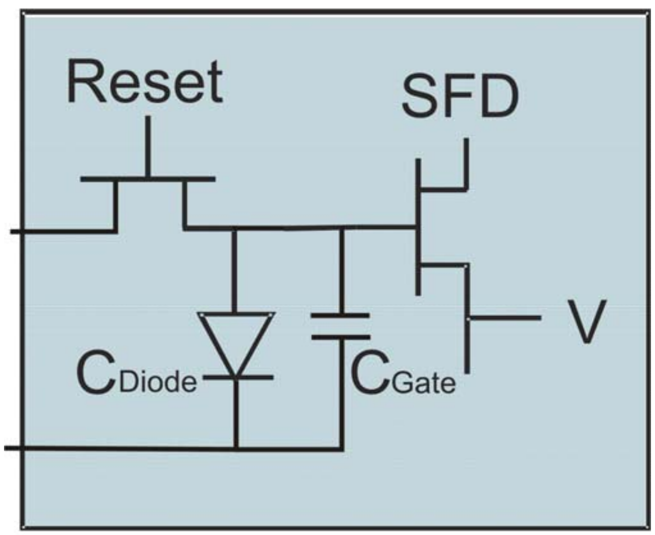

Detector

$C_0=C_D+C_G$

- Measurement of C(V) delivers
- built in voltage V_{bi}
  V_{bi} = 0.432V (at V_{reset}=0.5V)
- Doping density N_D
  N_D=1.2E14 cm^{-3}
- Gate and diode capacitance C_G , C_D
  C_G = 17.8 fF
  C_D = 9.5 fF
- diode capacitance is only 35 % of total capacitance
- recommendation to manufacturer: make C_G smaller to reduce readout noise
- Measurement of all physical parameters of junction for model of detector nonlinearity

Method to determine impulse response of capacitive coupling between pixels

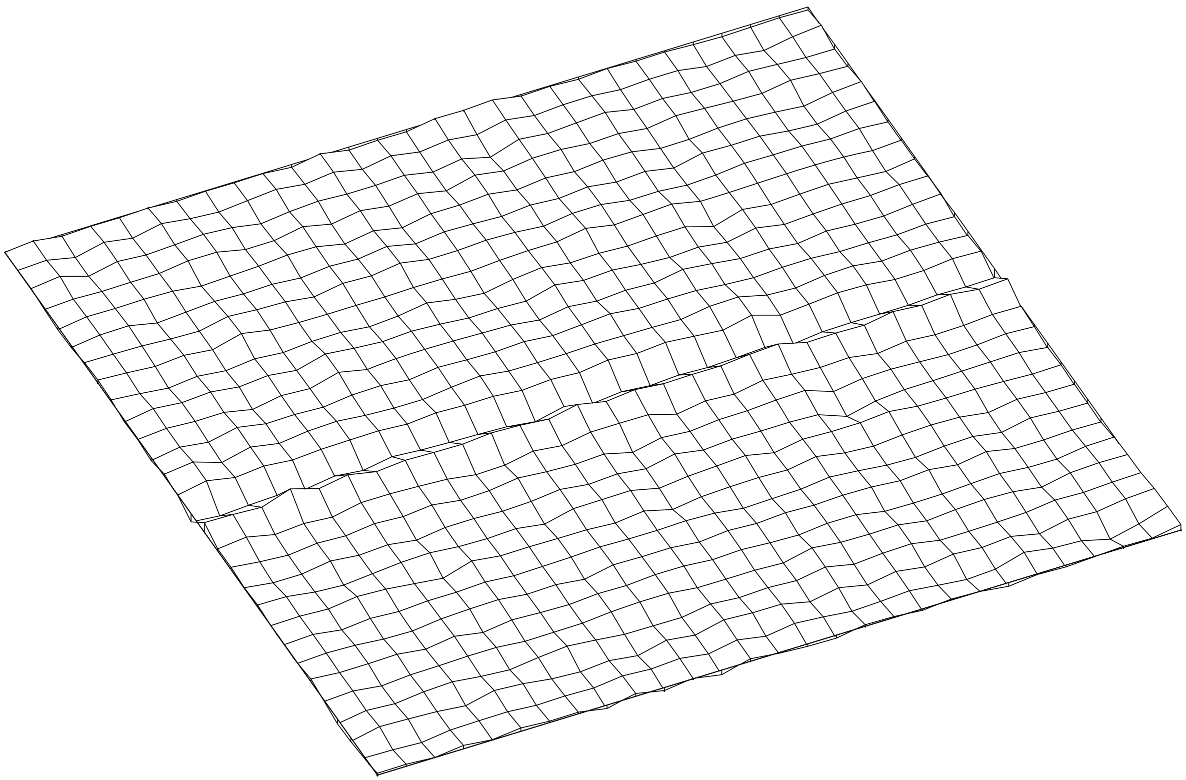

- uniformly illuminate array with high flux
  integration time 1 s
- Use guide mode of Hawaii-2RG mux
  guide window size 1x1
- Reset single pixel before readout
  integration time < 500μs

Method to determine impulse response of capacitive coupling between pixels

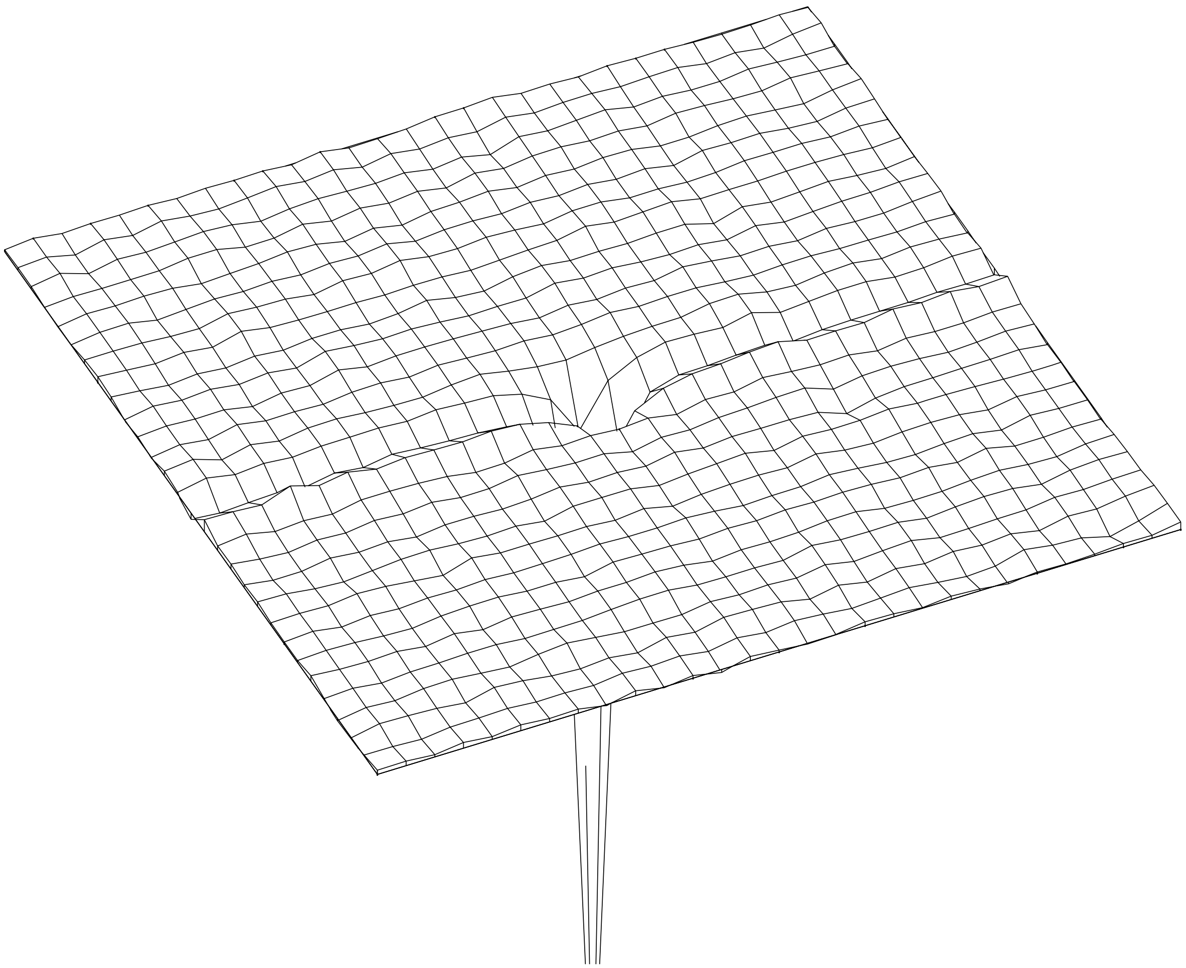

- uniformly illuminate array with high flux
  integration time 1 s
- Use guide mode of Hawaii-2RG mux
  guide window size 1x1
- Reset single pixel before readout
  integration time < 500μs
- Observe
  capacitive coupling
  on next neighbors

Impulse response of capacitive coupling by Single Pixel Reset

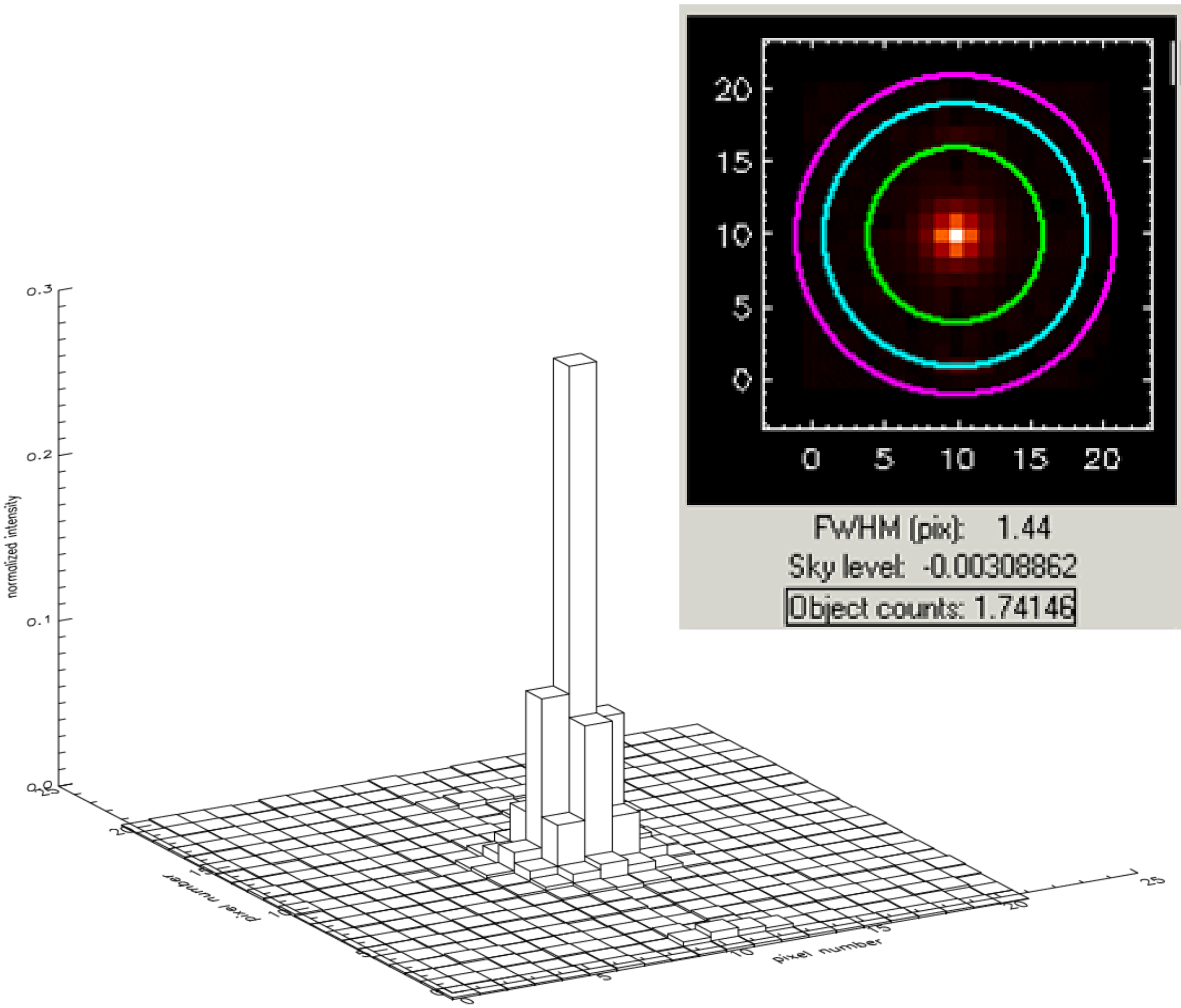

- Subtract images with single pixel reset off -on normalize to 1
- Result is PSF of capacitive coupling between pixels
- if normalized to unit area result is impulse response
- detector PSF can be used for deconvolution of image

Comparison of HgCdTe / Si-PIN PSF measured with single pixel reset

- Hawaii-2RG HgCdTe array
- 10 % of total energy in neighboring pixels
- Coupling to next neighbor 2.5 %

- Hawaii-2RG Si-PIN HyViSI array
- 42 % of total energy in neighboring pixels.
- Coupling to next neighbor 10 %.
- Confirmed by optical spot measurement on HyViSI (R. Dorn)

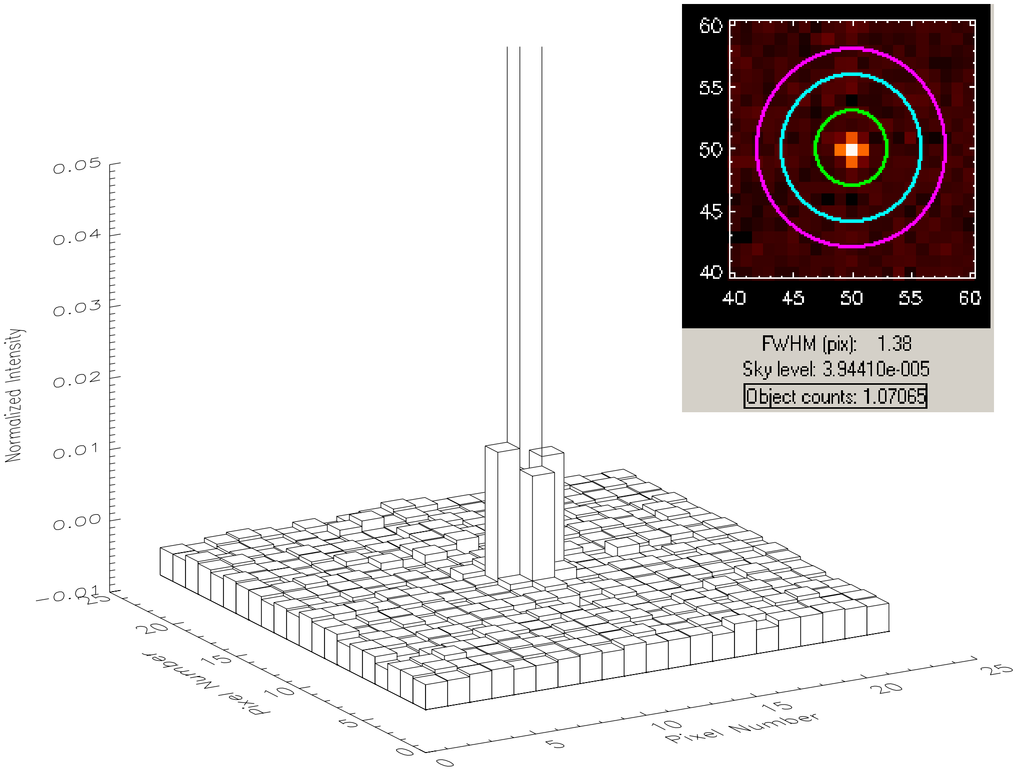

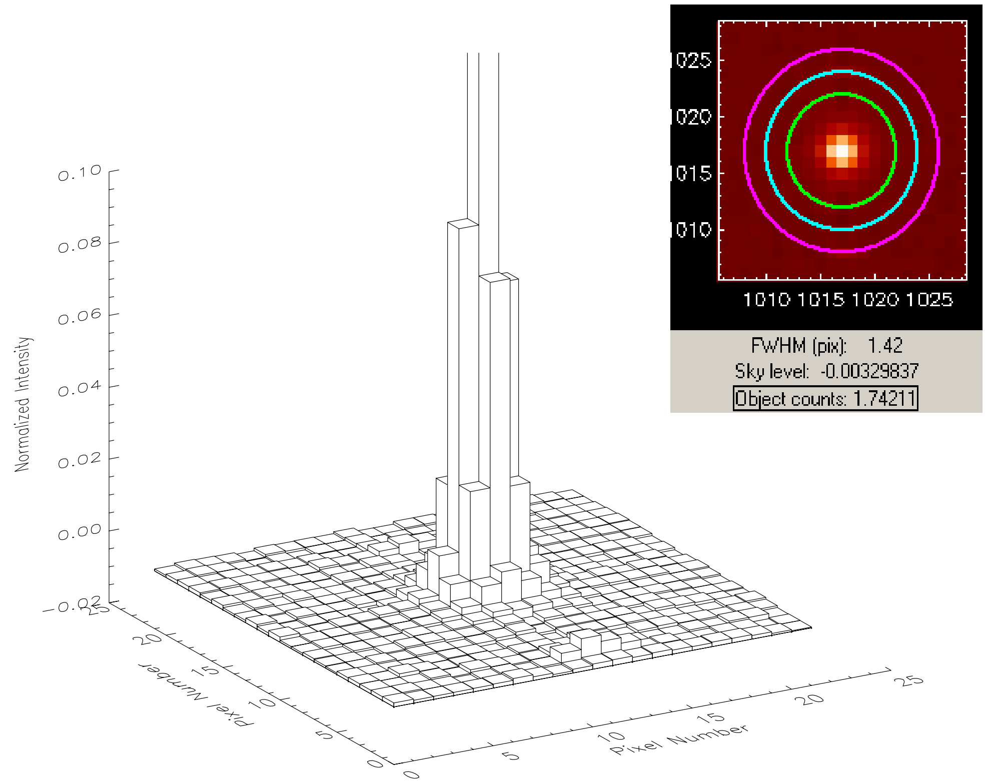

Comparison of HgCdTe / Si-PIN PSF measured with single pixel reset

- Hawaii-2RG HgCdTe array
- 10 % of total energy in neighboring pixels
- Coupling to next neighbor 2.5 %
- Download: www.eso.org/~gfinger

- Hawaii-2RG Si-PIN HyViSI array
- 42 % of total energy in neighboring pixels.
- Coupling to next neighbor 10 %.
- Confirmed by optical spot measurement on HyViSI (R. Dorn)

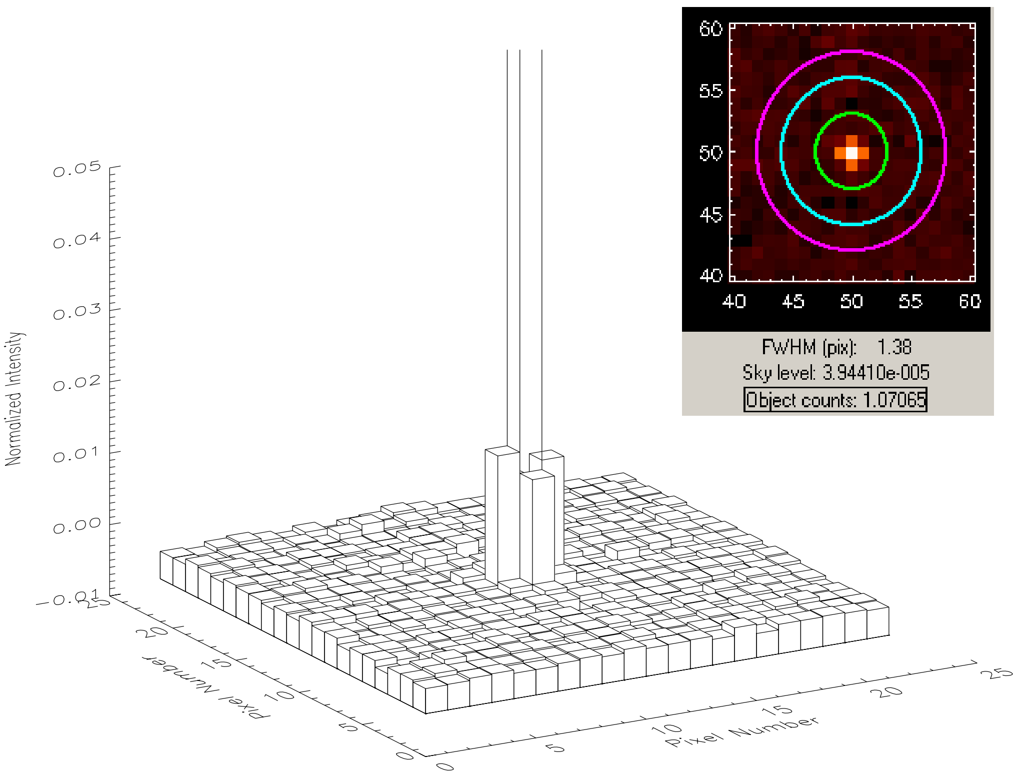

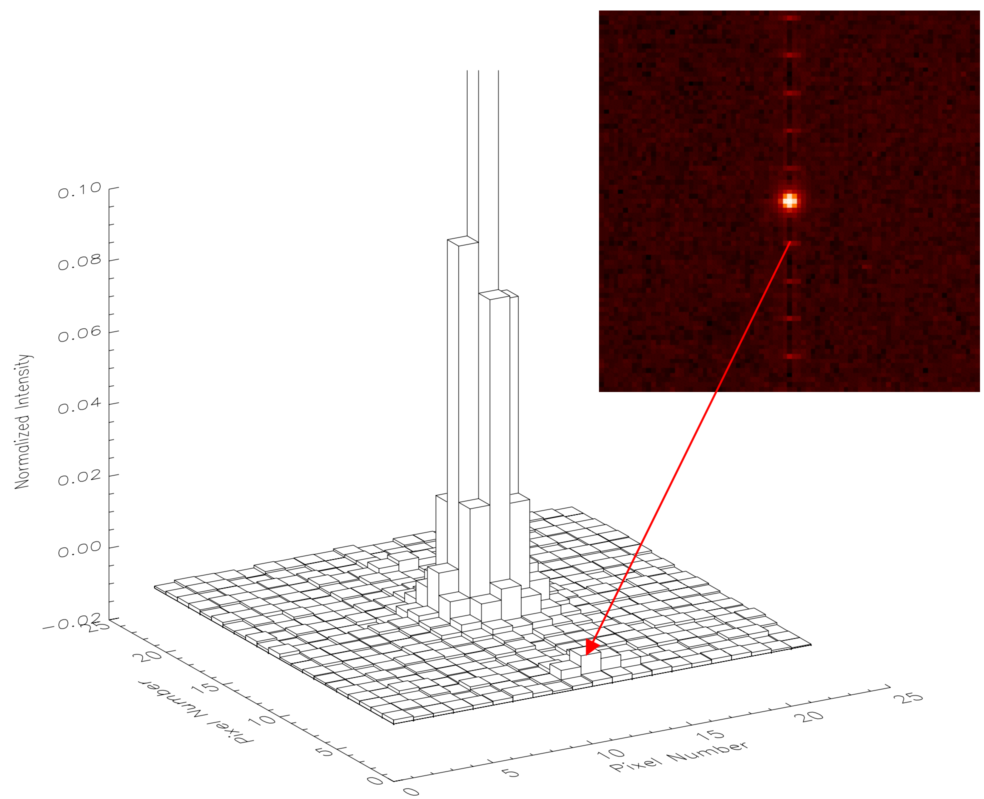

Structure of HgCdTe and Si-PIN Hawaii-2RG arrays

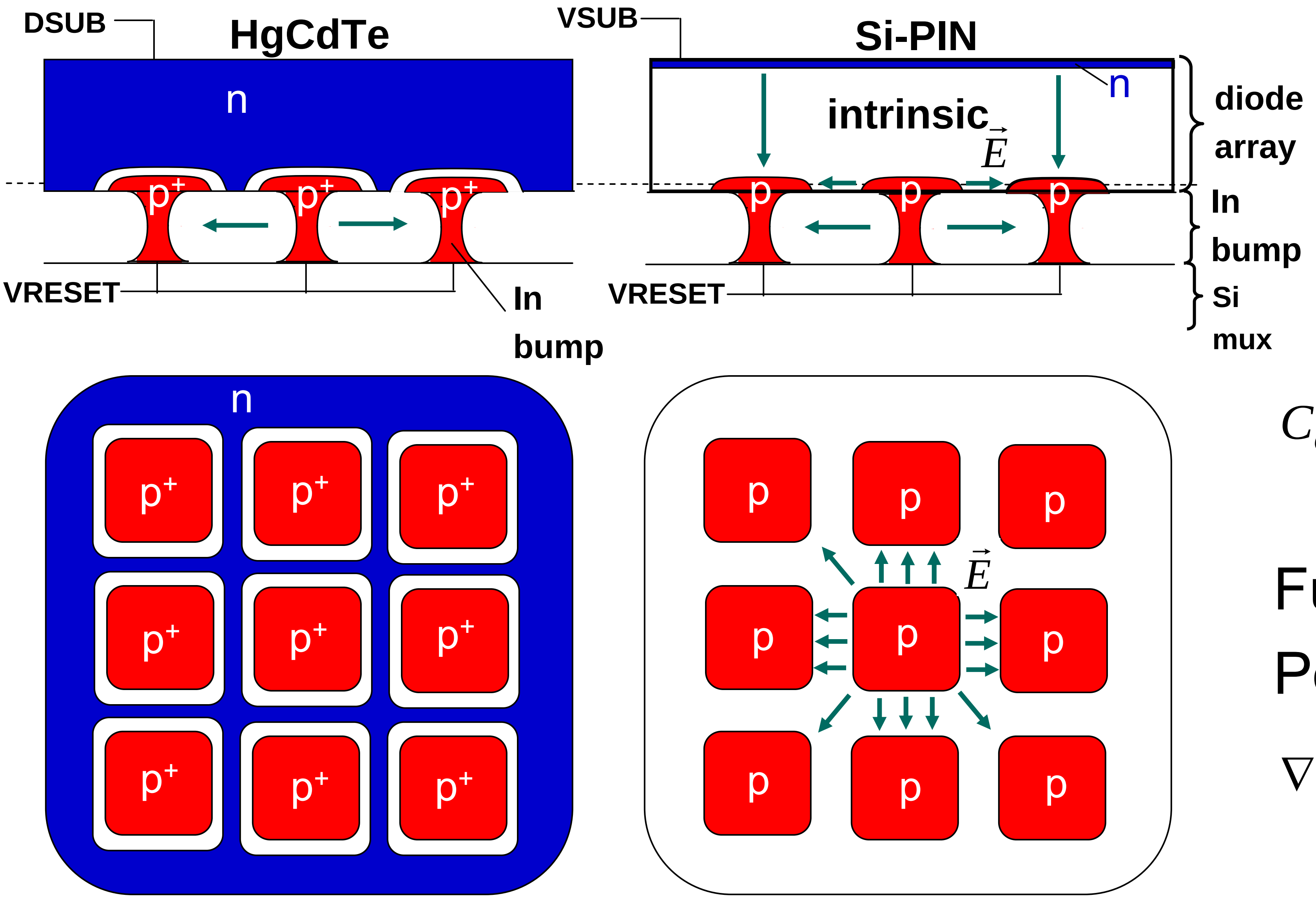

$$C_C = \frac{Q}{\int \vec{E} d\vec{x}}$$

Full solution Poisson:

$$\nabla^2 V = -\frac{\rho}{\varepsilon_0}$$

PSF of HgCdTe measured with cosmic rays and single pixel reset

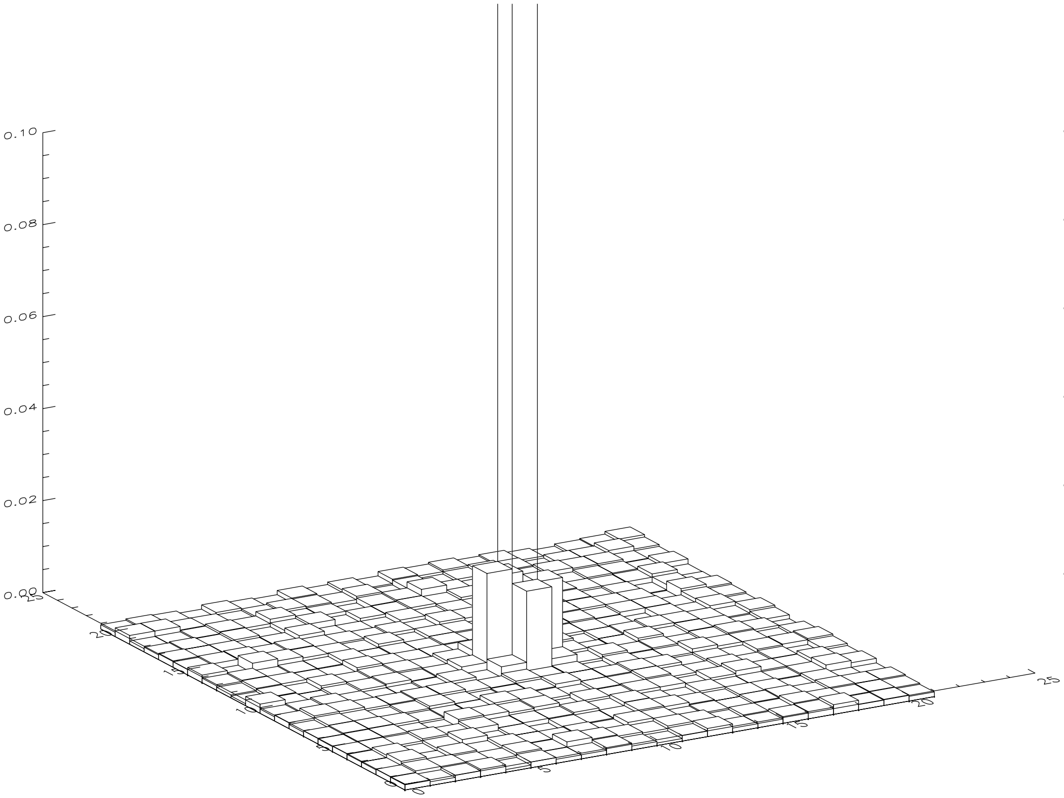

- Cosmic rays

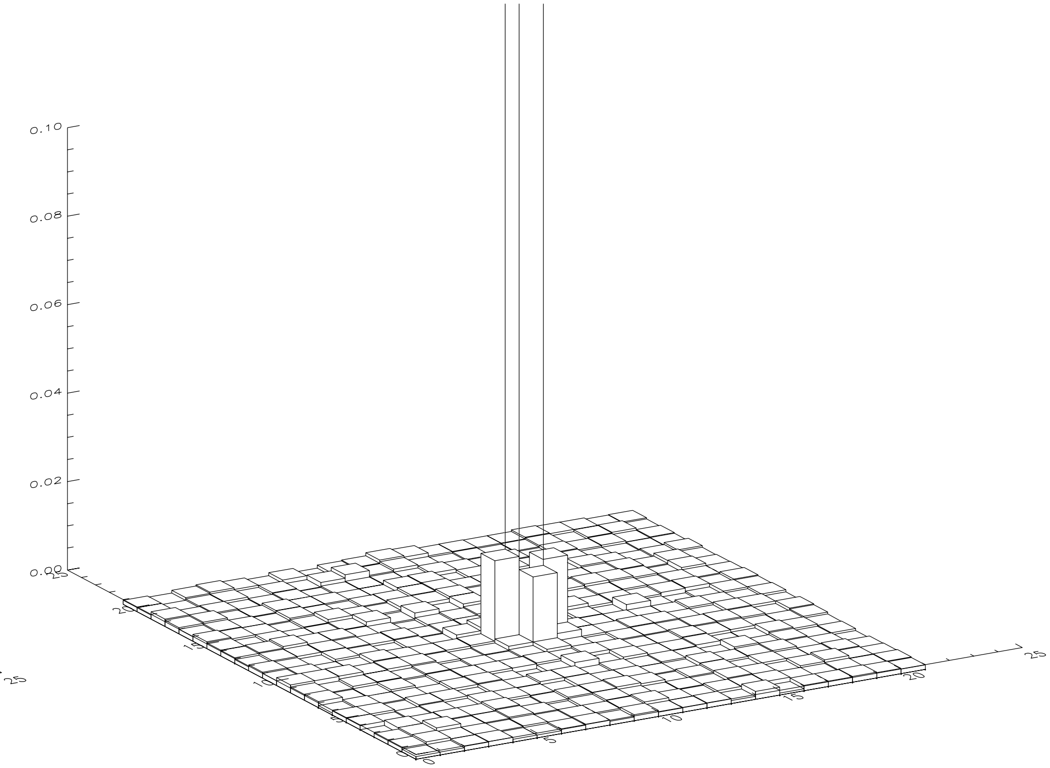

- Single pixel reset

- Cosmic ray and single pixel reset measurements show 2 % of coupling to next neighbors
- Capacitve coupling dominant, diffusion negligible

Noise estimator for photon shot noise: Integrated Autocorrelation replacing Variance

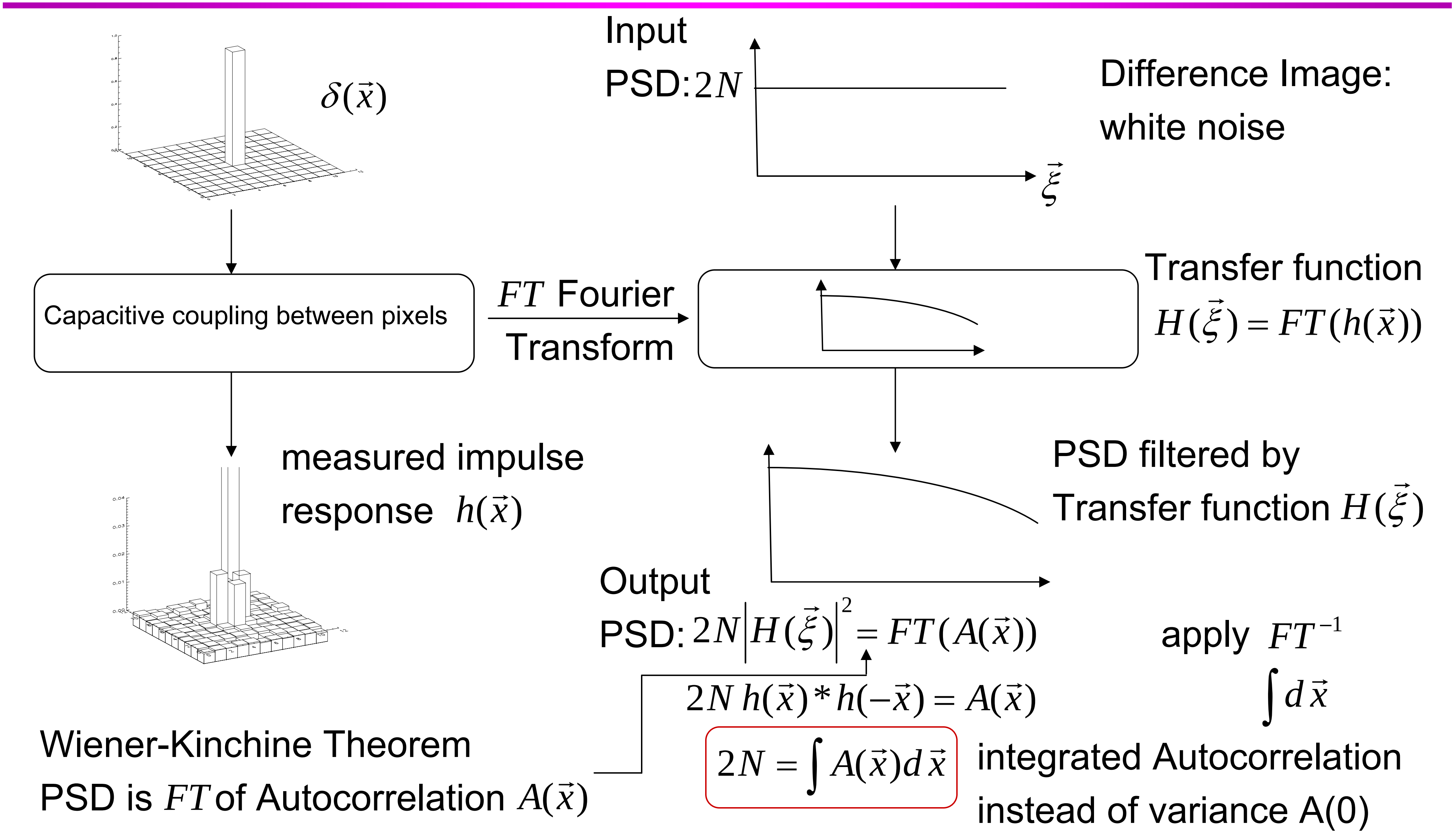

Noise estimator for photon shot noise: Integrated Autocorrelation replacing Variance

A. Moore: $2N = \int A(\vec{x})\, d\vec{x}$

$$2N = A(0) = \sigma^2 \Leftrightarrow A(\vec{x}) = 0 \;\; for\; \vec{x} \neq 0$$

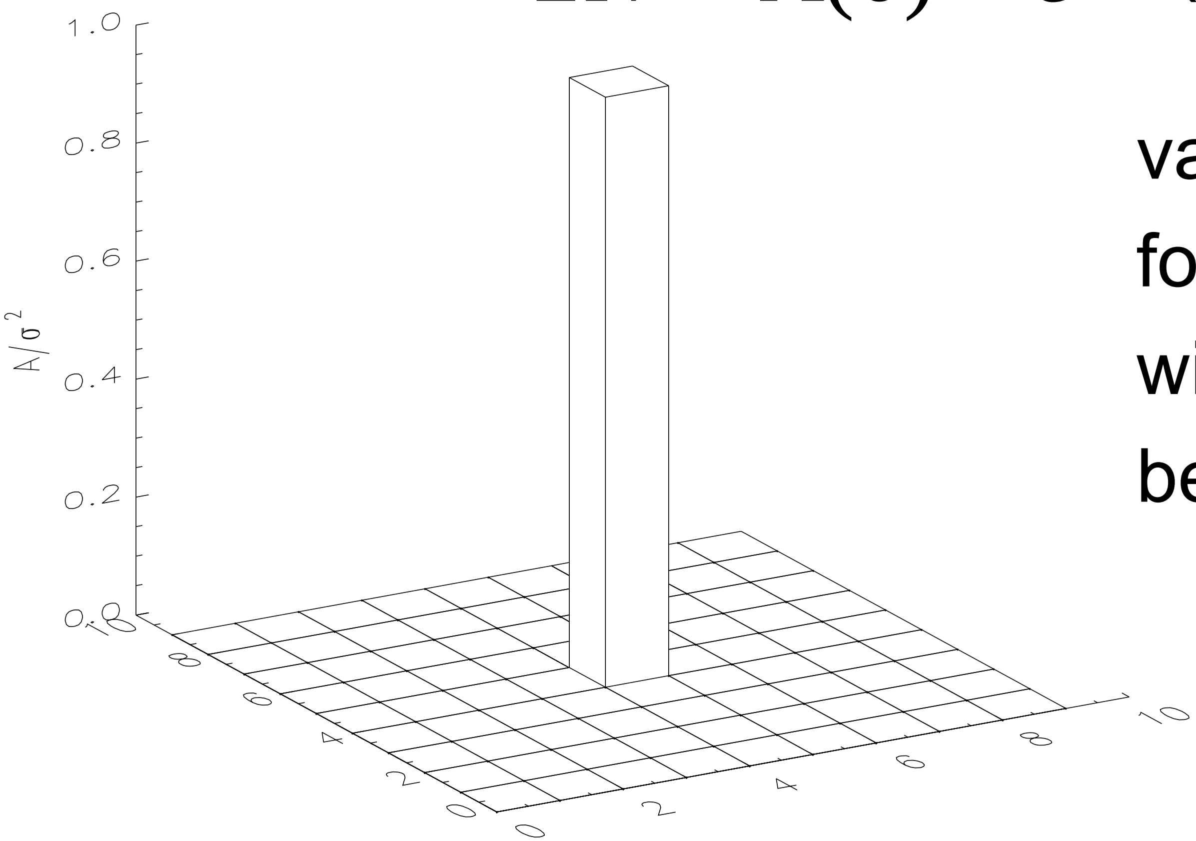

variance is good estimator for photon shot noise only without correlation between pixels

Noise estimator for photon shot noise: Integrated Autocorrelation replacing Variance

$$2N = \int A(\vec{x})\, d\vec{x}$$

$$2N = A(0) = \sigma^2 \Leftrightarrow A(\vec{x}) \neq 0 \;\; for\; \vec{x} \neq 0$$

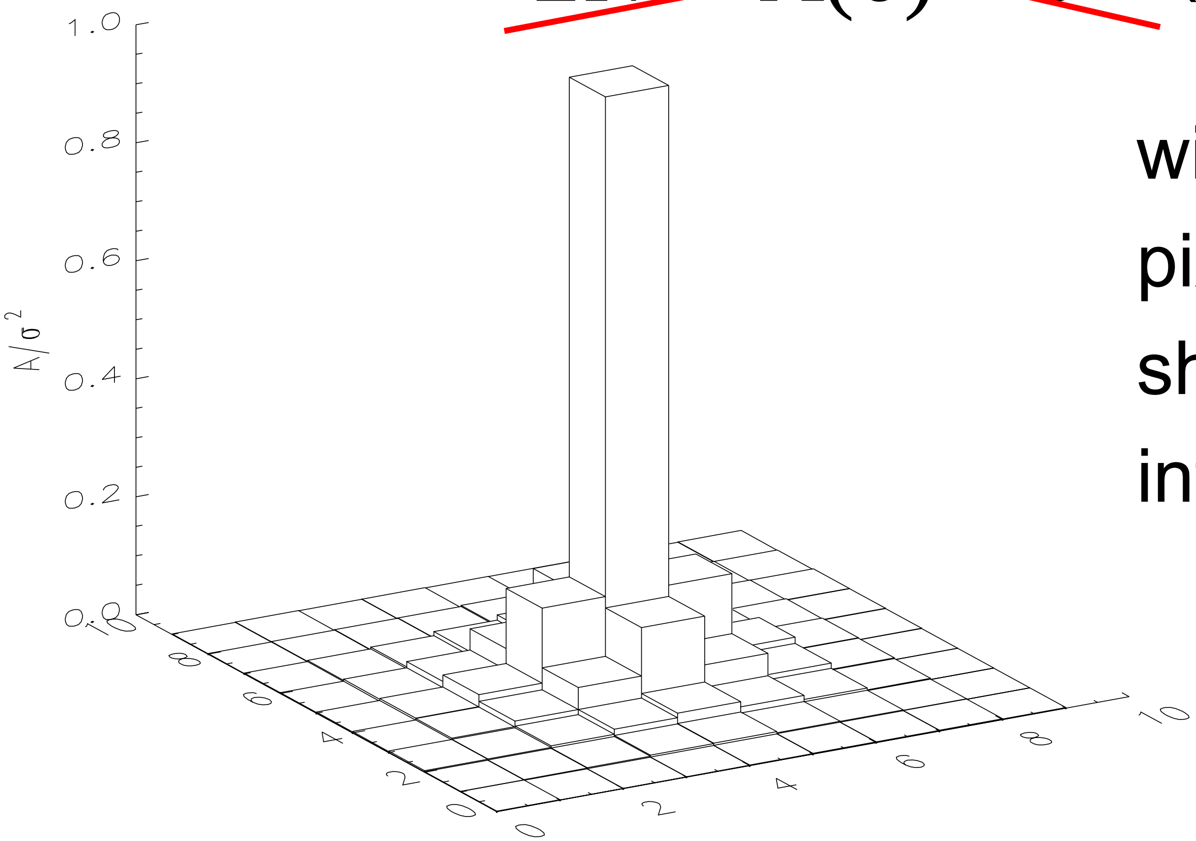

with correlation between pixels estimator for photon shot noise is integrated autocorrelation

Normalized Autocorrelation function R

- Normalized autocorrelation R=A / σ^2
- φ is correction factor by which σ^2 has to be multiplied for "noise squared versus signal" method

$$\varphi = \frac{\int A(\vec{x})\,d\vec{x}}{A(0)} = \sum_{m,n} R_{m,n}$$

$$R_{m,n} = \frac{\sum_{i,j} V_{i,j} V_{i+m,\,j+n}}{\sum_{i,j} V^2_{i,j}}$$

HgCdTe

φ=1.1

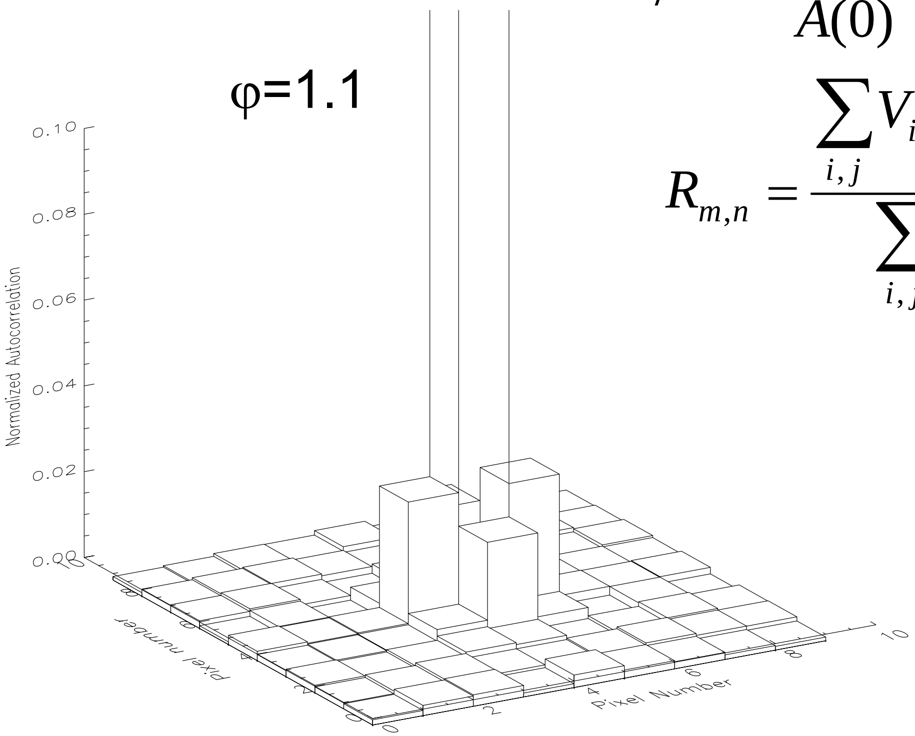

Si-PIN

φ=1.97

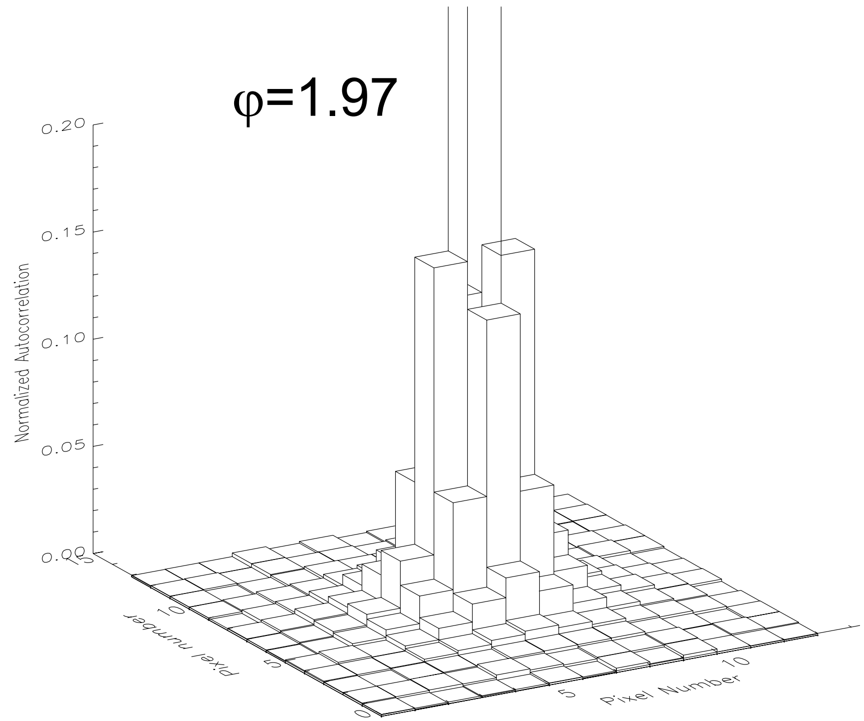

Calibration of acquisition system gain

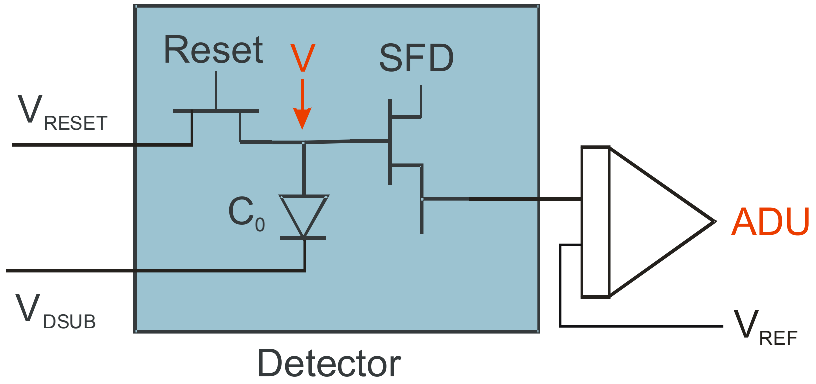

- refer ADU back to voltage V on C_0
- keep reset switch permanently closed
- vary V_{RESET} and $V_{REF,}$: measure ADU's
- SFD gain of Hawaii-2RG : 0.97

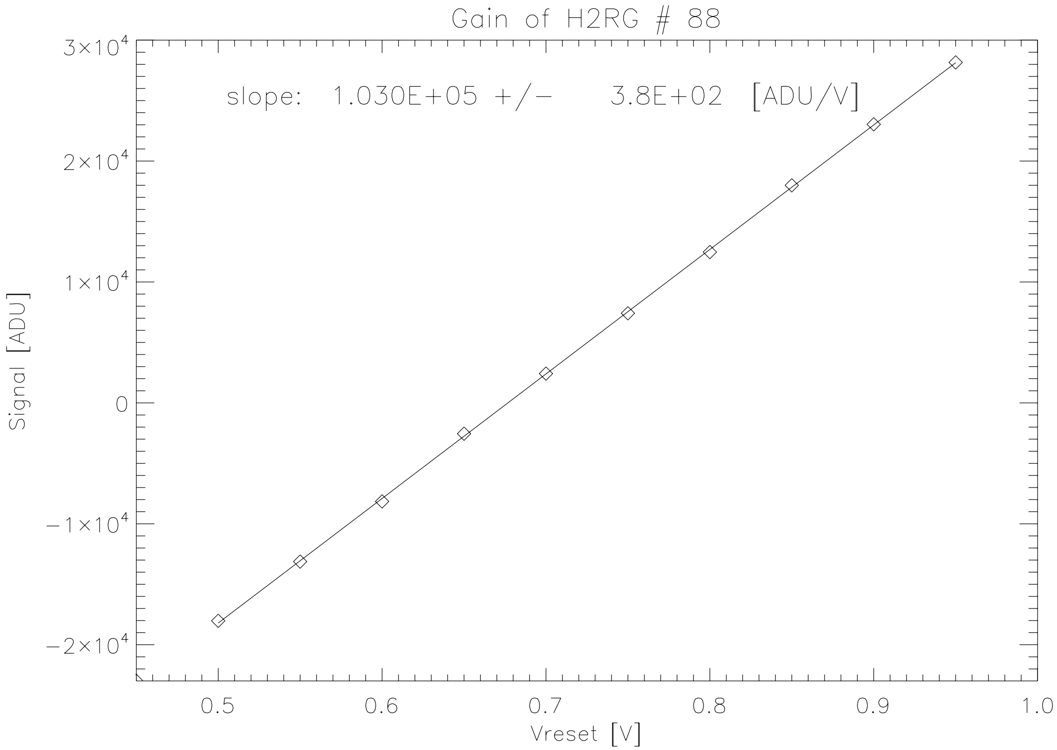

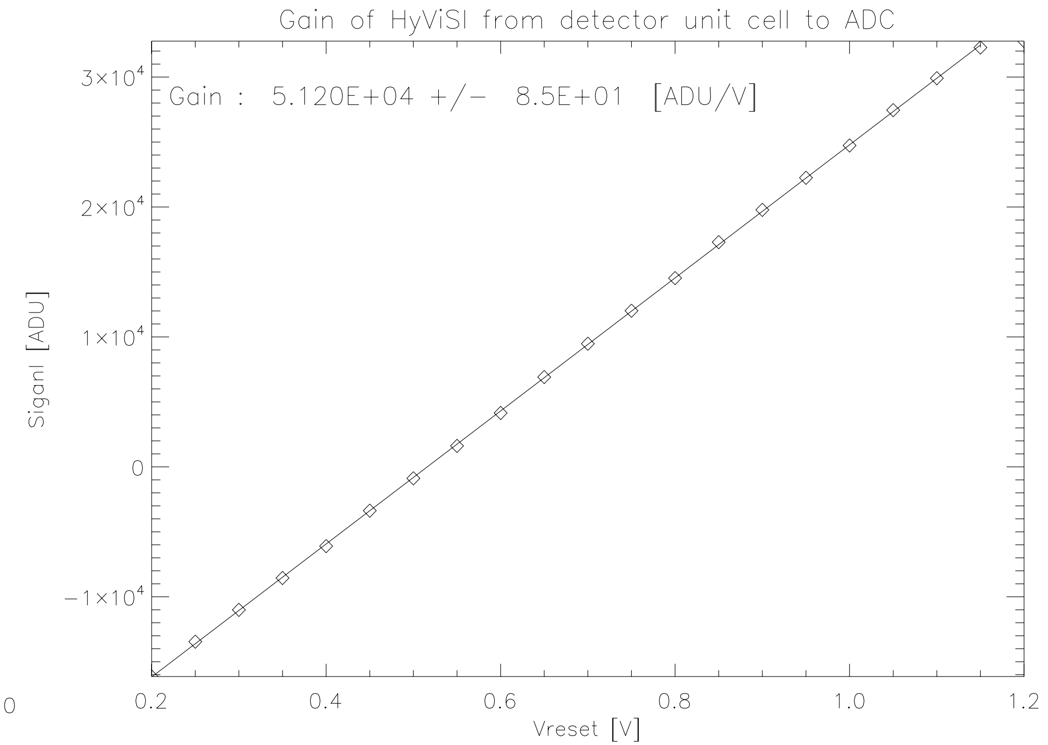

Conversion Gain HgCdTe Hawaii-2RG with Integrated Autocorrelation

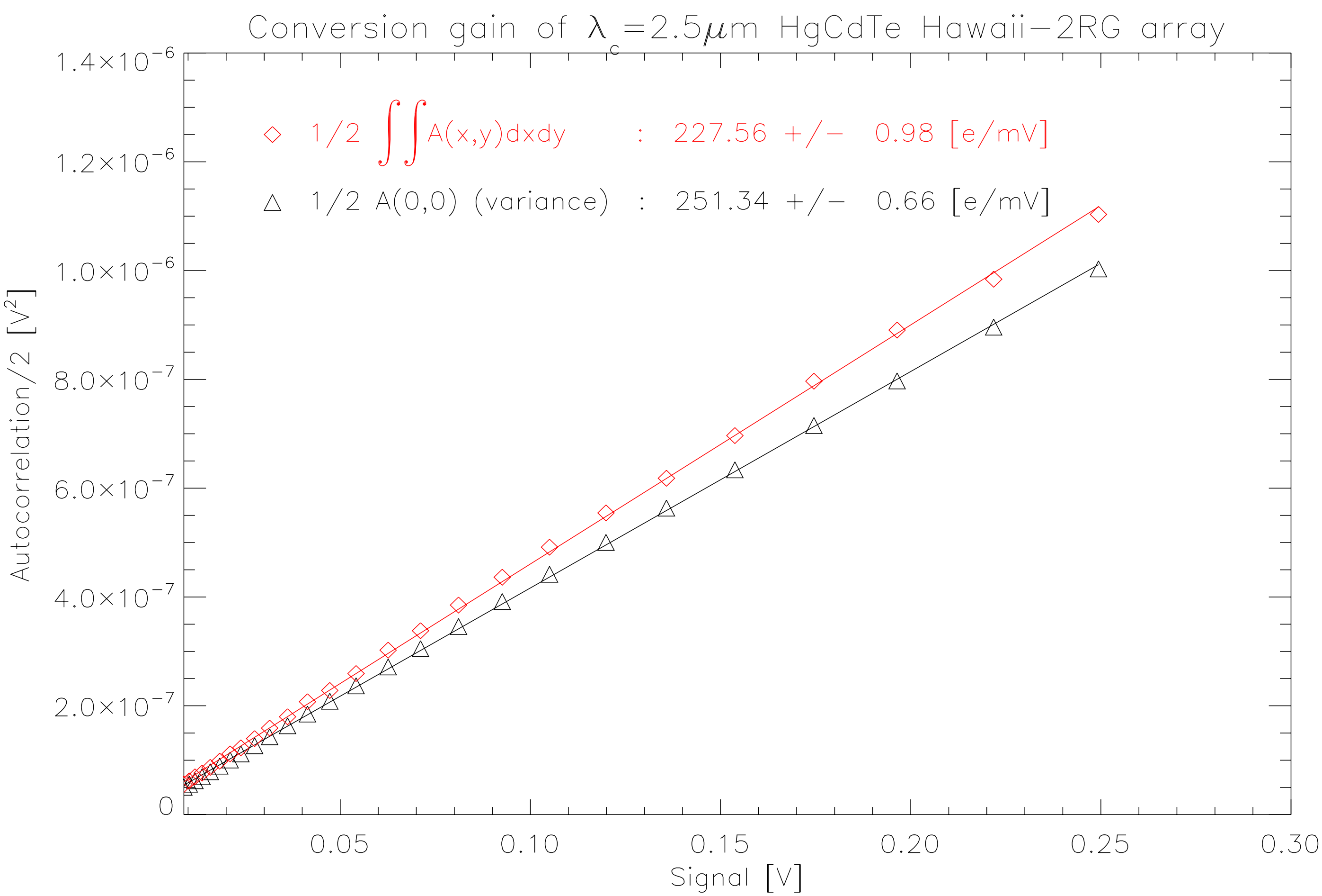

- Integrated autocorrelation $\int A(\vec{x})d\vec{x}$:
  C_0/e=227e/mV
  C_0=36 fF
- Variance A(0):
  C_0/e=251e/mV
  C_0=40 fF
- Variance overestimates conversion gain by 10 %

Conversion Gain Si-PIN Hawaii-2RG with Integrated Autocorrelation

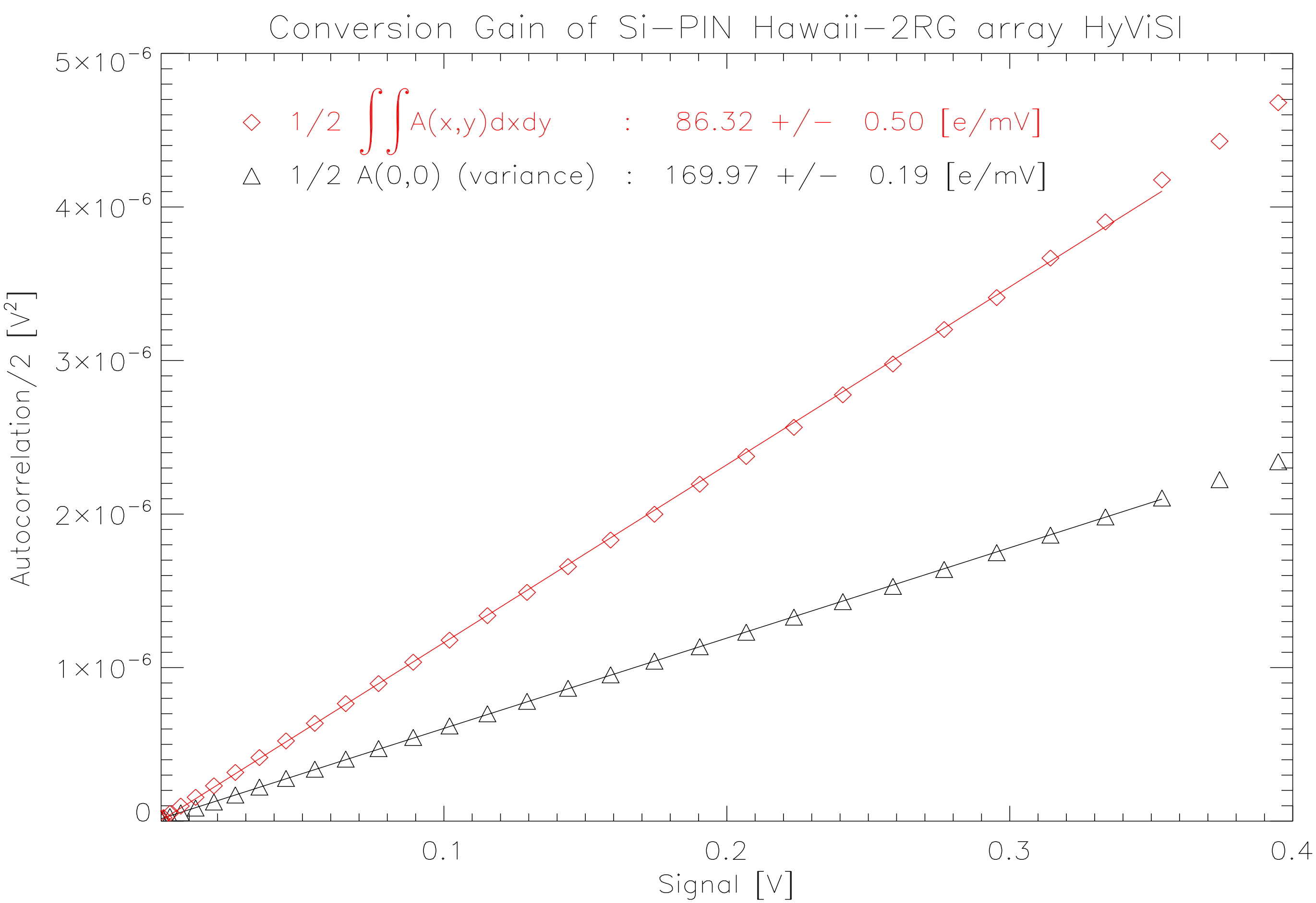

- Integrated autocorrelation $\int A(\vec{x})d\vec{x}$:
  C_0/e=86 e/mV
  C_0=13.8 fF
- Variance A(0):
  C_0/e=170e/mV
  C_0=27 fF
- Variance overestimates conversion gain by 97 %

Conversion gain

Method	Noise squared versus signal	Integrated Autocorrelation	Capacitance comparison	Fe^{55}
HgCdTe H2RG #88				
C_o/e [e/mV]	251.3	227.6	215	
C_o [fF]	40.3	36.4	34.5	
Si-PIN HyViSI				
C_o/e [e/mV]	170.0	86.3	85.1	86.8
C_o [fF]	27	13.8	13.6	13.9

- good quantitative agreement between capacitance comparison, integrated autocorrelation and Fe^{55} method
- overestimation of C_0 with "noise squared versus signal" method
  15 % for HgCdTe
  100 % for Si-PIN

Capacitive coupling between pixels

- shot noise method overestimates nodal capacitance C_0 and QE
  15 % for H2RG HgCdTe
  100 % for H2RG Si-PIN HyVisi
- capacitance comparison method directly yields nodal capacitance C_0
  validated with Fe55 on Si-PIN array
- $1/C^2$ reveals gate capacitance of unit cell source follower: C_G=17.8 fF , C_D=9.5fF
  built in voltage, donor concentration of diode junction
- Figure of merit C_0/C_c is measure of immunity against interpixel crosstalk
- Single pixel reset method gives impulse response of capacitive coupling
  which dominates optical PSF in Si-PIN arrays
- Noise estimator is integrated autocorrelation replacing variance
  for shot noise method
- Quantitative agreement of C_0/e determined
  capacitance comparison = integrated autocorrelation = Fe^{55}
- making pixels smaller is not a good way to increase array format
  if capacitive coupling is not addressed

Noise map of Hawaii-2RG
λ_c=2.5 µm MBE array

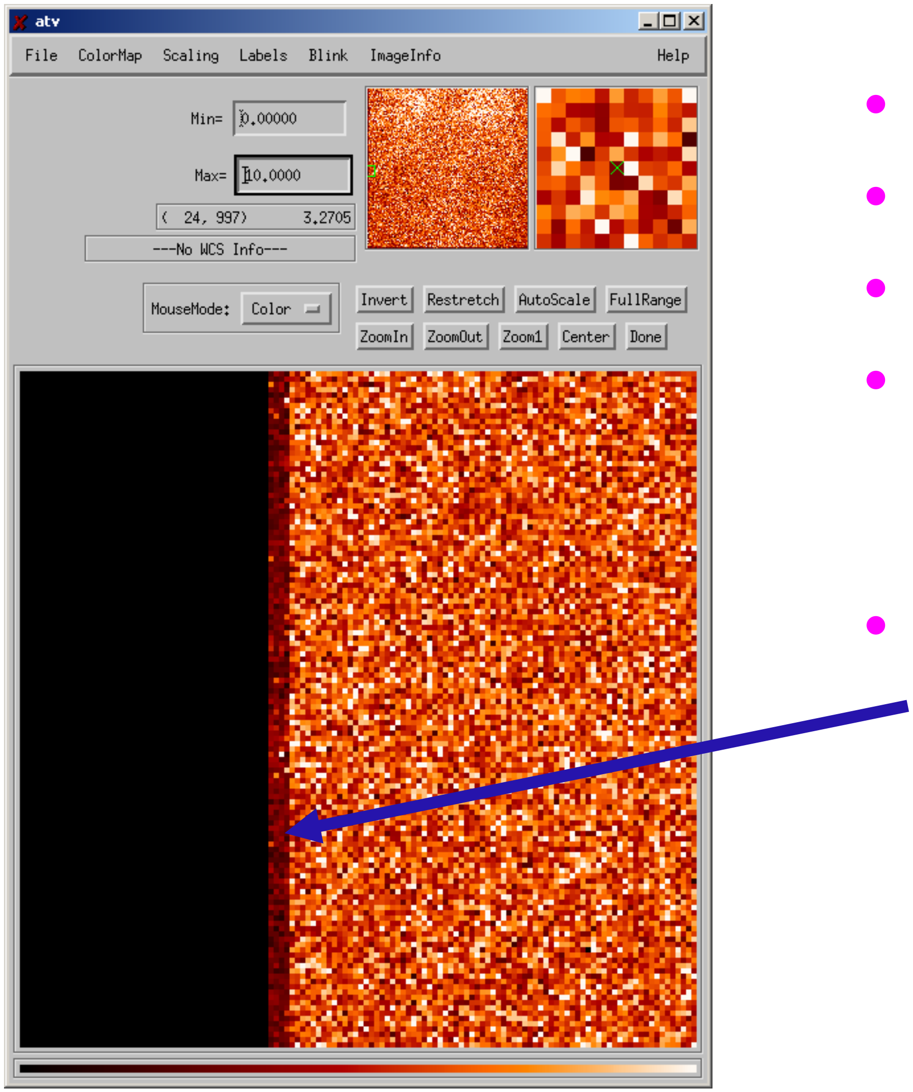

- Noise map for Hawaii-2RG
- 13.4 erms on active pixels
- 6.3 erms on reference pixels
- Dominant noise source is IR pixel, not mux or acquisition chain
- Clean set-up

4 columns of reference pixels on each side of the array

Noise map of Hawaii-2RG
λ_c=2.5 μm MBE array

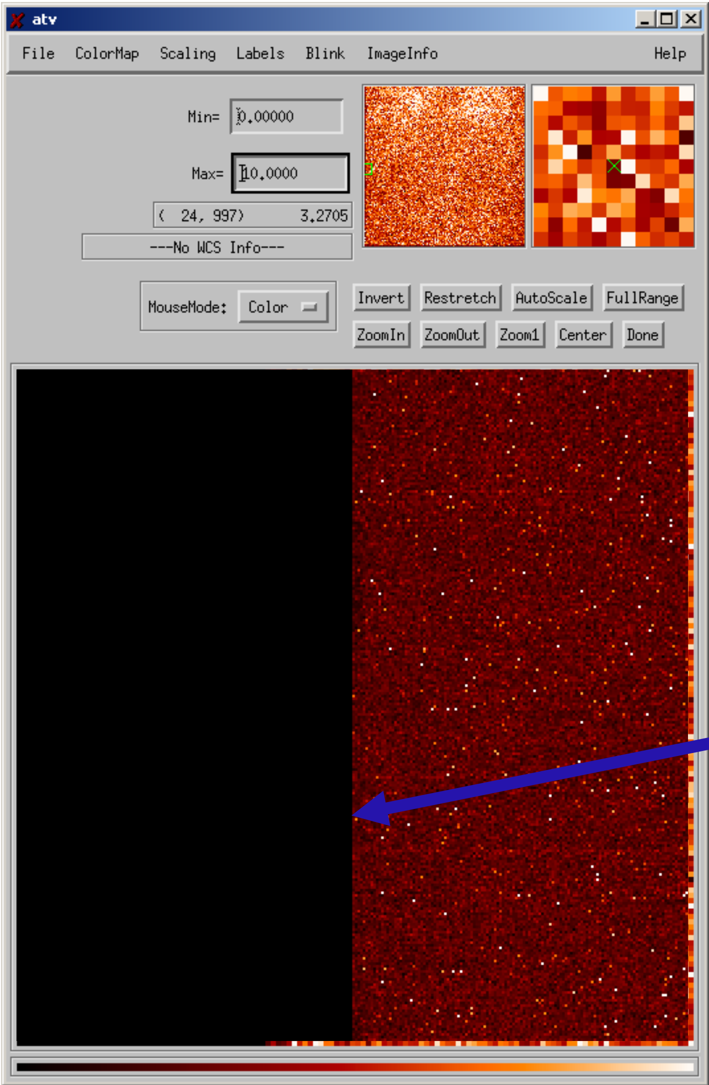

- Noise map for Hawaii-2RG # 49
- 8.6 erms on active pixels
- 8.6 erms on reference pixels
- Only on device #49 dominant noise source is not IR pixel, but mux and acquisition chain
- What is special with part #49 ?

4 columns of reference pixels on each side of the array

Noise reduction by multiple nondestructive readouts

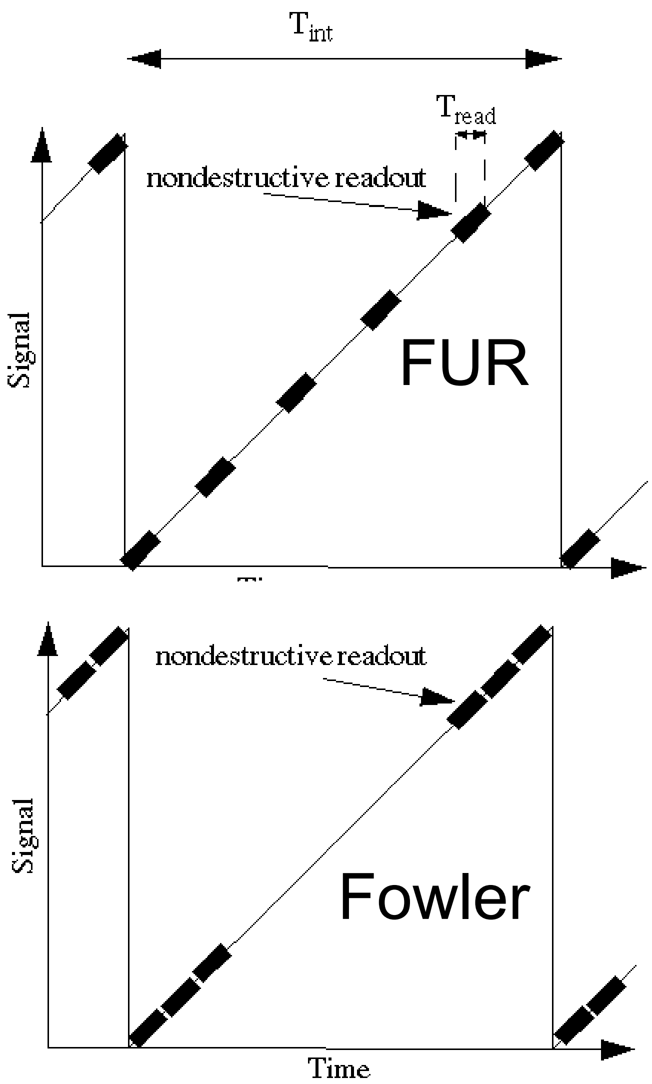

- Multiple readouts of array possible without disturbing ongoing integration : nondestructive readout
- Follow-up-the-ramp sampling (FUR):
  at equidistant time intervals nondestructive readouts
  least squares fit: slope of integration ramp

$$SNR_{FUR} = SNR_{DC}\sqrt{\frac{n(n+1)}{6(n-1)}}$$

- Fowler sampling:
  nondestructive readouts at start and at end of ramp
  least squares fit: slope of integration ramp
  for n>>1:

$$SNR_{Fowler} = SNR_{DC}\sqrt{\frac{n}{2}} \cong SNR_{FUR}\sqrt{3} \Leftrightarrow T_{\mathrm{int}} >> nT_{\mathrm{Re}ad}$$

Readout Noise versus number of nondestructive readouts

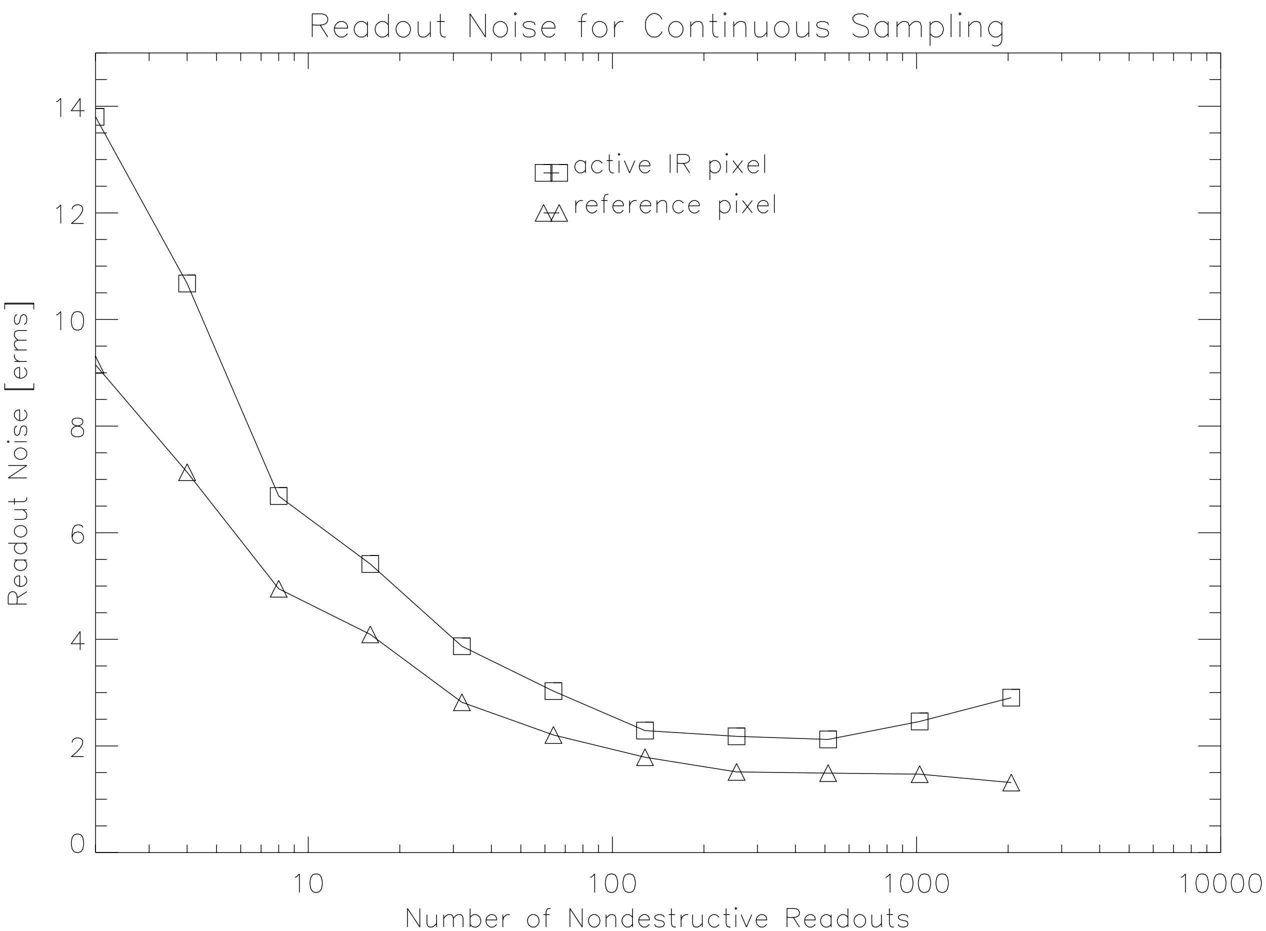

Fowler sampling:
number of readouts n proportional to integration time: 825 ms/readout

for 256 Fowler pairs
2.2 erms on IR pixels
1.3 erms on reference pixels
scales to subelectron noise for Si-pin diodes (HyVisi)

shielding multiplexer glow very efficient:
large number of nondestructive readouts possible with 32 channels

Readout Noise 256 Fowler pairs
2.5 µm MBE Hawaii-2RG

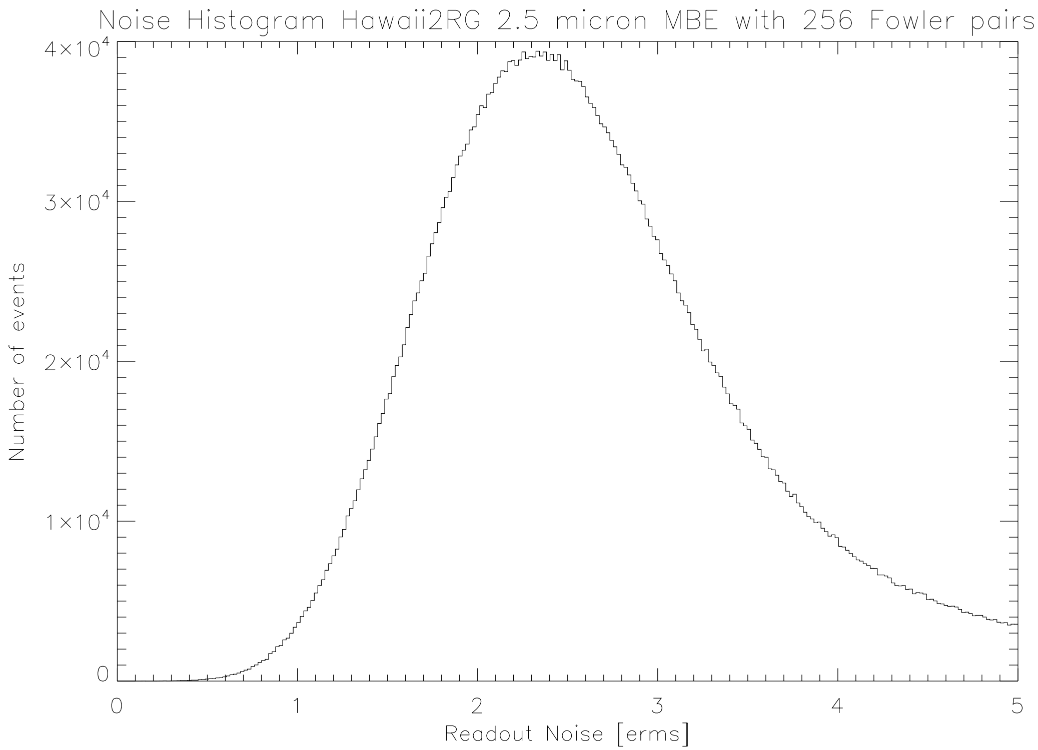

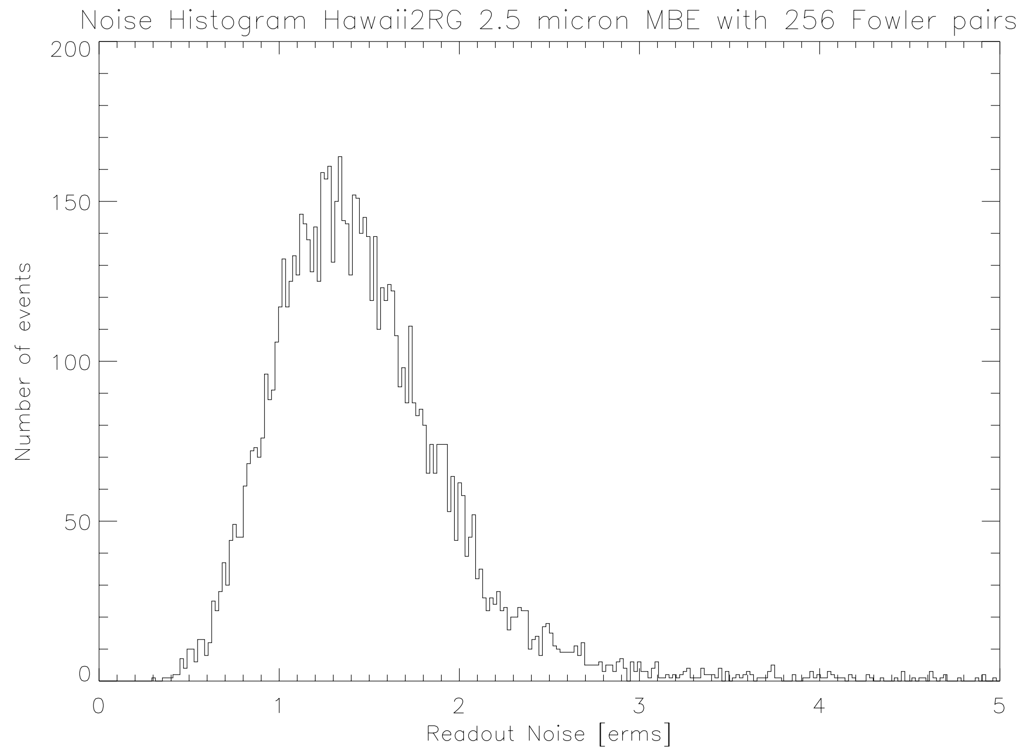

- 2.3 erms on active pixels
- 1.3 erms on reference pixels

Glow centers

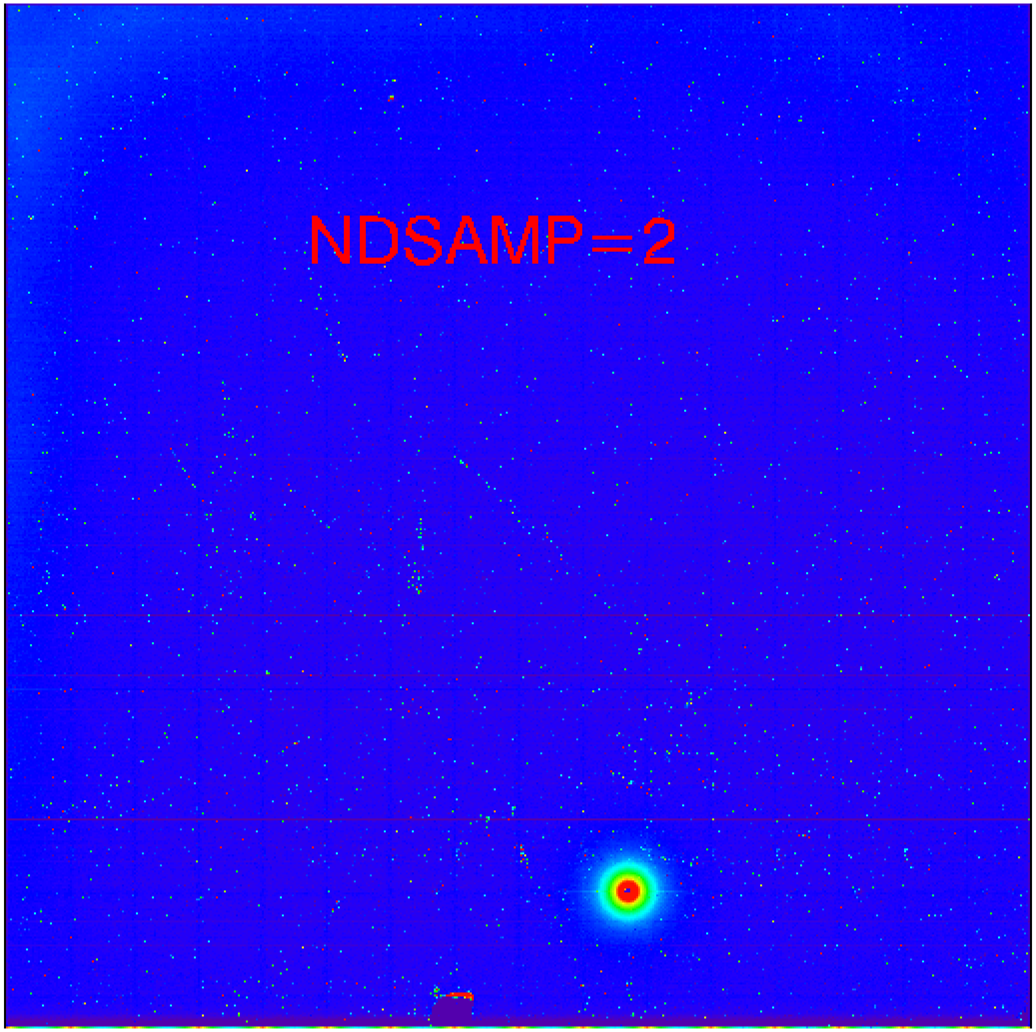

- For large number of nondestructive readouts engineering grade arrays show glow centers
- Fixed integration time 900s
- Vary number of nondestructive readouts

Intensity of glow centers

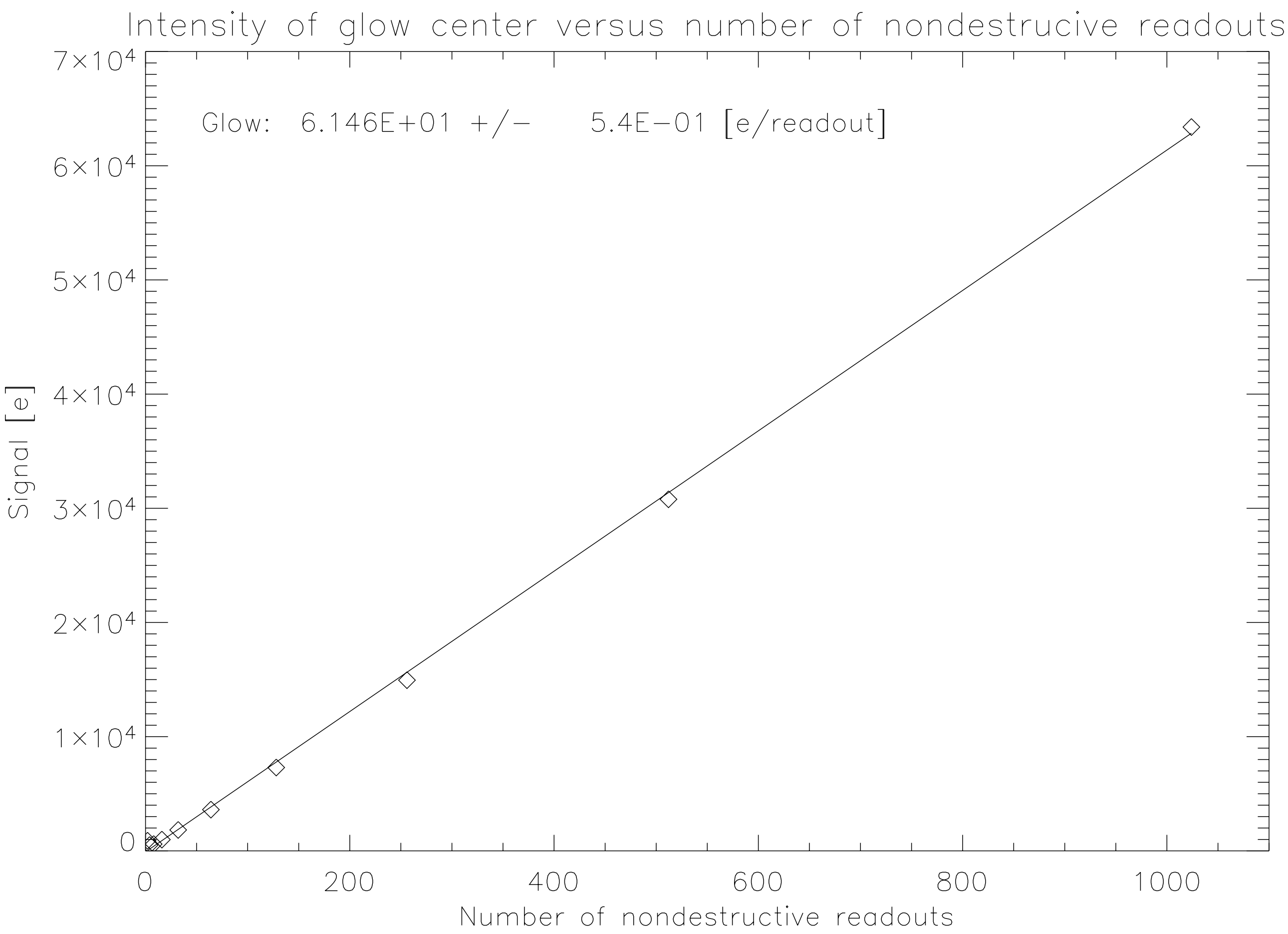

- Integration time 900 s
- Glow proportional to number of nondestructive readouts
- 27 pixels from center glow intensity is 61 e/frame

Glow centers

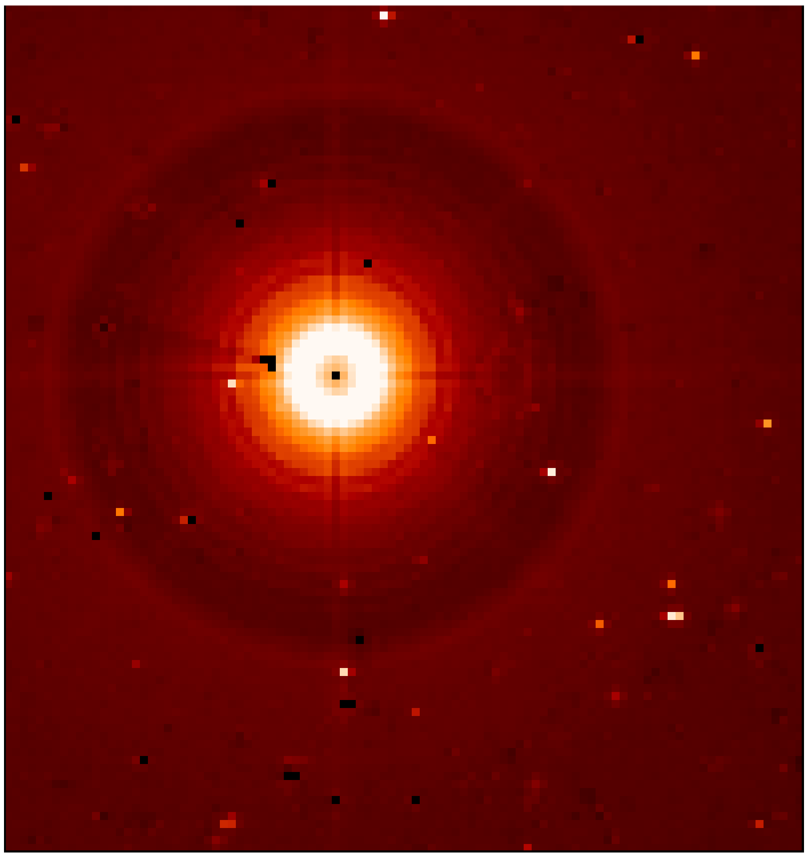

- several isolated glow centers for large number of readouts on engineering array
- No glow center on science array
- Diffraction like ring structure
- Selection criterium for science arrays
- Hole in metal shield of MUX ?

Persistence of
λ_c=2.5 μm HgCdTe Hawaii-2RG array

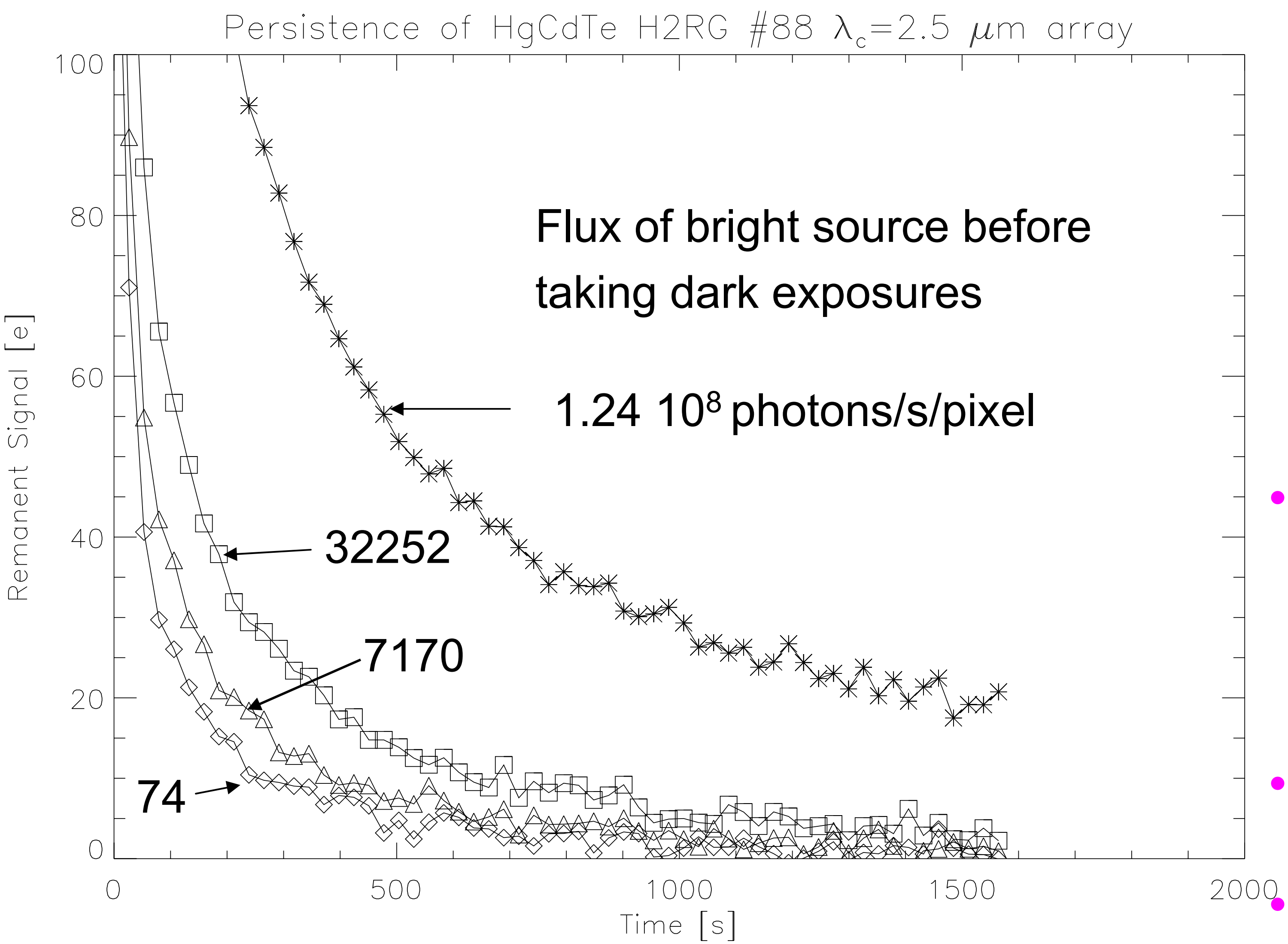

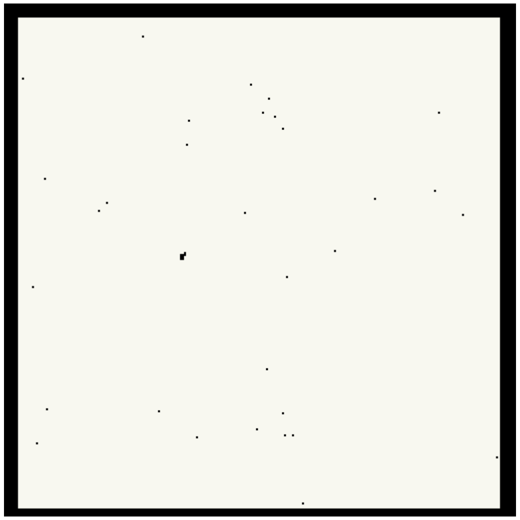

- replacing LPE with MBE does not eliminate persistence at λ_c=2.5μm
- latent image can be seen for hours
- persistence on all arrays measured

Persistence

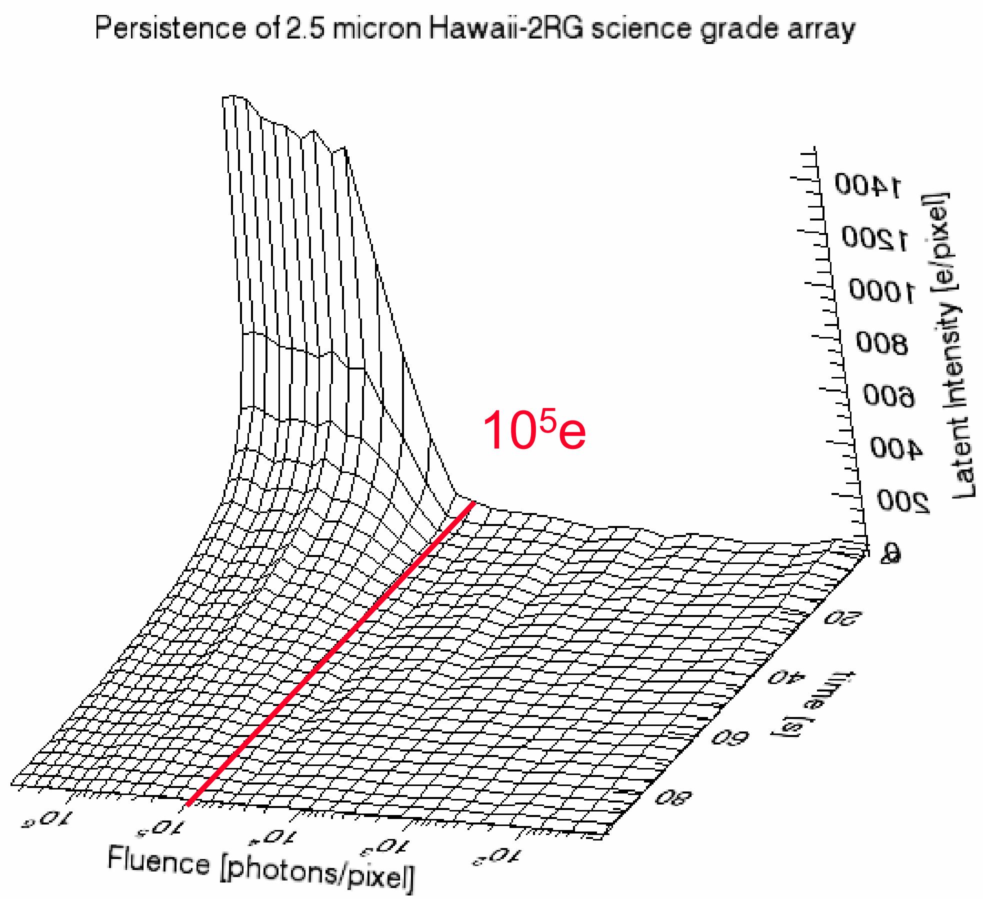

- depends on fluence not on flux
- $N<N_{saturation}=10^5$e no persistence
- switch from LPE to MBE does not eliminate persistence
- latent image can be seen for many hours
- Threshold of persitence because of traps close to the pn junction ?

low frequency noise suppression with embedded reference pixels

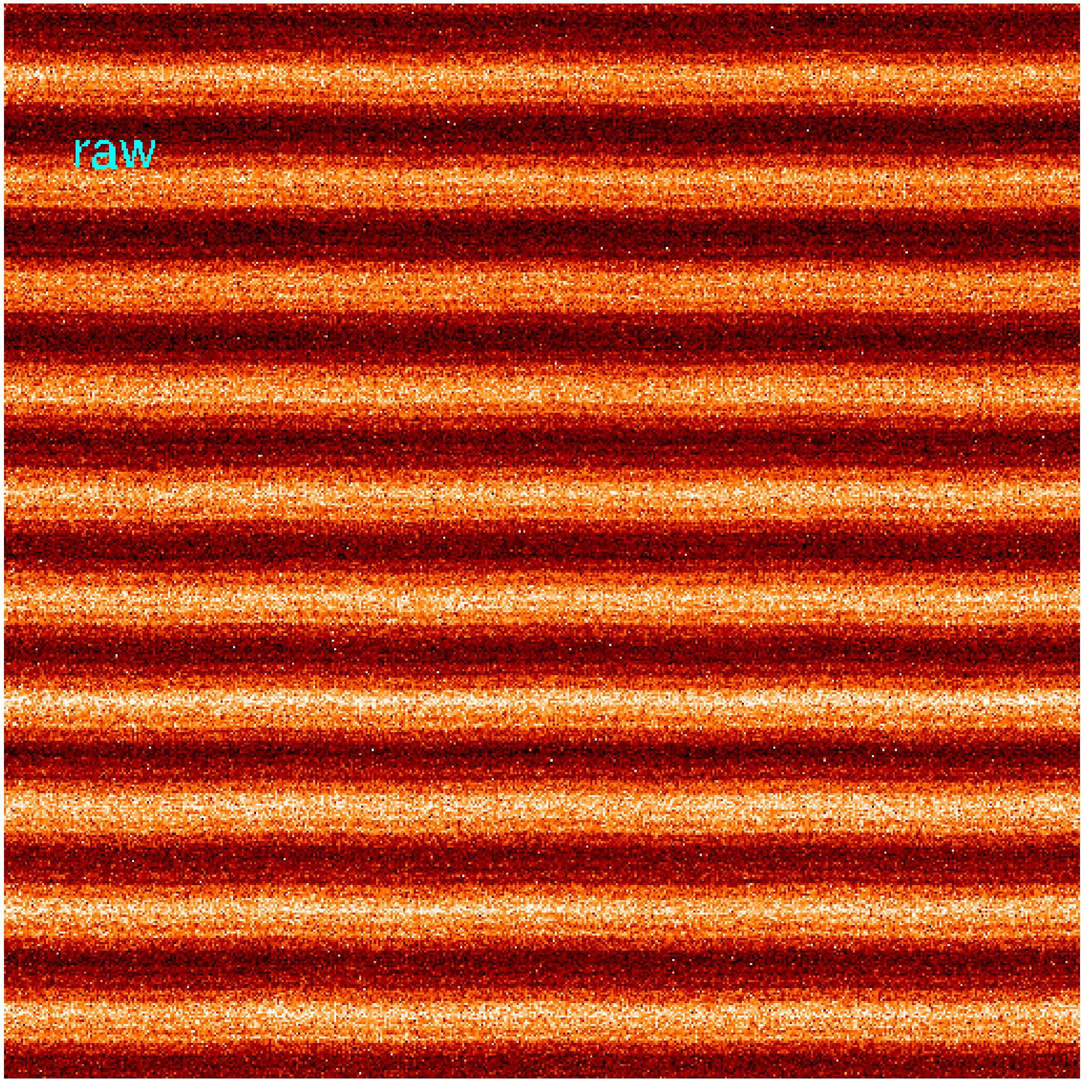

- Integration time 1.01 s
- high frequency stripes in direction of fast shift register are 50 Hz pickup
- Noise 45 erms
- For each row subtract average of 8 embedded reference pixels on right and left edge of the array
- With 32 channels reference pixels are read twice every 420 μs
- Noise 24 erms
- Linear interpolation of reference for each pixel using reference pixels of row and

Hawaii2GR in integral field spectrograph SPIFFI

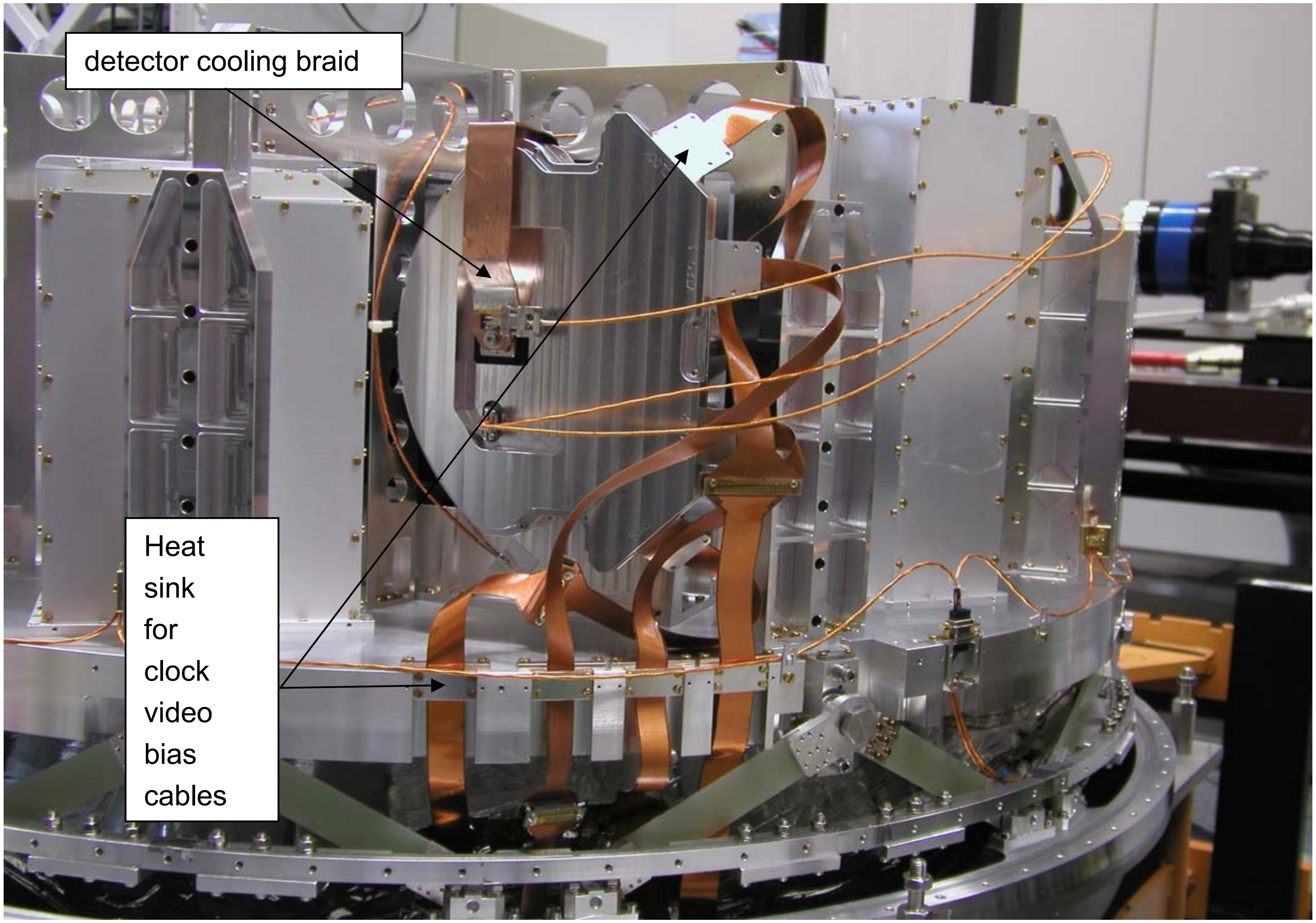

- Liquid bath cryostat $T_{detector}$ = 90 K
- λ_c=2.5 μm MBE Hawaii-2RG
- Heat sinking of cables

SPIFFI

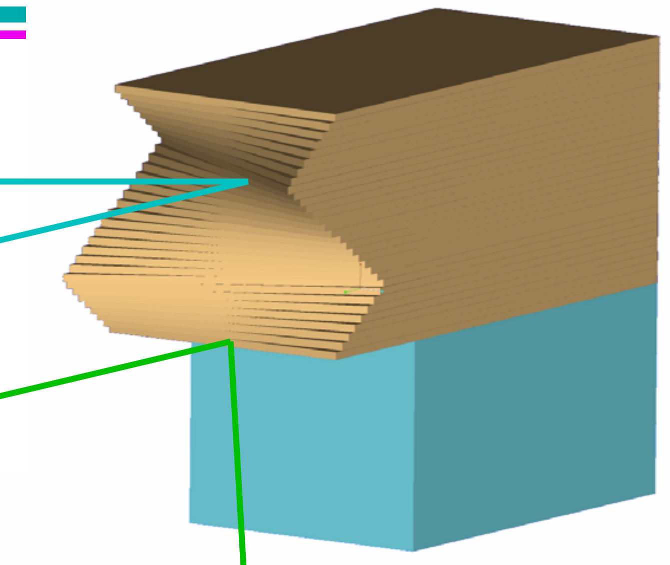

SPIFFI: SPectrometer for Integral Faint Field Imaging (MPE)

- Fully cryogenic spectrometer for the near infrared wavelength range from 1.0 – 2.5 µm
- Integral field unit with 32 x 32 pixels

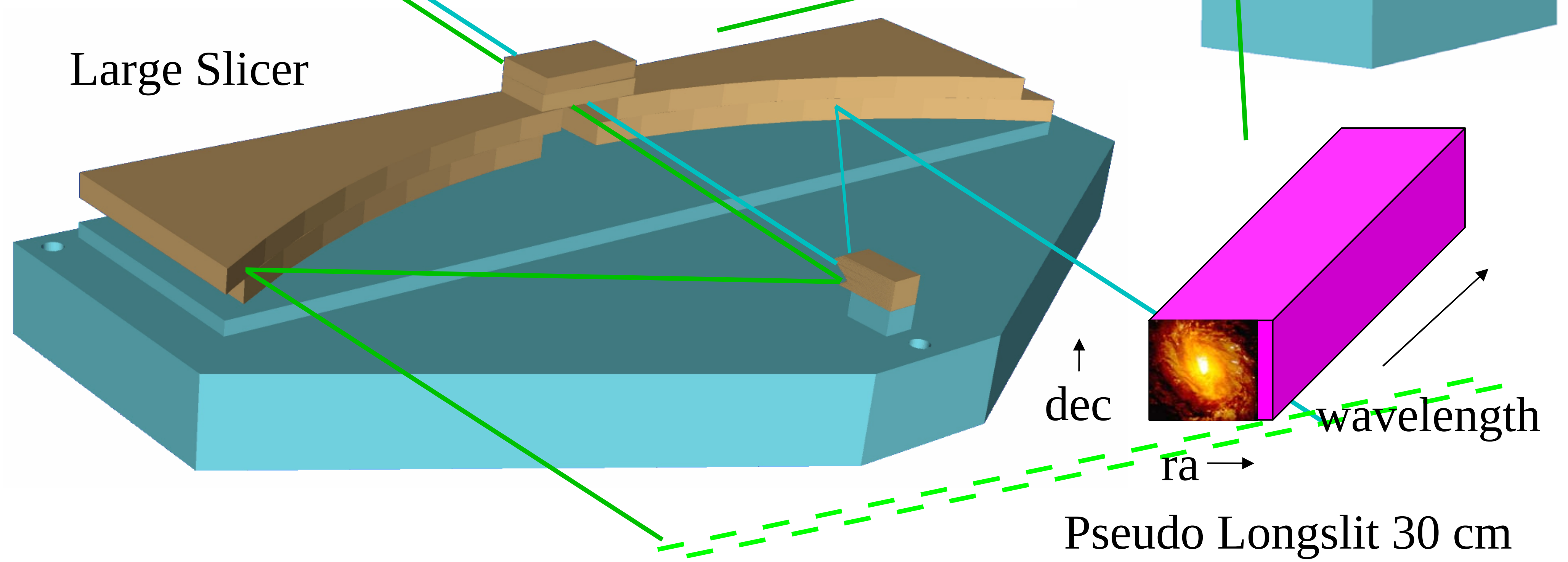

Hawaii2RG in integral field spectrograph SPIFFI

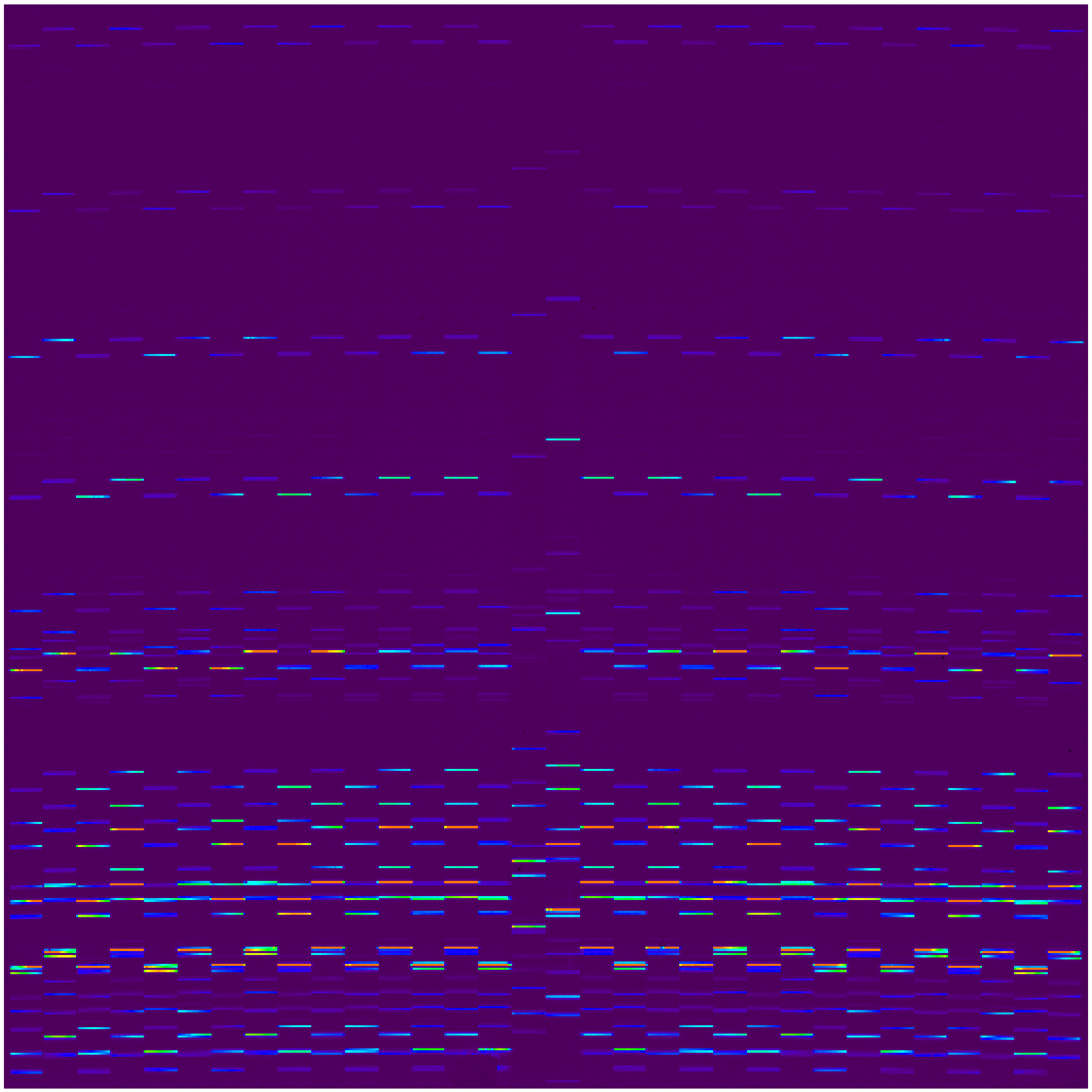

- K-band spectrum of Ne lamp
- Slitlets staggered because of image slicer
- Pixel scale 0.1 arcsec
- FWHM = 1.4 pixels
- Spectral resolution 6300

Hawaii2RG for Hawk-I

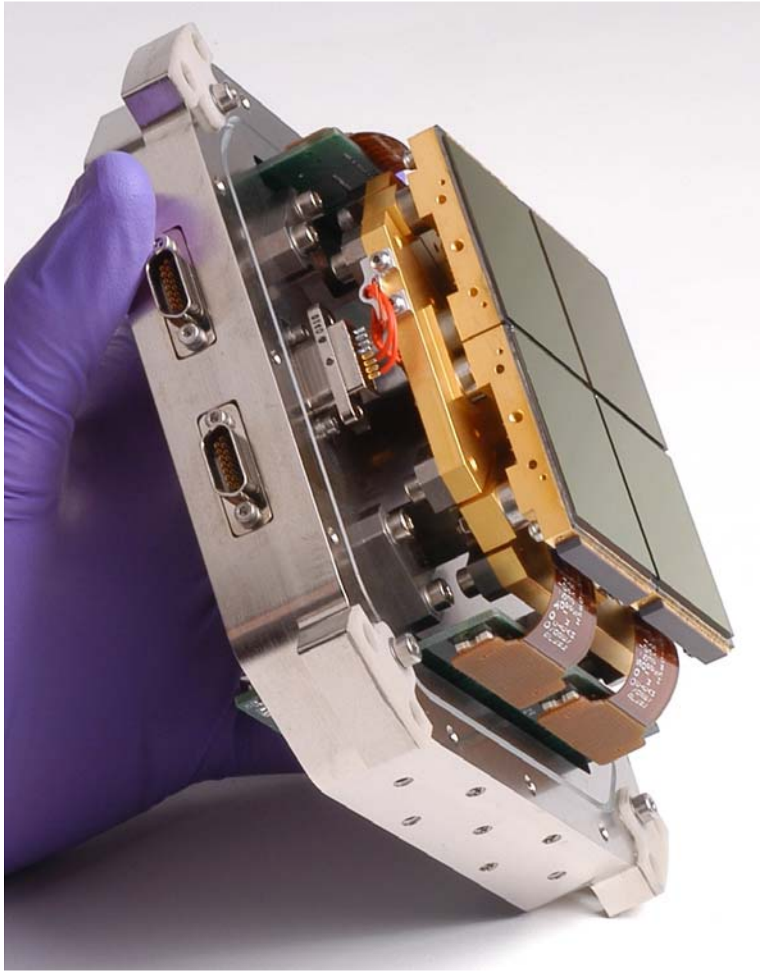

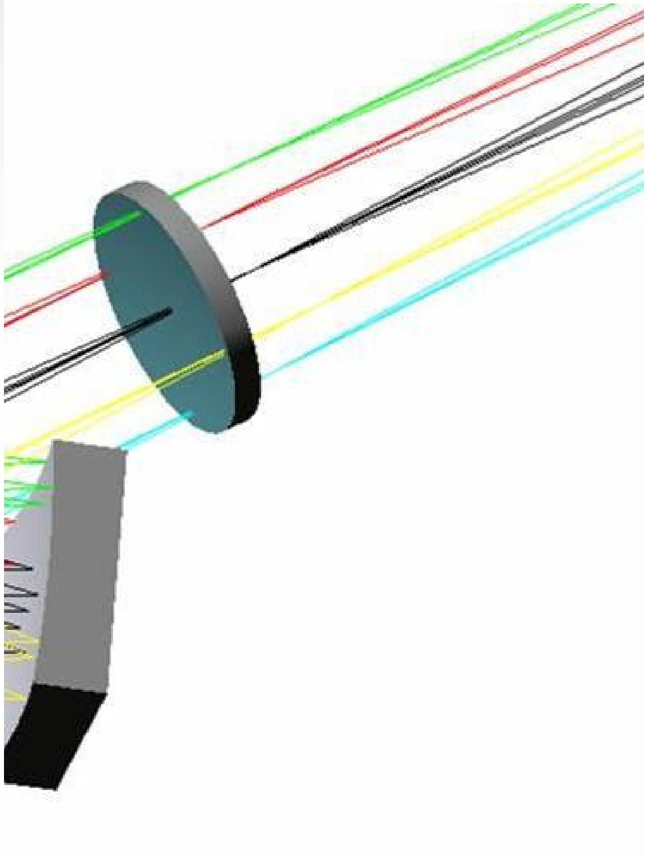

- 1-2.5μm
- All mirror optics
- 4kx4k mosaic detector
- 0.1” pixels 7.5x7.5’ field
- Designed for possible use with adaptive secondary +laser guide stars

Guide mode for tip-tilt correction with LGS-AO sytem

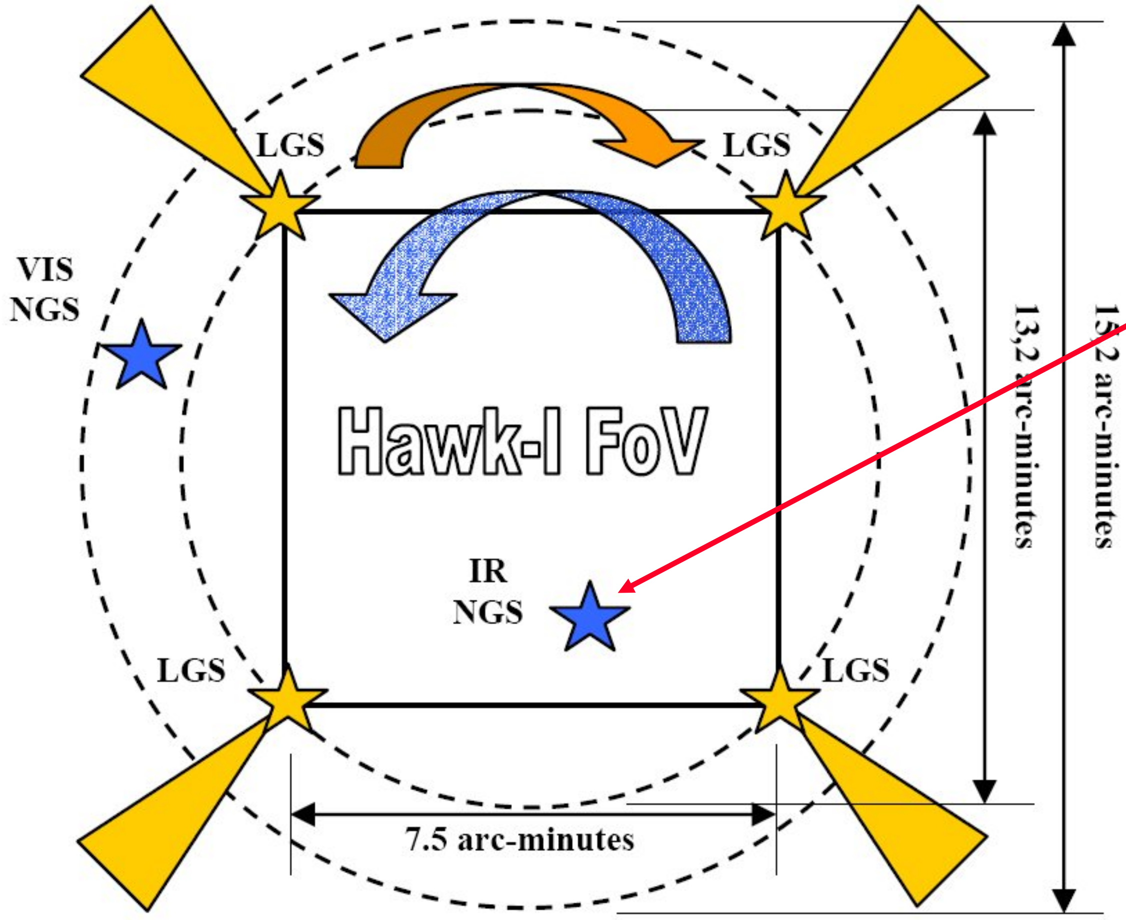

- Laser guide star AO system still need natural guide star for tip-tilt correction
- use guide mode of Hawaii-2RG arrays for tip-tilt correction with NGS

Interleaved readout of full field and guide window

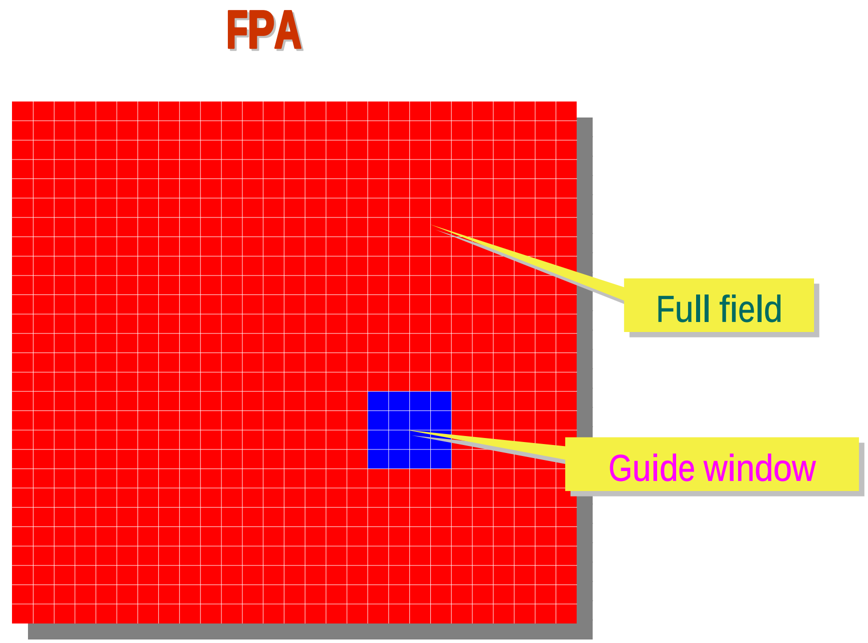

- Switching between full field and guide window is possible at any time
  ⇒any desired interleaved readout can be realized
- Three examples for interleaved readout:

1. Read guide window after reading part of the full field row
2. Read guide window after reading one full field row
3. Read guide window after reading two or more full field rows

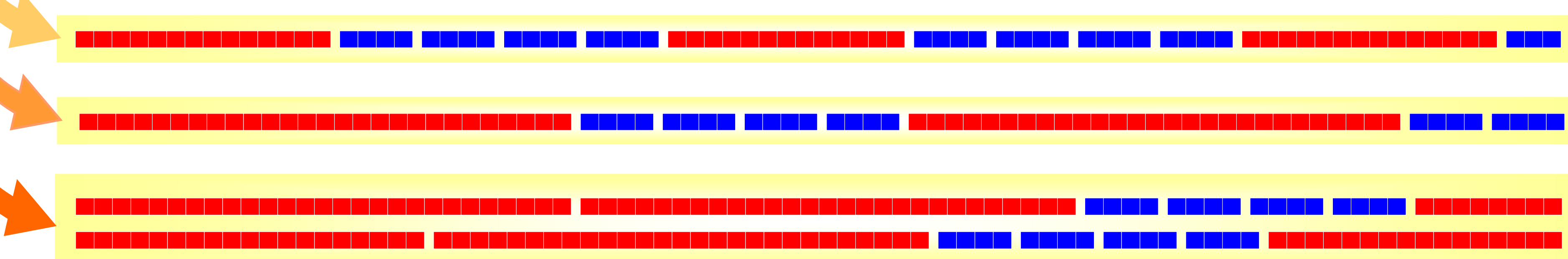

Timing of guide window readout

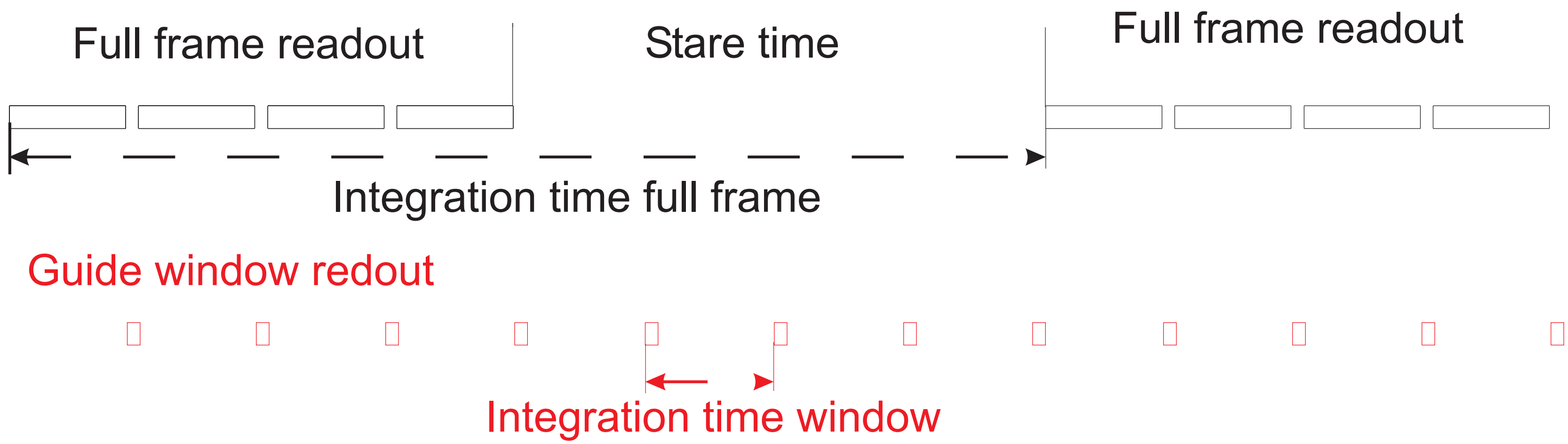

- Fowler or follow up-the-ramp sampling for science frame
- Interleave guide window readout with full science frame readout
- Guide window readout is nondestructive without reset: always subtract previous frame from new frame
- only one read needed per double correlated image
- Gain of 2 in bandwidth in comparison to read-reset read

Guide window
read-read-read

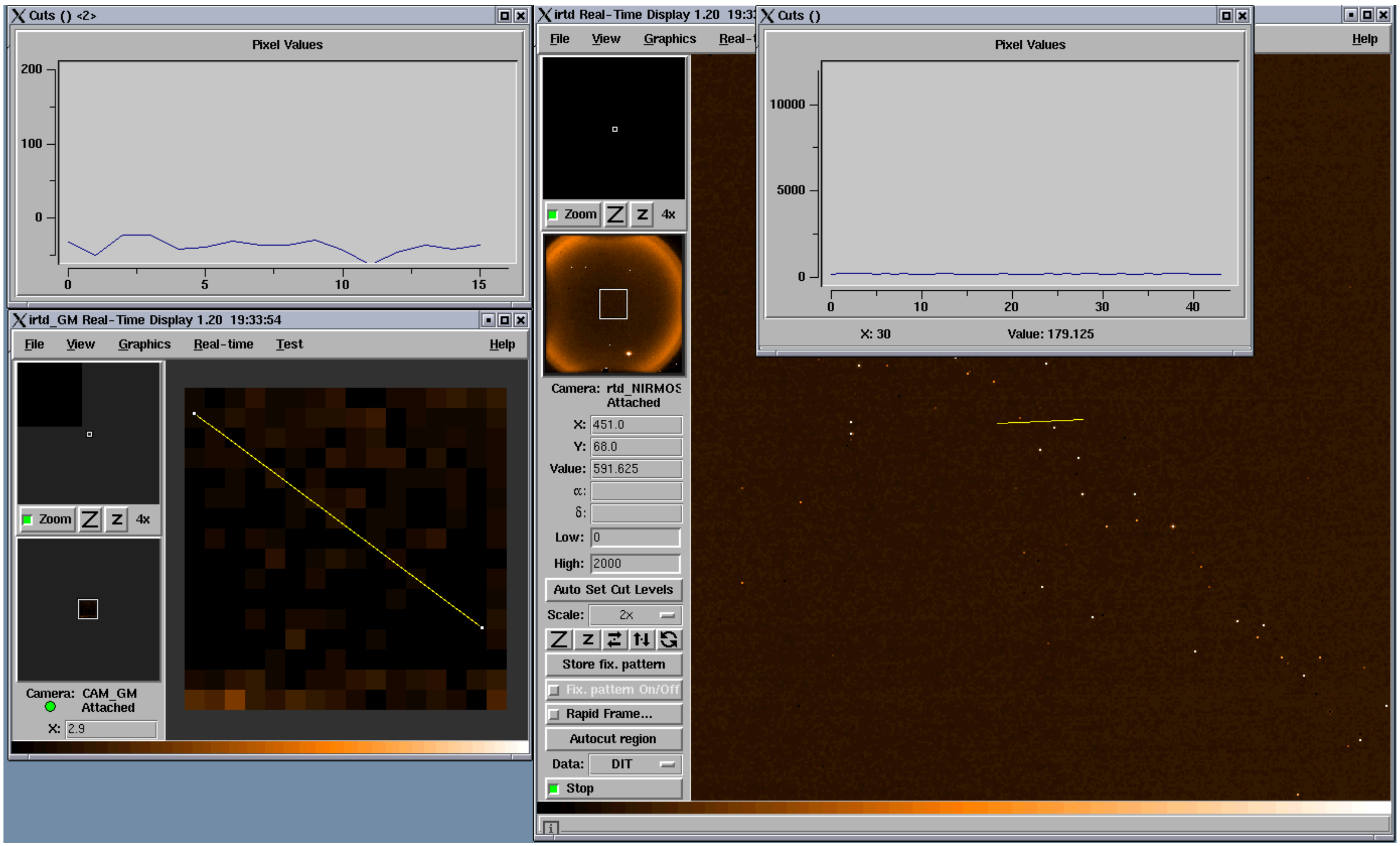

- Window 16x16
- Star mag 14
- 64 windows per full frame
- Frame rate 68 Hz
- Guide window is not lost for science frame

IRACE

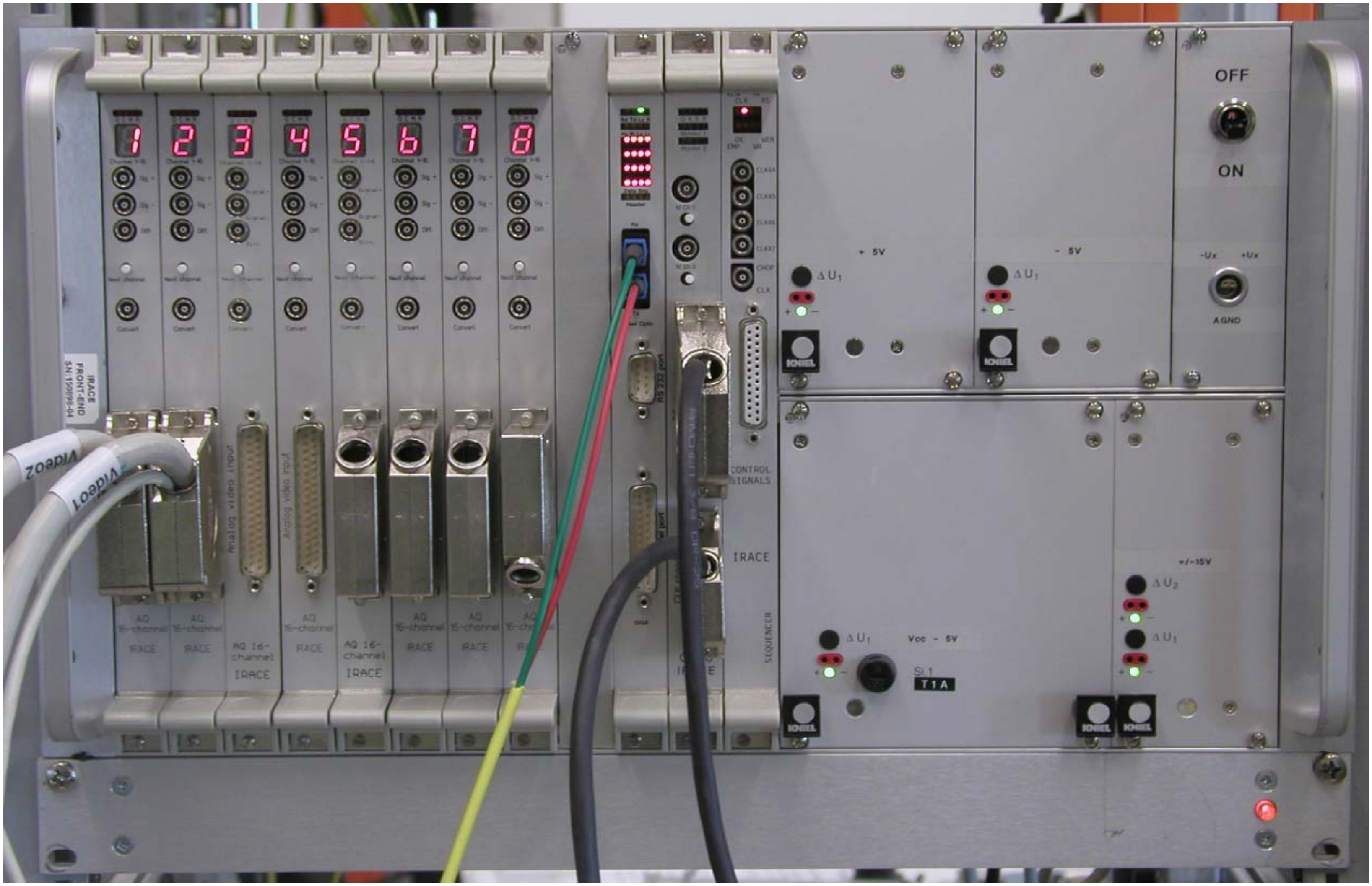

136 channel
IRACE system

similar system
already
operational
for CRIRES

IRACE for Hawaii2RG
32-channel and guide window

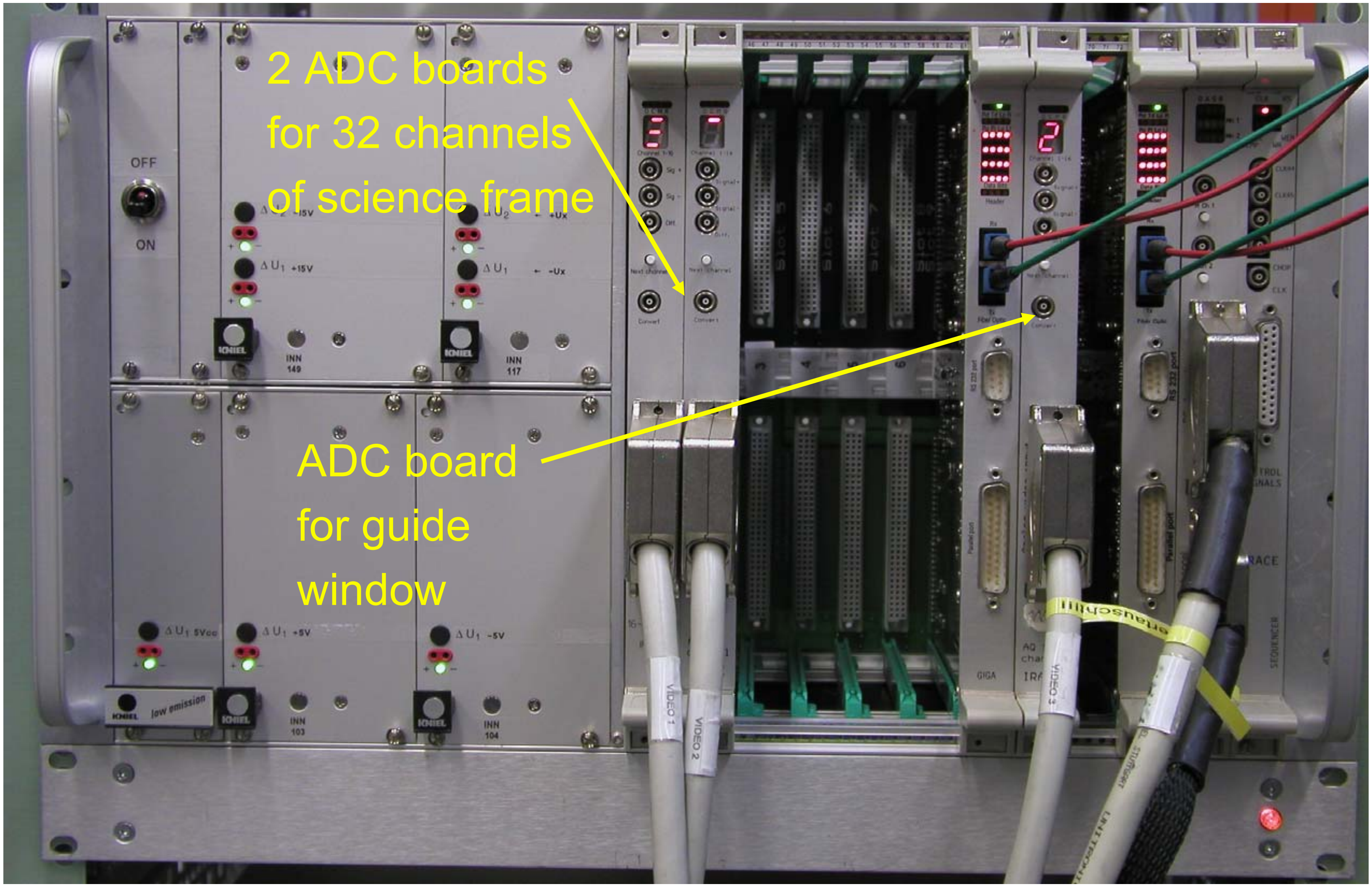

Add
ADC board and
2nd gigalink
for guide
window

IRACE for Hawaii2RG
32-channel and guide window

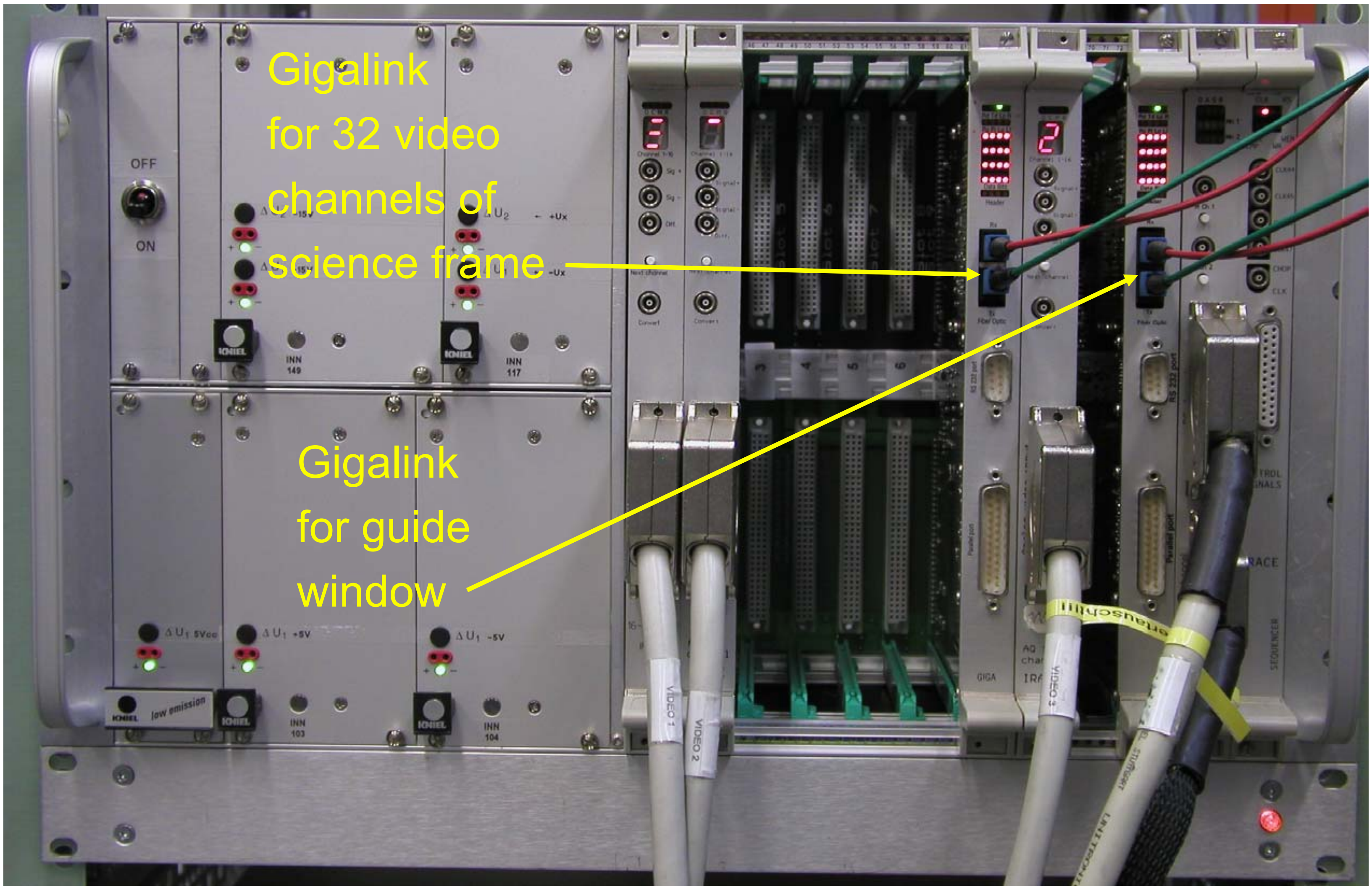

Additional ADC board and 2nd gigalink for guide window

IRACE is flexible architecture covering all Applications

Port flexibility to NGC

IRACE for 2x2 mosaic of Hawaii2RG's and guide mode

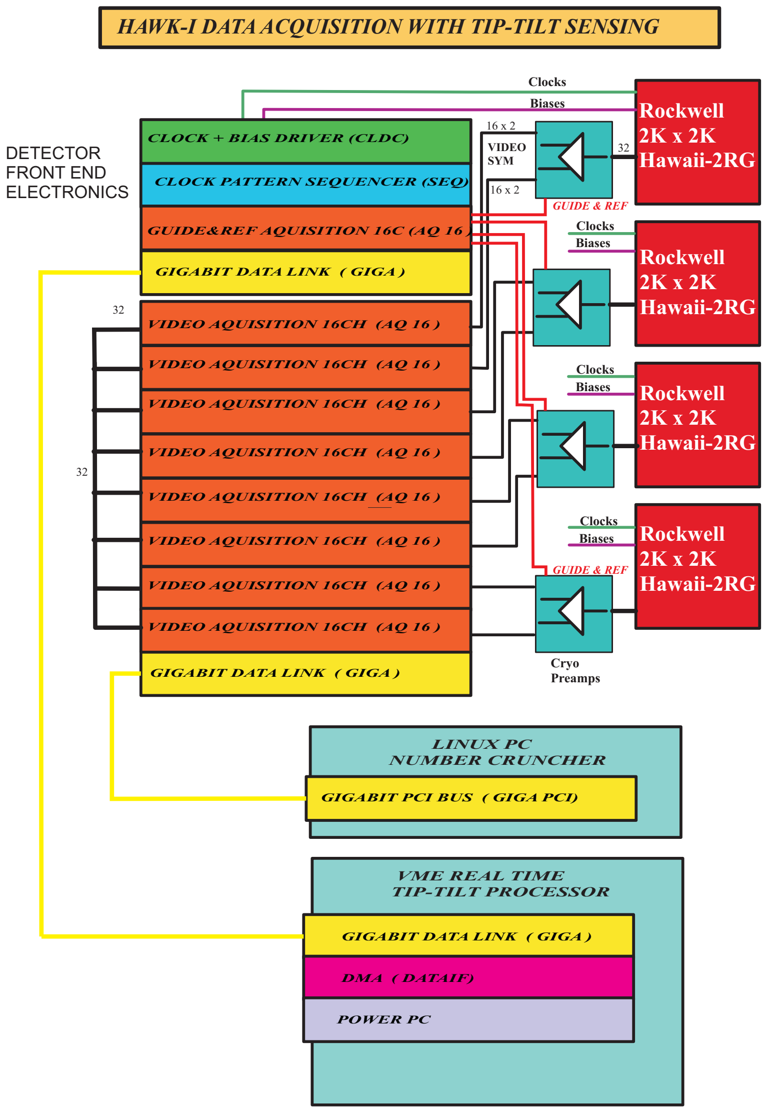

- 136 channel system
  16 bit 500 kHz

  4x32 video channels
  4x1 reference channels
  4x1 guide window channels
- Gigabit fiberlink
- cryo-opamps instead of ASIC
- Linux pc as number cruncher with home-made pci-bus gigalink interface

NGC Prototype
Minimum System (Four Channels)

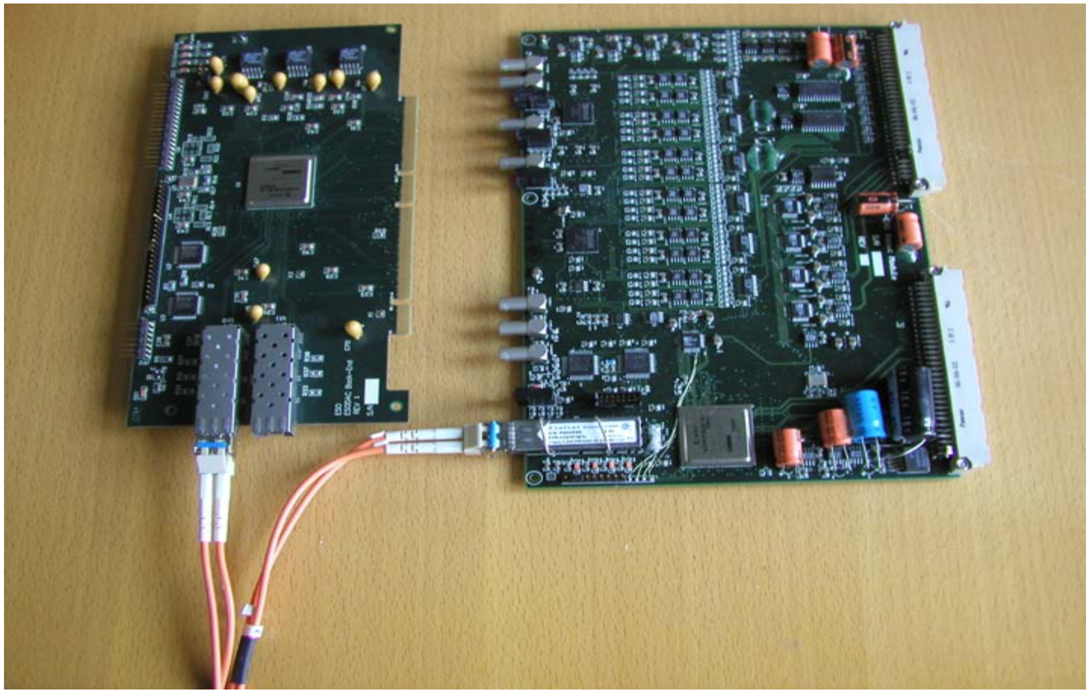

- NGC is a modular system for IR detector and CCD readout with a Back-end, a basic Front-end unit containing a complete four channel system on one card and additional boards like multi channel ADC units and more…
- There is no processor, no parallel inter-module data bus on the front-end side. Advanced FPGA link technology is used to replace conventional logic
- Connection between Back and Front-end with high speed fiber links at 2.5GBit/s
- Connection between Front-end modules with high speed copper links at 2.5GBit/s.
- Power Consumption on this Front-end is less than 10 Watts (Excluding power supply)
- This Front-End system does not require big cooling boxes

Status:

- Basic board and backplane operational
- 34-channel ADC board and add-on board tested and fully functional
- NGC software created (ngcb, ngcpp, ngcdcs)
- All components ready to read H2RG array

NGC controller

Manfred Meyer

main board   backplane   back board with fiber link connectors   32 channel ADC board

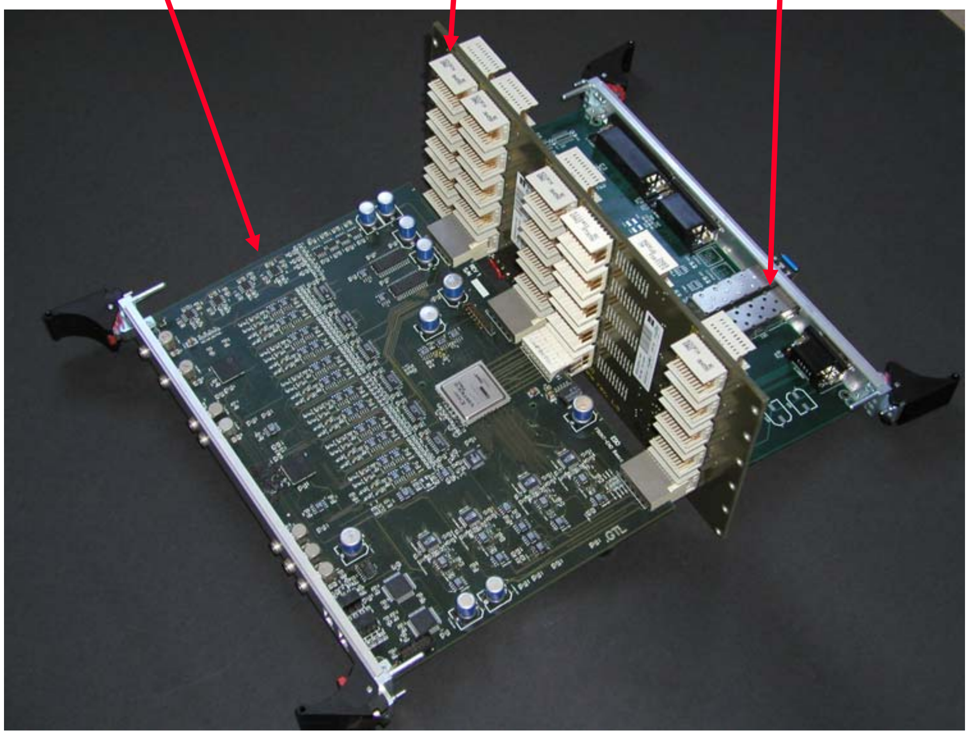

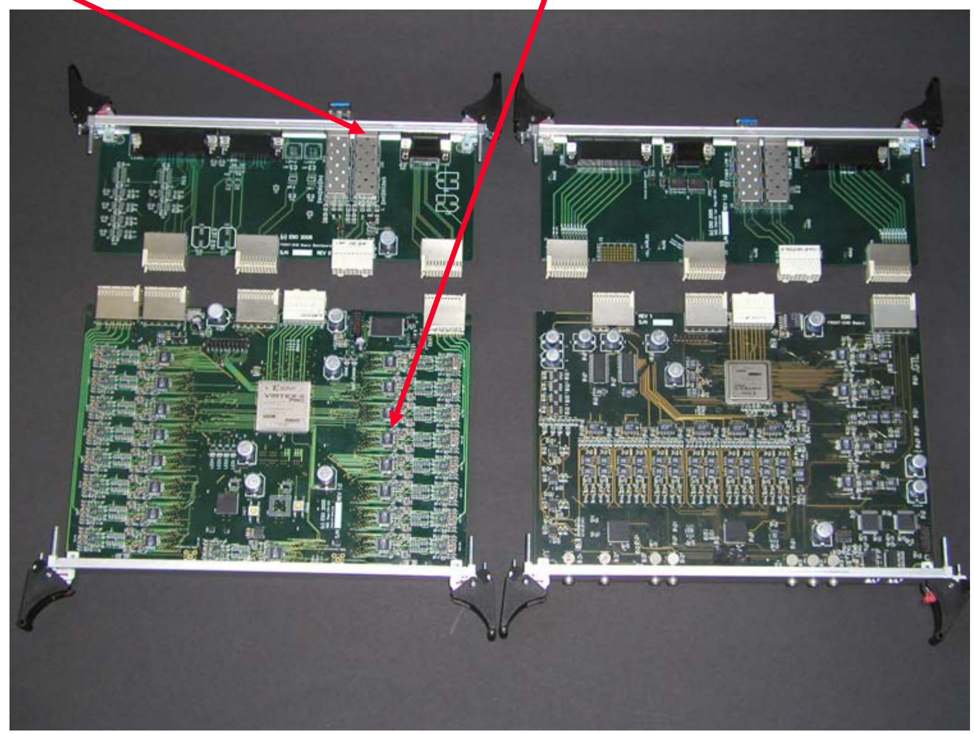

NGC prototype

- Read out independently
  2 Hawaii-2RG's
  and 1 Hawaii1 array
- 1 main board and
  1 ADC board required
  for each Hawaii-2RG
- 1 main board required
  for Hawaii1
- Total of 5 boards needed
  fits in 19'' 3HU rack at cryostat
- Power supply external
- Number cruncher

The SIDECAR ASIC
Control Electronics on a Chip

Replace this

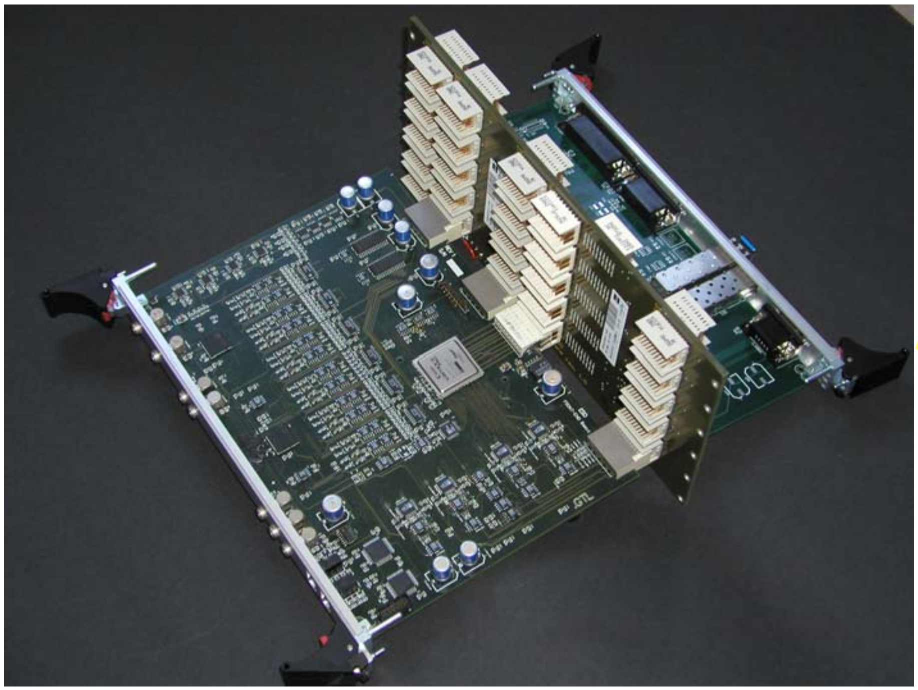

NGC controller

with this!

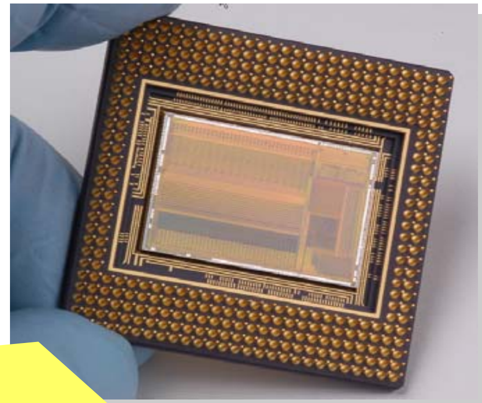

- complete controller on single chip operating at 40 K dissipating 4 mW
- programmable clocks and bias voltages
- digitize video signal on cold focal plane

  36 x16 bit100KHz ADC's
  32 x12 bit 5MHz ADC's
- digital interface to pc: USB2
- compare performance of ASIC and NGC

Sections Inside the ASIC

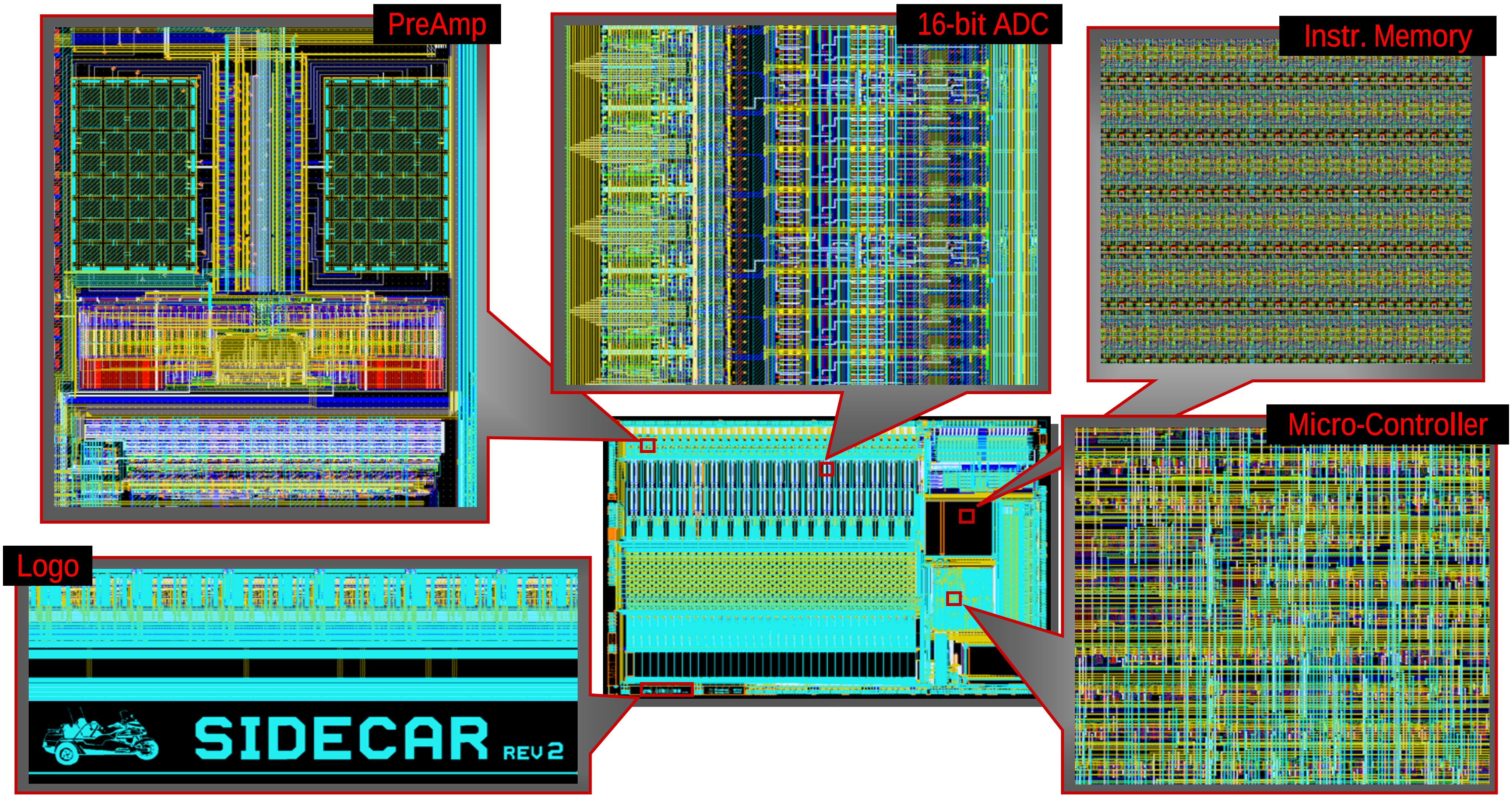

ASIC Flight Package for JWST

Exploded View

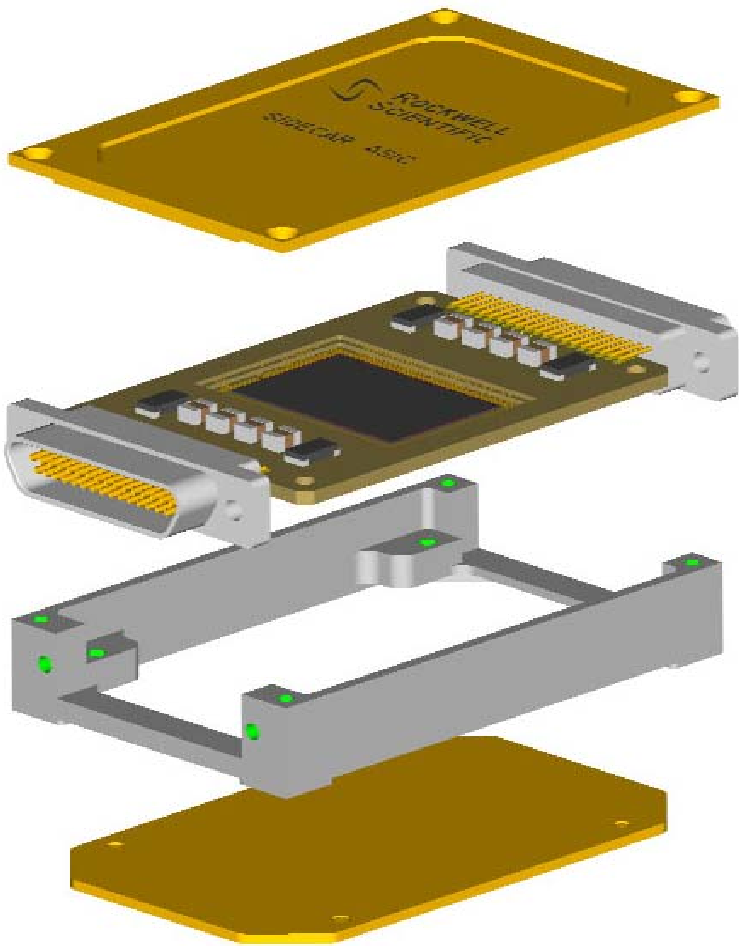

Detector + ASIC
Sub-System

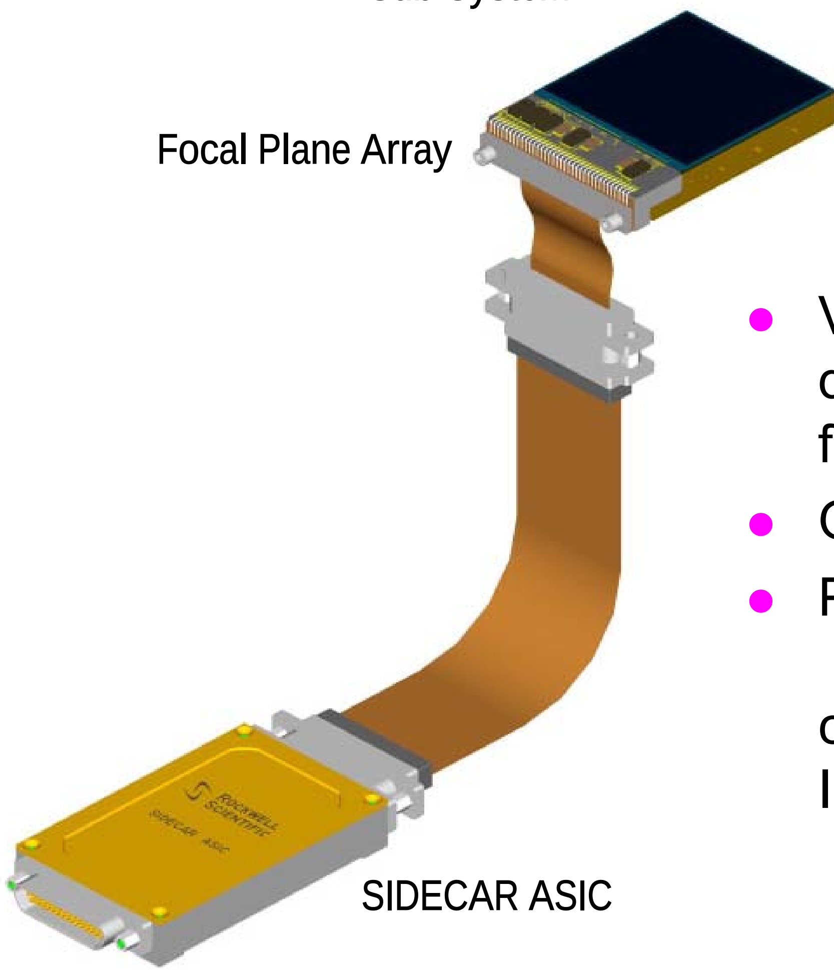

- Video signal digitized at cold focal plane
- Ordered by ESO
- Performance will be evaluated and compared with IRACE and NGC

Conclusions

- CCD's still competitive in the visible domain, but CMOS arrays improve
- Large detector formats achieved with array mosaics
- Sensor developments for AO: L3 CCD
  Geiger APD arrays
- BIB array development for ground based mid-IR: Si:As 1Kx1K Aquarius
- Work horse in infrared: HgCdTe arrays (Hawaii-2RG, VIRGO)
  - » QE high over the entire spectral range (K: 0.84, Z: 0.66) with correct PTF
  - » With MBE dark current < 0.01 e/s at T< 80 K
  - » For smaller pixel size interpixel capacitance has to be addressed and gain calibration has to take into account IPC
  - » Reference pixels eliminate drift and reduce pick-up: robust system
  - » Readout noise in IR with multiple sampling 2.2 erms
  - » Glow shielding on Hawaii-2RG efficient
  - » Persistence not yet solved
  - » Sophisticated mux with guide mode, which does not disturb science frame
- conventional detector controllers will eventually be replaced by ASIC's


The end